Terms and Conditions of Use of Digitised Theses from Trinity College Library Dublin

Copyright statement

All material supplied by Trinity College Library is protected by copyright (under the Copyright and Related Rights Act, 2000 as amended) and other relevant Intellectual Property Rights. By accessing and using a Digitised Thesis from Trinity College Library you acknowledge that all Intellectual Property Rights in any Works supplied are the sole and exclusive property of the copyright and/or other IPR holder. Specific copyright holders may not be explicitly identified. Use of materials from other sources within a thesis should not be construed as a claim over them.

A non-exclusive, non-transferable licence is hereby granted to those using or reproducing, in whole or in part, the material for valid purposes, providing the copyright owners are acknowledged using the normal conventions. Where specific permission to use material is required, this is identified and such permission must be sought from the copyright holder or agency cited.

Liability statement

By using a Digitised Thesis, I accept that Trinity College Dublin bears no legal responsibility for the accuracy, legality or comprehensiveness of materials contained within the thesis, and that Trinity College Dublin accepts no liability for indirect, consequential, or incidental, damages or losses arising from use of the thesis for whatever reason. Information located in a thesis may be subject to specific use constraints, details of which may not be explicitly described. It is the responsibility of potential and actual users to be aware of such constraints and to abide by them. By making use of material from a digitised thesis, you accept these copyright and disclaimer provisions. Where it is brought to the attention of Trinity College Library that there may be a breach of copyright or other restraint, it is the policy to withdraw or take down access to a thesis while the issue is being resolved.

Access Agreement

By using a Digitised Thesis from Trinity College Library you are bound by the following Terms & Conditions. Please read them carefully.

I have read and I understand the following statement: All material supplied via a Digitised Thesis from Trinity College Library is protected by copyright and other intellectual property rights, and duplication or sale of all or part of any of a thesis is not permitted, except that material may be duplicated by you for your research use or for educational purposes in electronic or print form providing the copyright owners are acknowledged using the normal conventions. You must obtain permission for any other use. Electronic or print copies may not be offered, whether for sale or otherwise to anyone. This copy has been supplied on the understanding that it is copyright material and that no quotation from the thesis may be published without proper acknowledgement.

Electromyography in the assessment of neuromuscular fatigue and biomechanical task specificity.

Neil Fleming

Thesis submitted for the award of PhD. to the Department of Physiology, Trinity College Dublin.

May 2012

DECLARATION

I declare that this thesis is all my own work and has/will not be submitted to this or any other university as part of any other post graduate programme. I grant permission to the Trinity College librarian to lend or copy this thesis in part on request.

Signature: _____ ~~October 2011~~. JUNE 2012

ABSTRACT

The use of EMG in the quantification of muscle fatigue has received much attention over the years. It has been used to identify the neuromuscular fatigue threshold at the aerobic-anaerobic transition during dynamic exercise (Lucia *et al.*, 1999) and the progressive changes in recruitment patterns during isometric fatiguing contractions (Mathur *et al.*, 2005). However, there is little or no published data comparing the EMG thresholds across a range of dynamic exercises. Furthermore, there is a lack of agreement as to the effect that training induced alterations to fatigue may have on the EMG signal. In addition to quantifying fatigue, EMG has been used to reveal intra- and inter-muscular adjustments to given internal and external exercise constraints (Li & Caldwell, 1998; Hug & Dorel, 2009). Nowicky *et al.* (2005) suggested that it may thus provide a means for the assessment of ergometer task specificity.

The aims of this research dissertation were therefore twofold. The first aim was to assess and compare the appearance of neuromuscular fatigue in a variety of biomechanical tasks and to establish if training could alter the EMG response to fatigue. The second aim was to assess the biomechanical task specificity of rowing and kayaking ergometry using the novel approach of comparing EMG data across conditions.

The research described in Chapter 3 of this dissertation investigated the appearance of neuromuscular fatigue at the aerobic-anaerobic transition across a range of dynamic sports. Three sub-groups of trained individuals performed graded incremental tests on ergometers specific to their discipline (rowing, kayaking and cycling). Aerobic-anaerobic thresholds based on EMG, blood lactate and ventilatory data were subsequently attained using the V-slope method. T_{EMG} was then compared against lactate and ventilatory thresholds and across sub-groups. The principal finding of this study was that T_{EMG} exhibited high correlation to the other thresholds across all sub-groups. Additionally, T_{EMG} and V_{T2} occurred at significantly higher workloads when comparing cycling to rowing ($P<0.01$), suggesting that they may be sensitive to alterations in the exercise protocol. However, a subsequent validation study (Appendix 4) did not support this hypothesis.

The second study (Chapter 4) compared the appearance of neuromuscular fatigue in a trained and untrained group, in order to establish if training induced resistance to fatigue could be identified via EMG. Participants performed fatiguing isometric knee extensions at

20 and 80% MVC. As expected, the trained group exhibited enhanced fatigue resistance, identified as greater time to failure (TTF). A significant difference in RF AEMG was observed during the 80% MVC trial, with the trained group exhibiting enhanced recruitment as fatigue progresses. No other differences in spectral or amplitude EMG amplitude were observed in any of the muscles assessed.

Chapters 5 and 7 detailed the assessment of biomechanical task specificity in kayaking and rowing ergometry, respectively. Participants performed matched exercise trials both on-ergometer and on-water, during which, EMG, force and kinematic data were recorded. The principal finding in these studies was that significant differences in EMG activity patterns recorded from discrete muscles existed between the on-water and on-ergometer stroke cycles in both kayaking (Chapter 5) and rowing (Chapter 7). A follow on study was therefore to assess the effect of the kayak ergometer loading mechanism on EMG activity and 3D kinematics (Chapter 6). During this study, kayakers performed matched exercise at varying levels of elastic recoil tension, during which EMG, force and 3D motion kinematics were recorded. The findings of Chapter 6 confirmed that with respect to AD activity, the ergometer loading mechanism which applies an elastic recoil force on the ergometer paddle shaft was responsible for the significant differences between on-water and on-ergometer kayaking.

Overall, the results of this dissertation highlight that with respect to neuromuscular fatigue, EMG is capable of identifying not only fatigue related alterations in recruitment at the aerobic-anaerobic transition in a variety of tasks, but also training induced changes in recruitment strategy, associated with enhanced fatigue resistance. In addition, the results of biomechanical task specificity trials suggest that ergometer exercise may not simulate the on-water scenario as accurately as desired, with respect to muscle recruitment patterns. Finally, the novel use of EMG to directly compare muscle recruitment patterns across conditions highlighted that it is a highly useful comparative tool in the assessment of task specificity. Moreover, the current EMG results allowed the author to make preliminary suggestions for improvements in ergometer design and use.

ACKNOWLEDGEMENTS

I will be forever grateful to so many people for their time, effort, support and encouragement during the past four years. Firstly, to Elisa who has supported me through thick and thin. Without her love and support, I could never have finished this work. To my parents, who instilled in me from an early age, both a passion for sport and the pursuit of knowledge. To my brothers Ciarán and Darragh who were always there to lend a hand in the laborious tasks involved in field based data collection. To my baby sister Áine for all of her help and support on campus over the last 2 years.

To Nick and Willy in the Department of Anatomy, who gladly performed all the medical examinations that were required.

To the many volunteers who freely gave of their time to participate in the research for this dissertation.

To all the staff in the Physiology Department for their support throughout this research.

To Cillin Condon and the staff in the School of Physiotherapy, for their time and help.

To Dave and Colin for their constant support and friendship.

Sincere thanks to David Fletcher for his tireless effort in the development of force measurement systems. Without his skill and knowledge, much of this research would not have been possible.

Thank you to my academic supervisor, Dr. Mikel Egana for his support and help especially over the past 6 months.

Finally, to Bernard for everything he has done for me. Words cannot describe how grateful I am to him, for his constant dedication, motivation and support. If I take one thing from my time in Trinity College, I hope it is Bernard's undying passion for science and the pursuit of excellence. Having first entered the Human Performance Laboratory as a young athlete aged 16, my first meeting with Bernard left such an impact that it completely changed the course of my life. I owe him more than any student could ever owe their teacher and will be forever in his debt.

20 and 80% MVC. As expected, the trained group exhibited enhanced fatigue resistance, identified as greater time to failure (TTF). A significant difference in RF AEMG was observed during the 80% MVC trial, with the trained group exhibiting enhanced recruitment as fatigue progresses. No other differences in spectral or amplitude EMG amplitude were observed in any of the muscles assessed.

Chapters 5 and 7 detailed the assessment of biomechanical task specificity in kayaking and rowing ergometry, respectively. Participants performed matched exercise trials both on-ergometer and on-water, during which, EMG, force and kinematic data were recorded. The principal finding in these studies was that significant differences in EMG activity patterns recorded from discrete muscles existed between the on-water and on-ergometer stroke cycles in both kayaking (Chapter 5) and rowing (Chapter 7). A follow on study was therefore to assess the effect of the kayak ergometer loading mechanism on EMG activity and 3D kinematics (Chapter 6). During this study, kayakers performed matched exercise at varying levels of elastic recoil tension, during which EMG, force and 3D motion kinematics were recorded. The findings of Chapter 6 confirmed that with respect to AD activity, the ergometer loading mechanism which applies an elastic recoil force on the ergometer paddle shaft was responsible for the significant differences between on-water and on-ergometer kayaking.

Overall, the results of this dissertation highlight that with respect to neuromuscular fatigue, EMG is capable of identifying not only fatigue related alterations in recruitment at the aerobic-anaerobic transition in a variety of tasks, but also training induced changes in recruitment strategy, associated with enhanced fatigue resistance. In addition, the results of biomechanical task specificity trials suggest that ergometer exercise may not simulate the on-water scenario as accurately as desired, with respect to muscle recruitment patterns. Finally, the novel use of EMG to directly compare muscle recruitment patterns across conditions highlighted that it is a highly useful comparative tool in the assessment of task specificity. Moreover, the current EMG results allowed the author to make preliminary suggestions for improvements in ergometer design and use.

ACKNOWLEDGEMENTS

I will be forever grateful to so many people for their time, effort, support and encouragement during the past four years. Firstly, to Elisa who has supported me through thick and thin. Without her love and support, I could never have finished this work. To my parents, who instilled in me from an early age, both a passion for sport and the pursuit of knowledge. To my brothers Ciarán and Darragh who were always there to lend a hand in the laborious tasks involved in field based data collection. To my baby sister Áine for all of her help and support on campus over the last 2 years.

To Nick and Willy in the Department of Anatomy, who gladly performed all the medical examinations that were required.

To the many volunteers who freely gave of their time to participate in the research for this dissertation.

To all the staff in the Physiology Department for their support throughout this research.

To Cillin Condon and the staff in the School of Physiotherapy, for their time and help.

To Dave and Colin for their constant support and friendship.

Sincere thanks to David Fletcher for his tireless effort in the development of force measurement systems. Without his skill and knowledge, much of this research would not have been possible.

Thank you to my academic supervisor, Dr. Mikel Egana for his support and help especially over the past 6 months.

Finally, to Bernard for everything he has done for me. Words cannot describe how grateful I am to him, for his constant dedication, motivation and support. If I take one thing from my time in Trinity College, I hope it is Bernard's undying passion for science and the pursuit of excellence. Having first entered the Human Performance Laboratory as a young athlete aged 16, my first meeting with Bernard left such an impact that it completely changed the course of my life. I owe him more than any student could ever owe their teacher and will be forever in his debt.

TABLE OF CONTENTS

LIST OF ABBREVIATIONS

μV	Microvolt
%	Percentage
°	Degree
Ω	Ohm
AD	*Anterior Deltoid*
ADP	Adenosine Diphosphate
AEMG	Average EMG
Ag	Silver
AgCl	Silver Chloride
AMP	Adenosine Monophosphate
ANOVA	Analysis of variance
ATP	Adenosine Triphosphate
BB	*Biceps Brachii*
BF	*Biceps Femoris*
BLa	Blood lactate
BMI	Body mass index
C	Carbon
Ca^{2+}	Calcium ion
Cl^-	Chloride ion
cm	Centimetre
CMRR	Common mode rejection ratio
CNS	Central nervous system
CV	Conduction Velocity
DFT	Discrete Fourier transform
EMG	Electromyography
ES	*Erector Spinae*
FER	Forced expiratory rate
FEV_1	Forced expiratory volume in 1 second
FFT	Fast Fourier transform
FVC	Forced vital capacity
G	Gram
GA	*Gastrocnemius*
H^+	Hydrogen ion
H_2O	Water
H_2O_2	Hydrogen Peroxide
Hct	Haematocrit
Hgb	Haemoglobin
h	Hour
Hz	Hertz
ICC	Inter-class correlation coefficient
IED	Inter-electrode distance
K^+	Potassium ion
kg	Kilogram
$kg.m^{-2}$	Kilogram per metre squared

kHz	Kilohertz
kΩ	Kilo-ohm
L	Litre
LD	*Latissimus Dorsi*
m	Metre
mm	Millimetre
MCT	Monocarboxylate transporter
MF	Median frequency
mg	Milligram
Mg^{2+}	Magnesium ion
min	Minute
mL	Millilitre
$mL.kg^{-1}.min^{-1}$	Millilitre per kilogram per minute
mmol	Millimole
MPF	Mean power frequency
ms	Millisecond
MU	Motor unit
mV	Millivolt
MVC	Maximum voluntary contraction
N	Newton
N_2	Nitrogen
Na^+	Sodium ion
NaCl	Sodium chloride
Nm	Newton metre
O_2	Oxygen
$O_2^{\bullet-}$	Superoxide radical
OBLA	Onset of blood lactate accumulation
$OH^{\bullet}$	Hydroxyl radical
P	Probability
pH	Potential Hydrogen
pK	Potential Potassium
PF	Peak expiratory flow
P_i	Inorganic phosphate
Pmax	maximum power
r	Pearson product moment correlation coefficient
RBC	Red blood cell count
RF	*Rectus Femoris*
Rev	Revolution
rms	Root mean squared
rmsEMG	Root mean squared EMG
SD	Standard deviation
SEM	Standard error of the mean
SENIAM	Surface electromyography for the non-invasive assessment of muscles
TA	*Tibialis Anterior*
TB	*Triceps Brachii*

TEM	Technical error of the measurement
T_{EMG}	EMG or neuromuscular fatigue threshold
T_{Lac}	Lactate threshold
TMS	Transcranial magnetic stimulation
TTF	Time to failure
UT	*Upper Trapezius*
$\dot{V}CO_2$	Volume of Carbon Dioxide production
$\dot{V}E$	Ventilation rate
$\dot{V}E/\dot{V}CO_2$	Ventilatory equivalent for Carbon Dioxide
$\dot{V}E/\dot{V}O_2$	Ventilatory equivalent for oxygen
VL	*Vastus Lateralis*
VM	*Vastus Medialis*
$\dot{V}O_2$	Volume of Oxygen consumption
$\dot{V}O_2max$	Maximum volume of Oxygen consumption
$\dot{V}O_2peak$	Peak volume of Oxygen consumption
vs.	Versus
V_{T1}	First ventilatory threshold
V_{T2}	Second ventilatory threshold
W	Watt
WBC	White blood cell count
yr	Year

LIST OF FIGURES

LIST OF TABLES

LIST OF PLATES

Chapter 1

Introduction

1.1: GENERAL OVERVIEW

Despite the wide usage of rowing and kayaking ergometers for both training and testing purposes, studies assessing the biomechanical task specificity of these machines, via direct comparison of on-water and on-ergometer exercise, are scarce. In addition, those limited studies which have assessed ergometer biomechanical task specificity have generally focussed on movement kinematics and force as a means of comparison (Elliott *et al.*, 2001; Kleshnev, 2005). Over the last two decades, surface electromyography (EMG) has been used as a novel means of comparing biomechanical movement (Clarys & Cabri, 1993; Nowicky *et al.*, 2005). The measurement of muscle activity provides insight into the internal mechanisms by which humans perform tasks and as such could provide a useful means of assessing ergometer task specificity. The quantification of muscle fatigue is another area in which EMG has been successfully utilised. Fatigue related changes around the metabolically derived aerobic-anaerobic transition have been studied using EMG for some time, however, there is limited data comparing this phenomenon across varying exercise modalities. In addition, it is possible that training induced alterations to fatigue may be quantified using EMG. The aim of the present introduction is therefore, to review the mechanisms involved in both muscle fatigue and biomechanical task specificity. This introduction will pay special attention to the mechanisms surrounding neuromuscular fatigue as it relates to the aerobic-anaerobic transition, the contrasting assessments of biomechanical task specificity in both kayaking and rowing and provide a detailed review of the current methodologies utilising EMG to assess both fatigue and task specificity.

1.2: MUSCLE FATIGUE

1.2.1: Muscle fatigue as a concept in physiology

Muscle fatigue is one of the key determining factors for performance in many competitive sports and as such, it is of great interest in the field of exercise physiology. In the context of physiology, fatigue is a general concept intended to denote an acute impairment of performance (Enoka & Stuart, 1992; Allen *et al.*, 2008). This impairment can include both an increase in perceived effort necessary to maintain a desired force or the eventual inability to produce this force (Asmussen, 1979). In addition to reduced force production, muscle fatigue can also manifest itself as a reduction in muscle fibre shortening velocity (Allen *et al.*, 2008). The endurance time in a contraction is defined as the time duration which the skeletal muscle can maintain a required force; when the muscle fails to do this, it is deemed to be fatigued (Hagberg, 1981). These definitions however, imply that fatigue occurs at a specific time point, a notion which is inconsistent with the concept of fatigue accepted in other scientific fields such as structural engineering and physics. The use of a failure point also carries with it some practical disadvantages, the most obvious being that fatigue is detected only after it occurs (De Luca, 1997). It is generally accepted that muscle fatigue is an ongoing process resultant from time-dependent physiological and biochemical processes which alter the means of generating force (De Luca, 1997). A quantitative means of monitoring changes in such processes is thus highly desirable when examining muscle fatigue (Asmussen, 1979).

Plate 1.1: Fatigue at the end of a rowing race.

1.2.2 Historical developments in the quantification of muscle fatigue

The earliest documented studies which examined muscle fatigue were by Ettienne-Jules Maray (1868). This work demonstrated fatigue induced changes in the mechanical response to stimulation of frog muscle (Figure 1.1). The first research examining human muscle fatigue was most likely the work of Mosso (1892). He developed an ergograph which recorded the effects of repetitive contractions of the middle finger with given loads, on a smoked drum (Figure 1.2). This early work by Mosso led to the concept of "central fatigue", in which deterioration in muscle performance originates in the central nervous system (CNS) (Gandevia, 2001). It was not until the 1950's and the arrival of reliable electromyographic techniques, that the distinction between "central" and "peripheral" fatigue slowly emerged (Asmussen 1979; Gandevia, 2001). Where central fatigue originates at the CNS, peripheral fatigue was defined as a deterioration in muscle performance originating downstream of the CNS at a myocellular level (Allen *et al.*, 2008). This distinction and the debate over each component's contribution to overall fatigue, remains the subject of considerable controversy. Since this differentiation between peripheral and central fatigue emerged, there has been a large body of literature which has attempted to quantify the contribution of each to the overall fatigue process.

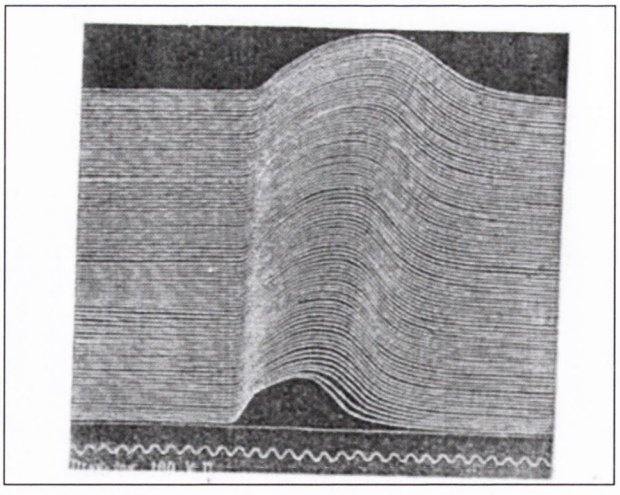

Figure 1.1: Superimposed contractions of a frog muscle (Marey, 1868). First contraction at bottom (Adapted from Asmussen, 1979).

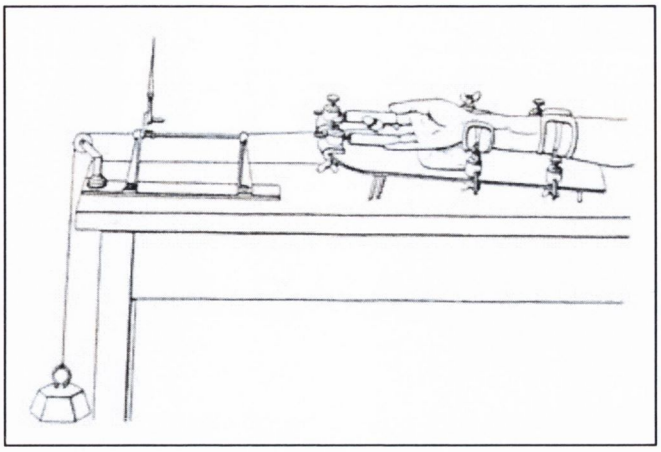

Figure 1.2: The classical finger ergograph developed by Mosso (1892) (Adapted from Asmussen, 1979).

Several extensive reviews of the literature examining muscle fatigue have been previously written. One of the first of these was by Erling Asmussen, who compiled an extensive review of early advances in the quantification of general "Muscle Fatigue" (Asmussen, 1979). Gandevia (2001) presented a more precise review of the technical and conceptual advances relevant to the examination of central fatigue. More recently Allen *et al.* (2008) provided an extensive review of advances in understanding of the cellular mechanisms underlying peripheral fatigue. In addition, a recent review by Enoka & Duchateau (2008) provided useful insight into the comparison of central and peripheral fatigue. For the purposes of this introduction however, I will highlight several key papers which have furthered our knowledge with regards to both central and peripheral muscle fatigue.

One of the first major steps forward in the comparison of "central" and peripheral" components of fatigue, was the development of the twitch interpolation technique by Merton (1954). This technique applies a super-maximal electrical stimulus to the active motor neuron, during maximal voluntary activation of the innervated muscle. Since the size of the interpolated twitch is inversely proportional to the strength of muscle activation, no interpolated twitch should be observed during a maximal voluntary contraction (Merton, 1954). Thus the twitch interpolation technique can quantify neural drive to a muscle and is therefore a useful means of quantifying centrally mediated reductions in force generating capacity or "central fatigue".

Bigland-Ritchie & Woods (1984) classified 3 potential sites of failure where fatigue may be manifested;

1) Failure within the CNS
2) Failure within the active muscle
3) Failure of peripheral neuromuscular transmission

Peripheral nerve stimulation and analysis of the resultant M-waves, is a technique which has been used for many years to assess the effects fatigue on neuromuscular pathways. M-waves are electrically elicited compound action potentials recorded from the surface of the muscle. This technique was first developed by Hoffmann, in 1910 and was used to examine neuromuscular properties of both afferent and efferent nerves. A stimulating electrode is placed on the surface of the skin, distal to the recorded muscle. Subsequent electrical stimulation of both afferent (sensory) and efferent (motor) neurons is recorded via EMG at the site of the recorded muscle (Palmieri *et al.*, 2004). The comparison of M-wave shape and size has provided a useful means of assessing if failure at the neuromuscular junction or transmission along the surface of the muscle cell plays a role in the generation of fatigue (Bigland-Ritchie & Woods, 1984). If neuromuscular transmission or muscle membrane excitability is impaired, a reduction in M-wave amplitude and area results (Bigland-Ritchie & Woods, 1984). It is now generally accepted that the integrity of neuromuscular transmission is maintained in the presence of fatigue (Merton *et al.*, 1981 cited in Bigland-Ritchie & Woods, 1984).

The more recent development of non-invasive techniques for the stimulation of the human cerebral cortex, such as transcranial magnetic stimulation (TMS), has allowed advances in the investigation of the central fatigue (Gandevia, 2001). The response to TMS is recorded at the active musculature using EMG and subsequent comparisons of fatigued and non-fatigued states can be made (Zijdewind *et al.,* 2000). In an active muscle, TMS evokes two main effects: a short-latency positive response (i.e. excitation, "muscle-evoked potential", MEP) and a longer latency negative response, a temporary interruption or decrease in EMG activity (TMS-evoked silent period) (Zijdewind *et al.,* 2000; Gandevia, 2001). Fatigue

affects both the MEP and TMS-evoked silent period. The MEP generally increases during sustained fatiguing contractions, however, there is a reduction in post-failure MEP amplitude compared to non-fatigued conditions (Taylor *et al.,* 1996; Zijdewind *et al.,* 2000; Gandevia, 2001). With respect to the TNS-evoked silent period, there is an increase in its duration both during and following sustained fatiguing contractions (Taylor *et al.,* 1996; Zijdewind *et al.,* 2000).

Finally, research by Bigland-Ritchie *et al.* (1986) highlighted the importance that feedback from small diameter muscle afferents such as Group III or IV can play in muscle fatigue. Group III and IV muscle afferents innervate free nerve endings that are plentiful and distributed widely throughout muscle. These afferents are either silent or maintain low background discharge rates (0.1 Hz). They respond to local mechanical, biochemical, and thermal events and can have a reflex inhibitory effect on motor unit output (Gandevia, 2001). Bigland-Ritchie *et al.* (1986) reported that the accumulation of muscle metabolites during sustained contractions led to reflex inhibition of the motor neurons via the Group III and IV afferent neurons. These findings confirmed a wide body of literature reporting similar effects in animal studies (Gandevia, 2001).

1.2.2: The use of electromyography to examine muscle fatigue

The use of electromyography allows physiologists to monitor changes in the electrical activity within muscles during sustained contractions and has become widely accepted as a non-invasive, objective means of quantifying muscle fatigue. It has long been established that a positive relationship exists between the force of a muscle contraction and magnitude of the electrical activity recorded from it via EMG (Lippold, 1952). This force-EMG relationship maintains that increases in force of a muscle contraction result in corresponding increases in the EMG recorded from that muscle. It is worth noting this relationship is highly variable based on the type of contraction, velocity of movement and specific muscle being analysed (Clarys et *al.,* 2010). In addition, even during isometric contractions, muscle intensity recorded via EMG is not always linearly related to the force (Clarys *et al.,* 2010). During the course of a sustained isometric contraction however, the electrical activity of the muscle progressively increases with no apparent increase in force (Edwards & Lippold,

1956). Thus if a muscle contraction is sustained at a constant force, the electrical activity will increase progressively throughout the course of the contraction. Edwards and Lippold (1956) postulated that this phenomenon was due to decreases in the contractility of fatigued muscle fibres and the subsequent recruitment of additional motor-units to compensate in order to maintain the desired force. This was the first study to show that EMG changes during sustained muscle contractions could quantify fatigue before the contraction failure point.

Since these early studies, it has been well documented that the electrical activity of the muscle progressively increases with time during fatiguing exercise both in static (Eason, 1960; Lippold, 1960; De Vries, 1968) and dynamic contractions (Zhukov, 1959; Potvin & Bent, 1997). The primary mechanism proposed for the increases in electrical activity within the fatiguing muscles, remains the recruitment of additional motor-units to compensate for loss of contractility within the fatigued muscle fibres (Lippold, 1960). However several other proposed factors may play a part in these fatigue induced changes. Such factors include the progressive synchronisation of motor-unit action potentials (Zhukov, 1959; Lippold, 1960), the firing of higher threshold motor units (De Vries, 1968), and muscle tremor caused by irradiation of electrical activity to antagonistic muscles (Lippold, 1960; Person, 1960).

According to Farina *et al.* (2002), the central nervous system (CNS) controls skeletal muscle force using two strategies; motor unit recruitment and motor unit firing rate modulation (rate coding). The combination of increased recruitment of additional motor units along with increased rate coding of already active motor units allows for smooth, controlled increases in muscle force. It has generally been accepted that EMG spectral variables shift towards higher frequencies as muscle force increases (Farina *et al.*, 2002) and it has been demonstrated that a positive linear correlation exists between spectral variables indicative of rate coding and amplitude variables indicative of motor unit recruitment as muscle force increases (Solomonow *et al.*, 1990). Thus under non-fatiguing conditions, increases in muscle force are accomplished by concurrent increases in motor unit recruitment and rate coding (Enoka & Stuart, 1992). However during sustained fatiguing isometric contractions,

it has been shown that there is a disassociation of the two mechanisms (Mathur *et al.*, 2005). When an individual performs a sub-maximal isometric contraction to exhaustion, the whole muscle EMG increases yet there is a decline in spectral variables (Person & Kudina, 1972; Bigland-Ritchie *et al.*, 1986; Mathur *et al.*, 2005). This indicates that while fatigue induces an increase in motor unit recruitment, there is an overall decrease in rate coding, or the velocity at which the action potentials are propagated.

It is widely accepted that a change in intramuscular ion and metabolite concentrations during fatiguing contractions is the primary cause of increases in EMG amplitude and spectral shift towards lower frequencies (Enoka & Stuart, 1992). The effect that hydrogen ions (H^+) and other metabolites have on reducing the contractility of muscle fibres requires the recruitment of additional motor-units to compensate, and thus EMG amplitude will increase. These same metabolites have also been shown to reduce the signal propagation and action potential conduction velocity along muscle fibres. Increased H^+ ion concentrations slow muscle fibre conduction velocity and fundamentally change the shape of action potentials along the muscle fibre (Brody *et al.*, 1991). Thus the increased acidity within fatiguing muscle will result in a shift towards lower EMG spectral frequencies and an increase in motor unit recruitment.

The mechanisms underlying fatigue induced shifts towards lower motor unit discharge frequencies have been debated for many years and there is still no unanimous interpretation of the spectral changes observed (Broman *et al.*, 1985). The most widely accepted explanation is a decrease in the myoelectric conduction velocity along the muscle fibre (Bigland-Ritchie *et al.*, 1981). As the muscle begins to fatigue, there is a decrease in the velocity at which an action potential passes along the active fibres (Brody *et al.*, 1991). Lindstrom *et al.* (1970) produced a mathematical model which illustrated that under constant conditions, the decreases in spectral variables could be explained entirely by decreases in muscle fibre conduction velocity (Lindstrom *et al.*, 1970). However constant conditions rarely appear in human physiology. As such, the hypothesis postulated by Lindstrom *et al.* (1970) was disputed by Broman *et al.* (1985). They reported that spectral variables decreased to a much greater magnitude than the muscle fibre conduction velocity during

sustained contractions of the *Gastrocnemius* muscle and it was concluded that other factors must also contribute to the fatigue induced frequency shifts (Broman *et al.*, 1985). Brody *et al.* (1991) examined the effect of pH on median frequency and muscle fibre conduction velocity from *in-vitro* muscle preparations and reported that along with a slowing of conduction velocity, fundamental changes in M-wave shape were identified (Brody *et al.*, 1991). They concluded that frequency changes were caused by more than just a slowing of conduction velocity and that pH was not the only causative factor. Other authors have suggested that other mechanisms may play a role in these spectral shifts, such as the derecruitment of fatigable motor-units (Asmussen, 1979) or low frequency motor unit synchronisation (De Luca & Erim, 2002; Boonstra *et al.*, 2008). Fatigue induced reductions in the EMG frequency spectrum may also be due to centrally mediated mechanisms (Enoka & Stuart, 1992). During sustained fatiguing contractions, there is a reduction in both the muscle fibre relaxation rate and the stimulus frequency necessary to elicit a given contractile force (Binder-Macleod & Guerin, 1990). This association of a concurrent decline in relaxation rate and motor neuron discharge rate has been referred to as "muscle wisdom" (Marsden *et al.,* 1971 cited in Gandevia, 2001). This was first observed by Marsden *et al.* in 1971 who by blocking the proximal *Ulnar* nerve, were able to observe the firing of individual motor units of the first *dorsal interosseous* muscle. They reported progressive decreases in firing rate which matched the altered contractile properties of the fatigued muscle. The term "muscle wisdom" was coined, to describe the strategy utilised by the CNS to optimise force production and ensure economical activation of fatiguing muscle (Marsden *et al.,* 1971 cited in Gandevia, 2001; Allen *et al.*, 2008). It is possible that muscle wisdom could also manifest itself as a progressive reduction in spectral EMG variables recorded from the fatiguing muscle. However, Gandevia (2001) cautioned against interpreting frequency shifts as being a root physiological cause of fatigue; "Changes in the frequency spectrum of the EMG accompany muscle fatigue, but they do not definitively cause it at a peripheral level, nor do they necessarily signify altered neural drive".

The EMG frequency spectrum is generally described either in terms of a median frequency (MF), or mean power frequency (MPF). Changes in these frequency variables over time are often used as a quantitative measure of neuromuscular fatigue (De Luca, 1997). The median

frequency (MF) is defined as the frequency that splits the power spectrum of the EMG in half (Bilodeau *et al.*, 1997). The mean power frequency is defined as the weighted average frequency of the power spectrum, where each frequency component is weighted against its power. Slopes of MF, MPF and average EMG (AEMG) amplitude are often used to describe shifts in these variables which may be associated with fatigue.

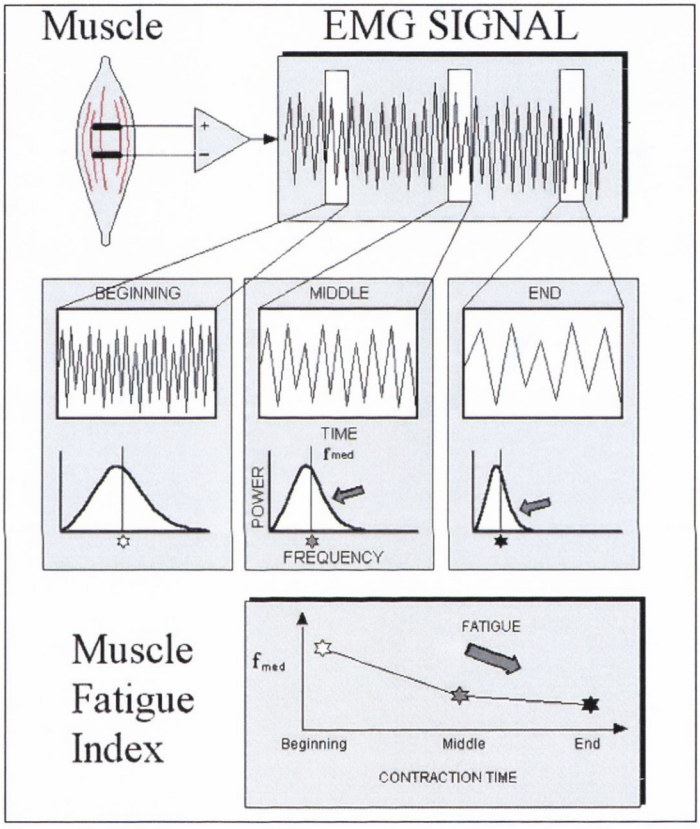

Figure 1.3: A diagrammatic explanation of the spectral modification which occurs in the EMG signal during sustained contractions. The muscle fatigue index is represented by the median frequency or mean power frequency of the spectrum (extract from De Luca, 1997).

1.2.3: Physiological mechanisms of peripheral muscle fatigue

Skeletal muscle contractions are activated by complex pathways which start in the motor cortex and lead to excitation of motor neurons in the spinal chord. The axon of the lower motor neuron carries the action potential to the neuromuscular junction of all muscle fibres

innervated by it, leading to the depolarisation of the muscle fibre and subsequent excitation-contraction coupling. The processes arising in the spinal chord and above are classified as central, whereas the processes occurring in the peripheral motor neuron, neuromuscular junction and the muscle itself are classified as peripheral. Therefore muscle fatigue can arise from both central and peripheral mechanisms. While there is unquestionably a central contribution to fatigue, the mechanisms surrounding it remain relatively unclear (Asmussen, 1979; Gandevia, 2001; Rasmussen *et al.*, 2007). It is universally accepted however, that a large proportion of muscle fatigue is due to peripheral mechanisms, many of which have been studied in detail through *in-vitro* and *in-vivo* muscle experimentation (Allen *et al.*, 2008). Asmussen's early works revealed two different peripheral sites susceptible to fatigue: the "transmission mechanism" (neuromuscular junction, muscle membrane and sarcoplasmic reticulum) and the "contractile mechanism" (muscle filaments) (Asmussen 1934 cited in Asmussen 1979). In either of these mechanisms, alterations in metabolite concentration can ultimately lead to decreasing force generating capacity.

It is now generally accepted that the transmission mechanism contributes little to the development of peripheral fatigue (Merton *et al.*, 1981 cited in Bigland-Ritchie & Woods, 1984). The traditional explanation for the contractile mechanism of peripheral fatigue is that a build-up of intramuscular lactate and H^+ ions causes impaired function of the contractile protein complex between actin and myosin (Fitts & Metzger, 1988 cited in Allen *et al.*, 2008). Accumulation of hydrogen ions has been shown to impair excitation-contraction coupling through inhibition of the sodium/potassium ATPase of the sarcolemna, the calcium ATPase of the sarcoplasmic reticulum and the myosin ATPase involved in actin-myosin interaction (Green & Patla, 1992). Other metabolites that have been proposed to interfere with actin-myosin coupling are P_i, K^+ and Mg-ADP (Edmans & Lou, 1990; Allen *et al.*, 2008). Myosin-actin cross bridge cycling converts ATP into ADP and P_i in order to achieve contractile force. Several *in-vivo* studies have shown that in the presence of high intramuscular [P_i], the rate of cross-bridge cycling is impaired, resulting in a reduction in muscle force generating capacity (Pate & Cooke, 1989; Millar & Homsher, 1990). In addition, P_i has been shown to impair Ca^{2+} re-uptake via inhibition of calcium ATPase (Millar & Homsher, 1990). Reactive oxygen species such as hydrogen peroxide (H_2O_2),

superoxide ($O_2^{\bullet-}$) and hydroxyl radicals ($OH^{\bullet}$) have also been shown to affect both Ca^{2+} sensitivity at Troponin C and Ca^{2+} release and re-uptake from the sarcoplasmic reticulum, thus further impairing muscle function (Allen *et al.*, 2008). During continual depolarisation of muscle fibres, there is substantial leaking of K^+ out of and Na^+ into the muscle cell. This has the effect of reducing action potential propagation both along the muscle fibre surface and down the T-tubules to the sarcoplasmic reticulum (Allen *et al.*, 2008). During fatiguing contractions, the rate at which metabolites (O_2, CO_2 and lactate) can be transferred to and from the muscle is of great importance. If skeletal muscle blood flow is impaired for any reason, homeostatic intramuscular metabolite concentrations cannot be maintained and function will inevitably become impaired (Allen *et al.*, 2008). Reductions in skeletal muscle blood flow and availability of O_2 can therefore be a significant factor in muscle fatigue. This is especially true during sustained isometric contractions (Allen *et al.*, 2008)

In general, peripheral muscle fatigue is resultant from several mechanisms including direct inhibition of myosin-actin cross bridge cycling, reduced Ca^{2+} release from the sarcoplasmic reticulum, reduced Ca^{2+} re-uptake via calcium ATPase, reduced muscle fibre and t tubule excitability, reduced voltage sensor activity, reduced blood flow and availability of O_2. The combination of all of these processes can impair the contractile properties within the fibre, thus requiring the central recruitment of additional fibres if complete exhaustion is to be avoided

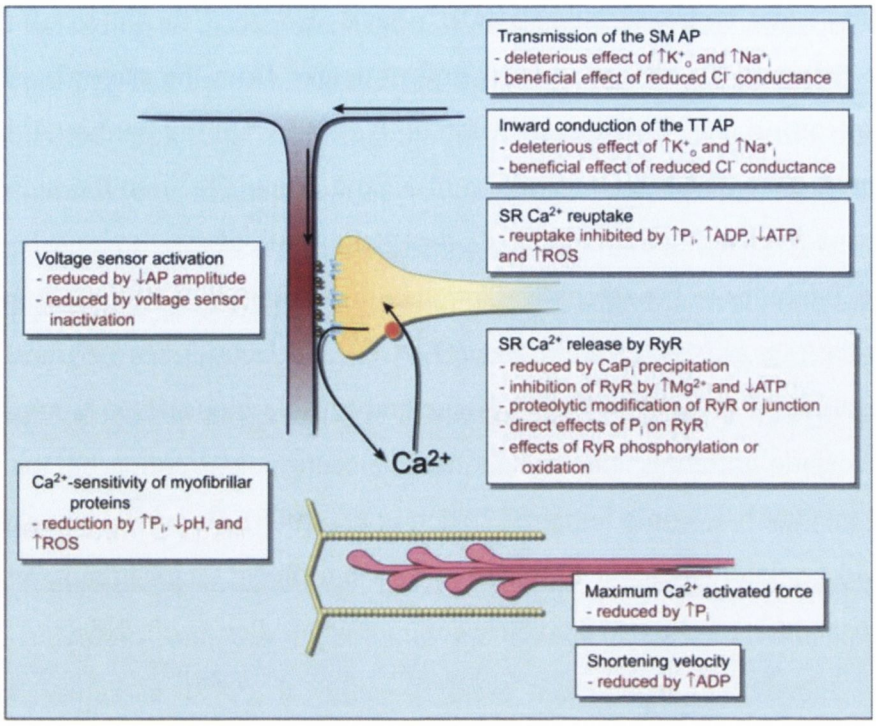

Figure 1.4: Diagram illustrating the major mechanisms that contribute to peripheral muscle fatigue (adapted from Allen 2008). Heading in each box identifies subcellular function, and the subsequent list indicates cellular changes occurring during fatigue that influence the subcellular function. (SM, surface membrane; TT, t-tubule; SR, sarcoplasmic reticulum; AP, action potential).

1.2.4: The aerobic-anaerobic transition

The term "anaerobic threshold" or "aerobic-anaerobic transition" was first used in 1964 to describe this critical point above which there is a disproportionate increase in plasma lactate concentrations (Wasserman & McIlroy, 1964). More recently, researchers have reported a dramatic increase in motor unit recruitment within the active skeletal muscle as the aerobic-anaerobic transition is passed (Moritani & De Vries, 1980). Since its discovery, the determination of the aerobic-anaerobic transition in athletes has become of critical importance as a performance predictor and in training prescription, particularly in endurance sports (Urhausen *et al.*, 2000). To this day, the physiological mechanisms underlying the aerobic-anaerobic transition are a cause of controversy amongst many research groups (Walsh & Banister, 1988).

1.2.5: The lactate threshold

The dramatic increases in circulating lactate which occur after the aerobic-anaerobic transition were first documented in detail in the early part of the 20th century (Hill & Lupton, 1923; Owles, 1930). This threshold has been defined in many ways since its introduction. Kindermann *et al.* (1979) set the lactate threshold as the workload corresponding to 4mmol.L^{-1} blood lactate accumulation and defined this arbitrary point as the onset of blood lactate accumulation (OBLA) (Kindermann *et al.*, 1979). Caiozzo *et al.* (1982) defined the lactate threshold as the point where there is a systematic increase in blood lactate concentration, while Brooks (1985) set the lactate threshold as the workload at which there is an abrupt increase in, or disproportionately high, non-linear increase in blood lactate concentration (Caiozzo *et al.*, 1982; Brooks, 1985). The lack of a unified definition for the lactate threshold extends further to a lack of agreement over the physiological mechanisms underlying the lactate threshold as it relates to the aerobic-anaerobic transition.

Initially, researchers hypothesised that an increase in lactate production as a result of local tissue hypoxia in the exercising muscles was the primary cause of the lactate threshold (Hill & Lupton, 1923; Wasserman & McIlroy, 1964; Wasserman *et al.*, 1973). Those supporting this hypothesis postulated that when oxygen perfusion to the skeletal muscle is not a limiting factor, all ATP was produced aerobically. Above a critical exercise intensity however, the rate of oxygen demand in the working muscles exceeded the rate of oxygen supply either due to increased metabolism or inadequate perfusion to the active motor units. This hypothesis has been challenged by several authors, primarily on the ground that subjects can exhibit a training induced reduction in lactate accumulation at any given absolute work rate with no net change in O_2 uptake (Holloszy, 1976; Ivy *et al.*, 1980).

Others have proposed that an increase in the rate of substrate utilisation through the glycolytic pathway leads to increased conversion of pyruvate to lactate (Gollnick *et al.*, 1974; Favier *et al.*, 1986; Gollnick, 1986). There is a finite rate of transfer of pyruvate into the mitochondria where it is subsequently broken down via the tricarboxylic cycle and oxidative phosphorylation. Once the exercise intensity exceeds the aerobic-anaerobic

transition and the demand for ATP continues to increase above this finite rate, excess ATP must be regenerated by increased substrate utilization via the glycolytic pathway. As a result of this increase in glycolytic flux, the excess pyruvate must be converted to lactate. Those supporting this hypothesis cite evidence of training induced increases in mitochondrial density reducing lactate concentrations at any given absolute work rate and hence shifting the lactate threshold to higher work levels (Favier *et al.*, 1986; Gollnick, 1986). Increased mitochondrial density provides a higher capacity for oxidative phosphorylation within working skeletal muscles.

A further mechanism which has been proposed is that an increased rate of lactate production linked with a decrease in the rate of removal is the primary mechanism underlying the lactate threshold (Brooks, 1985). Lactate is an excellent source of energy especially in tissues such as cardiac muscle, the liver and even skeletal muscle itself. A family of monocarboxylate (MCT) transporters, specifically MCT-1 and MCT-4 shuttle lactate across the mitochondrial and plasma membrane out into the circulation. Subsequently lactate can be taken up by other tissues where it can be used as a fuel source or even reconverted into glucose via gluconeogenesis (Brooks, 1986). A reduction in blood flow to tissues which actively remove lactate from the circulation would cause a net increase in blood lactate concentration. Donovan and Brooks (1983) hypothesised that as the aerobic-anaerobic transition is approached, there is a re-distribution of blood flow away from tissues such as the liver, and kidneys which are heavily involved in the uptake of circulating lactate (Donovan & Brooks, 1983). In addition, research has indicated that a saturation of uptake mechanisms within specific tissues can occur at the lactate threshold (Exton & Park, 1967; Naylor *et al.*, 1984). While there is a divergence of opinion on where the lactate threshold occurs during exercise and on the exact physiological mechanisms surrounding its occurrence, its existence has allowed testers to establish where the aerobic-anaerobic transition lies for individuals, through regular lactate estimation during incremental exercise. Consequently, lactate assessment during controlled laboratory based exercise protocols, and during training and competition in the field, has become one of the primary measurements used by the exercise physiologist.

1.2.6: The ventilatory threshold

While changes in respiratory exchange variables associated with the aerobic-anaerobic threshold have been known for many years (Owles, 1930), it was not until Wasserman *et al.* began using these gas exchange indices in their assessment of exercise performance in individuals with cardio-respiratory disease, that the potential use of respiratory variables as a means of identifying the aerobic-anaerobic transition became evident (Wasserman & McIlroy, 1964; Wasserman *et al.*, 1973). Since then, many investigators have used different gas exchange variables as a non-invasive means of detecting the aerobic-anaerobic transition. It has been shown that this transition can be determined as the work rate or volume of oxygen consumed ($\dot{V}O_2$) immediately preceding a non-linear increase in minute ventilation ($\dot{V}E$), volume of expired CO_2 ($\dot{V}CO_2$), ventilatory equivalent for O_2 ($\dot{V}E/\dot{V}O_2$), ventilatory equivalent for CO_2 ($\dot{V}E/\dot{V}CO_2$), and respiratory exchange ratio (RER) (Urhausen *et al.*, 2000). Several investigators documented that RER is the least sensitive of these gas exchange variables for the detection of the aerobic-anaerobic transition (Wasserman *et al.*, 1973; Davis *et al.*, 1976). In comparing four gas exchange variables, Caiozzo *et al.* (1982) reported that $\dot{V}E$ /$\dot{V}O_2$ was the most reliable and sensitive method of detecting the aerobic-anaerobic transition.

Regardless of what gas exchange variable is used to detect the aerobic-anaerobic transition, the physiological mechanisms underlying the principal remain the same. Due to its high pK, lactic acid is almost completely dissociated to lactate and hydrogen ions on formation within the muscle. Approximately 90-94% of the resultant hydrogen ions produced within the working muscles will immediately be buffered either by intracellular or plasma bicarbonate buffering systems (Wasserman *et al.*, 1986). The bicarbonate buffering system converts excess protons and bicarbonate into CO_2 and water (see Equation 1.1).

$$\mathbf{H^+ + HCO_3 <=> H_2CO_3 <=> CO_2 + H_2O}$$

Equation 1.1: Bicarbonate combines with excess protons to produce carbon dioxide and water. This bicarbonate buffering system is of critical importance in maintaining homeostatic pH within the body.

The resultant CO_2 produced via the bicarbonate buffering system is often referred to as "non-metabolic CO_2" (Anderson & Rhodes, 1989). Once the aerobic-anaerobic transition is passed, significant increases in lactic acid production will result in the liberation of large amounts of non-metabolic CO_2. These increases are detected by the peripheral chemoreceptors and cause a disproportionate increase in $\dot{V}CO_2$ and $\dot{V}E$ at what is known as the ventilatory threshold or V_T (Eston & Reilly, 2001). During incremental exercise to exhaustion, often 2 ventilatory thresholds will be detected. The first ventilatory threshold (V_{T1}) is best seen as the first breakpoint or non-linear increase in $\dot{V}E/\dot{V}O_2$ (Caiozzo *et al.*, 1982). This non-linear increase in minute ventilation occurs as a direct result of the increases in non-metabolic CO_2 production. A second ventilatory threshold (V_{T2}) can be seen as the first non-linear increase in $\dot{V}E/\dot{V}CO_2$ (Beaver *et al.*, 1986) or as a second breakpoint in $\dot{V}E/\dot{V}O_2$. V_{T2} occurs at higher exercise intensities when increased metabolic acidosis forces the body to resort to isocapnic buffering. At this point $\dot{V}E$ increases at a faster rate than $\dot{V}CO_2$. This takes place as a means of achieving respiratory compensation for the increased rates of metabolic acidosis occurring in the working muscles (Eston & Reilly, 2001). Since its initial discovery, the ventilatory threshold has become the primary non-invasive determinant of the aerobic-anaerobic transition.

1.2.7: Neuromuscular fatigue at the aerobic-anaerobic transition

The relationship between the aerobic-anaerobic transition and associated changes in electromyographic (EMG) signals recorded from the working muscles was first proposed by Moritani and De Vries (1980). Since then, non-linear increases in the amplitude of integrated or root mean squared EMG at the aerobic-anaerobic transition have been observed by several authors (Chwalbinska-Moneta *et al.*, 1998; Lucia *et al.*, 1999; Jurimae *et al.*, 2007). More recently, it has been shown that abrupt changes in spectral EMG variables such as median frequency (MF) also occur at the aerobic-anaerobic transition (Hug *et al.*, 2003). Both increased amplitude and decreased MF of the recorded EMG signal have long been established as reliable non-invasive determinants of neuromuscular fatigue (De Luca, 1997). As such, the abrupt changes in amplitude and frequency of the EMG signal

which occur at the aerobic-anaerobic transition have become known as the neuromuscular fatigue threshold or EMG threshold (T_{EMG}) for short.

The physiological mechanisms underlying T_{EMG} are still debated. Some authors argue that the changes in the myoelectric signal are entirely a result of local intramuscular changes which occur at the aerobic-anaerobic transition. Brody *et al.* (1991) documented an *in-vitro* study of the effect of pH changes on the myoelectric signal of muscle preparations and showed that increased acidity within the muscle resulted in decreased conduction velocities and MF along the active motor units. It was hypothesised that increased proton concentrations both intramuscularly and at the neuromuscular junction were delaying signal propagation both synaptically (at the neuromuscular junction) and post-synaptically (at the muscle fibres themselves). Thus intramuscular proton accumulation can be seen to alter the muscle fibre contractility and the recorded EMG signal via delayed propagation of the signal and by competitively inhibiting actin and myosin coupling (Brody *et al.*, 1991).

Other authors (Moritani & De Vries, 1980; Bigland-Ritchie *et al.*, 1986; Mateika & Duffin, 1994a) argue that central control of motor unit recruitment may contribute along with local changes within the active motor units. An increase in EMG activity has been shown to reflect the recruitment of additional motor units and an increase in motor unit rate coding to compensate for the deficit in contractility resulting from impairment of fatigued motor units, as the strength of a muscle contraction increases (Moritani & De Vries, 1980). Increased levels of muscle metabolites such as K^+ and H^+ ions has been shown to stimulate group III - IV muscle afferents, with activation of these muscle afferents eliciting an inhibitory effect on α-motor neurons thus leading to reduced motor output (Bigland-Ritchie *et al.*, 1986). Therefore, lactic acid can elicit central inhibition of motor unit recruitment via a sensorymotor feedback loop. Other authors have postulated that rapid central recruitment of fast-twitch Type II fibres at exercise intensities greater than the aerobic-anaerobic transition may potentiate the EMG threshold and indeed be a fundamental cause of the lactate threshold (Gollnick *et al.*, 1974; Baldwin *et al.*, 1977). Mateika and Duffin (1994) suggested that this threshold may be mediated by an increase in neural activity originating from higher motor centers or the exercising limbs, induced in response to the need to progressively

recruit fast twitch muscle fibers as exercise power output is increased and as individual muscle fibres begin to fatigue (Mateika & Duffin, 1994b, a).

Over the past 30 years there have been many studies examining the relationship between the aerobic-anaerobic transition and recorded EMG variables. Positive correlation between the breakpoint in EMG amplitude and the lactate threshold (Nagata *et al.*, 1981; Mateika & Duffin, 1994b; Chwalbinska-Moneta *et al.*, 1998), and correlation between EMG and the ventilatory threshold (Moritani *et al.*, 1993; Lucia *et al.*, 1999; Hug *et al.*, 2004) have been reported. More recently, positive correlation between spectral EMG measures, and the lactate threshold (Farina *et al.*, 2007) and ventilatory threshold (Hug *et al.*, 2003) have been reported. However, several authors (Viitasalo *et al.*, 1985; Taylor & Bronks, 1994) have published contradictory literature, reporting no correlation between EMG measures, and the aerobic-anaerobic threshold. Taylor and Bronks (1994) reported no signs of a breakpoint in EMG activity during incremental treadmill running, while Viitasalo *et al.* (1985) showed only linear changes in both spectral and amplitude based EMG variables during incremental cycling ergometry.

1.3: BIOMECHANICAL TASK SPECIFICITY

1.3.1: Ergometer exercise: Problems and analysis

The diversity of competitive sports which humans undertake highlights how the entire spectrum of our physical capability is exploited to perform an ever expanding range of tasks. Each sport involves the performance of a complex series of motor skills in a precise series of actions, in order to achieve the desired outcome. However, far from excelling in a wide range of skills however, it has long been known that elite athletes hone a specific set of physiological, psychological and biomechanical tools necessary to excel in their chosen discipline (Dal Monte & Lupo, 1989). The recognition of this specificity of fitness and performance in elite sport has led to the development of a range of specific ergometers appropriate to the demands within each sport (Reilly & Lees, 1984). Ergometers are primarily designed to simulate the biomechanical movements and physiological stresses associated with a specific sport, allowing exercise to be performed in a controlled indoor environment (Dal Monte *et al.,* 1988).

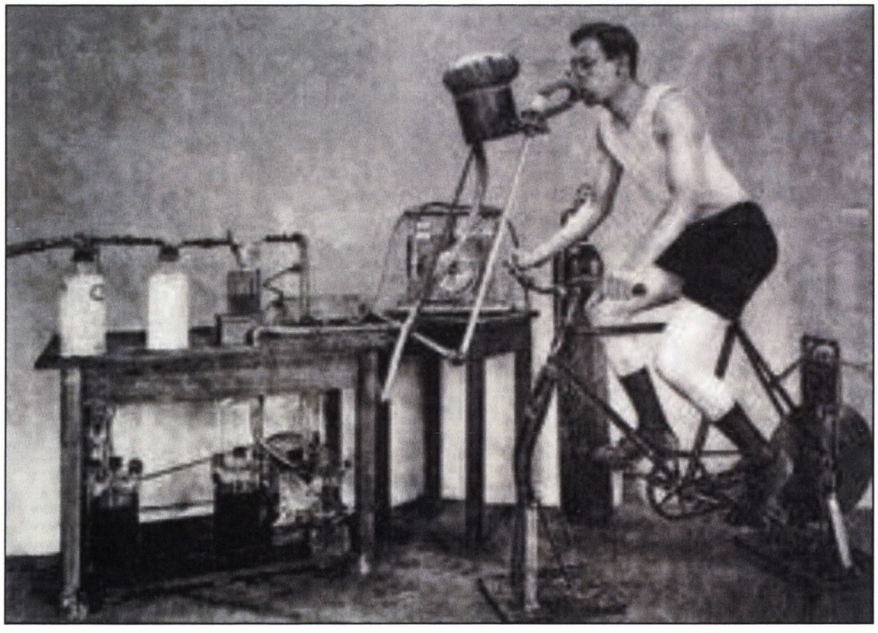

Plate 1.2: Early development of cycle ergometer testing (image location: http://www.exrx.net/Testing/YMCACycleTest.htm)

In the past, general field tests such as the Cooper 12 min run test and maximum weight lifted were used to assess endurance and muscular strength and for monitoring training improvements (Reilly, 1981). However, the necessity to obtain reliable and meaningful data for both the researcher and athlete led to the development of laboratory based testing protocols, which utilised specific ergometer exercise in order to simulate the sporting demands as accurately as possible (Dal Monte *et al.*, 1988). Dal Monte and Lupo (1989) recommended five parameters which should be considered with respect to sports specific laboratory based testing;

1) The specific action involved.
2) The position in space.
3) The movement frequency in competition.
4) The work load and exercise intensity involved.
5) The test duration necessary to simulate the energy sources utilised in competition.

(Dal Monte & Lupo, 1989)

Considering these parameters, it is clear that a quantitative assessment of task specificity is required, in order to validate sports specific ergometer testing protocols. The term "task specificity" refers to the accuracy with which an ergometer simulates the demands of the specific sport. While there is a substantial body of research assessing ergometer task specificity, much of this literature has compared the metabolic and physiological demands of the sport (Kenny *et al.*, 1995; Mitchell & Swaine, 1998; Van Someran *et al.*, 2000; de Campos Mello *et al.*, 2009). Kenny *et al.* (1995) compared the cardio-respiratory and physiological demands of sub-maximal cycle ergometry to field based cycling. Mitchell and Swaine (1998) compared on-water and on-ergometer kayaking at sub-maximal exercise intensities and reported significant differences in cardio-respiratory responses. Van Someran *et al.* (2000) subsequently reported contradictory findings of non-significant difference in cardio-respiratory response, comparing ergometer and on-water kayaking at maximal intensity. More recently, de Campos Mello *et al.* (2009) compared the energy system contributions of two rowing ergometer designs to the on-water scenario, concluding that

both ergometer designs underestimated the metabolic work which was performed during a maximal 2000m on-water race simulation (de Campos Mello *et al.*, 2009).

Van Someran *et al.* (2000) highlighted in their conclusions that while an ergometer may simulate the metabolic demands of a specific sport, biomechanical differences may still exist. Such biomechanical differences may have significant detrimental effects on the athlete, such as the increased risk of long term soft tissue damage (Bernstein *et al.*, 2002; Caldwell *et al.*, 2003) and the potential reinforcement of poor technical habits (Elliott *et al.*, 2001). It is therefore of great importance that biomechanical task specificity of the ergometer is assessed (Caldwell *et al.*, 2003; Nowicky *et al.*, 2005). Of the literature which has directly assessed ergometer biomechanical task specificity, the majority have used kinematic data (Swaine & Reilly, 1983; Lamb, 1989; Begon *et al.*, 2008) or a combination of kinematic and force data (Martindale & Robertson, 1984; Elliott *et al.*, 2001; Kleshnev, 2005) as a means of comparison. Swaine and Reilly (1983) compared stroke rates during maximal swimming in the water and on a biokinetic swim bench. The authors reported a high correlation (0.98) between optimal stroke rate during water swimming and stroke rate at $\dot{V}O_2$peak during swim bench trials (Swaine & Reilly, 1983). Lamb (1989) compared the kinematics of five body segments during ergometer and on-water rowing and reported that while the upper arm and forearm segments exhibited significant differences at the start and finish of each stroke, no significant differences in kinematic data were observed in any other segments (Lamb, 1989). Begon *et al.* (2008) compared 3D kinematic data obtained during kayak ergometry and compared it to on-water kayaking. While the authors reported closely matched 3D kinematics of the upper body segments, it is worth noting that their on-water scenario involved tethered kayaking in a pool (Begon *et al.*, 2008). It is unlikely that this condition truly reflects the biomechanics of flat-water kayaking. Both Elliott *et al.* (2001) and Kleshnev (2005) compared stroke force and kinematic data recorded during ergometer rowing and on-water sculling. Martindale and Robertson (1984) compared mechanical energy produced during rowing on a Gjessing ergometer and in a single scull and reported significant differences in the exchange of energy between the two conditions. While Elliott *et al.* (2001) reported force curves that were similar in shape between the two conditions, Kleshnev (2005) reported higher peak forces during ergometer rowing. Both authors did

however, report similar body positions and movement kinematics throughout the stroke cycle, when comparing on-water and on-ergometer rowing.

A novel approach to the assessment of task specificity was published by Nowicky *et al.* (2005). This approach utilised EMG as a means of comparing muscle activity patterns in contrasting conditions. While Nowicky *et al.* (2005) used this method to compare two contrasting rowing ergometer designs, the authors concluded that this approach may also be used to assess the accuracy with which rowing ergometers simulate the on-water scenario (Nowicky *et al.*, 2005). This approach provides useful insight into the internal mechanisms involved task performance and hence may highlight biomechanical differences not otherwise observed using conventional approaches. For example, a joint may consistently return to 90° flexion at the end of a movement cycle, regardless of test condition. Kinematics would therefore suggest the movement patterns are the same at this point. However, forces not visible to the observer, may be acting upon the joint in one condition and not in the other. These forces must be counteracted by increased muscle recruitment, in order to maintain joint position. While the external joint angle remains unchanged, internally the muscle recruitment patterns are entirely different between conditions. Combining the use of EMG, with kinematic and force data may therefore provide a complete biomechanical assessment of ergometer task specificity.

1.3.2: The physiology and biomechanics of kayaking

Flat-water kayaking has been an Olympic discipline since the Berlin Games of 1936. Races have typically been run over 1000 and 500m distances, however the introduction of 200m racing to the London 2012 Olympic programme at the expense of the 500m event will be a novel change to flat-water kayak racing. In the last 30 years, the physiological requirements for top performance in this sport have been studied by several authors. Elite kayakers have been reported to possess a total body maximal oxygen uptake in the order of 5.30-5.60 $L.min^{-1}$ (Tesch *et al.*, 1976) measured using treadmill running. When comparing $\dot{V}O_2max$ attained during paddling to data recorded during treadmill running, kayaking attained values in the region of 85-90% of that utilised during the whole body treadmill exercise (Tesch *et al.*, 1976). More recently, $\dot{V}O_2max$ data of 4.8 ± 0.6 (Fry & Morton, 1991), 4.1 ± 0.5 $L.min^{-1}$

(Van Someran *et al.*, 2000) and 5.1 ± 0.6 $L.min^{-1}$ (Fleming *et al.*, 2007), have been reported. These data clearly indicated that a high aerobic component is required for flat-water kayaking. The high aerobic adaptation elite kayakers undergo was further demonstrated from muscle biopsies attained from arm and shoulder muscles. Tesch (1983) reported 73% Type I slow oxidative fibre composition in the *Anterior Deltoid* musculature of elite male kayakers specialising in 1000m events. In contrast, the optimum ratio appears to be lower for sprint specialists (Cox, 1992a), with reports of Type 1 fibre composition in the range of 45 to 50% in the *Anterior Deltoid* muscle of 500m specialists (Gollnick *et al.*, 1972).

While elite kayakers show significant aerobic adaptations, they also have very high anaerobic power capacity. Tesch (1983) reported that male kayakers had significantly greater upper-body anaerobic capacity when compared with body builders or water skiers. The mean peak torque for isokinetic shoulder extension was significantly higher in kayakers (58±3 Nm) compared to bodybuilders (46±4 Nm). Significantly higher resistance to fatigue was also reported during continuous arm cranking exercise (24±4 compared to 44±4 % power reduction, Tesch, 1983). The need for anaerobic energy production during competitive kayaking was inferred by the high blood lactate data observed following racing, post-exercise blood lactate concentrations of 14.0±4.1 $mmol.L^{-1}$ have been recorded in elite kayakers (Tesch, 1983, 1984). To conclude, the two defining physiological characteristics reported for elite flat-water kayakers are high aerobic adaptations in the cardiovascular and skeletal muscle systems, in conjunction with adaptations towards increased lactate tolerance and anaerobic power capacity in the upper body skeletal musculature. It should be noted that the introduction of 200m event in the 2012 Olympic programme will undoubtedly alter the physiological profile of the elite flat-water kayaking population over the next decade. Athlete specialisation in either the longer (1000m) or shorter (200m) distance has already begun and will most likely result in two contrasting physiological groups.

The biomechanics of flat-water kayaking have been studies by many authors over the past 30 years (Mann & Kearney, 1980; Pflagenhoef, 1980; Logan & Holt, 1985; Kendal & Sanders, 1992; Sanders & Kendal, 1992; Sanders & Baker, 1998; Trevithick *et al.*, 2007). Since the introduction of the "wing" paddle in the early 90's, flat-water kayaking technique

has evolved significantly. As a result, earlier biomechanical studies into flat-water kayak technique are for the most part limited in relevance to generalised body segment movements. The flat-water kayaking stroke cycle is a contra-lateral movement cycle involving coordinated upper body movements of both the right and left side (Cox, 1992b). In describing the kayak stroke cycle, it is convenient to divide it into 4 distinct phases (a draw and transition phase for both right and left sides). The cycle begins when the paddle blade enters the water. The entry point initiates the draw (or pull) phase, where the paddle is pulled through the water. The draw phase ends when the paddle blade is removed from the water (exit). Once the paddle exits the water, a transition (or recovery) phase occurs where the kayaker moves from the end of one draw phase to the start the draw phase on the opposite side. Once the opposite draw phase is completed, a second transition phase brings the kayaker back to the original side for the onset of the next stroke cycle. One complete kayak stroke cycle involves the completion of both a right and left stroke. The ratio of draw to transition time has been assessed by several authors. Mann and Kearney (1980) reported a mean draw/transition ratio of 71.3% however Sanders and Kendal (1992) reported a lower ratio of 67%. Stroke rates during competition have been reported to be as high as 96 ± 5 strokes.min^{-1} using wing paddles, however during maximal sprints, the stroke rate can increase to greater than 120 strokes.min^{-1} (Sanders & Kendal, 1992).

Plate 1.3: Current Olympic champion Tim Brabants completing the draw phase of the kayak stroke cycle. (Image location www.guardian.co.uk/sport/2010)

Limited research assessing the contribution of muscle activity to the kayak stroke cycle have been published (Capousek & Bruggemann, 1990; Trevithick *et al.*, 2007). Capousek and Bruggemann (1990) used EMG analysis during kayak specific strength exercises and specific kayak movements performed in the laboratory to determine the most active muscles during the kayak stroke. Their data indicated that the *Anterior Deltoid* had the highest level of activation for the longest portion of the stroke. The *Upper Trapezius*, *Triceps Brachii* and *Rectus Abdominus* were also active during most phases of the stroke, but at a lower level relative to the *Anterior Deltoid* (Capousek & Bruggemann, 1990). More recently, Trevithick *et al.* (2007) assessed shoulder muscle recruitment patterns during kayak ergometry and correlated muscle activity to specific phases of the stroke cycle in *Subscapularis, Supraspinatus, Infraspinatus, Serratus Anterior, Rhomboid Major* and *Latissimus Dorsi* using fine-wire EMG and from *Medial Deltoid* and *Upper Trapezius*, using surface EMG. The authors hypothesised that the on-water scenario would elicit greater EMG activity from a number of the shoulder muscles recorded (Trevithick *et al.*, 2007). To date, no published data examining muscle recruitment patterns during on-water kayaking exist.

1.3.3: The physiology and biomechanics of rowing

The sport of rowing has been in existence for centuries (Halladay, 1990). It was first introduced to the Olympics at the 1900 Paris Games and has remained a part of the Summer Olympic programme ever since. At international standard, all races are competed on-water over a distance of 2000m (Soper & Hume, 2004). Competitive rowing consists of two contrasting styles, sculling (two oars) and sweep rowing (one oar). The physiological and anthropometric attributes of elite rowers have been studied for many years. Rowers are in general tall, heavy (excluding lightweight classes) and possess low percentage body fat. Hagerman *et al.* (1979) assessed more than 600 oarsmen and reported mean height of 192cm and body mass of 88kg. Mean percentage body fats of approximately 9% were also reported (Hagerman *et al.*, 1979). Maximal oxygen consumption in male rowers has been measured at 5.8 and 6.0 $L.min^{-1}$ for a paired crew during an on-water race simulation (DiPrompero *et al.*, 1971). More recently, mean ± S.D data for $\dot{V}O_2max$ was measured at 4.46 ± 0.33 and 4.48 ± 0.32 $L.min^{-1}$ for on-water and on-ergometer rowing (de Campos Mello *et al.*, 2009). Hagerman (1984) has highlighted however, that while outstanding $\dot{V}O_2max$ data have been

attained in rowing, the most impressive physiological attribute seems to be the rower's ability to sustain an extremely high percentage of their maximal O_2 consumption even after they have exceeded their anaerobic threshold (Hagerman, 1984). Anaerobic thresholds of 85 to 95% of $\dot{V}O_2max$ have been reported (Mickelson & Hagerman, 1982; Hagerman, 1984). This was confirmed more recently, when de Campos Mello *et al.* (2009) estimated the aerobic energy contribution during a simulated 2000m race was approximately 85% both on-ergometer and on-water.

Muscle samples obtained from the *Vastus Lateralis* muscle of elite rowers have revealed approximately 70% Type I fibres and the presence of very few Type IIb fibres (Mickelson & Hagerman, 1982; Hagerman & Staron, 1983). The results of these studies indicate that the relative proportions of fibre types in rowers are similar to those recorded in elite endurance athletes (Gollnick *et al.*, 1972; Saltin *et al.*, 1977). In addition to increased expression of Type I myosin heavy-chain isoforms, large cross sectional areas have also been reported for both Type I and II muscle fibres in rowers (Hagerman & Staron, 1983). Maximal isokinetic testing confirmed that rowers are capable of generating extremely high levels of force from their legs, but are not well adapted to high velocity actions (Hagerman, 1984). Knee extensor strength assessment in rowers produced greater isokinetic strength than elite swimmers, cyclists and canoeists at low joint velocities (0.5 to 2.1 $rad.s^{-1}$), but weaker at higher velocities (3.2 to 5.3 $rad.s^{-1}$). Hagerman (1984) suggested that the higher absolute strength was mostly due to rower's larger muscle mass, while the prominence of slow-twitch muscle fibres may explain the poorer performance at high velocities. To conclude, rowers exhibit physiological adaptations towards increased aerobic capacity and greater absolute leg strength. These adaptations are necessary due to the high aerobic demands of a 2000m race of 6 to 8 min in duration.

The biomechanics of rowing are in general, more simplistic than those of flat-water kayaking. Since the oars are fixed to the boat and the seat slides in a single axis along fixed rails, the degrees of biomechanical freedom are much lower than those experienced in kayaking. In addition, instead of contra-lateral movements of the right and left sides, the rowing stroke involves simultaneous activation of both sides. The rowing stroke cycle is

generally divided into two distinct phases, the drive and recovery (Soper & Hume, 2004). At the start of a stroke cycle, the rower's knees and hips are maximally flexed and their arm's fully extended in order to maximise stroke length at the oar entry. During the drive phase, rowers forcefully extend their knee and hip joints in order to pull the oar through the water whilst simultaneously moving back along the seat rails. The recovery phase involves removing the oar from the water, and subsequent flexion of the knees, hips and trunk in order to return to start position, ready for the next stroke cycle. Published literature assessing the biomechanics in rowing is substantial and has focused of many variables such as joint kinematics, stroke force and kinematics and muscle contribution to the stroke cycle (Soper & Hume, 2004). The most common variables assessed in rowing biomechanics are stroke rate, stroke length and drive: recovery ratio. Stroke rate has been shown to be significantly correlated to boat velocity (r=0.66), while stroke length is also correlated to both stroke rate and velocity (r=-0.99) (Martin & Bernfield, 1998). It has been suggested that the drive to recovery ratio is of most significance to boat velocity due to the effect of boat inertia during each recovery phase (Soper & Hume, 2004). Ideal rowing biomechanics maintains boat velocity as constant as possible throughout the stroke cycle (thus limiting the deceleration during recovery). Redgrave suggested a 1:2 drive to recovery ratio (or 0.5) in order to enable the rower to optimise the run of the boat during each stroke cycle (Redgrave, 1995).

Plate 1.4: Comparison of two man crews performing sweep rowing (Plate 1.4a) and sculling (Plate 1.4b). (Image location: www.carlosdinares.com, www.telegraph.co.uk/sport/olympics)

The muscle activity patterns involved in the body segment movements of the rowing stroke cycle have been examined by several authors over the past 20 years (Wilson *et al.*, 1988; Clarys & Cabri, 1993; Caldwell *et al.*, 2003; Nowicky *et al.*, 2005). Early studies identified the general patterns of muscle activity involved in the rowing stroke cycle (Wilson *et al.*, 1988; Clarys & Cabri, 1993). Wilson *et al.* (1988) reported the contribution of both knee and hip flexors and extensors to the development of the rowing stroke cycle. More recently, EMG has been used to compared activity patterns across ergometer design (Nowicky *et al.*, 2005) and to assess fatigue related changes in muscle activity during high intensity ergometer rowing (Caldwell *et al.*, 2003). Caldwell *et al.* (2003) identified fatigue induced increases in lumbar flexion and *Erector Spinae* activity during the course of a simulated 2000m ergometer rowing trial. Nowicky *et al.* (2005) reported no significant differences in hip and trunk muscle EMG and kinematics when rowing on two contrasting ergometer designs. To date no published literature examining muscle activity patterns during on-water rowing exist.

1.4: ELECTROMYOGRAPHY: CONCEPTS AND PROBLEMS

1.4.1: Factors influencing the EMG signal

De Luca (1997) stated that electromyography (EMG) is a seductive muse because it provides easy access to the physiological processes that cause the muscle to generate force and produce movement. While this ease of access is often considered one of EMG's advantages, it also remains one of the discipline's greatest pitfalls. EMG and more specifically surface EMG is too easy to use, and consequently too easy to abuse (De Luca, 1997). In an effort to standardise surface EMG methodology and thus minimise potential misuse in clinical and experimental settings, a European project on "Surface EMG for Non-Invasive Assessment of Muscles" (SENIAM) convened between 1997 and 1999, and published recommendations on the use of surface EMG (Hermens *et al.*, 2000). There are many physiological and non-physiological factors which must be fully taken into consideration before EMG signals can be produced with a high degree of confidence and fidelity (Farina *et al.*, 2004). The factors which combine to influence the detection and recording of EMG can be divided into extrinsic and intrinsic causative factors (De Luca, 1997). These causative factors each have a basic or elemental effect of the recorded EMG signal.

Extrinsic factors which influence EMG are those associated with the electrode structure and placement on the surface of the skin above the muscle. Such factors include;

1) The area and shape of the electrode detection surfaces (section 1.3.1.1).
2) The distance between electrode detection surfaces (section 1.3.1.2).
3) The location of the electrode with respect to the innervation zones and the myotendinous junction (section 1.3.1.3).
4) The location of the electrode on the muscle surface with respect to the lateral edge of the muscle (section 1.3.1.3).
5) The orientation of the detection surface with respect to the muscle fibres (section 1.3.1.4).

(Basmajian & De Luca, 1985; De Luca, 1997)

1.4.1.1: Area and shape of sensor

The area and shape of the recording surface is of importance as it determines the number of active motor units detected by virtue of the number of muscle fibres lying underneath the detection surface. An increase in the area of the detection surface will result in an increased number of active motor units detected. This can potentially reduce the fidelity of the EMG signal, as active motor units from neighbouring muscles may be recorded, leading to a phenomenon known as "muscle cross-talk". Muscle cross-talk has been defined as interference of EMG signals emanating from muscles other than the muscle directly under the recording electrode arrangement (Basmajian & De Luca, 1985).

1.4.1.2: The inter-electrode distance

The distance between electrode detection surfaces, or the inter-electrode distance (IED) has a significant influence on both the amplitude and power spectral density of the EMG signal. It is well known that a positive relationship exists between the IED and the absolute amplitude of the EMG signal (Roeleveld *et al.*, 1997; Hermens *et al.*, 2000; Beck *et al.*, 2005). However, there is a lack of agreement concerning to the range of IED's over which this positive relationship exists. Roelevand *et al.* (1997) reported that during sub-maximal isometric contractions, EMG amplitude increases with an increase in IED between 8 and 18mm. There was an increase to a lesser extent within the range 18 to 42mm, and EMG amplitude decreased within the range 42 to 84mm (Roeleveld *et al.*, 1997). More recent work by Beck *et al.* (2005) reported a positive relationship existing both in isokinetic and isometric actions, from 20mm up to 60mm. The hypothesis as to why this positive relationship exists, is that increasing the IED allows for detection of a larger number of active motor units deeper within the muscle (Solomonow *et al.*, 1990). Work by Fuglevand *et al.* (1992) and Roelevand *et al.* (1997) corroborated this hypothesis, reporting that increasing the IED increased the depth at which the electrodes detect action potentials, resulting in a greater pick-up volume from the muscle (Fuglevand *et al.*, 1992; Roeleveld *et al.*, 1997). Therefore an increase in IED and hence the pick-up volume, will increase the amplitude of the EMG signal.

While a positive relationship exists between IED and EMG amplitude, an inverse relationship exists with regard to spectral EMG variables such as MPF and MF (Zipp, 1978; Basmajian & De Luca, 1985; Elfving *et al.*, 2002). Increasing the IED has been shown to cause significant decreases in initial MF at fixed levels of contractile force in the *Erector Spinae* muscle (Elfving *et al.*, 2002) and for varying levels of isometric and isokinetic force in *Biceps Brachii* (Beck *et al.*, 2005). In order to understand the inverse relationship between IED and the EMG power spectrum, one must first understand that spectral EMG variables are a product of the conduction velocity (CV) along the muscle fibre. Since the EMG signal is a linear summation of motor unit action potentials that travel along and activate, skeletal muscle fibres (Basmajian & De Luca, 1985), the frequency of the EMG signal is intrinsically linked to the motor-unit CV. As with any measurement of velocity, the two determining factors are distance and time. In this case, velocity is equal to the time taken for an action potential to travel between two recording electrodes of fixed distance. Conversely, if CV is fixed, and inter-electrode distance is increased, action potentials will take longer to travel between the two recording electrodes, and the frequency of the EMG signal will decrease.

Recommendations as to the appropriate IED to use have been based on several factors, including the size of the muscle being examined, minimising the risk of cross-talk from adjacent muscles, and maximising the signal-noise ratio. Basmajian and De Luca (1985) suggested that greater selectivity is achieved by small IEDs due to reduced pick-up area and thus an IED of 10mm would minimise the risk of cross-talk to the greatest extent. However it has been argued that an IED of such small magnitude will produce a lower signal-noise ratio (Hermens *et al.*, 2000). It is clear that a compromise between selectivity and signal-noise ratio must therefore be reached. Based on this conclusion, SENIAM agreed that for large muscles an IED of 20mm would result in the greatest absolute EMG amplitudes values and therefore the highest signal-noise ratio, while relatively small muscles should be examined with an IED of less than one quarter the length of their muscle fibres (Hermens *et al.*, 2000). These recommendations were made on the basis that smaller muscles were more susceptible to muscle cross-talk due to the proximity of neighbouring muscles. As such, minimising cross-talk in smaller muscles was deemed to take priority over the signal-noise

ratio, while the opposite case was agreed for larger muscles where the risk of cross-talk is low (Hermens *et al.*, 2000).

1.4.1.3: Location of surface electrode

The location of the electrode with respect to innervations zones and myotendinous junctions influences both the amplitude and frequency characteristics of the EMG signal. Since EMG is a linear summation of motor unit action potentials (MUAP), it is important to understand where these action potentials come from. MUAPs travel from the site where they are innervated (at the motor end plates) to the tendons where they are attached, via the muscle fibres (De Nooij *et al.*, 2009). In muscles where the fibres run parallel, these motor endplates are generally situated closely together in one or more locations known as innervation zones. Several authors have stressed the need to avoid placing electrodes directly over innervation zones, since small shifts in surface electrodes relative to these zones have a major effect on EMG amplitude (Hermens *et al.*, 2000; Rainoldi *et al.*, 2000). Jensen *et al.* (1993) reported significant dips in the amplitude of EMG signals recorded directly over innervation zones. They explained their findings by illustrating that detection surfaces placed in opposite directions but at the same distance from a motor endplate will record similar waveforms. These similar waveforms are action potentials generated by the same motor endplate, propagating in different directions along the muscle fibres. After the subtraction necessary to obtain a bipolar derivation, almost no signal is left, resulting in a dip in the EMG amplitude (Jensen *et al.*, 1993). More recent work by Mesin *et al.* (2009) also outlined the need to avoid innervation zones due to their unstable effect on spectral and amplitude variables. They suggested that multichannel techniques and computer simulation to determine the location of innervation zones should be utilised to optimise electrode locations (Mesin *et al.*, 2009). The recommended location according to SENIAM is in the midline of the muscle belly between the nearest innervation zone and myotendinous junction (Hermens *et al.*, 2000).

The location of recording electrodes relative to the lateral edge of the muscle is of significant importance due to the influence of neighbouring muscles contributing to muscle 'cross-talk'. SENIAM recommendations with respect to electrode placement relative to

lateral edges of the muscle state that the sensors should be placed at the surface furthest away from the edges of the muscle so that the geometric distance to adjacent muscles is maximised (Hermens *et al.*, 2000). By placing the electrodes in the centre of the midline of the belly of the muscle being recorded, one is reducing the risk of muscle cross-talk, to the upper limits of experimental capability. A spatial filtering technique known as the "double differential technique" was developed by Broman *et al.* (1985) in order to detect and remove the appearance of muscle cross-talk from an EMG signal. This technique involves using a surface electrode with three detection surfaces equally spaced apart. Two differential signals are obtained, one from detection surfaces 1 and 2, the other from detection surfaces 2 and 3; then a differential signal is obtained from these two (Broman *et al.*, 1985). This differential technique significantly reduces the signal emanating from adjacent muscles but is not possible to achieve using conventional bipolar EMG electrodes (De Luca, 1997).

1.4.1.4: Orientation of recording electrodes

The orientation of surface electrodes with respect to muscle fibres is important as it not only affects the value of measured CV of action potentials and hence EMG spectral density, but also the amplitude of the EMG signal. The difference in voltage between two detection surfaces of a bipolar electrode at any given moment is what gives rise to the EMG signal amplitude. When detection surfaces are aligned parallel to the muscle fibres, MUAPs will travel down the fibres, directly past the first detection surface to the next. Any deviation from a parallel orientation will reduce the amplitude and potentially increase the power spectral density of the recorded EMG signal (Farina *et al.*, 2004). Due to differences in muscle shape, size, direction of fibres and articulation about joints, certain muscles appear more sensitive to electrode disorientation than others. For example, the *Trapezius* and *Biceps Brachii* muscles have been shown to be highly sensitive to electrode disorientation from the direction of muscle fibres (Jensen & Westgaard, 1997; Hermens & Vollenbroek-Hutten, 2004). However the same is not true for the *Vastus Lateralis* muscle, which has been reported to be less sensitive to electrode disorientation from the muscle fibre direction (Beck *et al.*, 2007). In addition one must also consider the type of muscle contraction which is being performed. Muscle fibre direction can change spatially within the muscle and dynamically during the course of a muscle contraction (Staudenmann *et al.*, 2010). Skeletal

muscle undergoes substantial three-dimensional changes in its geometry especially during dynamic contractions, due to the synchronous lengthening and shortening of large numbers of muscle fibres (Hodgson *et al.*, 2006). This will inevitably change the EMG electrode orientation with respect to the underlying musculature. While isokinetic and isotonic dynamic contractions result in greater changes in muscle morphology, it has been reported that isometric contractions at high levels of force (>80% MVC) can also cause a shift in muscle fibre orientation and the location of innervation zones within the muscle (Piitulainen *et al.*, 2009). While it is not possible to completely eradicate these potential shifts in orientation due to muscle fibre shortening and lengthening during the contraction, careful placement of electrodes in the appropriate location relative to the resting muscle fibre orientation and innervation zone location should minimise the effects of these shifts on the EMG signal to an acceptable level.

1.4.1.5: Intrinsic factors

In addition to the extrinsic causative factors which have been discussed, there are also a series of intrinsic factors which influence the EMG signal. De Luca (1997) described these factors as anatomical, physiological and biomechanical characteristics of the muscle which unlike extrinsic causative factors, are out of the control of the researcher due to limitations in current knowledge and available technologies (De Luca, 1997). In reporting the extraction of neural strategies from surface EMG, Farina *et al.* (2004) divided these intrinsic factors which affect the EMG signal into physiological and non-physiological factors, however for the purposes of this summery all intrinsic factors shall be dealt with as a single group. These intrinsic factors include;

1) The number of active motor units at any particular time of the contraction (1.3.1.6).
2) Fibre type composition of the muscle (section 1.3.1.7).
3) Blood flow in the muscle (section 1.3.1.7).
4) Muscle fibre diameter (section 1.3.1.8).
5) Depth and location of active fibres within the muscle with respect to the electrode detection surfaces (section 1.3.1.9).

6) The amount of subcutaneous tissue between the surface of the muscle and the electrode (section 1.3.1.10).

(Basmajian & De Luca, 1985; De Luca, 1997)

1.4.1.6: Number of active motor units recorded

The number of active motor units at any time during a contraction is of particular importance due to its direct contribution to the amplitude of the EMG signal. Skeletal muscle (as with smooth and cardiac muscle) obeys the all-or-none principle of motor unit recruitment. This principle states that once an action potential is propagated down a motor neuron, all muscle fibres innervated by that motor neuron will be stimulated and contract (Basmajian & De Luca, 1985). Conversely, if no action potential is propagated, no muscle fibres within that motor unit will contract. Another principal which skeletal muscles obey is Henneman's size principle which states that motor units are recruited in an orderly fashion from smallest to largest, as the contraction force increases (Henneman, 1957). Therefore as muscle contraction force increases, additional larger motor units are recruited via the all-or-none phenomenon and size principle, leading to an increase in detected EMG amplitude. The number of motor unit action potentials being recorded at any given time can also have another significant impact on the summated EMG signal amplitude (De Luca, 1997). It is generally accepted that the surface EMG underestimates the amount of motor unit activity, due to the loss of information that occurs when overlapping positive and negative phases of motor unit potentials cancel one another and reduce the amplitude of the signal (Figure 1.5). This concept is known as "EMG amplitude cancellation" and it has been reported that at maximal activation, amplitude cancellation can reach as high as 62% (Keenan *et al.,* 2004).

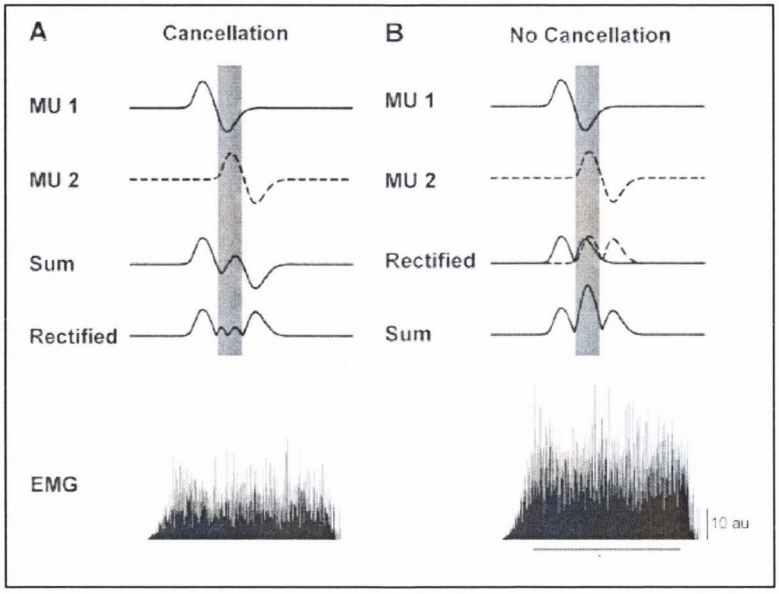

Figure 1.5: A demonstration of EMG amplitude cancellation. The summation of motor unit (MU) action potentials prior to rectification, leading to cancellation and significantly reduced EMG amplitude (adapted from Keenan *et al.*, 2004).

1.4.1.7: Fibre type composition and blood flow

The muscle fibre composition and the blood flow within the muscle are important factors in determining the fatigability of specific muscles. Human skeletal muscle is composed of three main fibre types, each determined by the particular myosin heavy chain isoforms present, and the degree of oxidative phosphorylation which takes place within the cells. Type I or slow oxidative skeletal muscle fibres are slow-twitch, low force, fatigue resistant muscle fibres. Type IIb or fast glycolytic skeletal muscle fibres are fast twitch, high force, and fatigable muscle fibres. In between these two isoforms is a third intermediate type, Type IIa or fast oxidative fibres. An increased proportion of Type II muscle fibres (especially type IIb) will lead to increased accumulation of lactate, and hence lactic acid which is one of the primary factors associated with muscle fatigue. Increased intramuscular lactic acid concentration will reduce the pH of the muscle interstitial fluid. Both the lactate molecule itself, and a reduction in pH can disrupt excitation contraction coupling (Fitts & Metzger, 1988; Favero *et al.*, 1997) and in addition, slow the conduction velocity along the muscle fibre (Brody *et al.*, 1991). Both these effects will play a role in altering both the spectral and amplitude content of the EMG signal. The amount of blood flow within the muscle will

determine the rate at which metabolites such as lactate are cleared from the muscle. A higher rate of clearance will allow the muscle to maintain normal contractile function for longer, thus improving fatigue resistance.

1.4.1.8: Muscle fibre diameter

Muscle fibre diameter (or cross-sectional area) influences both the amplitude and CV of the action potentials which constitute the EMG signal. Several authors have reported positive correlations between spectral EMG variables and muscle fibre cross-sectional area (CSA) (Kupa *et al.*, 1995; Gerdle *et al.*, 2000; Larsson *et al.*, 2006). However, there is a lack of agreement in the literature as to whether this correlation is uniform throughout the various muscle fibre types. Kupa *et al.* (1995) only detected a positive correlation between spectral variables and muscle fibre CSA in the *Extensor Digitorum Longus* muscle, which has a fibre composition of 99% Type II. In other muscles with a more heterogeneous mixture of fibre types, such a relationship did not exist (Kupa *et al.*, 1995; Larsson *et al.*, 2006). Hence, structure and capacity of the electrical conduction system seem to differ among the various muscle fibre types (Larsson *et al.*, 2006). This may be due to morphological differences between fibre types, such as the greater fibre diameters generally observed in Type II compared with Type I (Maughan & Nimmo, 1984). In addition, the varying number of muscle fibres within any given motor unit makes it difficult to distinguish muscle fibre type and diameter on the basis of CV (Farina *et al.*, 2004). While increased muscle fibre CSA has been shown to increase amplitude and frequency components of the EMG signal, the exact mechanism remains to be fully elucidated. What is clear however, is that muscle fibre CSA is a major contributing factor behind the waveform of the MUAP and its CV and hence on the EMG signal (Larsson *et al.*, 2006). This has been shown in mathematical modeling (Lindstrom *et al.*, 1970; Basmajian & De Luca, 1985) and more recently through human *in-vivo* studies (Gerdle *et al.*, 2000; Larsson *et al.*, 2006)

1.4.1.9: Depth and location of active fibres

As was discussed earlier (see extrinsic factors), the EMG surface electrode is more sensitive to the detection of motor units close to the surface of the muscle, however varying the IED can allow for greater recording depth or pick-up volume. The depth and location of active

fibres during a contraction is thus an important intrinsic factor which can influence the EMG signal. During sub-maximal contractions, not all motor units within the muscle will be recruited, and as such, variations in the depth and location of the active motor units will become an issue. This is especially important because it can dramatically affect the EMG signal characteristics (De Luca, 1997). As the distance between active fibres and the detection surface varies, two important concerns arise. Firstly, the spatial filtering characteristics change, thus altering the amplitude and frequency characteristics of the MUAPs that are within the pick-up volume of the electrode. Secondly, the movement of the electrode and the active fibres may be sufficient to place new active motor units within the detection volume and conversely, remove some other active motor units from it (De Luca, 1997). Thus, if muscle fibre length changes during a contraction (as is the case in dynamic contractions such as isokinetic or isotonic), electrode size must change accordingly in order to maintain appropriate spatial filtering. With current surface EMG techniques, it is not possible to change electrode shape and size during contractions. As such, signal stability can only be approached if the contraction remains isometric (De Luca, 1997). This issue limits the capability of EMG to determine the intensity of muscle contraction force during dynamic actions, but does not impact on its capacity to determine the timing of muscle activation (De Luca, 1997; Campanini *et al.*, 2007).

1.4.1.10: Subcutaneous tissue

The amount of tissue between the surface of the muscle and the recording electrode will affect the spatial filtering of the EMG signal. Such tissues include adipose tissue, skin, subcutaneous capillaries, sweat glands and hair follicles; however the adipose tissue layer is of greater importance to the signal than any other. The effect of fat layers on bipolar EMG recordings has been largely studied using models (Kleine *et al.*, 2000; Farina *et al.*, 2002). With regard to amplitude and spectral variables, the subcutaneous layer thickness reduced the amplitude of the propagating EMG components more than the spectral density, thus introducing a bias in favour of CV and other frequency estimates (Farina *et al.*, 2002; Cescon *et al.*, 2008). The subcutaneous tissue layer therefore causes overestimation of spectral variables and underestimation of amplitude variables through a reduction in the signal-noise ratio (Cescon *et al.*, 2008). This effect of subcutaneous tissue layer once again

raises the importance of spatial filtering in cases where this layer is large enough to have a perceived effect on the EMG signal. The double differential technique (as described earlier) is one such spatial filtering technique which has been shown to produce CVs closer to physiological values than a standard bipolar array.

When one considers the multitude of intrinsic and extrinsic factors which influence the EMG signal, it is clear that extracting meaningful quantitative data from the signal becomes more difficult than at first glance. These limitations in surface EMG techniques are often not appreciated, which sometimes lead to erroneous interpretations of results and conflicting reports in the literature (Farina *et al.*, 2004). So how can one attain meaningful results from surface EMG? Through careful consideration of the many factors which influence the signal, adherence to the recommendations of SENIAM in order to minimise the impact of many of these factors, and through appropriate signal processing and normalisation techniques (which will be dealt with in the next section), one can produce EMG signals which are representative of the physiological processes occurring within the muscle.

1.4.2: Normalisation of the EMG signal

In order to overcome the effect of both intrinsic and extrinsic factors influencing the EMG signal and to allow comparison between different muscles, across time, and between individuals, the EMG signal should be normalised (Yang & Winter, 1984; Mathiassen *et al.*, 1995; De Luca, 1997). This procedure involves expressing EMG data relative to a reference value obtained during standardised and reproducible conditions (Burden & Bartlett, 1999). The importance of normalisation has long been recognised by researchers and clinicians recording EMG data during dynamic tasks (Yang & Winter, 1983; Ounpuu & Winter, 1989; Hug & Dorel, 2009). EMG was first normalised during gait analysis in 1951 (Eberhart & Inman, 1951) using a method that divided each point which constituted the processed EMG by the peak data recorded from the same set of EMG data. This method which is subsequently referred to as the peak dynamic method is still widely used by electromyographers (Jacobson *et al.*, 1995; Nowicky *et al.*, 2005; Trevithick *et al.*, 2007). Dubo *et al.* (1976) introduced an equally popular method by which each EMG data point during the dynamic task was divided by the peak EMG recorded from an isometric maximal

voluntary contraction (MVC) recorded from the same muscle (Dubo *et al.*, 1976). The isometric MVC method is generally performed prior to the dynamic task and at a fixed joint angle, in the middle of the range of motion (Burden *et al.*, 2003). This method is favoured by many electromyographers analysing EMG from a variety of dynamic actions (Marsh & Martin, 1995; Hunter *et al.*, 2002; Diederichsen *et al.*, 2007). Yang and Winter (1984) proposed a previously unpublished method known as the mean dynamic method as part of a study comparing various EMG normalisation procedures used in gait analysis. This method, which is similar to the peak dynamic method, involves dividing each data point within the processed EMG by the mean value recorded from the same EMG. The mean dynamic method was shown to reduce inter-individual variability of EMG data relative to other normalisation methods (Yang & Winter, 1984; Shiavi *et al.*, 1987). As a result, Winter chose to use the mean dynamic method in subsequent studies (Winter & Yack, 1987).

There has been much debate as to the most appropriate method for normalising EMG attained during dynamic tasks, and to date there has been little or no agreement on the best normalisation procedure to be adopted (Hug & Dorel, 2009). The key criterion for selecting the best method of normalisation is its ability to reduce the inter-individual variability of the EMG data (Yang & Winter, 1984). However, several authors have warned that the reduction of inter-individual variability should not be at the expense of true biological variance within a group (Allison *et al.*, 1993; Knutson *et al.*, 1994).

The most common criticism of the mean dynamic method or the peak dynamic method is that neither has the potential to give any information as to the level of activity the muscle is performing at during a dynamic task (Burden *et al.*, 2003). The reason for this lies in the denominator being used to normalise the data. Since both these methods attain their denominator directly from the EMG data being analysed, no information as to the level of activation can be attained. The isometric MVC method does not suffer from this problem, and as such has the potential to reveal how active a muscle is during a dynamic task relative to a maximum reference value. Several authors however, have called into question the validity of normalising EMG data from a dynamic task, using a denominator attained from a non-dynamic task (Dubo *et al.*, 1976; Mirka, 1991). During a dynamic task, the muscle

being analysed is shortening and lengthening as it moves the joint through a range of angles. As a result, the number of active motor units within the range of the surface electrodes may change at any particular time during a dynamic contraction (De Luca, 1997). This is not true during an isometric contraction as there is no lengthening or shortening of the muscle fibres and no change in joint angle. Despite this criticism, both SENIAM and the Journal of Electromyography and Kinesiology have endorsed its use as a normalisation method (Burden, 2010). However, practical application of this method has shown that it can yield outputs in excess of 100%, especially during rapid, forceful contractions (Jobe *et al.*, 1984; Nowicky *et al.*, 2005; Burden, 2010). Jobe *et al.* (1984) reported EMG amplitude recorded from the Serretus Anterior during over arm throwing, to be 226% of that recorded during isometric MVCs. It has also been shown that EMG recorded during isokinetic MVCs of knee extensor muscles increases with increasing angular velocity during concentric contractions (Amiridis *et al.*, 1996). Nowicky *et al.* (2005) more recently reported that their attempts at normalising using the isometric MVC method were unsuccessful as higher peak EMG activity was recorded during the rowing movement compared with the reference isometric MVC manoeuvre. The EMG signal attained from an isometric MVC may not therefore represent the maximum activation capacity of the muscle (Burden & Bartlett, 1999). In a recent review of the limitations of EMG recording, Clarys *et al.* (2010), the authors suggested that the isometric MVC approach may be unreliable for several reasons;

1) Different maxima may be observed within the same subject repeating at different occasions.

2) Different maxima are observed at different angles of movement, both in eccentric and concentric movement modes.

3) The values measured during isotonic dynamic ballistic- complex sports movements (or heavy lifting tasks) may exceed the 100% MVC.

(Clarys *et al.*, 2010)

Several authors have published papers outlining an isokinetic MVC method of normalisation, in an attempt to attain a more biologically relevant denominator for normalising EMG during dynamic tasks. Kellis and Baltzopoulos (1996) attained significantly greater ($P<0.05$) normalised muscle activation amplitudes compared with the isometric MVC method, when both methods were used to normalise EMGs from knee flexors and extensors during isokinetic knee flexion and extension actions (Kellis & Baltzopoulos, 1996). However Burden and Bartlett (1999) did not show any significant differences between the isokinetic and isometric MVC methods of normalisation. More recently, Burden *et al.* (2003) concluded that the isokinetic MVC method should be rejected by electromyographers as it does not reduce intra- or inter-individual variability to any greater extent than existing methods, nor does it provide a more representative measure of muscle activation during gait than the isometric MVC method.

Considering all variations and limitations of normalisation techniques, Soderberg and Knutson (2000) recommended that the isometric MVC method be used for normalising kinesiological EMG data until a more appropriate means of normalisation was developed (Soderberg & Knutson, 2000). More recently a paper published by Rouffet and Hautier (2007) recommended a novel approach to the normalisation of EMG data attained during a cycling task. They advocated the use of a maximal torque-velocity sprint test in order to attain reference EMG data which were specific to the range of movements associated with cycling. This normalisation method, referred to as the torque-velocity method allows EMG to be normalised using a maximal reference data specific to the dynamic task being analysed. This normalisation method appears to provide an appropriate, task specific means of normalising EMG data (Rouffet & Hautier, 2008), however further research and methodological refinement is necessary before it can be fully accepted (Hug & Dorel, 2009).

1.4.3: Signal processing and spectral analysis

In order to attain meaningful data from the recorded EMG data, the signal must first be processed. Processing involves the filtering of undesired signals and the rectification of the differential EMG signal. The myoelectric signal is low in amplitude with respect to other

ambient signals (De Luca, 1997). As a result, it is necessary to record surface EMG using a differential electrode configuration (Basmajian & De Luca, 1985). A differential electrode configuration involves the use of two detection surfaces, with the resultant signals being subtracted from one another prior to amplification. De Luca (1997) stated that this differential electrode arrangement in effect acts as a high pass filter, removing many of the unwanted frequencies from the EMG signal. Further band pass filtering of the EMG signal is recommended between 20 and 500 Hz with a common mode rejection ratio (CMRR) greater than 80dB (De Luca, 1997).

Amplitude processing of raw EMG data generally involves rectification, amplitude estimation and smoothing of the differential signal. Several methods of estimation exist and there is no unanimous recommendation as to which method is most appropriate (De Luca, 1997). Root mean squaring (rms), integration and averaging after rectification are all common methods used. De Luca (1997) stated during voluntary elicited contractions, the rms technique may be more appropriate because it represents the signal power and thus has a clear physical meaning. However, it should be noted that the rms processed EMG signal is affected by both the number and frequency of the recruited motor units, without allowing any clear distinction between the two (De Luca, 1997).

Spectral EMG processing is mostly carried out using the Fourier transform. This is a mathematical process which decomposes a signal into its constituent frequencies. While Fast Fourier transforms (FFT) are almost exclusively used in the literature as an estimation of the EMG spectral composition, there is much variation in the FFT methods used to attain power spectral density from the EMG signal (Rainoldi *et al.*, 1999; Mathur *et al.*, 2005). Rainoldi *et al.* (1999) used an FFT window of 500ms with 0% window overlap. In contrast, Mathur *et al.* (2005) used an FFT window of 250ms with a window overlap of 300%. The first 250ms of each second of EMG data was therefore processed for spectral analysis. This protocol effectively eliminated 75% of the overall temporal data processed to frequency power spectra. In addition, variations in the windowing function may further compound variations. Several windowing functions such as Hamming, Hanning, Bartlett and Welch exist. In conclusion, while FFT methods are commonly used to estimate the power spectral density of

the EMG signal, there is no unanimous interpretation as to the most appropriate methods to utilise.

There has however, been some criticism of the FFT method of spectral EMG analysis (Bilodeau *et al.,* 1997; Kumar *et al.,* 2003). This criticism is based on the fact that Fourier transforms assume that the signal being process is stationary. A random process is considered stationary if the moments of its probability density function are time independent (Bilodeau *et al.,* 1997). In most studies where spectral analysis of EMG signals is performed, stationarity is seldom tested and more often presumed (Bilodeau *et al.,* 1997). During isometric contractions at a fixed force, where the muscle length and contractile force remain unchanged, stationarity can be assumed. Several authors have corroborated this assumption during isometric tasks (Popivanov & Todorov, 1986; Paiss & Inbar, 1987 cited in Bilodeau *et al.,* 1997) over a short time period (1 s). However, there is an inherent danger in assuming stationarity during dynamic or variable force contractions. There is a growing body of literature, arguing in favour of wavelet transforms as a more valid means of quantifying the spectral content of the EMG signal (Karlsson & Gerdle, 2001; Kumar *et al.*, 2003). The argument in favour of using wavelet transforms is that unlike Fourier transforms, they are time variant, and therefore can be used to process both stationary and non-stationary signals (Kumar *et al.*, 2003). In fact, Karlsson & Gerdle (2001) have reported that wavelet transforms had better accuracy and precision compared to FFT analysis of both stationary and non-stationary EMG signals.

1.5: AIMS AND OBJECTIVES

The aims and objectives of this study are twofold. The first set of aims deal with the subject of neuromuscular fatigue and its manifestation in both dynamic and static conditions. Identification of the neuromuscular fatigue threshold via EMG may provide a novel means of determining the aerobic-anaerobic transition, however there is little or no published data verifying that this fatigue related phenomenon occurs across the full spectrum of dynamic exercise conditions. In addition, it is possible that other factors, not directly related to muscle fatigue, such as training induced alterations in recruitment strategy may play a role in its manifestation. By assessing neuromuscular fatigue across a range of dynamic exercise conditions and by comparing neuromuscular fatigue between trained and untrained individuals during isometric fatiguing contractions, it is hoped to clarify some of the mechanisms through which these fatigue induced EMG changes appear. The aim therefore, is to assess and compare the appearance of T_{EMG} around the aerobic-anaerobic transition across a range of biomechanical tasks. An additional aim is to assess if training induced alterations to fatigue are identifiable using EMG.

The second set of aims deal with the assessment of biomechanical task specificity in both kayaking and rowing ergometry. There has been no definitive biomechanical comparison of on-ergometer and on-water exercise in either rowing or kayaking. Moreover, much of the published literature comparing the two is contradictory in its findings. While Mitchell and Swaine (1998) reported metabolic differences between kayak ergometry and the on-water scenario, Van Someran *et al.* (2000) observed no significant differences in cardio-respiratory responses. Elliott *et al.* (2001) concluded that the Rowperfect ergometer was similar in stroke kinematics to on-water sculling, however, Lamb (1989) reported significant differences in arm kinematics. In addition, little or no data exists with regards to muscle recruitment patterns during on-water exercise in either sport. The aim therefore, is to use the novel approach of EMG analysis, in combination with more common biomechanical measures, as a means of assessing the biomechanical task specificity of kayaking and rowing ergometers.

Chapter 2

General Methodology.

2.1: EMG recording

EMG recordings were made from the surface of the skin using an ME6000 system (MEGA Electronics, Kuopio, Finland). The ME6000 is a 4-channel, 14 bit AD converter with a common mode rejection ratio (CMRR) of 110 dB. Raw EMG signals were band-pass filtered between 8 and 500Hz, amplified and converted from analogue to digital at a sampling rate of 1 kHz. These data were transmitted from an integrated memory card (compact flash memory, 256Mb) to computer via wireless telemetry and subsequently synchronised to recorded 2D video kinematic data prior to storage for further processing and analysis (Megawin Version 2.3, MEGA Electronics, Kuopio, Finland).

Plate 2.1: ME6000 4-channel portable EMG recorder

All efforts were made to conform to the recommendations of SENIAM throughout EMG recordings (Hermens *et al.*, 2000). Prior to the application of electrodes, participants were seated and the recorded sites were shaved, abraded and cleaned with an alcohol swab in order to minimise skin impedance. The electrodes used throughout this study were 3M pre-gelled surface monitoring electrodes (Paediatric Red Dot, 3M, Minnesota, USA). This electrode consists of a circular Ag/AgCl disk of 8mm diameter beneath a pre-gelled sponge of 15mm diameter, all of which is embedded on an adhesive pad of 45mm diameter, see Plate 2.2a. Chapters of the adhesive pad were removed from a pair of electrodes in order to attain inter-electrode distance of 20 mm for each bipolar EMG sensor, see Plate 2.2b.

Bipolar sensors were applied to the midpoint of the palpated muscle belly approximately halfway between the motor endpoint area and the distal part of the muscle, longitudinally to the muscle fibres, with a fixed inter-electrode distance of 20mm maintained throughout. Anatomical positioning of the sensors for the most part adhered to the recommendations outlined by SENIAM (www.seniam.org). A full description of anatomical locations for each muscle assessed is provided in Appendix 2. Reference electrodes were placed over electrically neutral sites. When recording EMG data during dynamic exercise, recording electrodes and leads were fixed to the skin using elasticised strapping (Prowrap, Meuller Sports Medicine, Wisconsin, USA), to minimise potential movement artefacts. Surface electrode positions were marked with a permanent marker and digital photographs recorded to ensure correct electrode replacement during repeat visits.

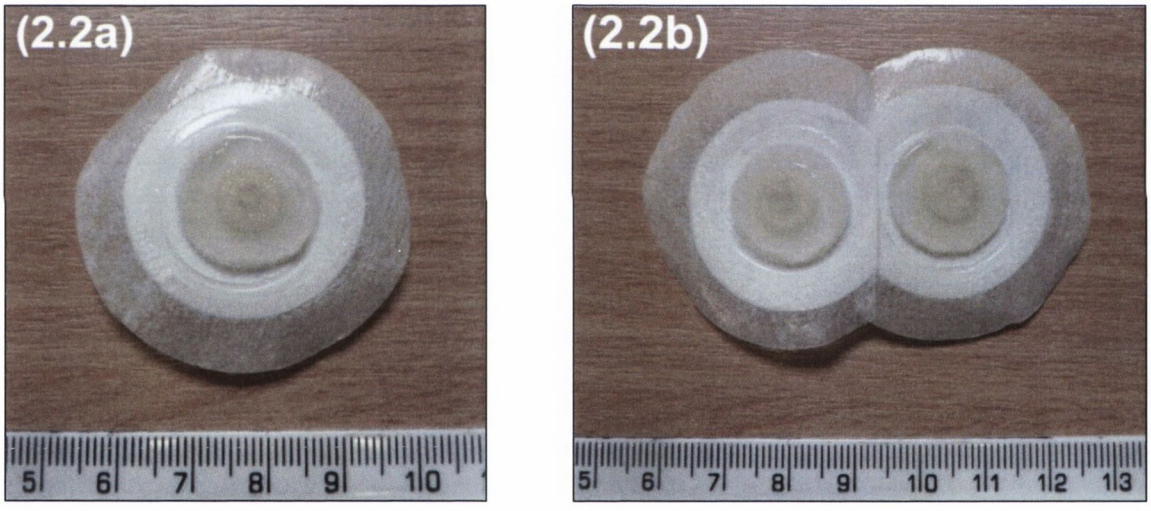

Plate 2.2: Shown are a single surface electrode (2.2a) and a pair of surface electrodes (2.2b) which have been modified and combined to produce a bipolar configuration with an IED of 20mm.

2.2: Synchronisation of EMG and 2D video data

In order to identify the temporal location of EMG activity within a specific movement, a record of the onset of each movement cycle was required. This was facilitated via the recording of 2D video kinematic data during all EMG recording phases, using a 50 Hz digital video camera (JVC, Yokohama, Japan) positioned orthogonally to the sagittal plane of the participant. Synchronisation of EMG and video data using an audio-sync trigger

(MEGA Electronics, Koupio, Finland) facilitated identification of the onset of each cycle within the EMG recording. The audio-sync trigger simultaneously transmitted a high frequency audio pulse to the video camera and a digital marker to the ME6000 system via wireless telemetry. Trigger pulses generated at the start and end of each recording phase were automatically aligned via the recording software (Megawin Version 2.3, MEGA Electronics, Koupio, Finland). The onset of the rowing stroke cycle was identified as the first video frame where rowing ergometer handle (on-ergometer) or oar handle (on-water) was moved away from the maximal forward position (see Plate 2.4a). The onset of the cycling revolution was defined as the video frame corresponding closest to top-dead centre (see Plate 2.4b). In order to identify the onset of the on-ergometer kayak stroke cycle, the height of the kayak seat above the water line was measured and used to mark a reference line (virtual water line) along the length of the ergometer relative to the seat. A paddle reference point was set up by adding an extension element to the end of the ergometer paddle shaft equating to each kayaker's actual paddle length (range 215 to 221cm, see Plate 2.3). Onset of stroke cycle was identified as the first video frame on paddle entry into the water (on-water trials) or the first video frame in which the paddle reference point crossed below the virtual water line (on-ergometer trials, see Plate 2.4c).

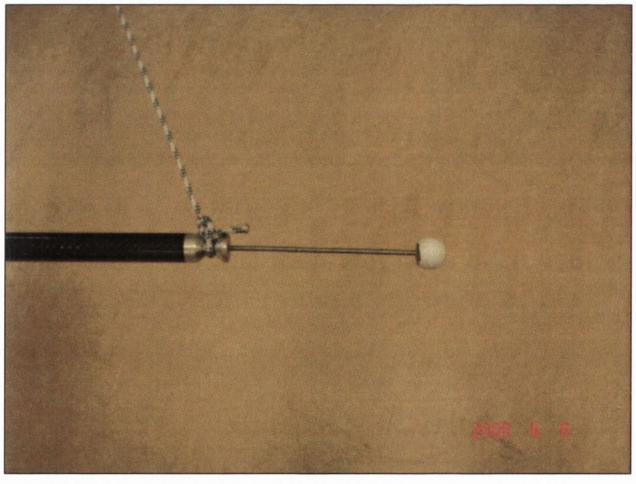

Plate 2.3: Adjustable extension which was added to the ergometer shaft, in order to match to on-water paddle length. The reference point on the extension was required to identify stroke cycle onset during ergometer kayaking.

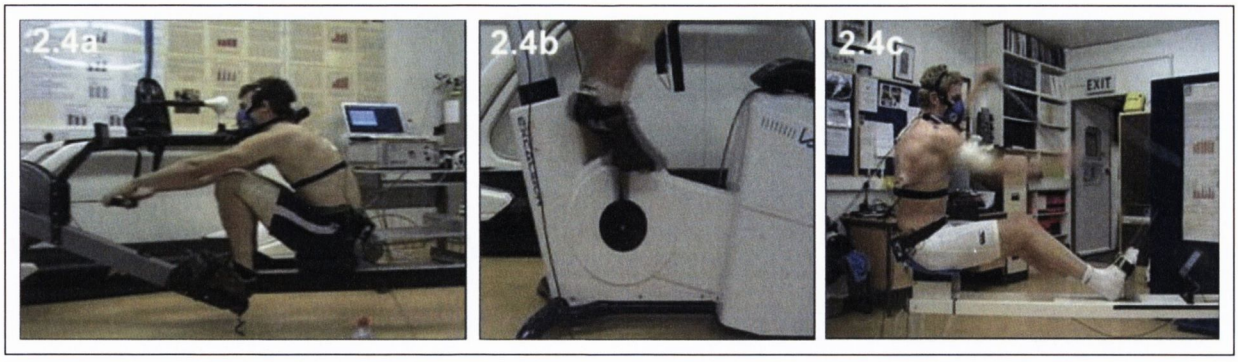

Plate 2.4: The onset of the movement cycle during ergometer rowing (2.4a), cycling (2.4b) and kayaking (2.4c) as identified from 2D kinematic data.

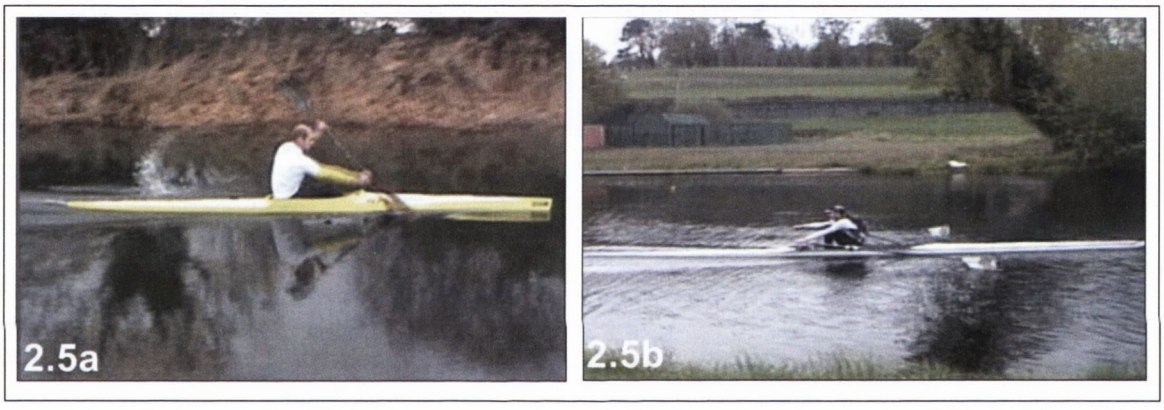

Plate 2.5: The onset of the movement cycle during on-water kayaking (2.5a) and rowing (2.5b) as identified from 2D kinematic data.

2.3: EMG amplitude processing

Unless stated otherwise, all EMG amplitude processing was performed was via root mean squaring (rms) of the raw EMG signal (see Equation 2.1 and Figure 2.1a). The length of the averaging window was maintained at 20 ms throughout with 0% overlapping of windows. Since raw EMG data were sampled at a frequency of 1 kHz, the number of data points within each averaging window equated to 20. All amplitude processing was performed via automated programmes written in Matlab (Mathworks, Massachusetts, USA) and rmsEMG data were expressed in μV.

$$f_{rms} = \sqrt{\frac{1}{T_2 - T_1}\int_{T_1}^{T_2}[f(t)]^2 dt}$$

Equation 2.1: Shown is the rms formula for a continuous waveform f(t) defined over the interval $T_1 \leq t \leq T_2$. For the purposes of the current study, $T_2=T_1+20$.

2.4: EMG amplitude normalisation

In order to reduce the inter-individual variability with regards to surface EMG amplitude, the EMG signal must be normalised to a reference (see Chapter 1). Unless stated otherwise, EMG amplitude data were normalised to isometric MVC contractions recorded prior to data collection. Isometric MVC was performed prior to all task specificity trials to normalise EMG data against a maximal reference for each muscle (Table 2.1 for specific joint position and action). Joints were positioned at the appropriate angle and all isometric actions were resisted by an adjustable chain attached to fixed horizontal climbing bars (Hintermeister *et al.*, 1998). Individuals were instructed to push maximally and hold for 5 s, each isometric MVC was repeated 3 times with a rest period of 55 s between successive actions. Raw EMG data were recorded during each isometric MVC and subsequently root mean squared. The maximal amplitude recorded from each muscle was identified as the reference and all subsequent rmsEMG data recorded from that muscle were then expressed as a percentage of this reference, see Figure 2.1b.

Muscle	Joint position	Action
Triceps Brachii	0° shoulder flexion 90° elbow flexion	Elbow extension
Latissimus Dorsi	0° elbow flexion, 30° shoulder abduction and internally rotated	Shoulder extension and internal rotation
Anterior Deltoid	0° elbow flexion 45° shoulder flexion	Shoulder flexion
RF, VL, VM	90° knee flexion, seated position	Knee extension
Biceps Femoris	45° knee flexion, prone position	Knee flexion
Erector Spinae	45° hip and lumbar flexion, prone position	Hip and lumber extension

Table 2.1: Joint positions and actions for the specific isometric MVC performed on investigated muscle prior to task specificity trials.

2.5: Temporal normalisation and ensemble averaging

In order to account for variations in the duration of each movement cycle, temporal normalisation was performed. Cubic splines were applied to each cycle and rmsEMG data were interpolated at each 2% interval of the movement cycle (Figure 2.1c). This process not only eliminated variations in the number of data points per movement cycle, but also had an additional smoothing effect on the EMG data (Figure 2.1c). Data were then averaged over 10 consecutive cycles (Figure 2.1d) before finally being expressed as a mean ensemble average at each 2% interval of the cycle. Both temporal normalisation and ensemble averaging were performed using automated programming written in Matlab (Mathworks, Massachusetts, USA).

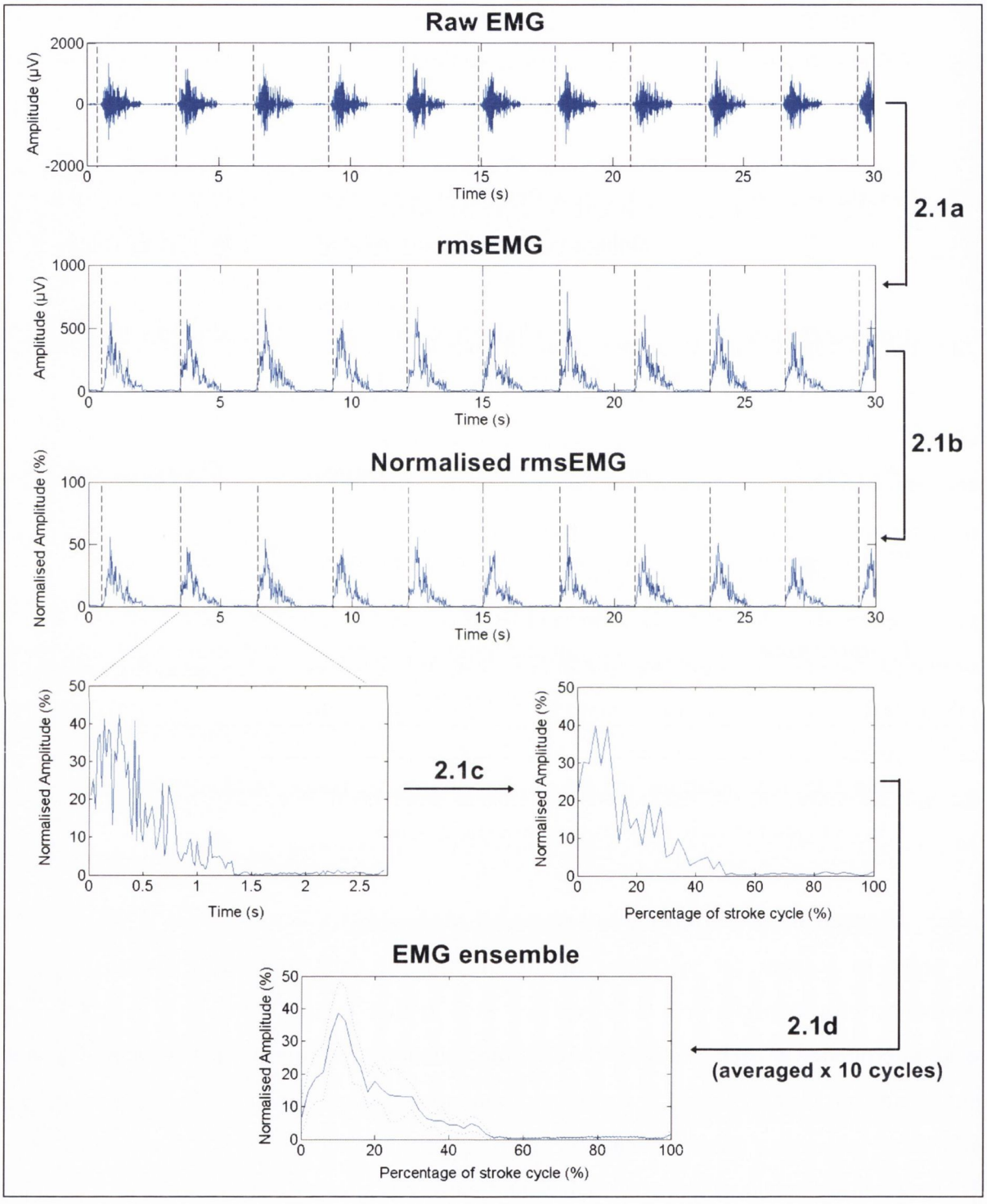

Figure 2.1: Timeline of EMG processing. Raw EMG data is initially root mean squared (2.1a) and amplitude normalised (2.1b). Temporal normalisation of each cycle is then accomplished via cubic spline interpolation (2.1c) before 10 consecutive cycles are averaged (2.1d) to produce an average EMG ensemble.

2.6: FFT and spectral analysis

Median frequency (MF), mean power frequency (MPF) and average EMG amplitude (AEMG) were calculated from the power spectral densities of the non-rectified EMG signal, using discrete fast Fourier transform (FFT) methods. All FFT methods utilised Hamming window processing, with a window length of 256 samples and a window overlap of 192 samples (75%).

$$X_k = \sum_{n=0}^{N-1} x_n e^{-i2\pi k \frac{n}{N}} \qquad k = 0, \ldots\ldots\ldots, N-1$$

Equation 2.2: Shown is the formula for a Discrete Fourier transform (DFT). FFT methods produce the same result as DFT methods, however this is accomplished in fewer iterations.

In order to quantify spectral changes associated with neuromuscular fatigue, the line of best fit for each variable was plotted through FFT spectral and amplitude data points throughout the duration of specific fatiguing contractions and rates of change across time were subsequently calculated ($Hz.min^{-1}$ or $\mu V.min^{-1}$).

2.7: Stroke force measurements

As part of the assessment of ergometer task specificity, force measurements were attained during the rowing and kayaking stroke cycles (Chapters 5 to 7). In order to achieve this in the kayaking scenario, the development of a strain gauge system capable of measuring stroke force from the bending moment of paddle shaft both on-ergometer and on-water was required.

A series of 2mm aluminium foil strain gauges (RS 632-146, RS Components, Northants, UK, Plate 2.6), combined with laser trimmed strain gauge amplifiers (RS Components, Northants, UK), were integrated in a Wheatstone bridge array with temperature compensation (Figure 2.2) onto two identical commercially available carbon kayak shafts

(Jantex, Sokolovce, Slovakia). These strain gauges have a resistance of 120 Ω, a measurable strain of 3 to 4% and can operate in a temperature range of -30 to 180 °C. Separate quad strain gauge arrays were fitted at fixed distances of 20cm either side of the midpoint of both shafts (Plate 2.7), facilitating assessment of stroke force data during left and right paddle strokes via resultant bending moments. The integration of one shaft onto the kayak ergometer and the addition of commercially available carbon paddles (Jantex Alpha M+; Jantex, Sokolovce, Slovakia) to the other shaft facilitated assessment of stroke force profiles during both on-water and on-ergometer task specificity trials. Paddle shafts were adjusted to match the length and angle of the kayaker's normal paddle set-up. All shafts were calibrated with 10 and 20 kg loads prior to both trials. Strain gauge data recording bending moments on left and right sides of the paddle shaft resultant from the applied propulsive force were amplified (Dataq, Ohio, USA) and data logged at a frequency of 100Hz under software control (Windaq Pro Data Acquisition Software V2.0, Dataq, Ohio, USA). The onset of each stroke cycle was identified as the point at which force increased above a 10N threshold (Benson *et al.*, 2011).

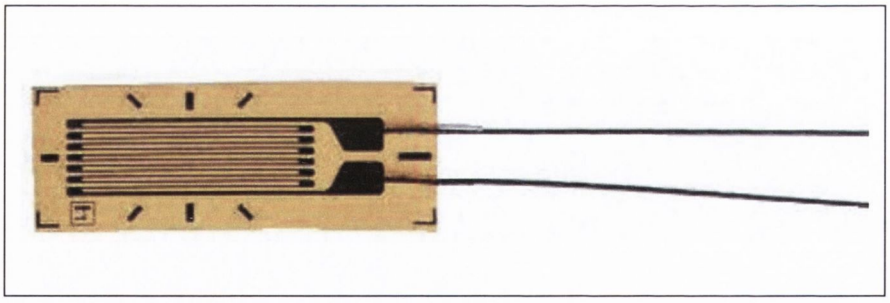

Plate 2.6: The RS 632-146 2mm aluminium foil strain gauge, used to measure tensile and compressive forces. Four such strain gauges were integrated along with laser trimmed amplifiers in a Wheatstone bridge array, onto carbon paddle shafts.

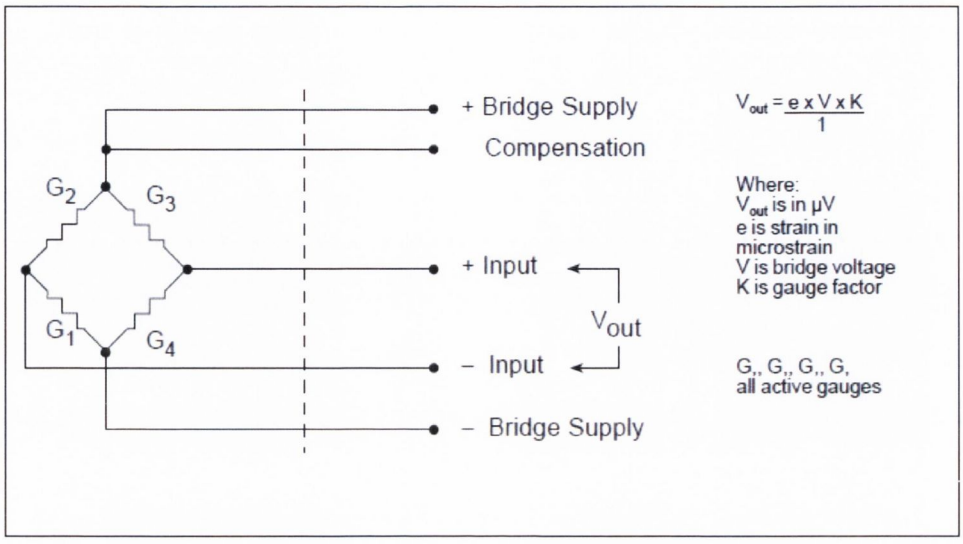

Figure 2.2: The Wheatstone bridge array with temperature compensation used to record tension and compression associated with the bending moment of carbon paddle shafts. G_1 to G_4 represent the four 2mm strain gauges integrated onto the shaft in the described circuit.

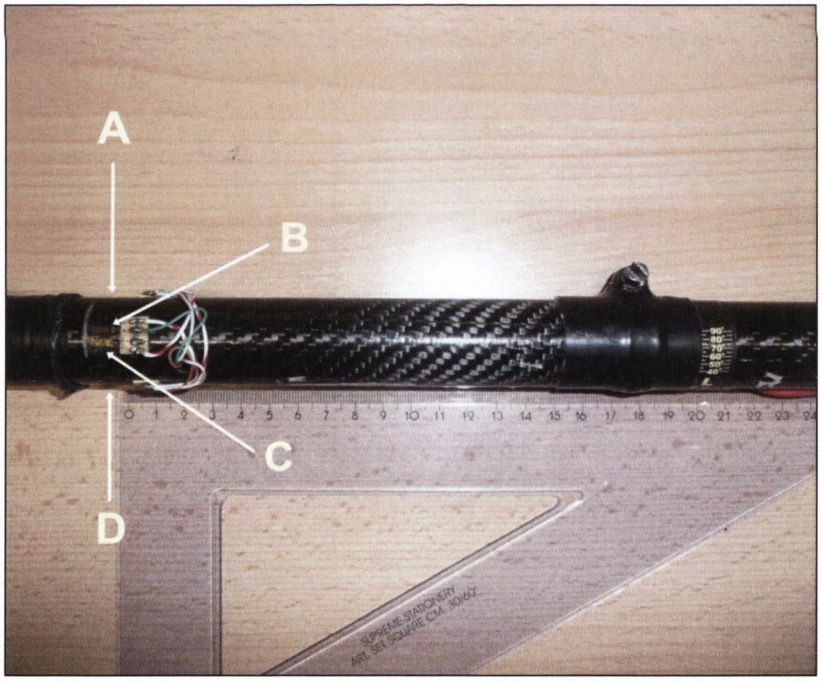

Plate 2.7: Integration of a strain gauge array onto the carbon paddle shaft. Strain gauges were integrated 20cm both sides of the centre point. Gauges at (A) and (D) are responsible for the measurement of tension and compression, while strain gauges at (B) and (C) are responsible for temperature compensation.

Throughout all ergometer rowing trials, stroke force data were measured using a load cell attached to the ergometer handle (see Plate 2.8). This quad strain gauge load cell (Tedea-Huntleigh, Model 616, Cardiff, UK) measured compressive and tensile forces up to 5000N. The load cell was calibrated with a 10 kg load prior to ergometer task specificity trials. The load cell output was amplified (Dataq, Ohio, USA) and data logged at a frequency of 100Hz under software control (Windaq Pro Data Acquisition Software V2.0, Dataq, Ohio, USA). The onset of each stroke cycle was identified as the point at which force increased above a 10N threshold (Benson *et al.*, 2011).

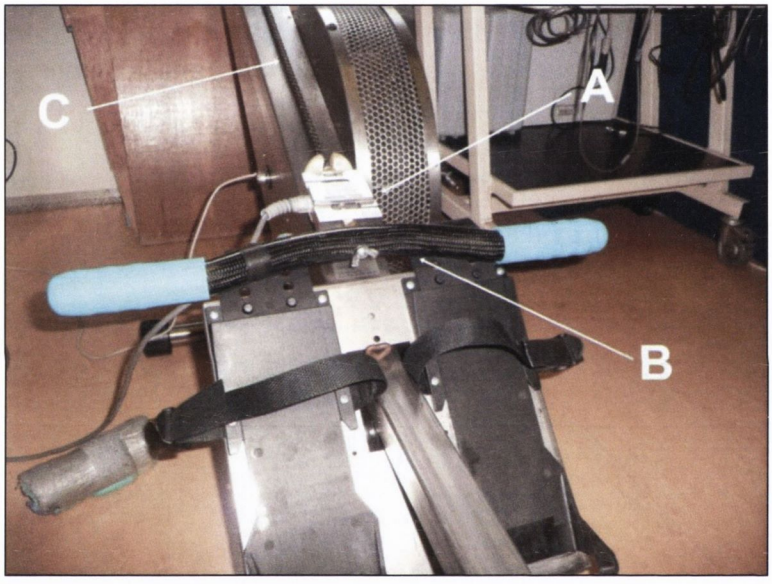

Plate 2.8: The integration of a load cell (A) onto the ergometer handle (B) and chain (C) facilitated handle forces to be quantified during ergometer rowing stroke cycles.

2.8: Maximal incremental testing

Several of the study methodologies involved participants performing a maximal incremental test, either as a means of identifying specific individual exercise intensities which were used for subsequent task specificity trials (Chapters 5 to 7) or as a direct means of inducing neuromuscular fatigue (Chapter 3). All participants performed the maximal incremental test in the Human Performance Laboratory, Anatomy Department, Trinity College Dublin, on ergometers specific to their chosen sport. Gas exchange variables, heart rate, blood lactate

concentration, stroke rate (kayaking and rowing) and in some cases raw EMG data (Chapter 3) were recorded during each increment of the test. The rowing tests were performed on a air-braked rowing ergometer (Concept 2, Vermont, USA). The foot-stretcher and flywheel drag factor were both adjusted pre-test to account for anthropometric and body mass variations between rowers. An air-braked kayak ergometer (Dansprint, Hvidovre, Denmark) was used for the kayaking tests. Once again, seating position and flywheel drag-factor were adjusted to account for variations in anthropometric and body mass variations between kayakers. In both rowing and kayaking ergometry, flywheel drag-factor was adjusted by increasing or decreasing the surface area of the flywheel covered by an air damper. Flywheel drag settings were adjusted to on-board computer calibarations for rowing ergometry and based on body mass displacement tables for kayak ergometry (www.dansprint.de). An electromagnetically loaded cycling ergometer (Lode, Groningen, The Netherlands) was used in the cycling tests. Cyclists adjusted the saddle and handlebar height, and fore-aft distance from the crank in order to attain their normal cycling position. Both the rowing and kayaking tests utilised an intermittent incremental protocol, while the cycling test utilised a continual incremental protocol, see Figure 2.3. Participants were instructed to refrain from intense physical exertion in the 24 hours prior to incremental testing, in order to minimise the risk of fatigue impacting on subsequent measurements.

Rowing

The rowing incremental test began with a 10 min warm-up on the ergometer at a mean power output of 80 to 120W. This was followed by 3 min resting period during which non-exercising data were recorded while they sat quietly on the ergometer. Rowers then performed a series of 3 min exercise bouts at fixed workloads (starting workload 120W, duration 3 min, increment 40W). They were instructed to attain the target power output within the first 30s of commencing each increment and then to maintain this power output constant for the duration of the 3 min exercise element. Heart rate, stroke rate, and respiratory variables were recorded and averaged over the final minute of each increment. A 1 min resting period between exercise bouts facilitated lactate sampling from the earlobe, see Figure 2.3a. No restriction was placed on stroke rates. The test finished when rowers

reached a target workload which they were unable to maintain for the full 3 min of exercise elements.

Kayaking

The kayak incremental test began with a 10 min warm-up on the ergometer at a mean power output of 70 to 90W. This was followed by 3 min resting period during which non-exercising data were recorded while the kayakers sat quietly on the ergometer. They then performed a series of 3 min exercise bouts at fixed workload (starting workload 90W, duration 3 min, increment 20W). In a similar fashion to the rowing test, kayakers were instructed to attain the target power output within the first 30s of commencing each increment and then to maintain this power output constant for the duration of the 3 min exercise element. Once again, no restriction was placed on stroke rate. Heart rate, stroke rate, and respiratory variables were recorded and averaged over the final minute of each increment. A 1 min resting period between exercise bouts facilitated lactate sampling from the earlobe, see Figure 2.3a. The test finished when kayakers reached a target workload which they were unable to maintain for the full 3 min of the exercise element.

Cycling

The cycling incremental test began with a 10 min warm-up on the cycle ergometer at a fixed power output of 120W. This was followed by 3 min resting period during which non-exercising data were recorded while the cyclist sat quietly on the ergometer. They then performed a series of 3 min exercise bouts at fixed workload (starting workload 120W, duration 3 min, increment 40W). Unlike the rowing and kayaking tests, no rest period between exercise bouts was necessary during the incremental cycling test, as it was possible to collect earlobe blood samples while the cyclist exercised. The cycling test was a continuous incremental trial where workload increased in a stepwise fashion every 3 min, see Figure 2.3b. Also unlike the rowing and kayaking tests, the target workloads for the cycling test were pre-programmed into an on-board computer which automatically adjusted the electromagnetic loading of the ergometer so that the target workload was always maintained throughout the test, regardless of pedalling cadence. Cyclists were simply instructed to maintain a comfortable cadence within a pre-selected range, for the duration of the test. Heart rate and respiratory variables were recorded and averaged over the final

minute of each increment. The test finished when cyclists could no longer overcome the applied resistance necessary to continue pedalling.

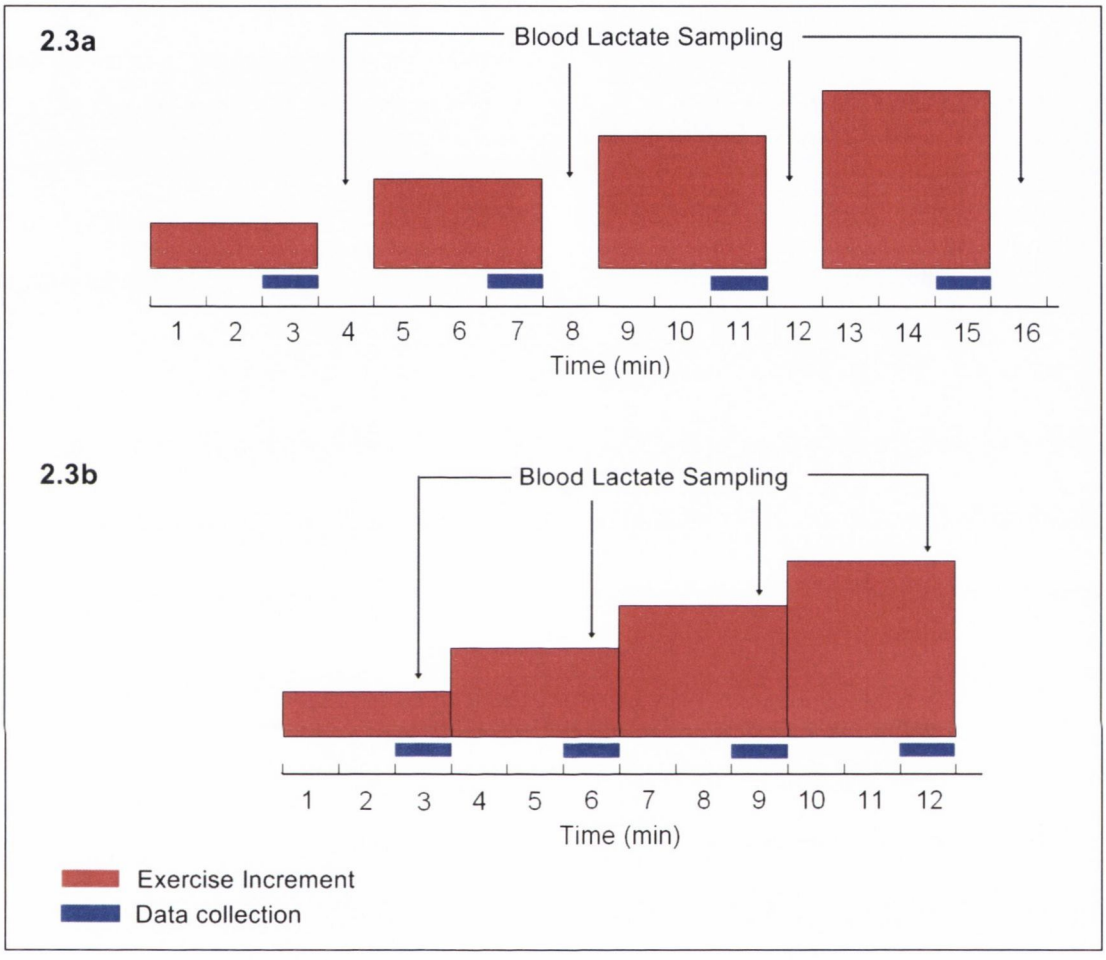

Figure 2.3: Protocol for intermittent (Figure 2.3a) and continuous (Figure 2.3b) maximal incremental test. The time-points at which blood lactate sampling were performed are indicated by the arrows. EMG, heart rate, stroke rate and respiratory data were recorded and averaged in the final minute of each exercise increment, indicated by the blue boxes in Figures 2.3a and 2.3b.

2.9: Respiratory data

Gas exchange variables were recorded using a Quark B^2 (Cosmed, Rome, Italy) breath-by-breath pulmonary gas exchange analyser during all stages of incremental testing. This system consisted of a flowmeter, a Zirconia-oxygen analyser and an infra-red carbon dioxide analyser. The flowmeter used a bi-directional digital turbine with air passing through helical

conveyors, causing the rotation of the turbine rotor. The rotating blade interrupted an infrared light beam emitted by the three diodes of the optoelectronic reader. Every interruption represented 16.6% turn of the rotor; this allowed for accurate measurement of the number of rotations in a fixed time ($rev.s^{-1}$). There was a constant ratio between the air passing through the turbine and the number of turbine rotations thus allowing for the accurate measurement of volume and flow rate. The Zirconia oxygen analyser had a range of 1 to 100% Oxygen (O_2), a response time of <120 ms and an accuracy of <0.05% O_2. The fast carbon dioxide analyser measured CO_2 concentration by infra-red radiation absorption (response time <150 ms). The CO_2 that passed through the sensor cell absorbed a certain amount of radiation; the absorption was proportional to the quantity of CO_2 in the sample line.

The respiratory variables of importance measured during the test were:

1. Oxygen consumption ($\dot{V}O_2$) in $mL.min^{-1}$ or when corrected for body mass, $\dot{V}O_2$ measured in $mL.kg^{-1}.min^{-1}$
2. Carbon dioxide production ($\dot{V}CO_2$) in $mL.min^{-1}$
3. Minute Ventilation ($\dot{V}E$) in $L.min^{-1}$
4. Respiratory frequency in $breath.min^{-1}$
5. Ventilatory equivalent for oxygen ($\dot{V}E/\dot{V}O_2$)
6. Ventilatory equivalent for carbon dioxide ($\dot{V}E/\dot{V}CO_2$)

Participants wore a facemask (Hans Rudolf, USA) connected by a nafion tube (Permapure, New Jersey, USA) to the Quark B^2 analyser. Air inspired from the room was expired and analysed for volume, O_2 and CO_2 content before the respiratory data were displayed and recorded on a PC. It was necessary to attach the mask as tightly as possible with the adjustable straps in order to maintain a tight seal and avoid any volume losses during the test.

The Quark B^2 analyser was calibrated prior to each incremental test for O_2 and CO_2 using room air and a standardised α-certified gas (15% O_2, 5% CO_2 and balance N_2, BOC, Surrey, UK), calibration of the volume transducer was performed daily using a 3L gas calibration

syringe (Cosmed, Rome, Italy). Having connected the sampling line to the sampling socket on the front of the unit, the gas sensor was easily calibrated using the system software (Quark B^2, Version 2.0, Cosmed, Rome, Italy). The gas analysers were calibrated twice prior to each incremental test using both room air and the certified gas mixture. A volume calibration was performed using a 3-litre calibration syringe attached to the flowmeter. The syringe piston was moved in and out for 5 inspiratory strokes and 5 expiratory strokes before the first measurements appeared on the calibration screen. A further 10 inspiratory and expiratory strokes were then performed, and the percentage errors were displayed before the new calibration factors were stored. This volume calibration was repeated until an average percentage error reading of less than 0.5% was attained. All respiratory data were exported as Excel files and stored for later analysis.

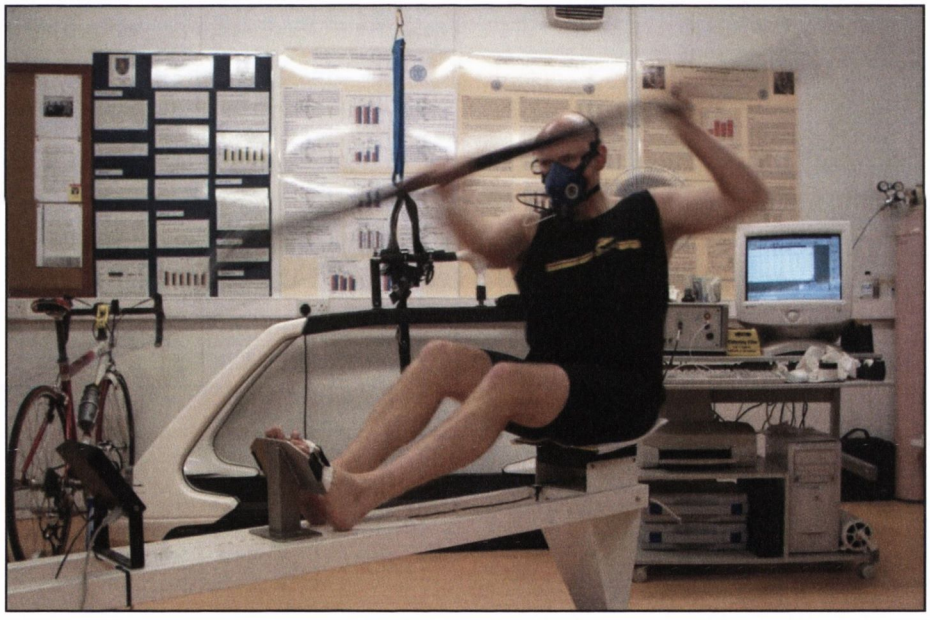

Plate 2.9: Kayaker with face mask attached to Quark B^2 metabolic analyser during maximal incremental test on a Dansprint kayak ergometer.

2.10: Blood lactate data

Blood lactate (BLa) concentration was measured using an YSI 1500 Sport lactate analyser (Yellow Springs Instruments, Ohio, USA) calibrated prior to each test using a 5mmol.L^{-1} lactate standard. Blood samples were obtained from the right earlobe during all tests using a sterile lancet following dry swab cleaning. The earlobe was lanced with a sterile lancet

(Solofix, Braun, Bratislava, Slovakia) prior to the start of each incremental test. After each exercise increment, the participant's earlobe was wiped clean of any sweat or dried blood. A fresh sample of blood was then squeezed from the earlobe and drawn via capillary action into a heparinised capillary tube (Marienfeld Laboratory Glassware, Laud-Konigshofen, Germany). A 25μL sample of this blood was then collected from the capillary tube and transferred into the lactate analyser using a syringe pipette (Yellow Springs Instruments, Ohio, USA).

The measurement of blood lactate concentration [BLa] involved a series of chemical reactions within the sensor probe of the YSI lactate analyser. The probe consisted of a silver cathode and platinum anode. A three layered membrane consisting of polycarbonate, immobilized L-lactate oxidase and cellulose acetate covered the probe. When a blood sample was injected in the reaction chamber using the 25 μL syringe, some of the sample diffused through the membrane. The outer membrane was porous and resisted diffusion of enzymes but was large enough to allow the passage of O_2, H_2O, H_2O_2, NaCl and lactate. The inside membrane of cellulose acetate was permeable to H_2O_2, but impermeable to ascorbic acid and other substances with a molecular weight greater than 200. When the lactate in the blood sample diffused through the outer polycarbonate membrane and came into contact with the L-lactate oxidase membrane, the lactate was rapidly oxidised producing H_2O_2 and pyruvate in the reaction below:

<u>Reaction 1:</u> L-Lactate + O_2 $\xrightarrow{\text{L-Lactate Oxidase}}$ H_2O_2 + Pyruvate

The H_2O_2 produced passed through the inner membrane of cellulose acetate and was oxidised at the platinum anode producing electrons:

<u>Reaction 2:</u> H_2O_2 $\xrightarrow{\text{At the platinum electrode}}$ $2H^+ + O_2 + 2e^-$

The circuit was completed at the silver reference cathode where the following reaction occurred:

Reaction 3: $2\,AgCl + 2e^- \longrightarrow 2Ag + 2Cl^-$

The current produced was linearly proportional to the lactate concentration in the sample chamber. The analyser calculated the lactate concentration of the sample by comparing the current produced by the sample with a reference sample of known lactate concentration. Prior to each test, the analyser was calibrated. A 25µL sample of 5mmol.L^{-1} lactate standard solution was passed into the reaction chamber using the syringe pipette. The analyser was calibrated to a precision of ±0.1mmol.L^{-1}.

Plate 2.10: YSI 1500 Lactate Analyser with 25µL syringe pipette

2.11: Heart rate data

Heart rate data were recorded by radio-telemetry using a Cardiosport GT1 heart rate monitor (Cardiosport, Hampshire, UK) consisting of a coded transmitter belt and monitor. A small

amount of ultrasound transmission gel (Aquasonic 100, Parker, New Jersey, USA) was placed on the transmitter electrodes to allow for more accurate and consistent readings. Heart rate was transmitted from the belt to the monitor at a 1 s sampling rate. The monitor was positioned on the participant's back attached to the belt out of their view during all tests. Heart rate data was monitored and recorded every 15 s during laboratory testing. During field based testing, heart rate data were recorded by radio telemetry using a Garmin Forerunner 310 (Garmin, Kansas, USA). Field based heart rate data were downloaded to a laptop post-exercise via a USB interface.

Plate 2.11: Cardiosport heart rate monitor and transmitter with ultrasound transmission gel.

2.12: Anthropometric measurements

Participant's height (cm) and body mass (kg) were measured using a stadiometer and counterbalance scales (Seca, Hamburg, Germany) to a precision of 0.1cm and 0.1kg, respectively. Participants were weighed in their Lycra training shorts having removed their footwear. Body mass index (BMI) was then calculated using Equation 2.3 (McArdle *et al.*, 2005).

Equation 2.3: BMI ($kg.m^{-2}$) = Body Mass (kg) / Height^2 (m^2)

2.13: Percentage body fat

A Harpenden skinfold caliper (Baty, Sussex, UK) was used to assess percentage body fat. Measurements were taken from four discrete anatomical sites; biceps, triceps, subscapular and suprailiac on the dominant side. The skinfold measurement was assessed with the participant standing on a level surface. Using the left hand, a fold of skin and subcutaneous tissue was picked up, the plates of the caliper held in the right hand were allowed to exert full pressure ($10g.cm^{-2}$) below the position of the left hand before recording skinfold thickness to the nearest 0.2 millimetre (mm). The mean of three measurements at each site was recorded.

1. Triceps: Skinfold thickness was recorded from the midpoint of a line connecting the acromion and the olecranon process while the arm was hanging loosely with the elbow extended.

2. Biceps: Skinfold thickness was recorded directly above the centre of the cubital fossa at the same level at which the triceps reading was taken.

3. Subscapular: Skinfold thickness was recorded just beneath the inferior angle of the scapula in a direction obliquely downwards and outwards at 45° angle.

4. Supra-iliac: Skinfold thickness was recorded 5 to 7 cm above the anterior superior iliac spine (ASIS) at an angle of 45° above the horizontal.

The sum of the four skinfold thicknesses was calculated and used to estimate percentage body fat from the equivalent fat content tables (Durnin & Womersley, 1974) grouped by age and gender. Lean body mass (LBM in kg) was also calculated by subtracting the computed fat mass (kg) from the overall body mass, see Equation 2.4.

Equation 2.4: Lean Body Mass (kg) = Total body mass (kg) – computed fat mass (kg)

Plate 2.12: Harpenden skinfold calipers

2.14: Pulmonary function tests

Lung function data were assessed before and after each incremental test using the Microlab microspirometer (Micro Medical, Blessingstoke, UK). A disposable unidirectional cardboard mouthpiece was attached to the spirometer. The procedure was explained to each participant and was subsequently performed on two or more occasions until results with less than 2% variation were achieved, as recommended by the European Respiratory Society. Wearing a nose clip, to eliminate nasal breathing, the participant was instructed to inhale maximally from the room and then, having placed the mouthpiece in their mouth, exhale maximally for as long and as fast as possible. Verbal encouragement was provided in order to ensure that full expiratory reserve volume was expelled from the lungs during each test.

The following four variables were recorded:

1. Forced Vital Capacity (FVC) in litre (L)
2. Forced Expiratory Volume in one second (FEV_1) in L
3. Peak Expiratory Flow (PF) in litre per second ($L.s^{-1}$)
4. Forced Expiratory Rate (FER) in %

Plate 2.13: Microlab microspirometer

2.15: Haematological analysis

A blood sample was collected aseptically from the medial cubital vein in the anticubital fossa of the left arm using the vacutainer system; this system involved the use of a 21G 1.5 inch needle (Precision Glide, BD Diagnostics, Plymouth, UK) and a 4mL EDTA tube (Vacutainer, Plymouth, UK). The blood sample was analysed in an automated cell counter (Coulter Counter System, Model Act Diff, Coulter Electronics, UK). Data for the variables haemoglobin (Hgb) in $g.dL^{-1}$, haematocrit (Hct) in %, red blood cell count (x $10^{12}.L^{-1}$) and white blood cell count (x $10^{9}.L^{-1}$) were recorded for each participant who undertook incremental testing.

Chapter 3

Assessment of neuromuscular fatigue at the aerobic-anaerobic transition during varying dynamic exercise.

3.1: INTRODUCTION

Physiologists have long recognised the existence of a critical exercise intensity above which a dramatic increase in blood lactate accumulation and associated changes in respiratory exchange variables occur. However, it was not until 1964 that the term "anaerobic threshold" or "aerobic-anaerobic transition" was coined to describe this critical point above which there is a disproportionate increase in plasma lactate concentrations (Wasserman & McIlroy, 1964). This definition was later extended to include associated changes in gas exchange variables which occurred above this exercise intensity (Wasserman *et al.*, 1973). Since its discovery, the determination of the aerobic-anaerobic transition has become of critical importance as a performance predictor and in training prescription, particularly in endurance sports (Urhausen *et al.*, 2000). The velocity at the aerobic-anaerobic transition has been shown to be a more accurate predictor of performance than $\dot{V}O_2max$ in marathon runners (Tanaka & Matsuuram, 1984) and a more objective determinant of training intensity in elite rowers (Mickelson & Hagerman, 1982). While the identification of non-linear increases in plasma lactate concentration remains the most common method of determining the aerobic-anaerobic transition, the novel use of EMG has received more recent attention due to its potential as a non-invasive means of determining this critical exercise intensity.

An increase in amplitude and a decrease in the MF of the recorded EMG signal have long been established as reliable non-invasive determinants of neuromuscular fatigue (De Luca, 1997). To date, there have been many studies documenting non-linear increases in the amplitude of EMG signals at the aerobic-anaerobic transition (Chwalbinska-Moneta *et al.*, 1998; Lucia *et al.*, 1999; Jurimae *et al.*, 2007). Positive correlation between the breakpoint in EMG amplitude and the lactate (Mateika & Duffin, 1994a; Chwalbinska-Moneta *et al.*, 1998) and ventilatory thresholds (Moritani *et al.*, 1993; Lucia *et al.*, 1999; Hug *et al.*, 2004) have been reported. However, other authors have reported no correlation between EMG measures and the aerobic-anaerobic threshold (Viitasalo *et al.*, 1985; Taylor & Bronks, 1994). Taylor and Bronks (1994) reported no signs of a breakpoint in EMG activity during incremental treadmill running, while Viitasalo *et al.* (1985) showed only linear changes in both spectral and amplitude based EMG variables during incremental cycle ergometry. In addition, the majority of the published literature examining the EMG threshold has been

performed within the scope of dynamic cycling exercise. Of the 15 or more published articles examining EMG changes about the aerobic-anaerobic transition, only two papers have used a non-cycling based protocol (Taylor & Bronks, 1994; Maestu *et al.*, 2006) and of these studies, only Maestu *et al.* (2006) reported a positive correlation between T_{EMG} and ventilatory threshold (V_T). It thus remains to be seen if the changes in EMG variables which appear about the aerobic-anaerobic transition in cycling exercise, are detectable in other dynamic exercise conditions. Furthermore, if there exists a universal relationship between the T_{EMG} and other estimates of the aerobic-anaerobic transition, is its relationship consistent across exercise condition?

3.2: AIMS AND HYPOTHESIS

The primary aim of this study was to examine the occurrence of T_{EMG} across varying exercise conditions and compare these with metabolic and ventilatory based determinants of the aerobic-anaerobic transition. A secondary aim was to compare T_{EMG} across different exercise conditions and investigate if its relationship to the aerobic-anaerobic transition was independent of exercise condition.

Our hypothesis was that T_{EMG} determined via non-linear increases in rmsEMG amplitude of investigated muscles, would lie within the range of the aerobic-anaerobic transition measured via ventilatory and metabolic means. As such, we expected to find that the power at T_{EMG} (W) would lie between the power at V_{T1} and V_{T2} when comparing T_{EMG} to ventilatory derived thresholds, and between power at T_{Lac} (measured via the V-slope method) and OBLA when comparing T_{EMG} to metabolically derived thresholds. We hypothesised that no significant differences in the relationship between T_{EMG} and other measures of the aerobic anaerobic threshold across exercise conditions would be observed.

3.3: MATERIALS AND METHODS

3.3.1: Experimental design

This study involved performing a standard incremental test to volitional failure on one of three sports specific ergometers (rowing, cycling or kayaking ergometers) while metabolic, gas exchange and electromyographic data were collected. Participants were required to visit the laboratory on one occasion only. All participants were fully informed of the procedures involved in the current study and provided informed consent to participate, see Appendix 3. Ethics approval was granted from the Trinity College Health Sciences research ethics committee prior to commencing the study.

3.3.2: Participant group

40 healthy male volunteers (n=40) formed the overall study group for this investigation. This group comprised of trained club level athletes from rowing (n=14), kayaking (n=12) and cycling (n=14). The overall study group had a mean age (mean ± SEM) of 23 ± 1 yr, height of 184.9 ± 0.9 cm and mass of 80.4 ± 1.3 kg. All participants were informed of experimental procedures, benefits and risks and when satisfied, provided written informed consent in accordance with the Declaration of Helsinki (Appendix 3). For juniors, written consent was also obtained from their parent or legal guardian. Prior to participation, all volunteers completed a detailed medical questionnaire (Appendix 3) and underwent a medical examination by a qualified medical practitioner. Exclusion criteria for participants included any cardiac or respiratory abnormalities, hypertension, diabetes, or any muscular conditions or injuries suffered in the previous 2 months which had adversely affected their training.

3.3.3: Medical examination

On arrival, all participants were required to complete a detailed medical questionnaire, outlining medical history and details of any past sporting injuries (see Appendix 3). A medical practitioner performed a general physical examination; blood pressure was measured using an automated sphygmomanometer (Omron, Tokyo, Japan). A venous blood sample obtained by standard venepuncture technique using a 21G needle and Vaccutainer

system was analysed for Hgb, Hct, RBC and WBC to rule out anaemia, sub-clinical infection and dehydration prior to exercise testing, see Chapter 2.15. Anthropometric measurements, percentage body fat and lung function tests were also performed prior to exercise testing, see Chapter 2.12, 2.13 and 2.14, respectively.

3.3.4: Data collection

All participants performed a sport specific maximal incremental test to volitional failure, see Chapter 2.8. While cyclists performed a continuous protocol, all rowers and kayakers performed an intermittent protocol, see Figure 2.3. Earlobe blood lactate concentration was assessed at the end of each increment, see Chapter 2.10 and respiratory exchange data recorded on a breath-by-breath basis was averaged over 15s intervals using the Quark b^2 software, see Chapter 2.9. Mean data for respiratory exchange variables recorded during the final 90s of each increment was used during data analysis. The maximal $\dot{V}O_2$ and $\dot{V}E$ data recorded in any 15s interval for the duration of the incremental test was identified as $\dot{V}O_2$peak and $\dot{V}E$max. The recorded data were then graphed as a function of workload before the lactate threshold (T_{Lac}) and ventilatory thresholds (V_{T1} and V_{T2}) were identified using the V-slope method (Beaver *et al.*, 1986). The first ventilatory threshold (V_{T1}) was defined as the first breakpoint or non-linear increase in $\dot{V}E/\dot{V}O_2$ (Caiozzo *et al.*, 1982). The second ventilatory threshold (V_{T2}) was defined as the first non-linear increase in $\dot{V}E/\dot{V}CO_2$ (Beaver *et al.*, 1986). In order to compare our results with previously published literature, power at onset of blood lactate accumulation (OBLA) defined as a fixed blood lactate concentration of 4 $mmol.L^{-1}$ was also identified.

Raw EMG data were recorded from 4 specific muscles involved in each sport (Table 3.1) during the final minute of each increment, see Chapter 2.1. EMG see data were synchronised to 2D kinematic data, see Chapter 2.2 and processed over 10 consecutive movement cycles, see Chapter 2.3. The average rmsEMG data for each muscle were then plotted as a function of workload in a similar fashion to the blood lactate and metabolic data. EMG thresholds (T_{EMG}) for each muscle were identified in the graphical plots which showed non-linear increases in activity using the V-slope method (Beaver *et al.*, 1986) in a similar fashion to

the lactate and ventilatory thresholds (Figure 2.8). Data from muscles which did not exhibit non-linear increases in amplitude were not included in the statistical analysis.

	Muscle 1	Muscle 2	Muscle 3	Muscle 4
Cycling	*Rectus Femoris*	*Vastus Medialis*	*Tibialis Anterior*	*Gastrocnemius*
Rowing	*Rectus Femoris*	*Vastus Lateralis*	*Biceps Femoris*	*Upper Trapezius*
Kayaking	*Triceps Brachii*	*Biceps Brachii*	*Anterior Deltoid*	*Latissimus Dorsi*

Table 3.1: Muscles assessed for T_{EMG} for each athletic sub-group in the current study.

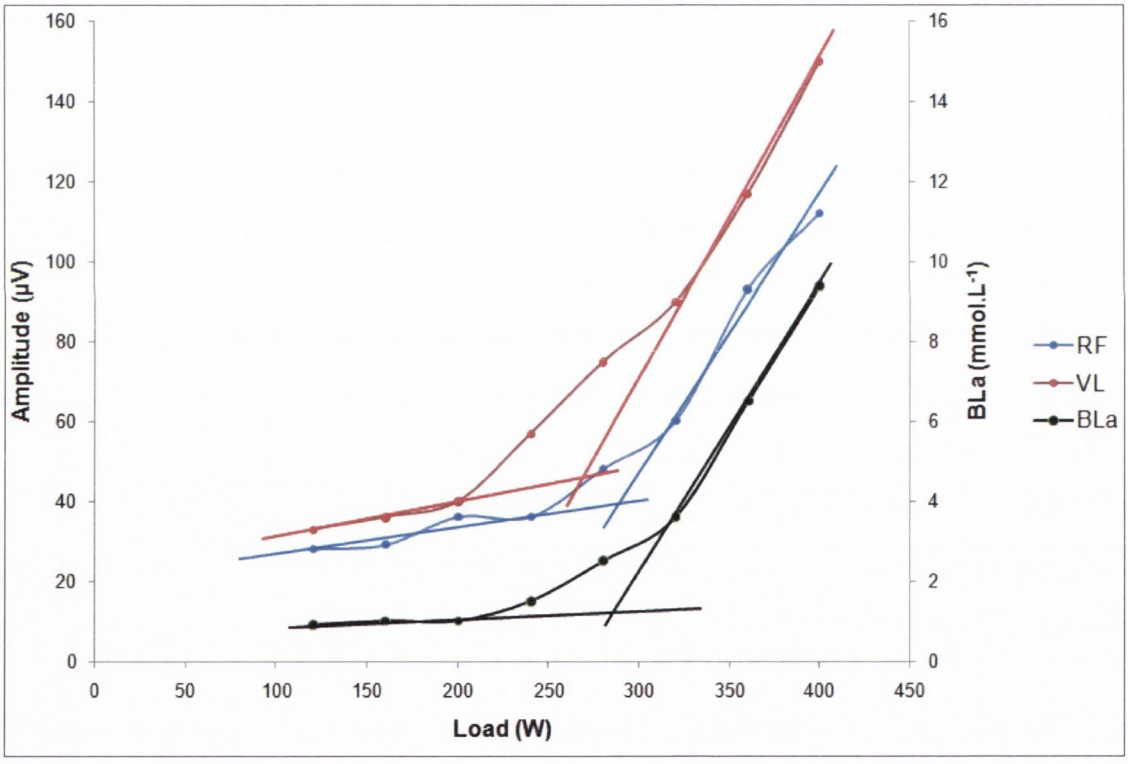

Figure 3.1: The rmsEMG data for RF (RF), VL (VL) and blood lactate concentrations (BLa) at increasing workloads measured during a rowing incremental test. The intersection of the lines of best fit plotted for the initial data points corresponding to the aerobic phase and the final data points corresponding to the anaerobic phase yielded a threshold for each variable (V-slope method). The power (W) corresponding to each threshold could then be interpolated.

3.3.5: Statistical Analysis

Individual values of T_{Lac}, OBLA, V_{T1}, V_{T2} and T_{EMG} were expressed in terms of $\dot{V}O_2max$ ($mL.kg^{-1}.min^{-1}$), % of $\dot{V}O_2peak$, % Pmax (the maximum power attained within the test) and in power (W). Data are presented as group mean ± SEM unless otherwise stated. Pearson product correlation coefficients were applied to evaluate the association of T_{EMG} to the other estimates of the aerobic-anaerobic transition. A single factor, repeated measures ANOVA with *post-hoc* Tukey tests, established if any significant differences ($P<0.05$) existed between these data sets. Subsequent analysis across exercise condition was performed by attaining a mean individual T_{EMG} for each participant. These data were then expressed relative to each individual's Pmax and analysed across exercise condition using a single factor ANOVA.

3.4: RESULTS

3.4.1: Anthropometric and physiological characteristics

The anthropometric, physiological, haematological and pulmonary characteristics describing the study sub-groups are shown in Table 3.2. No significant differences were observed for height, BMI, percentage body fat, $\dot{V}O_2$peak or any of the haematological variables across the three participant sub-groups. However, the cycling sub-group were significantly ($P<0.01$) older than the rowing or kayaking sub-groups. This is most likely attributed to the fact that both the rowing and kayaking participants were recruited from collegiate clubs or under-23 national squads, respectively. The rowing sub-group were significantly heavier ($P<0.05$) than the kayaking or cycling sub-groups. The rowing sub-group recorded significantly greater FVC and FEV1 than the cycling sub-group ($P<0.05$).

	Cycling	Rowing	Kayaking
Age (yr)	29 (2) **	21 (1)	21 (1)
Height (m)	1.83 (0.09)	1.87 (0.11)	1.84 (0.20)
Mass (kg)	78.0 (2.4)	85.5 (1.7) *	77.1 (2.0)
BMI ($kg.m^{-2}$)	23.2 (0.6)	24.3 (0.5)	22.8 (0.5)
Body fat (%)	12.3 (0.9)	13.8 (0.6)	11.8 (0.7)
$\dot{V}O_2$peak ($mL.kg^{-1}.min^{-1}$)	58.9 (1.7)	60.6 (1.5)	57.9 (2.0)
Hct (%)	44.1 (0.6)	44.8 (0.8)	43.5 (0.6)
Hgb ($g.dL^{-1}$)	15.7 (0.2)	15.5 (0.3)	15.4 (0.2)
RBC ($x10^{12}.L^{-1}$)	4.8 (0.1)	4.9 (0.1)	4.8 (0.1)
FVC (L)	5.57 (0.17)	6.51 (0.23) #	5.91 (0.22)
FEV1 (L)	4.53 (0.15)	5.33 (0.19) #	4.97 (0.24)
PF ($L.min^{-1}$)	658 (20)	677 (38)	656 (24)

Table 3.2: Mean (SEM) physiological, haematological and pulmonary characteristics describing each sub-group. Asterisk infers significant difference compared to two other groups. Hash symbol infers significant difference compared to cycling only (one symbol, $P<0.05$; two symbols, $P<0.01$).

3.4.2: Appearance of T_{EMG}

T_{EMG} was assessed in 4 discrete muscles for each sport (Table 3.1) and compared to more conventional estimators of the aerobic-anaerobic transition such as ventilatory and lactate derived thresholds. Of the 14 participants tested in the rowing sub-group, only 1 failed to exhibit any signs of non-linear increases in rmsEMG activity, most likely due to deterioration in electrode contact with the skin as the test proceeded. As a result, all data for this participant, including metabolic and ventilatory derived thresholds were excluded from statistical analysis. In total, 13 participants exhibited non-linear increases in EMG activity in RF and VL, 10 participants exhibited non-linear increases in EMG activity in BF while only 9 exhibited non-linear increases in EMG activity in UT (Table 3.3). Of the 12 participants tested in the kayaking sub-group, all exhibited non-linear increases in rmsEMG activity in TB and LD while 9 participants exhibited non-linear increases in rmsEMG activity in BB (Table 3.3). Unexpectedly, only 1 participant exhibited signs of non-linear increases in rmsEMG activity in AD. In fact, the majority of participants in this sub-group (n=8) registered a decrease in AD activity as power increased. As such, we were unable to attain T_{EMG} in AD and data from this muscle was excluded from further analysis. In the course of the cycle testing, 1 participant was unable to complete the maximum incremental test due to muscular cramping during the protocol. Results for the cycling group are therefore expressed with a group total of 13 (n=13). When assessing T_{EMG} in the four muscles, all 13 participants exhibited non-linear increases in rmsEMG in RF, 12 exhibited non-linear increases in VM activity, while 9 exhibited non-linear increases in the TA. Unexpectedly, only 3 participants exhibited non-linear increases in GA activity with the majority exhibiting linear increases (Table 3.3). Consequently, GA data were not included in the statistical analysis.

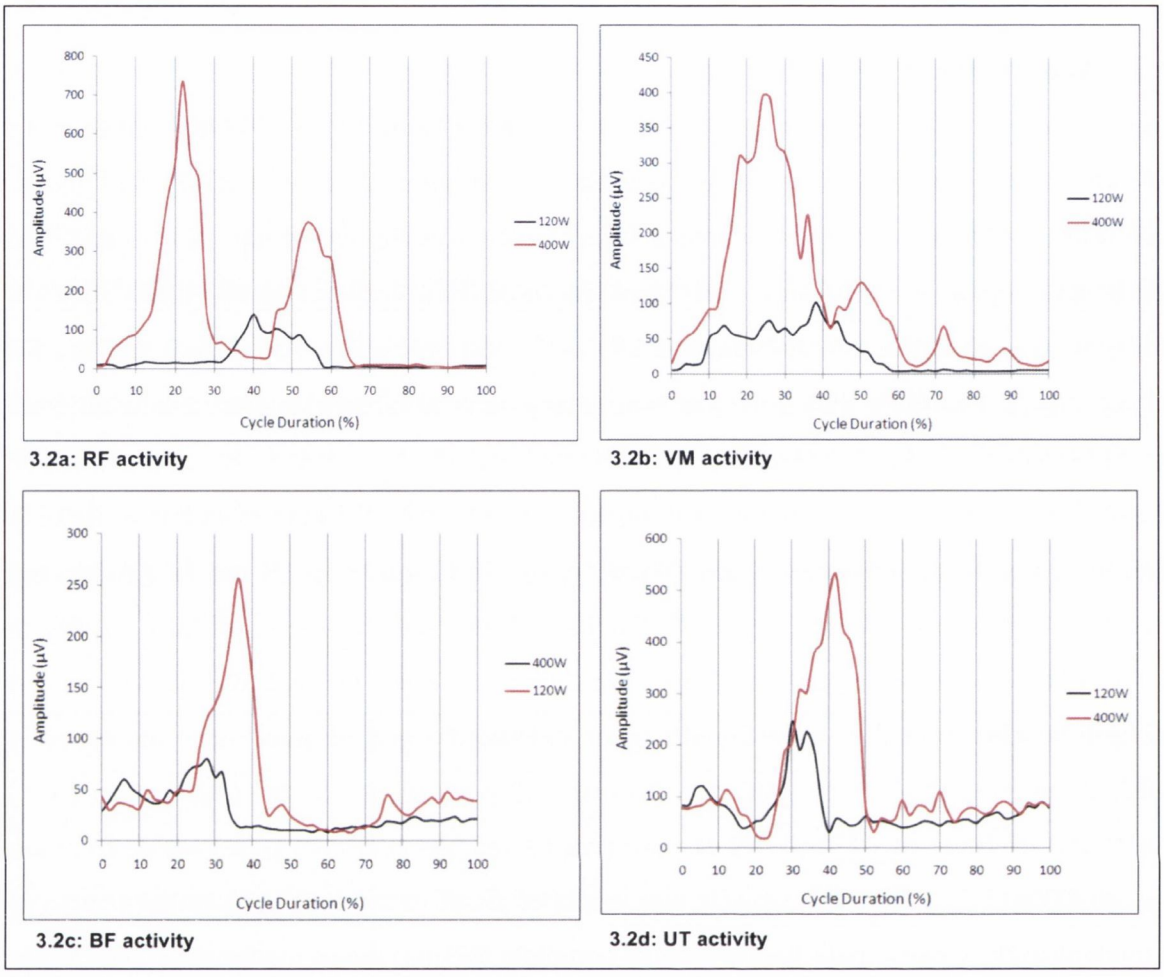

Figure 3.2: Un-normalised rmsEMG ensemble averages for 10 consecutive rowing stroke cycles in a participant exercising at 120 and 400W. Average rmsEMG data (μV) are presented relative to percentage of stroke cycle duration (%). RF, VL, BF and UT are shown in Figure 3.2a to Figure 3.2d, respectively.

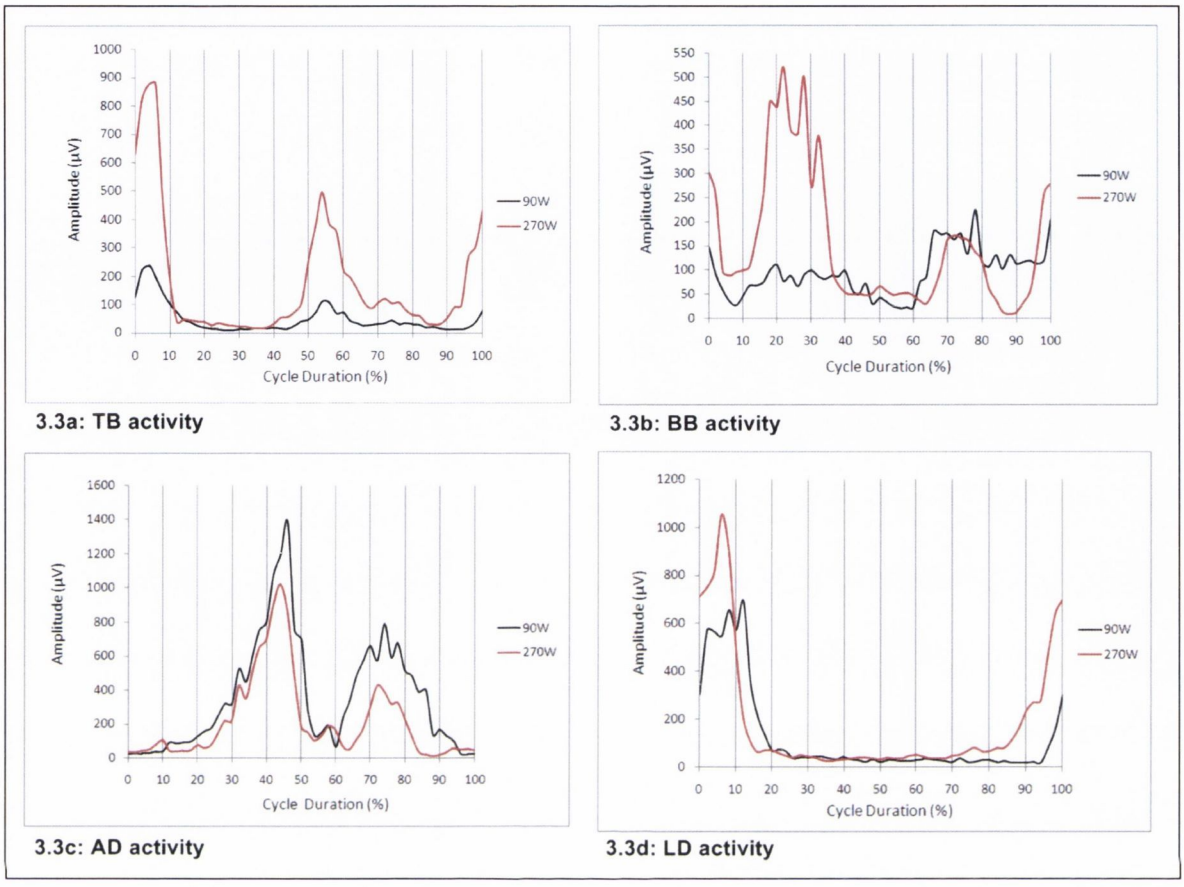

Figure 3.3: Un-normalised rmsEMG ensemble averages for 10 consecutive kayaking stroke cycles in a participant exercising at 90 and 270W. Average rmsEMG data (μV) are presented relative to percentage of stroke cycle duration (%). TB, BB, AD and LD are shown in Figure 3.3a to Figure 3.3d, respectively. Note the unexpected decrease in AD activity as power increased (Figure 3.3c).

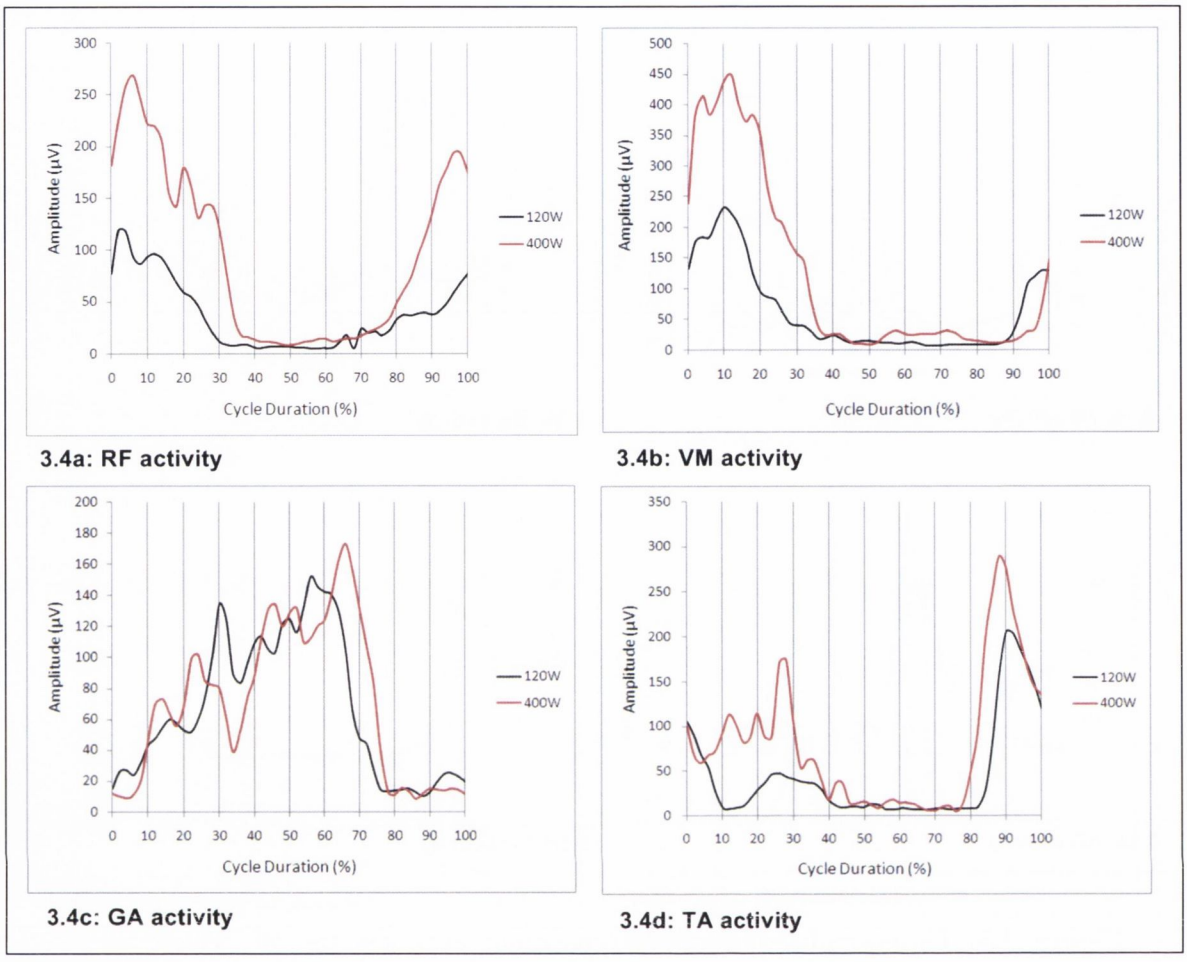

Figure 3.4: Un-normalised rmsEMG ensemble averages for 10 consecutive cycling pedal cycles in a participant exercising at 120 and 400W. Average rmsEMG data (μV) are presented relative to percentage of pedaling cycle duration (%). Activity in RF, VM, GA and TA are shown in Figure 3.4a to Figure 3.4d, respectively.

	Cycling (n=13)	Rowing (n=14)	Kayaking (n=12)
T_{EMG} muscle 1	13	13	13
T_{EMG} muscle 2	12	13	9
T_{EMG} muscle 3	9	10	1
T_{EMG} muscle 4	3	9	12

Table 3.3: The number of participants within each sub-group who exhibited non-linear increases in EMG within the discrete muscles assessed. See Table 3.1 for the specific muscles used within each sporting condition.

3.4.3: Comparison to ventilatory and lactate thresholds

When comparing the appearance of T_{EMG} to that of ventilatory and lactate derived thresholds, it appears that the knee extensor and flexor muscles are the most appropriate muscles for identifying the aerobic-anaerobic transition in both rowing (RF, VL and BF) and cycling (RF and VM) while in kayaking, TB and LD appear most appropriate. This is due to participants consistently exhibiting non-linear increases in EMG in these muscles (Table 3.5), and the high correlation between T_{EMG} in these muscles and the more conventional determinants of the aerobic-anaerobic transition (Tables 3.7, 3.8 and 3.9, respectively).

In general, T_{EMG} consistently occurred at higher power than T_{Lac}. Of the 10 muscles used in statistical comparison, 6 of the muscles had T_{EMG} occurring at significantly higher power than that of T_{Lac} (Table 3.4). As expected, OBLA occurred at significantly higher power than T_{Lac}, as did V_{T2} ($P<0.05$). V_{T2} also occurred at significantly higher power than V_{T1} ($P<0.05$), in all sub-groups (Table 3.4). Linear regression analysis revealed higher correlation coefficients comparing T_{EMG} to lactate thresholds (T_{Lac} and OBLA) than ventilatory thresholds, in both cycling and rowing, see Tables 3.5 and 3.6, respectively. However, correlation coefficients were equally high for both lactate and ventilatory thresholds in kayaking, see Table 3.7. In general T_{EMG} correlation to the more conventional estimators of the aerobic-anaerobic transition to was high, with the exception of TA in cycling which showed relatively poor correlation (0.51-0.66, see Table 3.5). When comparing T_{EMG} data from within each exercise condition, no significant differences were

seen amongst the muscles in cycling or rowing. However in kayaking, T_{EMG} in TB occurred at significantly lower percentage of Pmax when compared to LD ($P<0.05$) see Figure 3.6.

	Cycling	Rowing	Kayaking
T_{EMG} muscle 1	277 (13)	267 (5)	152 (9)**
T_{EMG} muscle 2	292 (20)**	268 (5)	146 (10) $
T_{EMG} muscle 3	290 (17)*	270 (8)*	NA
T_{EMG} muscle 4	NA	274 (10)**	159 (10) ***##
V_{T1}	285 (14)**	264 (5)	148 (10)
V_{T2}	300 (15)***#	279 (7)***#	161 (10)***##
T_{Lac}	264 (16)#	256 (7)	140 (8)
OBLA	290 (17)*	281 (9)***##	152 (9)**

Table 3.4: Group mean (SEM) power (W) at EMG, ventilatory and lactate thresholds. See Table 3.1 for specific muscles used in each sporting condition. Asterisk infers significant difference from T_{Lac}. Hash symbol infer significant difference from V_{T1}. Dollar symbol infers significant difference from Muscle 4 (one symbol, $P<0.05$; two symbols, $P<0.01$; three symbols, $P<0.001$).

	V_{T1}	V_{T2}	T_{Lac}	OBLA
RF	0.84	0.83	0.96	0.93
VM	0.82	0.84	0.95	0.92
TA	0.61	0.58	0.55	0.61

Table 3.5: Pearson's product moment correlation coefficients comparing T_{EMG} in each muscle to the ventilatory and metabolically derived thresholds attained during cycling ergometry.

	V_{T1}	V_{T2}	T_{Lac}	OBLA
RF	0.75	0.81	0.87	0.93
VL	0.58	0.66	0.73	0.83
BF	0.63	0.72	0.80	0.89
UT	0.76	0.86	0.73	0.80

Table 3.6: Pearson's product moment correlation coefficients comparing T_{EMG} in each muscle to the ventilatory and metabolically derived thresholds attained during rowing ergometry.

	V_{T1}	V_{T2}	T_{Lac}	OBLA
TB	0.94	0.96	0.91	0.91
BB	0.89	0. 91	0.85	0.82
LD	0.94	0.94	0.96	0.93

Table 3.7: Pearson's product moment correlation coefficients comparing T_{EMG} in each muscle to the ventilatory and metabolically derived thresholds attained during kayaking ergometry.

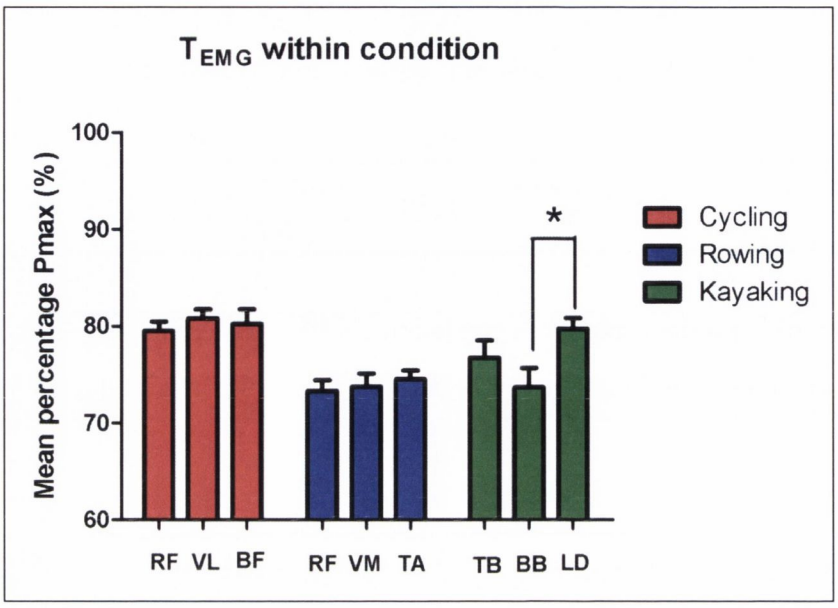

Figure 3.5: Mean± SEM of T_{EMG} data for 3 muscles within each exercise condition.

3.4.4: Comparison across exercise condition

Power at threshold for each data set were normalised to Pmax in order to statistically compare variables across exercise condition. This was done in order to eliminate the variations in power associated with the different exercise conditions. Since EMG was recorded from different muscles within each participant group, it was not possible to directly compare T_{EMG} data from discrete muscles across exercise condition. However, an indirect comparison was made, by attaining a global T_{EMG} response within each sub-group, by averaging the T_{EMG} data from all muscles within each condition. Results are expressed as mean ± SEM percentage of Pmax (%) and are presented in Table 3.8. No significant differences were observed between participant sub-groups for T_{Lac} or OBLA. However significant differences were observed between participant sub-groups for V_{T1} and V_{T2}. Both V_{T1} and V_{T2} occurred at significantly higher percentages in cycling when compared to kayaking and rowing ($P<0.05$), see Figure 3.5a and 3.5b. Analysis revealed that global T_{EMG} in cycling also occurred at a significantly greater percentage of Pmax when compared to rowing ($P<0.01$), see Figure 3.7. One unique characteristic of the cycling thresholds were the apparently delayed occurrence of both ventilatory derived thresholds. V_{T1} occurred at

significantly higher power that T_{Lac} in the cycling sub-group, an observation that was not observed in the other conditions. Methodological differences in the cycling incremental exercise protocol and in the identification of the ventilatory threshold in this sub-group may explain these observed differences (see Chapter 3.4 for further discussion).

	Cycling	**Rowing**	**Kayaking**
T_{Lac}	74.3 (1.2)	70.5 (1.1)	70.4 (1.2)
OBLA	80.5 (1.4)	76.7 (1.2)	77.7 (1.5)
V_{T1}	81.0 (1.2)**#	72.8 (1.4)	74.5 (1.9)
V_{T2}	85.0 (1.2)**	76.8 (1.5)	80.3 (1.7)
Global T_{EMG}	80.1 (0.7)**	73.9 (1.0)	76.7 (1.4)

Table 3.8: Mean (SEM) global T_{EMG}, ventilatory and metabolic thresholds for each exercise sub-group nomalised to Pmax (%). Asterisk infers significant difference compared to rowing, while hash symbol infers significant difference compared to kayaking (one symbol, $P<0.05$; two symbols, $P<0.01$).

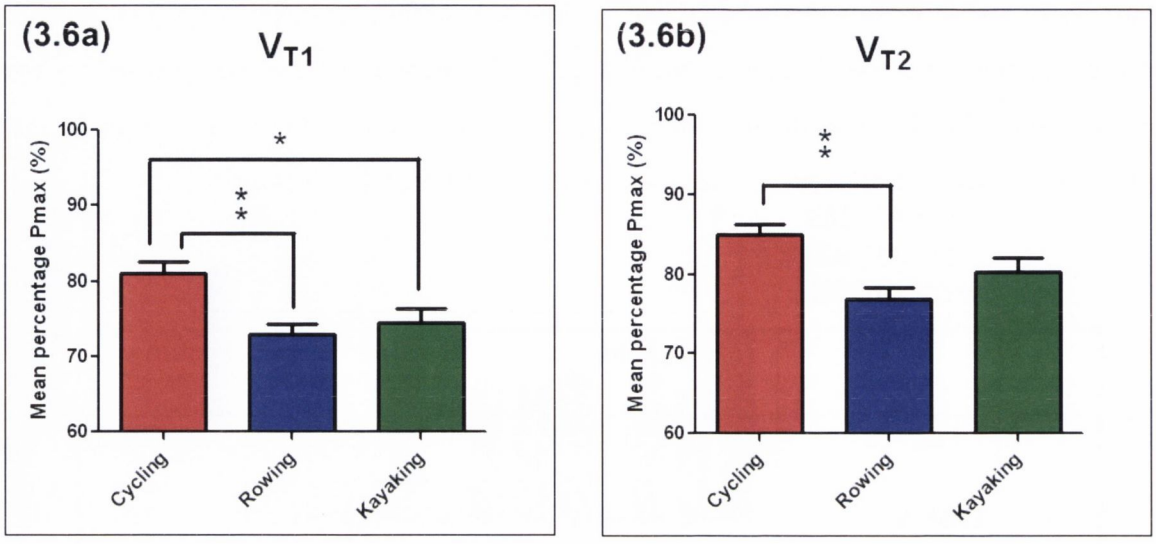

Figure 3.6: Mean ± SEM for V_{T1} (3.6a) and V_{T2} (3.6b) across exercise conditions.

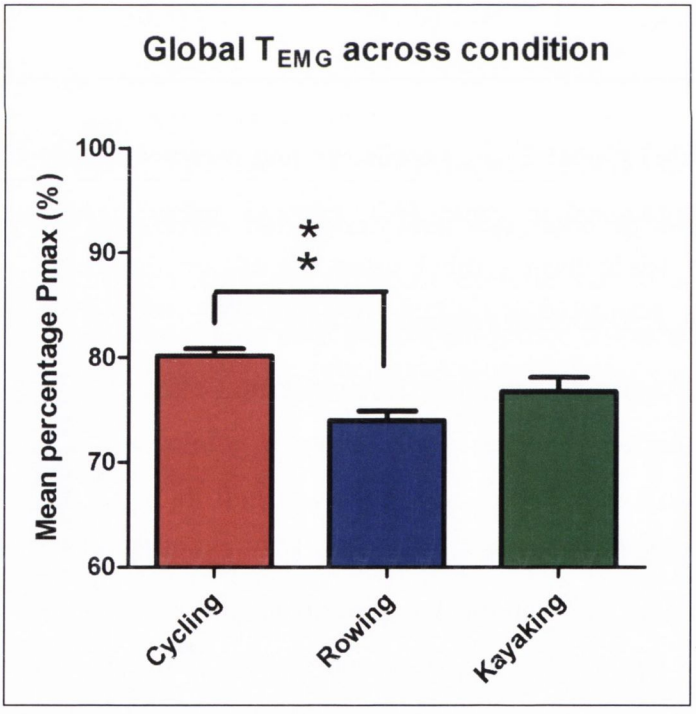

Figure 3.7: Mean ± SEM for the global T_{EMG} in each exercise condition. Threshold data from muscles within each exercise condition were averaged together in order to attain an overall mean T_{EMG} for each exercise condition, for comparison across exercise conditions.

3.5: DISCUSSION

The primary aim of the current study was to investigate if the appearance T_{EMG} was consistent across a variety of exercise conditions. Muscles selected for the assessment of T_{EMG} in each sub-group were chosen based on previous literature which had identified each muscle as playing a key role in the movement patterns associated with that sport (Capousek & Bruggemann, 1990; Hagerman, 2000; Hug & Dorel, 2009). The attainment of T_{EMG} from a discrete muscle involved the identification of non-linear increases in signal amplitude, as exercise intensity increased during the incremental test. To this end, T_{EMG} was identified in 117 out of a possible 156 EMG traces investigated, see Table 3.3. This equates to a 75% success rate in the attainment of T_{EMG} across all exercise conditions. The failure to identify non-linear increases in some discrete muscles may lie with their unique role within the movement pattern of the sporting task. This would appear the case for AD activity in kayaking. However, in other cases, namely GA in cyclists, linear increases were the most common observation and the reason why non-linear increases in EMG amplitude were absent remains to be elucidated. Correlation analysis of T_{EMG} to more common determinants of the aerobic-anaerobic threshold suggests that the occurrence of T_{EMG} is more closely associated with the occurrence of lactate thresholds in cycling and rowing, while T_{EMG} is highly correlated to both ventilatory and lactate thresholds in kayaking (Tables 3.5 to 3.7).

One of the most interesting findings of the current study is that a comparison of global T_{EMG} across exercise condition identified differences between the cycling and rowing sub-groups which were also identified in the ventilatory thresholds (Figures 3.6 and 3.7). Global T_{EMG}, V_{T1} and V_{T2} were significantly higher in cycling when compared to rowing. While this anomaly is most likely due to methodological differences in the incremental testing protocol, it is interesting that similar differences across conditions were not observed in either T_{Lac} or OBLA. It has been well documented that increased hyperventilation can be utilised as a means of buffering H+ ions within the blood (Anderson & Rhodes, 1989; Mateika & Duffin, 1995; Chicharro *et al.*, 2000). By blowing off excess CO_2 produced via the bicarbonate buffering system, hyperventilation can offset the increases in both H^+ and CO_2 concentrations within the bloodstream (Mateika & Duffin, 1995). During an intermittent

incremental protocol, participants are afforded a 1 min recovery period between increments. At higher workloads, post-exercise hyperventilation during this recovery is a common response. It is likely that this hyperventilation may provide a reserve capacity for increased CO_2 production during the subsequent exercise increment and may therefore alter the onset of both V_{T1} and V_{T2} when compared to a continual incremental protocol. It is not surprising therefore, that differences in V_{T1} and V_{T2} are observed between rowing and cycling sub-groups, since contrasting exercise protocols were used. What is surprising, however, is that similar differences were observed in global T_{EMG}. This would suggest a potential link between ventilatory changes associated with the aerobic-anaerobic transition and increased central recruitment of additional motor units. Mateika and Duffin (1994a) have suggested that changes in both the ventilatory motor unit recruitment response about the aerobic-anaerobic transition may be centrally mediated. This suggestion has been backed by evidence from incremental tests performed at normoxia, hypoxia and hyperoxia (Mateika & Duffin, 1994b). The current results may also point towards central mediation of the aerobic-anaerobic threshold, however further research is warranted.

Decreases in AD activity were observed as exercise intensity increased during kayak ergometry. This inverse relationship between exercise intensity and EMG activity was unexpected and may be as a result of the unique role of AD in the kayak stroke cycle. On examination of the muscle responses to increasing exercise intensity in kayaking, the most striking finding was the absence of increasing EMG activity in ADs. In fact, 8 of the 12 participants exhibited decreasing AD activity over the course of the incremental protocol (Figure 3.3c). Activity in AD was for the most part isolated to phases of the stroke cycle not involved in generating propulsive forces (Figure 3.3). A previously published hypothesis which postulated that increased stroke force on-water at higher exercise intensities would lead to increased shoulder muscle recruitment (Trevithick *et al.*, 2007). The results of the current study suggest that increasing exercise intensity in kayaking is brought about by additional motor unit recruitment from muscles active during the initial phases of the cycle (TB, LD and BB) and not from muscles involved in other phases of the stroke (AD).

When undertaking this study, our choice of participant sub-groups was made with the aim of investigating the occurrence of T_{EMG} across a broad spectrum of dynamic movements. Our choice of cycling, kayaking and rowing thus allowed us to investigate lower limb (cycling), upper limb (kayaking) and whole body (rowing) dynamic movements. In addition to investigating a broad range of dynamic movements, it was intended to examine participant sub-groups with contrasting physiological characteristics due to the nature and demands of the training within their chosen sports. The physiological demands of both cycling and rowing require a high degree of aerobic endurance in order to compete at a high level. As such, it has been shown that elite male cyclists and rowers have undergone a high degree of aerobic adaptation through training. Coyle *et al.* (1992) observed a positive correlation between the percentage of Type I muscle fibres and cycling efficiency. An elite group of cyclists in their study showed a mean percentage of 67% Type I muscle fibres in the VL (Coyle *et al.*, 1992). Olympic level American rowers have been shown to exhibit 71% Type I muscle fibres with 24% Type IIA, and approximately 5% Type IIB in the VL (Hagerman, 2000). In contrast, Olympic sprint kayaking is a discipline involving a high degree of anaerobic power. Tesch *et al.* (1976) examined a group of Olympic male Swedish kayakers and observed a ratio of 53% to 47% Type I to Type II muscle fibres in the AD. For athletes specialising in the 500m kayak race, the mean percentage of Type II muscle fibres increased to 56% due to the greater anaerobic contribution required for this shorter sprint distance (Tesch *et al.*, 1976). Ivy *et al.* (1980) reported significant positive correlations ($P<0.01$) between percentage Type I muscle fibre and absolute ($r=0.74$) and relative ($r=0.70$) lactate thresholds. These results suggested that the proportion of Type I muscle fibres plays a role in determining the anaerobic threshold (Ivy *et al.*, 1980). Therefore the variations in fibre type composition reported to exist between trained athletes in these sports meant that the possibility of contrasting EMG threshold responses identifying the aerobic-anaerobic transition could not be ruled out.

In addition to variations in muscle fibre type composition amongst elite rowers, cyclists and kayakers, differences also exist in maximal oxygen consumption in these sports. Competitive male rowers have been shown to exhibit a mean ± SD $\dot{V}O_2max$ of 68.9 ± 8.9 $mL.kg^{-1}.min^{-1}$, when exercising on air-braked rowing ergometers (Maestu *et al.*, 2006).

Elite male cyclists have been shown to exhibit a $\dot{V}O_2$max of 67.5 ± 8.9 mL.kg^{-1}.min^{-1} (Jurimae *et al.*, 2007) and 69.9 ± 6.4 mL.kg^{-1}.min^{-1} (Lucia *et al.*, 1999). It has been reported that elite kayakers exhibit lower maximum oxygen uptake data. Tesch *et al.* (1976) reported $\dot{V}O_2$max data of 57.5 ± 2.5 mL.kg^{-1}.min^{-1}, while Fry and Morton (1991) reported $\dot{V}O_2$max data of 59.3 ± 7.4 mL.kg^{-1}.min^{-1} (Tesch *et al.*, 1976; Fry & Morton, 1991). In a more recent study, a group of well-trained flat-water kayakers exhibited a $\dot{V}O_2$max of 55.2 ± 7.5 mL.kg^{-1}.min^{-1} (Van Someran *et al.*, 2000). The $\dot{V}O_2$peak values exhibited by our rowing sub-group (60.6 ± 5.7 mL.kg^{-1}.min^{-1}) and cycling sub-group (58.9 ± 6.5 mL.kg^{-1}.min^{-1}) appear markedly lower than published data in the literature. However this may be explained by our selection of participants. Our rowing group comprised of intermediate and senior varsity oarsmen while the current cycling group consisted of club level cyclists who would not be of the physical fitness level as elite cyclists used in the studies by Lucia *et al.* (1999) or Jurimae *et al.* (2007). The $\dot{V}O_2$peak data in our kayaking group (57.9 ± 7.1 mL.kg^{-1}.min^{-1}) were comparable to the published literature and again this is due to the training level of participants undertaking the study. Our kayaking group comprised of senior and under-23 kayakers who were all representing Ireland at international competition. The fact that no significant differences in $\dot{V}O_2$peak were observed between the cycling, rowing or kayaking sub-groups appears to show that our choice of participants and their varying level of training may have resulted in a more homogenous data set than would have been expected. Although we were unable to perform muscle biopsies in the current study, it may be assumed that our cycling and rowing sub-groups did not exhibit as high a degree of muscle fibre adaptation than has been observed in the elite participant groups studied by Coyle *et al.* (1992) and Hagerman *et al.* (2000), respectively.

3.6: CONCLUSION

From the current study we have established that EMG thresholds are attainable not only in a variety of dynamic exercise conditions, but from a variety of muscles involved in each condition. However caution must be aired in choosing appropriate muscles to record from, as the varying contribution each muscle has within a given dynamic exercise means that one may not always attain a T_{EMG}, especially from muscles recruited secondary within the movement. This was highlighted both by the AD muscle in kayaking and the GA muscle in cycling where inconsistent increases and even decreases relative to increasing power were often observed. These variations made it difficult if not impossible to attain T_{EMG} data. Choosing muscles which provide a high contribution to force production and propulsion within the given movement is recommended. Such was the case with RF and VL in rowing, RF and VM in cycling and TB and LD in kayaking. All these muscles exhibited consistent non-linear increases in EMG relative to power and showed strong correlation to both ventilatory and metabolically derived thresholds. EMG thresholds in general appear to show a close association with OBLA and the ventilatory thresholds, and less association to T_{Lac} measured by the V-slope method. This was illustrated by the significant differences exhibited by many of the muscles compared to T_{Lac}.

When comparing thresholds across exercise condition, it appears that the ventilatory and EMG thresholds are sensitive to variation in exercise protocol. Surprisingly, the metabolic thresholds (T_{Lac} and OBLA) did not exhibit sensitivity to these protocol variations. While the shared sensitivity of the ventilatory and EMG thresholds may suggest a physiological link between muscle activity and ventilation, further research examining this anomaly is warranted. In order to test the validity of this theory, an additional validation study comparing intermittent and continual cycling incremental testing was performed, see Appendix 4.

Having explored the neuromuscular fatigue thresholds at the aerobic-anaerobic transition in varying dynamic exercise modalities, another important area in our attempt to better understand neuromuscular fatigue is to explore if EMG indices are altered between training and untrained individuals. The next experimental chapter will explore this.

Chapter 4

A comparison of neuromuscular fatigue in trained and untrained groups, during sustained isometric contractions of the knee extensors.

4.1: INTRODUCTION

Short-term resistance training (duration less than 6 weeks) induces significant increases in maximal strength with no apparent increases in muscle mass (Sale, 1988). These changes have been linked to neural adaptations involving increased agonist muscle synchronisation, decreased antagonist co-activation, and enhanced motor unit recruitment and rate coding (Sale, 1988; Carolan & Cafarelli, 1992; Pucci *et al.*, 2006; Duchateau & Baudry, 2010). In contrast, long-term resistance training increases muscle force generating capacity through both neuromuscular adaptations and increases in sarcomere cross-sectional area (CSA) (Wilmore *et al.*, 2008). It has previously been reported that hypertrophic increases in muscle CSA accounted for 40% of the increase in force generating capacity; the remaining 60% being accounted for primarily by adaptations in neural activation (Narici *et al.*, 1989). Long-term dynamic endurance training increases the proportion of Type I muscle fibres in elite runners (Fink *et al.*, 1977), rowers (Hagerman, 2000) and cyclists (Coyle *et al.*, 1992). Since Type I muscle fibres are more fatigue resistant than Type IIa or IIb fibres, a greater proportion of Type I fibres within muscle may enhance fatigue resistance.

Electromyography (EMG) allows monitoring of changes in electrical activity within muscles during the course of sustained contractions and is widely accepted as a non-invasive, objective means of quantifying muscle force production and neuromuscular fatigue (De Luca, 1997). Hakkinen and Komi (1983) reported that short-term resistance training improvements in knee extensor force were accompanied by significant increases in integrated EMG amplitude of the associated muscles. They concluded that marked increases in force in the early stages of training resulted from significant increases in neural activation assessed by iEMG, while longer-term improvements were of a smaller magnitude and were not accompanied by detectable changes in iEMG (Hakkinen & Komi, 1983). More recently, long-term resistance training induced an altered spectral EMG response in swimmers performing a dry-land isotonic swim bench protocol to volitional failure (Ganter *et al.*, 2007). In addition, De Souza *et al.* (2009) reported that short-term resistance training protocols altered the frequency and amplitude of muscle fatigue indices during sustained isometric contractions of *Biceps Brachii,* inferring that training induced neural adaptations increase both muscle strength and endurance (De Souza *et al.*, 2009).

During sub-maximal isometric contractions to exhaustion, whole muscle EMG increases yet there is a progressive decline in spectral variables (Person & Kudina, 1972; Bigland-Ritchie *et al.*, 1986; Mathur *et al.*, 2005). While the mechanism proposed for increasing EMG activity within fatiguing muscles remains the recruitment of additional motor-units to compensate for loss of contractility within fatigued fibres (Lippold, 1960), the mechanisms underlying the decline in motor unit discharge frequencies are still debated. The most widely accepted explanation is a decrease in the myoelectric conduction velocity (Bigland-Ritchie *et al.*, 1981). As the muscle begins to fatigue, a build up of metabolites and reduction in intramuscular pH decreases the velocity at which an action potential is propagated along the active fibres (Brody *et al.*, 1991). Other factors however, may also contribute to these fatigue induced frequency shifts (Broman *et al.*, 1985). Masuda *et al.* (1999) argued that changes in myoelectric conduction velocity only partly explained the spectral shift in EMG since changes in median frequency during non-ischemic, dynamic contractions were not accompanied by a slowing of muscle fibre conduction velocity (Masuda *et al.*, 1999). Other authors have proposed that derecruitment of fatigable motor-units (Type IIa, IIb) may play a role in these spectral shifts (Asmussen, 1979) along with low frequency motor unit synchronisation (De Luca & Erim, 2002; Boonstra *et al.*, 2008).

4.2: AIMS AND HYPOTHESIS

The primary aim of this study was to compare spectral and amplitude derived EMG indices of neuromuscular fatigue in trained and untrained groups at varying relative intensities of isometric contraction. In contrast to previous literature (Hakkinen & Komi, 1983; Ganter *et al.*, 2007; De Souza *et al.*, 2009), the current study aimed at directly comparing trained and untrained groups for EMG indices of neuromuscular fatigue in their knee extensors. In addition the trained group used in the study was both resistance and endurance trained and consequently would be expected not only to exhibit neural adaptations to force production, but also intramuscular adaptations towards fatigue resistance brought about by endurance training. We hypothesised that potential altered responses to fatigue in this group of trained individuals may provide a starting point for the identification of training induced alterations in muscle function and morphology. A secondary aim of this study was to quantify and compare reliability indices between trained and untrained volunteers. We hypothesised that the trained group would exhibit enhanced force production and an altered neuromuscular response to fatigue illustrated by higher levels of knee extensor moment, a reduction in rates of change of EMG fatigue variables and enhanced reliability indices compared to the untrained group.

4.3: MATERIALS AND METHODS

4.3.1: Participants

Twenty volunteers were tested on two occasions with a minimum of 2 and a maximum of 7 days between both tests. Healthy male volunteers (mean ± SD; age 23±4 yr, mass 82.3±8.7 kg) were divided into trained (n=10, age 22±2 yr, mass 84.5 ± 10.0 kg) and untrained groups (n=10, age 23±4 yr, mass 80.0±7.1 kg). Club level rowers were selected as the trained group since significant increases in Type I muscle fibre composition of the knee extensors have been reported in rowers (Hagerman, 2000). In addition, all trained volunteers had performed a minimum of 2 resistance training sessions per week for the previous 6 months as part of their regular training. The untrained group comprised of physically active 3rd level students. All participants were fully informed of the procedures involved and provided informed consent to participate, see Appendix 3. Ethical approval for this study was granted from the Trinity College Health Sciences ethics committee.

4.3.2: Knee extensor moment assessment

Isometric moment measures were performed on a Cybex II Humac Norm System (Model 770, Computer Sports Medicine, Massachusetts, USA) isokinetic dynamometer. This unit is designed as a single chair system with the head assembly in a fixed position (see Plate 4.1). The servomotor controls and monitors the velocity and force applied to the dynamometer allowing for application and assessment of isokinetic, isotonic and isometric protocols. The dynamometer is located in the head assembly. Information on dynamometer shaft, or lever-arm, position and direction are communicated to the computer interface via electrical signals derived from the dynamometer's servo potentiometer. The torque board inside the dynamometer housing provides the system with moment data recorded at the input shaft and the dynamometer is controlled by a microprocessor. Isometric moment measurements were recorded from the dynamometer and relayed to the computer interface at a frequency of 100 Hz. The dynamometer's rotation, height and tilt are all adjustable as is the dynamometer's chair. In addition, the chair's back can be adjusted to account for variations in femoral length and sitting position.

Participants were seated on the dynamometer and the backrest and seat angle were adjusted so that the hips were fixed at approximately 80° of flexion. They were then securely strapped to the seat using shoulder and pelvic belts in order to minimise any body movement other than the desired knee extension. The axis of dynamometer rotation was aligned to the knee joint line, and the cuff (load cell) was placed at a distance equivalent to 50% of each participant's tibial length. The knee joint was placed at 70° of flexion relative to maximum voluntary knee extension. All adjustments made to the dynamometer were noted to ensure the same placement for the second testing session. A visual feedback of produced force was provided on the computer interface screen during all trials in order for the participants to maintain a constant desired moment. Throughout all isometric contractions performed, participants remained sitting still with their arms folded across their chest.

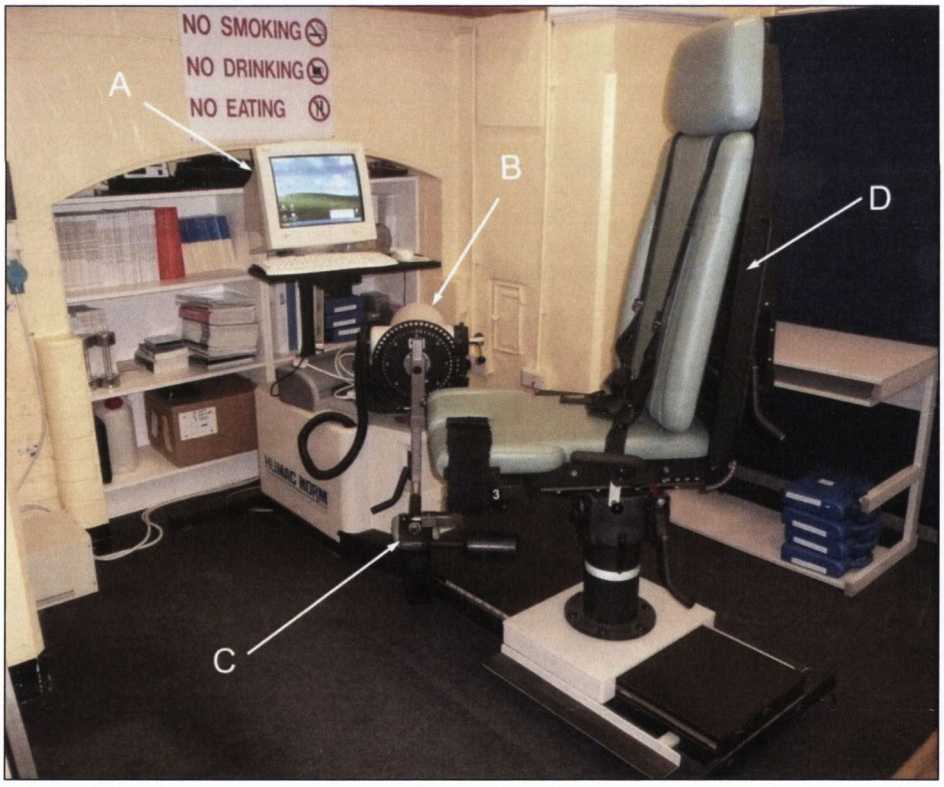

Plate 4.1: Cybex II dynamometer. Shown is the interface screen (A), the head assembly (B) within which the dynamometer is located, the knee joint adapter with ankle cuff (C) and the adjustable seat (D).

4.3.3: Exercise protocol

Volunteers initially exercised dynamically on a weight-loaded cycle ergometer (Monark, Varberg, Sweden) at a power of 90W for 10 min. A subsequent series of three maximal voluntary isometric contractions (MVC) of the knee extensors were performed on each leg. Volunteers were instructed to "push as hard as possible" and hold for a 5 s period. Visual feedback and consistent verbal encouragement were provided during each effort and a 1 min rest period separated MVC trials. MVC data were assessed on both legs, on both testing days, in order to calculate the target moment for subsequent endurance trials. Calculation of target moment was performed by averaging isometric moment data across the time period from 1.5 to 4.5s during each MVC. Maximum data for each leg were identified from the three attempts and individual target moments for 80 and 20% MVC calculated.

Endurance assessments consisted of time to failure (TTF) trials performed at 80% MVC on one leg and at 20% MVC on the other leg. Random selection determined that eleven volunteers (n=11) performed their 80% MVC trial on their dominant side and nine (n=9) performed their 20% MVC trial on their non-dominant side. Visual feedback of target and applied moment were provided and constant verbal encouragement given by the tester to maintain the pre-set target for as long as possible. TTF was defined as the point where the applied moment dropped 5Nm below target during the 20% MVC trial and 10Nm below target during the 80% MVC trial, despite verbal encouragement. A 10 min rest period between TTF trials was provided for static stretching and to reduce any potential effects of central fatigue on the subsequent TTF trial. All isometric moment data were downloaded post-exercise and standard deviation from pre-set target quantified and expressed as %MVC.

Plate 4.2: Participant performing maximal voluntary isometric knee extensions on the Cybex II dynamometer.

4.3.4: EMG recording

Surface EMG recordings were collected from the 3 superficial muscles of the knee extensor musculature; *Vastus Lateralis* (VL), *Vastus Medialis* (VM) and *Rectus Femoris* (RF), see Chapter 2.1. For each TTF trial, median frequency (MF), mean power frequency (MPF) and average EMG amplitude (AEMG) were calculated from the power spectral densities of the non-rectified EMG signal, using discrete fast Fourier transform (FFT) methods, see Chapter 2.6. The line of best fit for each variable was plotted through FFT spectral and amplitude data points from attainment of pre-set moment to failure during each TTF trial and rates of change across time subsequently calculated ($Hz.min^{-1}$ or $\mu V.min^{-1}$). Data collected over a 5s window following attainment of the target and preceding the failure point were also averaged using discrete FFT methods to obtain a single estimate for initial and final MF, MPF and AEMG data.

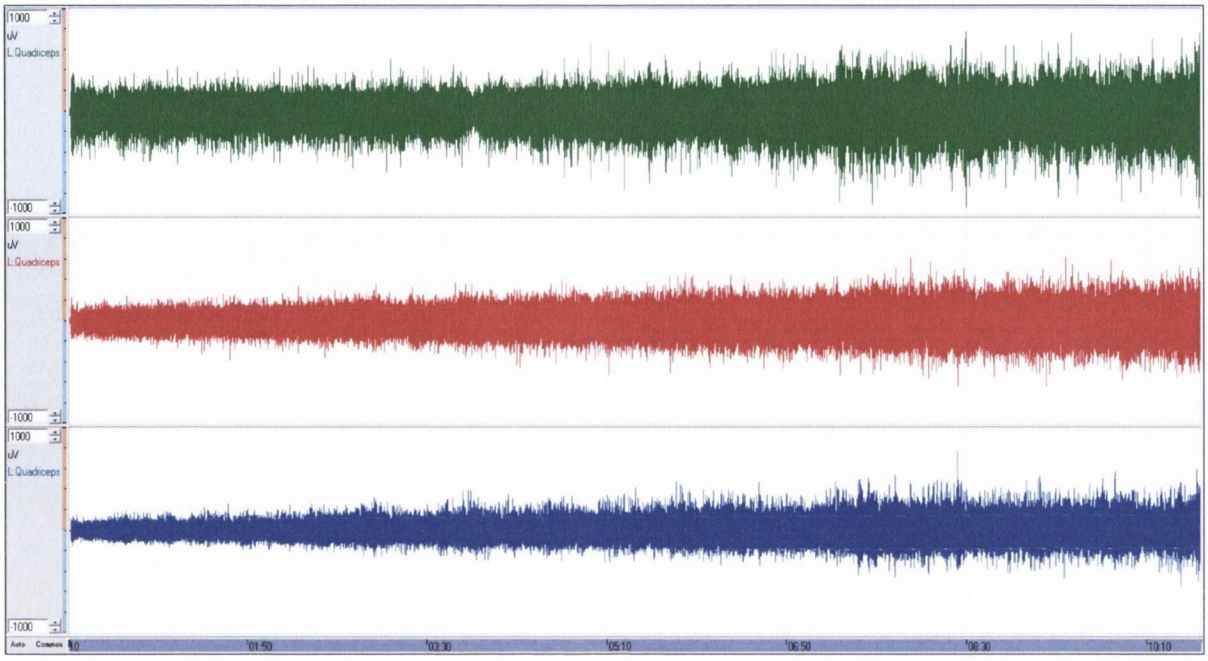

Figure 4.1: Sample raw EMG traces (bipolar scale: ±1000 μV per channel) recorded from RF (green data) VL (red data) and VM (blue data) during a 20% TTF trial.

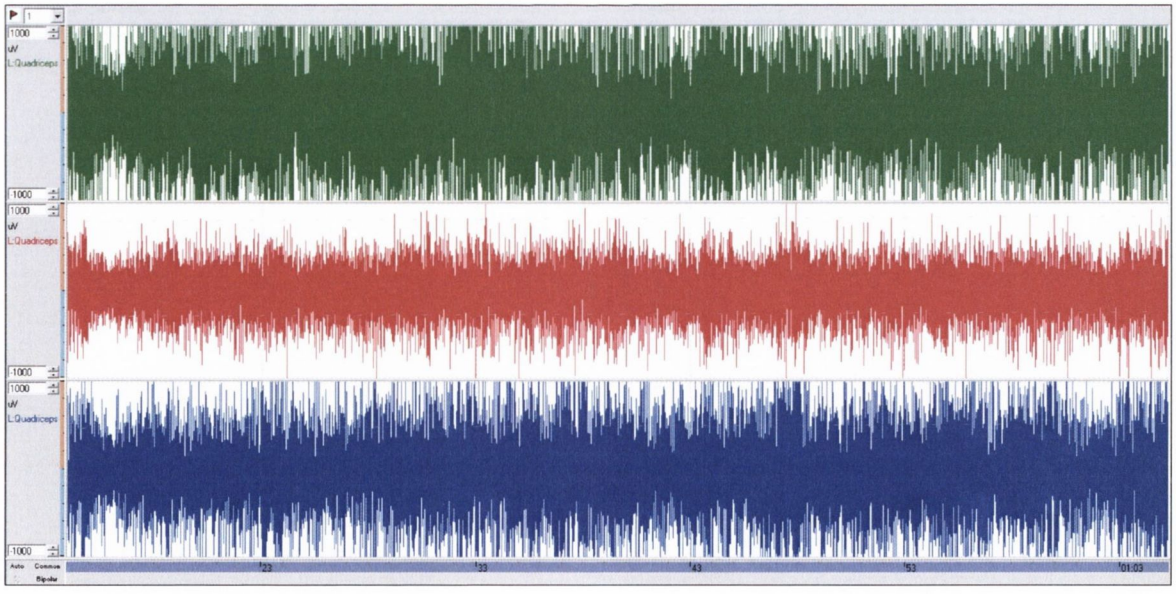

Figure 4.2: Sample raw EMG traces (bipolar scale: ±1000 μV per channel) recorded from RF (green data) VL (red data) and VM (blue data) during an 80% TTF trial.

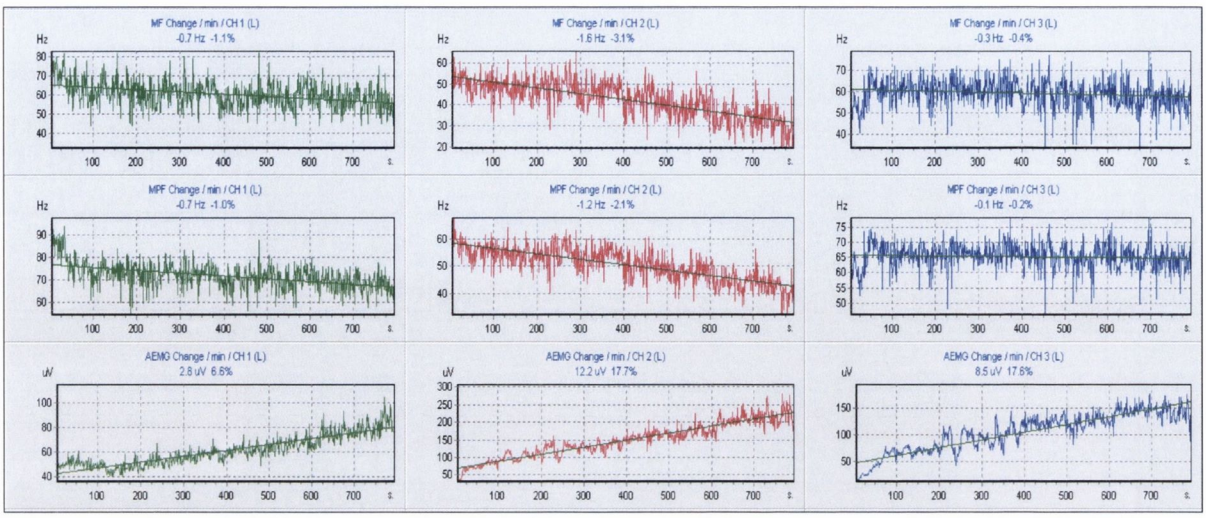

Figure 4.3: Sample of fatigue indices calculated for *Rectus Femoris* (green data) *Vastus Lateralis* (red data) and *Vastus Medialis* (blue data) during the 20% TTF trial (Figure 4.2). MF data are shown across the first row, MPF data are shown across the second row and AEMG data are shown across the third row.

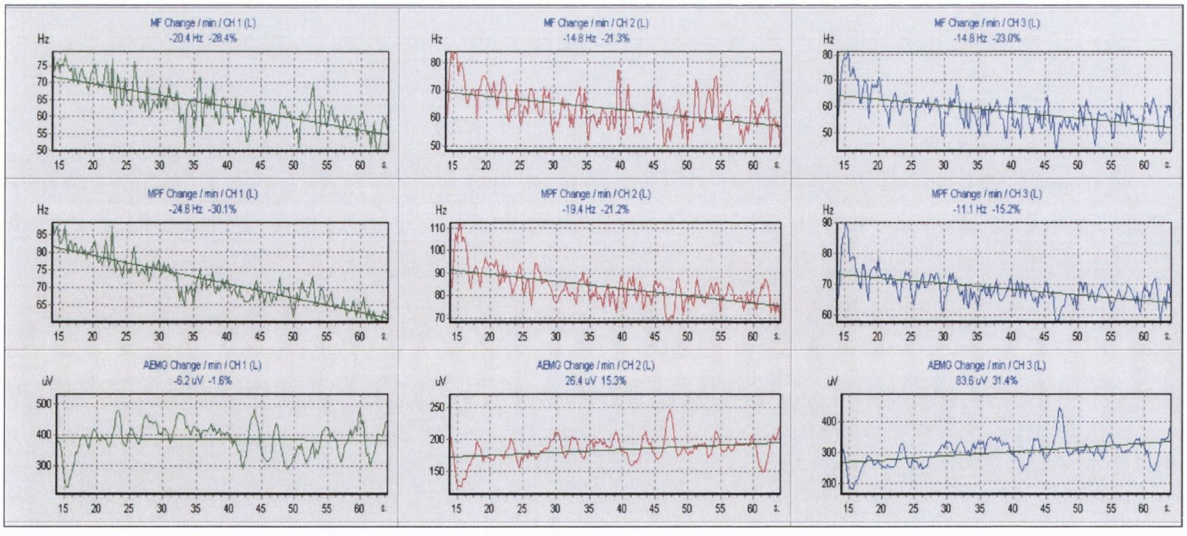

Figure 4.4: Sample of fatigue indices calculated for *Rectus Femoris* (green data) *Vastus Lateralis* (red data) and *Vastus Medialis* (blue data) during the 80% TTF trial (Figure 4.3). MF data are shown across the first row, MPF data are shown across the second row and AEMG data are shown across the third row.

4.3.6: Statistical analysis

Statistical analyses were performed using Graphpad Prism (Graphpad Software, California, USA). Unless otherwise stated, data were expressed as group mean ± SEM. Scatter-plots of data were inspected to ensure no outliers existed before analysis. Comparison of variables across muscles within group were performed on day 2 data, using a single factor ANOVA, *post-hoc* Tukey tests quantified detected differences, $P<0.05$ inferred statistical significance. Comparison of variables between groups was performed on day 2 data using unpaired Student's T-tests. Interclass correlation coefficients (ICC) comparing day 1 and day 2 data expressed relative reliability of measures. Munro's descriptors for reliability coefficients were used to describe the degree of reliability: 0.00 to 0.25 – little, if any correlation; 0.26 to 0.49 – low correlation; 0.50 to 0.69 – moderate correlation; 0.70 to 0.89 – high correlation; and 0.90 – 1.00 – very high correlation (Mathur *et al.*, 2005). Technical error of the measurement (TEM) expressed absolute reliability and reproducibility of the data (Norton *et al.*, 2000). TEM was calculated from the square root of the error variance (the mean of standard deviations from day 1 and day 2) and has the same units as the tested variable. Smaller values of TEM reflect more reproducible measures (Norton *et al.*, 2000).

4.4: RESULTS

4.4.1: Maximal isometric force and muscular endurance

Significant differences between trained and untrained groups were observed in isometric MVC data. The trained group produced significantly greater maximal isometric knee extensor moment in their left (280±18 vs. 210±11 Nm, $P<0.01$) and right leg (288±23 vs. 227±9 Nm, $P<0.05$), see Figure 4.5. When MVC data was normalised relative to body mass these significant differences still existed for left (3.26±0.16 vs. 2.67±0.14 $Nm.kg^{-1}$, $P<0.05$) and right legs (3.41±0.18 vs. 2.89±0.12 $Nm.kg^{-1}$, $P<0.05$), suggesting that the greater body mass of the trained group was not a factor influencing maximum strength (Figure 4.6). In addition, trained volunteers recorded greater muscular endurance, illustrated by significantly longer TTF for both 80% (102±12 vs. 59±4 s, $P<0.01$) and 20% MVC (603±39 vs. 411±28 s, $P<0.001$) trials, see Figure 4.7. Accuracy of task performance was assessed by analysing deviation from target moment during both 80 and 20% MVC trials. During the 20% MVC trial, both groups recorded a standard deviation from target of 1.2% MVC. During the 80% MVC trial the standard deviation from target in the trained and untrained groups were 2.5 and 4.3% MVC, respectively. While greater deviations were observed in both groups during the 80% MVC trial, these deviations were almost 2 fold higher in untrained despite significantly lower applied moment. This result indicated that the trained group were more successful at maintaining their target moment during the higher % MVC trial.

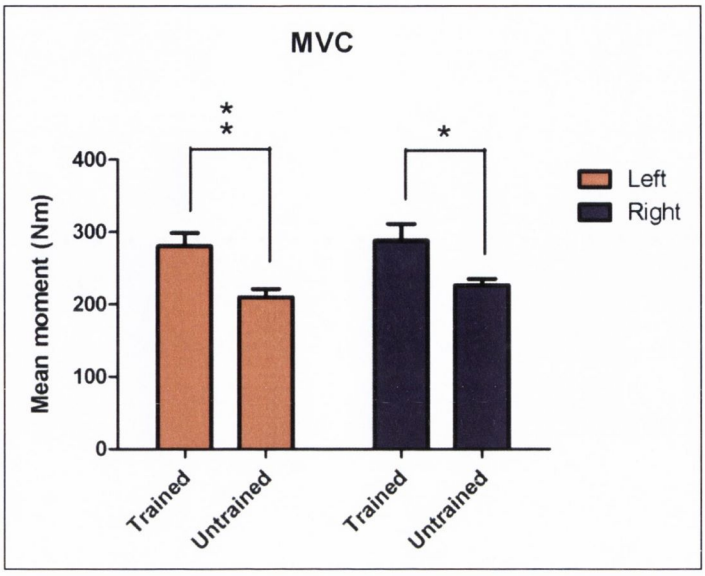

Figure 4.5: Mean ± SEM moment for trained and untrained participants during MVC contractions on both left and right legs. Asterisks infer significant differences between groups (one symbol, $P<0.05$; two symbols, $P<0.01$).

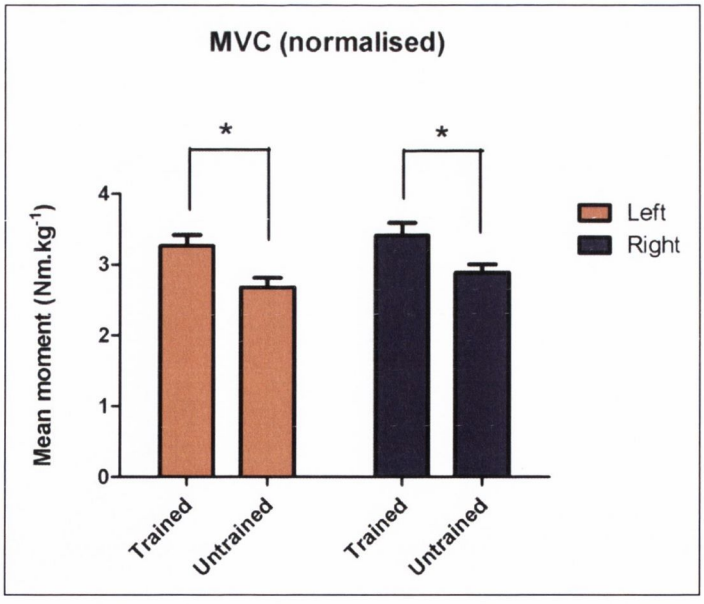

Figure 4.6: Mean ± SEM moment for trained and untrained participants normalised relative to body mass, during MVC contractions performed on both left and right legs. Asterisk infer significant difference between groups ($P<0.05$).

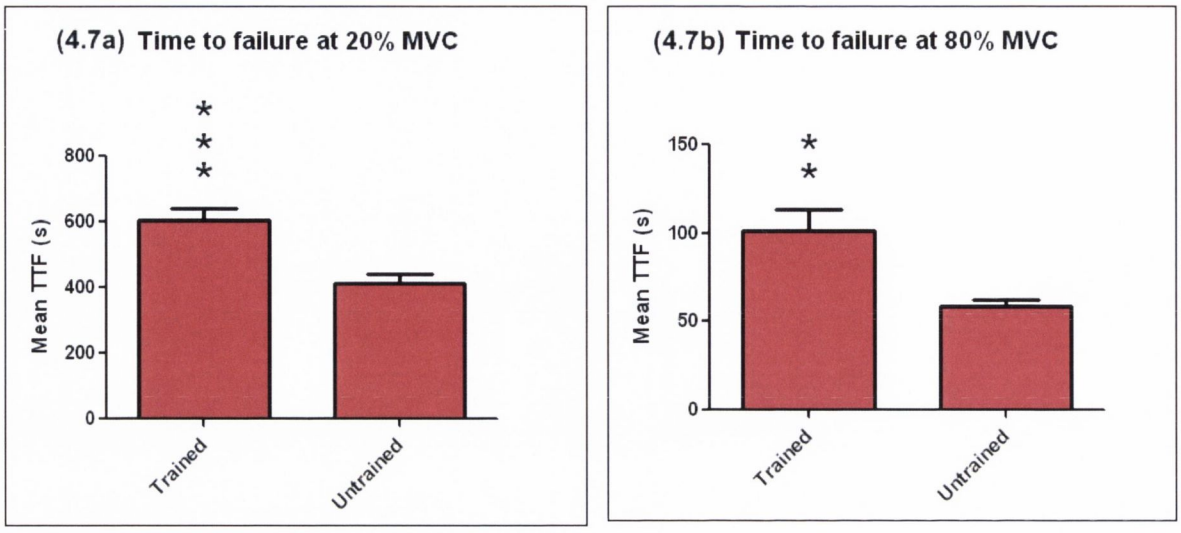

Figure 4.7: Mean ± SEM TTF data performed at 20% (4.7a) and 80% (4.7b) MVC for trained and untrained groups. Asterisks infer significant differences between groups (** $P<0.01$, *** $P<0.001$).

4.4.2: Untrained group

Spectral EMG variables (MF and MPF) decreased across time during the 20 and 80% MVC trials (Tables 4.1 and 4.2, Figure 4.8 to 4.11). This was observed in all investigated muscles as lower final compared to initial MF and MPF data and negative slopes. Progressive increases in AEMG were observed for the *Vastii* during both the 20 and 80% MVC trials (Table 4.3 and Figures 4.12 and 4.13). Mean AEMG in RF exhibited progressive increases during the 20% MVC trial, but unexpectedly exhibited decreases during the 80% MVC trial (Table 4.3 and Figure 4.13, negative slope for RF).

When comparing data across muscles no significant differences were observed between the *Vastii* for any of the spectral or AEMG variables during the 20 or 80% MVC trials. In contrast, RF exhibited significant differences to the *Vastii* for MF, MPF and AEMG data during TTF trials. Differences in frequency variables for RF included significantly greater ($P<0.05$) initial MF and MPF during both trials, significantly greater ($P<0.01$) final MF and MPF during the 20% MVC trial and significantly ($P<0.01$) more negative slope data for MF and MPF during the 80% trial (Table 4.1 and 4.2, respectively). Overall, AEMG data in RF

differed from the *Vastii* with significantly lower ($P<0.01$) final amplitude during the 20% MVC trial and significantly more negative AEMG slope data ($P<0.001$) during the 80% MVC trial (Table 4.3). Initial AEMG for RF in the 20% MVC trial was lower than both *Vastii*; however this difference was only statistically significant ($P<0.05$) in VL.

	Rectus Femoris		***Vastus Lateralis***		***Vastus Medialis***	
20% MVC	**Day 1**	**Day 2**	**Day 1**	**Day 2**	**Day 1**	**Day 2**
Initial (Hz)	63.2 (0.9)	64.6 (0.9) * $	56.3 (1.0)	56.8 (0.7)	56.7 (1.6)	56.2 (0.7)
Final (Hz)	60.6 (0.8)	59.4 (0.6) *** $$	50 (0.8)	47.7 (0.8)	54.2 (2.7)	51.2 (0.8)
Slope (Hz.min^{-1})	-0.4 (0.1)	-0.3 (0.1)	-0.8 (0.1)	-0.8 (0.2)	-0.4 (0.2)	-0.5 (0.1)
80% MVC						
Initial (Hz)	78 (1.0)	76.7 (1.1) ** $$	63.3 (1.1)	59.9 (0.9)	57.3 (2.0)	58.2 (0.7)
Final (Hz)	56.6 (1.1)	56.3 (1.0)	55.6 (0.9)	50.8 (0.4)	50 (1.6)	52.2 (0.9)
Slope (Hz.min^{-1})	-21.5 (0.9)	-20.3 (1.1) ** $$	-7.7 (0.7)	-8.4 (0.7)	-7.2 (0.7)	-7.5 (0.5)

Table 4.1: Mean (SEM) for MF data in untrained group. Shown are the initial, final, normalised and slope of MF data during 20 and 80% TTF trials on both days.

	Rectus Femoris		***Vastus Lateralis***		***Vastus Medialis***	
20% MVC	**Day 1**	**Day 2**	**Day 1**	**Day 2**	**Day 1**	**Day 2**
Initial (Hz)	74.1 (1.0)	75.6 (1.0) * $	65.4 (1.5)	65.9 (1.1)	63.7 (0.6)	62.4 (0.7)
Final (Hz)	70.1 (0.9)	69.3 (0.7) *** $$	58.4 (1.0)	56.6 (0.8)	62 (1.0)	59.1 (1.0)
Slope (Hz.min^{-1})	-0.5 (0.1)	-0.3 (0.0)	-0.8 (0.1)	-0.9 (0.1)	-0.2 (0.1)	-0.3 (0.1)
80% MVC						
Initial (Hz)	86.9 (1.4)	85.5 (1.5) * $	72.9 (1.5)	68.1 (1.3)	66 (1.2)	64.5 (1.1)
Final (Hz)	63.6 (1.3)	63.6 (1.3)	65 (1.2)	59.8 (0.7)	59.3 (1.2)	59.1 (1.2)
Slope (Hz.min^{-1})	-23.9 (1.0)	-22.0 (1.1) ** $$	-9.8 (0.7)	-7.8 (0.8)	-6.5 (0.5)	-6.5 (0.5)

Table 4.2: Mean (SEM) for MPF data in untrained group. Shown are the initial, final, normalised and slope of MPF data during 20 and 80% TTF trials on both days.

	Rectus Femoris		*Vastus Lateralis*		*Vastus Medialis*	
20% MVC	**Day 1**	**Day 2**	**Day 1**	**Day 2**	**Day 1**	**Day 2**
Initial (μV)	61 (3)	46 (2) *	67 (3)	68 (3)	71 (3)	62 (2)
Final (μV)	110 (5)	93 (4) ** $$	178 (10)	177 (13)	173 (8)	167 (8)
Slope ($\mu V.min^{-1}$)	5.0 (0.3)	8.8 (1.5)	12.3 (0.8)	14.4 (1.5)	12.6 (0.7)	15.2 (1.5)
80% MVC						
Initial (μV)	300 (13)	295 (15)	285 (12)	267 (15)	306 (13)	300 (15)
Final (μV)	283 (15)	274 (11)	356 (18)	315 (15)	415 (23)	368 (19)
Slope ($\mu V.min^{-1}$)	-21.0 (3.2)	-21.1 (4.5) ***$$$	79.3 (7.4)	63.1 (6.1)	112.1 (11.6)	81.4 (6.0)

Table 4.3: Mean (SEM) for AEMG data in untrained group. Shown are the initial, final, normalised and slope of AEMG data during 20 and 80% TTF trials on both days.

4.4.3: Trained group

Spectral EMG variables (MF and MPF) decreased across time during the 20 and 80% MVC trials (Table 4.4 and 4.5, Figures 4.8 to 4.11). This was observed in all investigated muscles as lower final compared to initial MF and MPF data and negative slopes. Progressive increases in AEMG were observed for the *Vastii* during both the 20 and 80% MVC trials, see Table 4.6 and Figures 4.12 and 4.13. Mean AEMG in RF exhibited progressive increases during both the 20 and 80% MVC trial

No significant differences were observed between VL and VM for any EMG variables. RF exhibited significant differences from the *Vastii* for MF data during the 80% MVC trial and for AEMG data during the 20% MVC trial (Tables 4.4 and 4.6, respectively). During the 20% MVC trial, final AEMG was significantly lower than VL ($P<0.01$) and VM ($P<0.05$), as was AEMG slope data ($P<0.01$). Initial MF for RF was significantly higher than VL ($P<0.001$) and VM ($P<0.01$) and MF and MPF slope data in RF was significantly lower ($P<0.01$), see Tables 4.4 and 4.5, respectively. In contrast to the untrained group, spectral variables in RF were not significantly different from the *Vastii* during the 20% MVC trial, and no significant differences in AEMG variables were observed during the 80% MVC trial.

	Rectus Femoris		*Vastus Lateralis*		*Vastus Medialis*	
20% MVC	Day 1	Day 2	Day 1	Day 2	Day 1	Day 2
Initial (Hz)	67.4 (0.6)	68.1 (0.6)	61.2 (1.1)	62.1 (1.0)	55.9 (0.6)	60.3 (0.8)
Final (Hz)	57.9 (0.6)	59.1 (0.6)	52.0 (1.3)	51.0 (1.3)	52.1 (0.9)	55.6 (0.9)
Slope ($Hz.min^{-1}$)	-0.5 (0.0)	-0.4 (0.0)	-1.3 (0.2)	-1.2 (0.2)	-0.3 (0.1)	-0.3 (0.0)
80% MVC						
Initial (Hz)	70.7 (1.6)	72.8 (0.4) *** $$	58.9 (0.8)	60.9 (0.8)	60.7 (0.7)	61.5 (0.8)
Final (Hz)	51.8 (2.5)	51.4 (0.8)	48.9 (0.9)	51.6 (0.9)	53 (0.9)	45.9 (1.8)
Slope ($Hz.min^{-1}$)	-17.3 (0.8)	-16.4 (0.7) ** $$	-9.4 (0.7)	-9.3 (0.7)	-8.6 (0.4)	-8.6 (0.4)

Table 4.4: Mean (SEM) MF data in trained group. Shown are the initial, final and slope of MF data during 20 and 80% TTF trials on both days.

	Rectus Femoris		*Vastus Lateralis*		*Vastus Medialis*	
20% MVC	Day 1	Day 2	Day 1	Day 2	Day 1	Day 2
Initial (Hz)	79.1 (0.7)	79.3 (0.6)	74.0 (1.8)	73.9 (1.7)	66.3 (0.8)	69.6 (0.9)
Final (Hz)	69.1 (0.8)	69.5 (0.6)	60.8 (1.4)	59.4 (1.4)	63.1 (0.9)	65.8 (0.9)
Slope ($Hz.min^{-1}$)	-0.6 (0.1)	-0.5 (0.1)	-1.5 (0.2)	-1.5 (0.2)	-0.3 (0.1)	-0.3 (0.1)
80% MVC						
Initial (Hz)	80.8 (0.6)	82.9 (0.7)	73.4 (2.3)	77.9 (2.3)	69.3 (1.0)	71.1 (1.1)
Final (Hz)	57.6 (1.0)	56.8 (1.0)	61.5 (2.2)	64.3 (2.2)	59.7 (1.2)	58.7 (1.2)
Slope ($Hz.min^{-1}$)	-20.5 (1.1)	-19.9 (1.0) ** $$	-12.2 (1.0)	-11.8 (0.9)	-9.0 (0.6)	-9.3 (0.4)

Table 4.5: Mean (SEM) MPF data in trained group. Shown are the initial, final and slope of MPF data during 20 and 80% TTF trials on both days.

	Rectus Femoris		*Vastus Lateralis*		*Vastus Medialis*	
20% MVC	**Day 1**	**Day 2**	**Day 1**	**Day 2**	**Day 1**	**Day 2**
Initial (μV)	52 (1.9)	53 (2)	72 (4)	74 (4)	65 (4)	61 (3)
Final (μV)	86 (2.5)	95 (3) ** $	182 (9)	196 (9)	159 (9)	172 (10)
Slope ($\mu V.min^{-1}$)	4.4 (0.9)	5.9 (0.6) ** $$	14.5 (1.6)	16.1 (1.6)	12.7 (1.3)	13.1 (1.3)
80% MVC						
Initial (μV)	300 (10)	276 (10)	328 (17)	309 (15)	367 (16)	366 (15)
Final (μV)	366 (12)	331 (9)	408 (17)	424 (22)	477 (24)	493 (23)
Slope ($\mu V.min^{-1}$)	39.8 (3.6)	41.3 (3.2)	56.1 (4.9)	77.9 (6.2)	78.0 (7.4)	74.2 (4.2)

Table 4.6: Mean (SEM) AEMG data in trained group. Shown are the initial, final and slope of AEMG data during 20 and 80% TTF trials on both days.

4.4.4: Comparison across groups

Initial and final data for MF, MPF and AEMG performed by the trained and untrained groups are presented graphically, see Figures 1 to 4. No significant differences were observed between groups for any variables in VL or VM during the 20 or 80% MVC trials. No significant differences were observed between groups for any variables in RF during the 20% MVC trial. However, a significant difference between trained and untrained groups for AEMG slope data in RF was observed during the 80% MVC trial (+41.3±3.2 vs. -21.1±4.5 $\mu V.min^{-1}$, $P<0.01$), see Figure 4.13. The negative slope for AEMG in RF exhibited by the untrained group was the only temporal EMG fatigue index which did not conform to the normal EMG responses to fatigue and was unexpected.

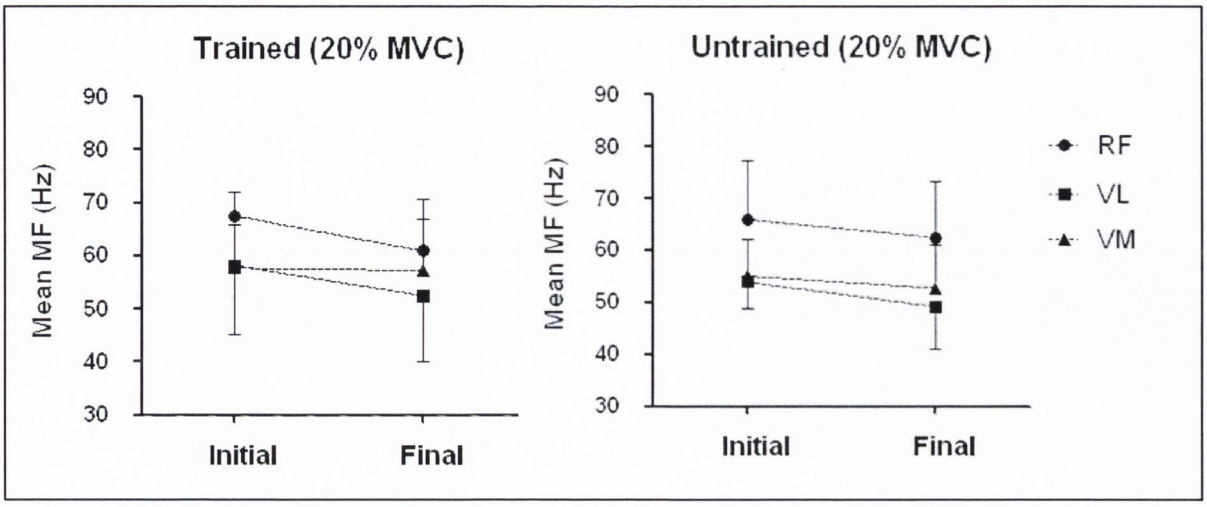

Figure 4.8: Mean ± SD initial and final MF during 20% MVC trials in trained and untrained groups. No significant differences were observed for initial, final or slope data between groups.

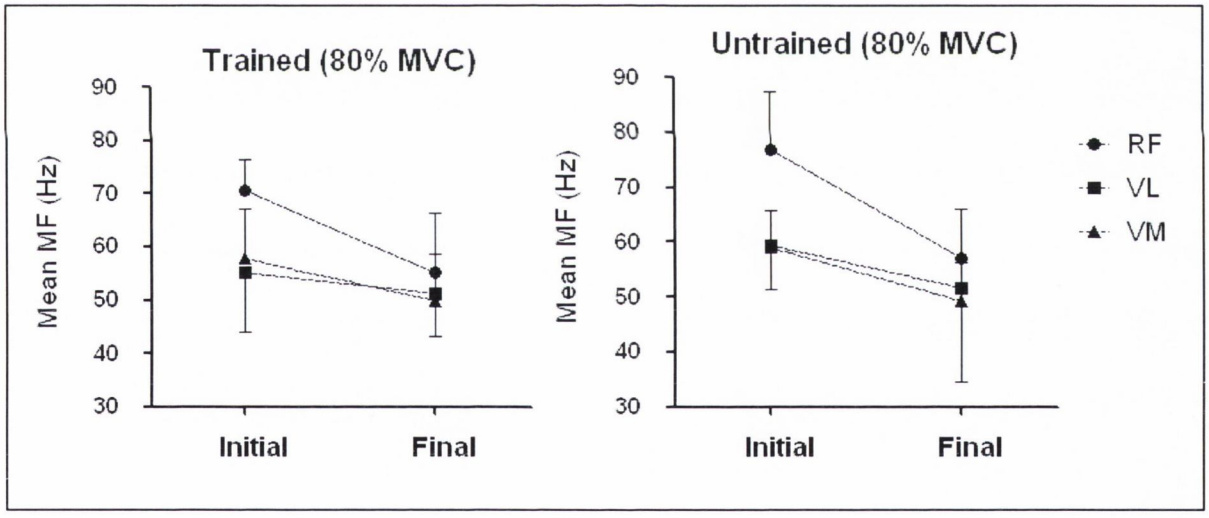

Figure 4.9: Mean ± SD initial and final MF during 80% MVC trials in trained and untrained groups. No significant differences were observed for initial, final or slope data between groups.

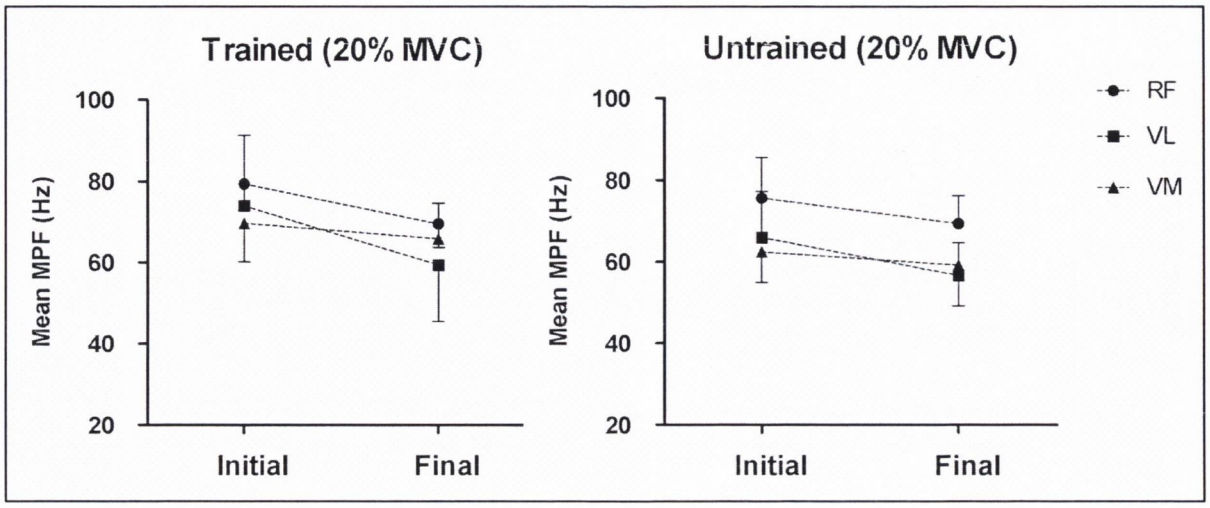

Figure 4.10: Mean ± SD initial and final MPF during 20% MVC trials in trained and untrained groups. No significant differences were observed for initial, final or slope data between groups.

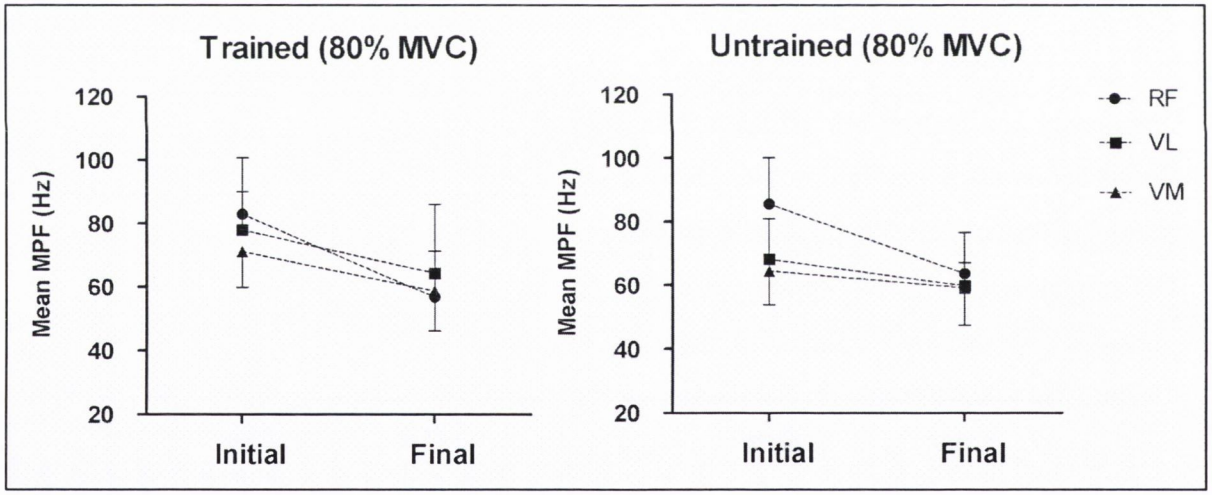

Figure 4.11: Mean ± SD initial and final MPF during 80% MVC trials in trained and untrained groups. No significant differences were observed for initial, final or slope data between groups.

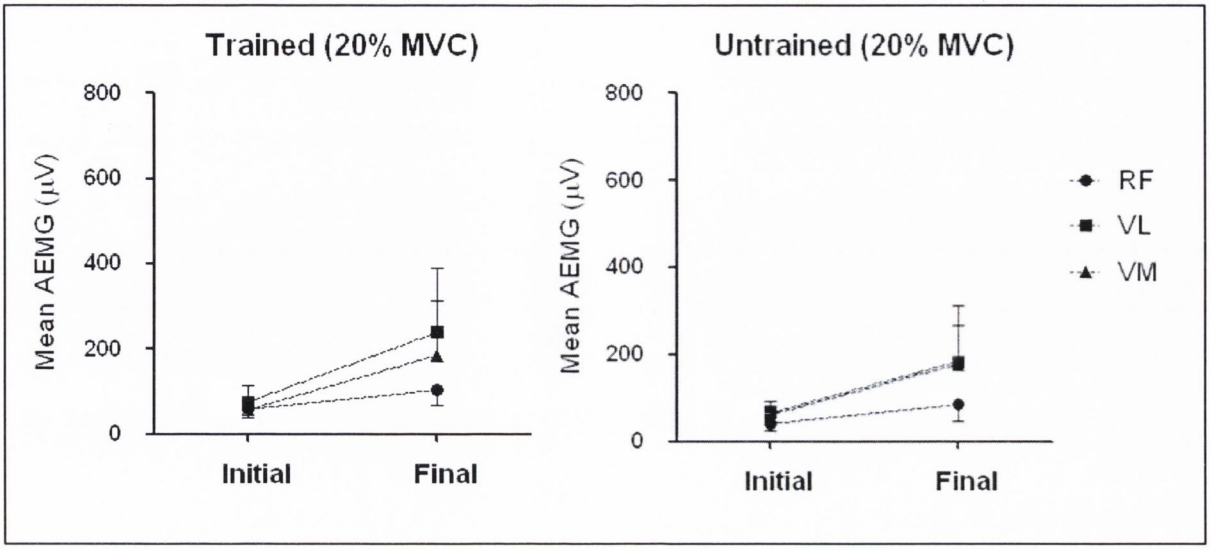

Figure 4.12: Mean ± SD initial and final AEMG during 20% MVC trials in trained and untrained groups. No significant differences were observed for initial, final or slope data between groups.

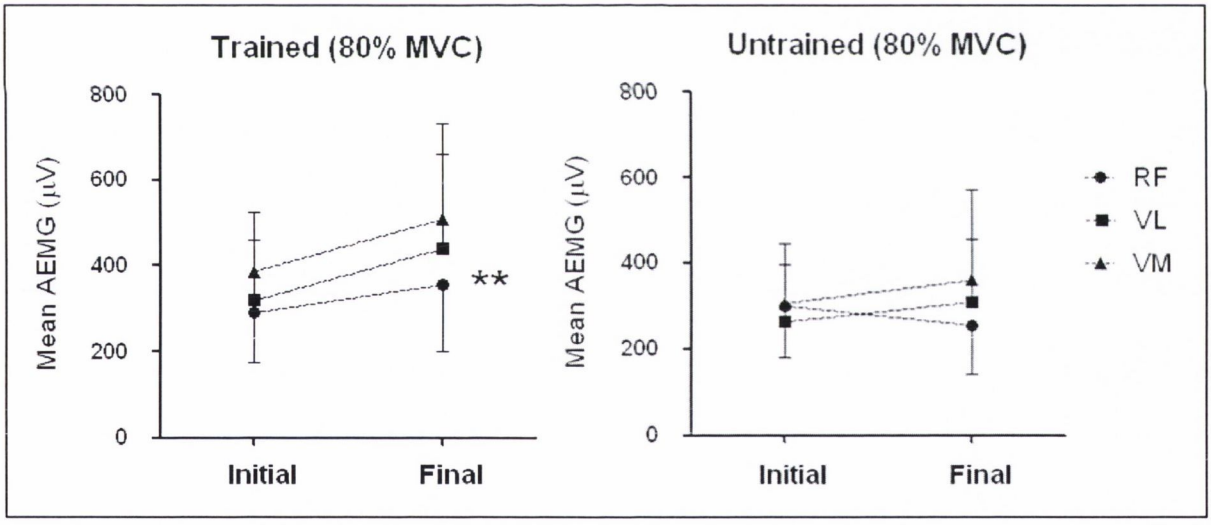

Figure 4.13: Mean ± SD initial and final AEMG during 80% trials in trained and untrained groups. ** denote significantly different RF slope compared to untrained group ($P<0.01$).

4.4.5: Reliability and reproducibility

The trained group showed high to very high relative reliability assessed by ICC (0.70 to 0.98) for all MF variables during their 20% MVC trial. In contrast, the untrained group showed low to high reliability for MF variables (0.18 to 0.89) during their 20% MVC trial. During the 80% trial, the trained group showed moderate to very high reliability for MF variables (0.51 to 0.93). The untrained group showed little if any reliability for slope of MF in RF (0.35) and VL (0.26) and low to very high reliability for other MF variables (0.47 to 0.87). In general, the trained group showed better reproducibility illustrated by the lower TEM data for most MF variables (with the exception of final MF in VM, see Table 4.7).

	Rectus Femoris		*Vastus Lateralis*		*Vastus Medialis*	
20% MVC	**Trained**	**Untrained**	**Trained**	**Untrained**	**Trained**	**Untrained**
Initial (Hz)	0.84 (2.38)	0.63 (5.11)	0.94 (2.54)	0.82 (3.47)	0.74 (3.70)	0.82 (2.47)
Final (Hz)	0.89 (1.89)	0.70 (3.88)	0.89 (4.01)	0.69 (4.14)	0.88 (2.92)	0.78 (3.89)
Slope (Hz.min^{-1})	0.88 (0.13)	0.31 (0.48)	0.97 (0.23)	0.67 (0.63)	0.98 (0.17)	0.75 (0.29)
80% MVC						
Initial (Hz)	0.89 (2.09)	0.88 (3.54)	0.93 (1.95)	0.68 (5.59)	0.86 (2.92)	0.54 (4.33)
Final (Hz)	0.87 (2.68)	0.91 (2.89)	0.89 (3.01)	0.22 (6.42)	0.57 (9.27)	0.41 (6.04)
Slope (Hz.min^{-1})	0.91 (2.1)	0.68 (5.71)	0.87 (1.64)	0.55 (4.45)	0.95 (0.8)	0.35 (4.06)

Table 4.7: ICCs (TEM) for MF data in the trained and untrained groups during TTF trials at 20 and 80% MVC.

For MPF, the trained group exhibited moderate reliability for initial MPF in VM (0.69) and high to very high relative reliability for all other variables (0.76 to 0.98) during the 20% trial. The untrained group exhibited low reliability for slope in RF (0.34). All other variables exhibited moderate to high reliability (0.51-0.89) during the 20% trial. During the 80% trial, the trained group exhibited high to very high reliability for all other variables (0.74 to 0.95). The untrained group exhibited low reliability for final MPF in VL (0.42), and slope of MPF in VM (0.49). All other variables exhibited moderated to very high reliability (0.53-0.92). In

general, the trained group showed better reproducibility illustrated by the lower TEM data for nearly all MPF variables (Table 4.8).

	Rectus Femoris		***Vastus Lateralis***		***Vastus Medialis***	
20% MVC	**Trained**	**Untrained**	**Trained**	**Untrained**	**Trained**	**Untrained**
Initial (Hz)	0.98 (2.1)	0.51 (6.8)	0.98 (2.1)	0.89 (4.24)	0.69 (4.82)	0.69 (3.65)
Final (Hz)	0.92 (3.71)	0.65 (4.55)	0.92 (3.71)	0.67 (4.97)	0.82 (3.64)	0.85(3.68)
Slope ($Hz.min^{-1}$)	0.97 (0.29)	0.34 (0.45)	0.97 (0.28)	0.78 (0.52)	0.96 (0.21)	0.85 (0.19)
80% MVC						
Initial (Hz)	0.89 (2.15)	0.87 (4.8)	0.85 (8.69)	0.79 (6.14)	0.85 (3.93)	0.53 (7.75)
Final (Hz)	0.89 (3.24)	0.92 (3.31)	0.91 (6.44)	0.42 (7.6)	0.96 (2.3)	0.57 (7.48)
Slope ($Hz.min^{-1}$)	0.93 (2.65)	0.6 (6.57)	0.98 (0.9)	0.83 (3.02)	0.91 (1.6)	0.49 (3.56)

Table 4.8: ICCs (TEM) for MPF data in the trained and untrained groups during TTF trials at 20 and 80% MVC.

For AEMG, the trained group exhibited high to very high reliability for all variables (0.71 to 0.95) during their 20% MVC trial while the untrained group exhibited moderate to very high reliability (0.65 to 0.91). During the 80% trial, the trained group again showed high to very high reliability for all variables (0.84 to 0.97). In contrast, the untrained group showed little if any reliability for final AEMG in VL (0.23), initial AEMG in VM (0.23) and low reliability for slope data in VM (0.38). All other variables exhibited moderate to high reliability (0.41 to 0.84). Once again, the trained group showed better reproducibility illustrated by the lower TEM data for all AEMG variables, see Table 4.9.

	Rectus Femoris		*Vastus Lateralis*		*Vastus Medialis*	
20% MVC	**Trained**	**Untrained**	**Trained**	**Untrained**	**Trained**	**Untrained**
Initial (μV)	0.87 (6.90)	0.13 (23.00)	0.98 (4.89)	0.78 (12.93)	0.89 (12.23)	0.72 (12.40)
Final (μV)	0.86 (9.50)	0.66 (27.10)	0.92 (23.90)	0.92 (31.30)	0.97 (15.9)	0.91 (22.50)
Slope ($\mu V.min^{-1}$)	0.90 (1.59)	0.87 (1.16)	0.94 (3.40)	0.71 (6.15)	0.96 (2.28)	0.67 (6.50)
80% MVC						
Initial (μV)	0.93 (26.90)	0.86 (49.40)	0.91 (46.10)	0.76 (64.00)	0.92 (42.7)	0.82 (57.70)
Final (μV)	0.83 (42.90)	0.85 (43.20)	0.91 (64.40)	0.78 (77.10)	0.95 (48.80)	0.76 (99.80)
Slope ($\mu V.min^{-1}$)	0.87 (11.9)	0.28 (34.00)	0.74 (27.80)	0.47 (48.40)	0.83 (28.50)	0.52 (60.00)

Table 4.9: ICCs (TEM) for AEMG data in the trained and untrained groups during TTF trials at 20 and 80% MVC.

4.5: DISCUSSION

The most pertinent observation in the current study was the altered response to fatigue for RF in the trained group (Figure 4.13). This was evident only during the 80% MVC trial and illustrates the trained group's enhanced ability to recruit RF during fatiguing contractions, especially at higher levels of contractile force. This adaptation towards progressive co-activation of the *Vastii* and RF as fatigue sets in, was entirely absent from the untrained group's results. The trained group's ability to increase agonist co-activation of their knee extensors, especially towards the latter stages of the trial, undoubtedly aided in maintaining the 80% MVC contraction for significantly longer. This response may also explain the group's enhanced accuracy of task performance, illustrated by the smaller deviations from target during their 80% MVC trial.

We initially speculated that increased knee extensor moment observed in the trained group was primarily due to increased muscle CSA, as a result of muscle hypertrophy and hyperplasia (Holloszy, 1976). It has previously been reported that rowers recorded large CSA in Type I and Type II muscle fibres (Hagerman & Staron, 1983). Increased CSA especially in Type II muscle fibres in rowers have been shown to be comparable to increases exhibited by weightlifters and are highly correlated with increased force production (Prince *et al.*, 1976; Hagerman, 1984). However, due to the altered response to fatigue observed in the 80% MVC trial, increased agonist co-activation of the knee extensors cannot be ruled out as another major contributing factor. Absolute MVC data in the trained group in the current study are comparable with isometric knee extensor data reported in male rowers by Parkin *et al.* (2001) but less than data reported by Hagerman and Staron (1983) in international oarsmen performing knee extension exercise. However in agreement with Parkin *et al.* (2001) no significant left-right asymmetries were observed for knee extensors in the current study.

The difference in endurance times between trained and untrained groups may not only be due to enhanced co-activation, but also long-term intramuscular adaptations to endurance exercise. Elite oarsmen have 71% Type I, 24% Type IIA and approximately 5% Type IIB muscle fibres in VL (Hagerman, 2000). In addition to an increased ratio of Type I muscle

fibres, increased CSA of Type I fibres has also been reported (Hagerman, 1984). Both these intramuscular adaptations to endurance training would theoretically increase oxidative capacity and endurance. The differences in knee extensor MVC and endurance observed in the current study could be explained by intramuscular adaptations to training observed in previous rowing groups. Normal physiological adaptations to training reported in rowers are increases in muscular power, and at the same time endurance capacity (Hagerman, 1984, 2000). Increases in CSA of both Type I and more specifically Type II fibres, will increase maximal force production. In addition, the increased number of Type I oxidative muscle fibres and the concurrent increases in CSA enhances the muscle's oxidative and endurance capacity. The current results would appear to reflect both these unique training adaptations in rowers reported by Hagerman (1984, 2000).

Overall, RF registered higher rates of fatigue compared to the *Vastii*, especially at the higher load of 80% MVC. This was illustrated by the significantly greater negative slope observed in MF and MPF during the 80% MVC compared to the corresponding slopes of the *Vastii*, see Figures 4.9 and 4.11, respectively. This response was observed in both trained and untrained groups and may possibly be due to anthropometric and physiological properties of RF. While the VM and VL are mono-articulate, RF is bi-articulate and it has previously been suggested that bi-articulate and mono-articulate muscle groups may exhibit different electrophysiological behaviour which may contribute to differences in fatigue responses (Ebenbichler *et al.*, 1998). In addition, anatomical studies (Polger *et al.*, 1973; Rainoldi *et al.*, 2001) have reported significantly larger Type II muscle fibre diameter in RF (74μm) compared to VM (65μm) or VL (67μm) and higher Type I muscle fibre proportions in the VL. During higher force contractions such as 80% MVC, there is a greater recruitment of Type II fibres (Vollestad, 1997) which most likely results in greater recruitment of RF compared to the *Vastii*. Previously, RF has been shown to be the most fatigable muscle in the knee extensors (Polger *et al.*, 1973; Mathur *et al.*, 2005) and has been shown to exhibit the lowest fatigue thresholds during cycle ergometry (Housh *et al.*, 1995). The current results which showed higher rates of fatigue in the RF especially at 80% MVC are in agreement with previous literature.

While the AEMG differences observed in RF in the current study may indeed be a product of resistance training induced adaptations (Pucci *et al.*, 2006; Carolan & Caferelli, 1992; Sale, 1988), they may also be due to the functional biomechanical demands of rowing. Due to the bi-articulate nature of RF, it involved in both knee extension and hip flexion. Rowing involves knee and hip extension during the drive phase, and knee and hip flexion during the recovery phase (Steer *et al.*, 2006). As such, RF is the only knee extensor muscle actively participating in both distinct phases of the rowing stroke cycle. This unique role of RF in rowing stroke may induce a heightened proprioception and control over recruitment which may otherwise be absent in a sedentary population.

It seems likely that the enhanced fatigue resistance of the trained group during the 80% trial, was at least in part due to enhanced knee extensor synergy. This manifest itself as enhanced RF contribution during the trial, which aided the work being performed by the *Vastii.* The altered pattern of activation between the *Vastii* and RF observed in the current study is in agreement with previous literature. Mathur *et al.* (2005), also reported progressive decreases in RF activity during high intensity (80% MVC) sustained isometric contractions. In addition, Place *et al.* (2006) reported altered RF activity during sustained isometric contractions, performed using target EMG feedback. When feedback was provided from the Vastii, RF activity progressively declined. However, when feedback was provided from the RF, subjects successfully maintained the appropriate level of activity (Place *et al.,* 2006). In both of these studies however, untrained sedentary individuals formed the cohort. Further research examining trained individuals response to fatigue, using EMG biofeedback is therefore warranted.

De Luca (1997) previously suggested that EMG fatigue indices may in the future be capable of determining differences in muscle fibre type thereby providing a non-invasive "electrophysiological muscle biopsy". In addition, it has been shown that initial MF is positively correlated to the proportion of Type II muscle fibres (Macintyre *et al.*, 1998). As a result it may be possible to identify increases or decreases in muscle fibre type proportions from analysis of spectral EMG variables. While initial MF for RF during the 80% MVC trial in the trained group was less than the untrained group (Tables 4.4 and 4.1, respectively), a

finding which based on the results of Macintyre *et al.* (1998) could potentially indicate a decrease in Type II muscle fibre proportions, these results did not attain statistical significance. No differences between trained and untrained groups were observed for any spectral variables in the *Vastii*. The only EMG variable which showed a significant training effect was AEMG slope in RF during the 80% MVC trial, see Figure 4.13. As previously discussed, this result is most likely due to a training induced adaptation towards enhanced co-activation of the knee-extensors as fatigue sets in and is unlikely to represent intramuscular alterations in muscle fibre proportions of the RF. It appears from the current results, that the spectral and amplitude EMG variables assessed were for the most part unable to detect intramuscular differences between a group of trained rowers and a relatively untrained group of college students.

In general, the trained participant group demonstrated better reliability and reproducibility of EMG measures from a test-retest scenario. This was evident by higher ICC and lower TEM data computed for most MF, MPF and AEMG variables during the 20 and 80% MVC trials. In the current study, with one or two exceptions, moderate to very high reliability was observed for initial and final MF during both trails for all muscles investigated, see Table 4.7. This is in accordance not only with Mathur *et al.* (2005) but also with other studies examining sustained contractions of elbow flexors (Bilodeau *et al.*, 1997), back muscles (Elfving *et al.*, 1999) and ramp contractions of knee flexors (Kellis & Katis, 2009). It is likely that improved reliability and reproducibility of measures recorded by the trained group were as a result of better performance of isometric tasks, illustrated during the higher level contractions by smaller deviation from target exhibited in the trained group (2.5 vs. 4.3% MVC). This was most likely due to enhanced synchronisation and co-activation of the knee extensors as described earlier, however improved sensorimotor skills brought about by resistance training may also have played a role (Wong & Ng, 2010). Little or no differences in ICC or TEM between MF and MPF were observed in the current study (Tables 4.7 and 4.8, respectively), suggesting that both are equally reliable measures of EMG frequency.

4.6: CONCLUSION

In conclusion, enhanced co-contraction of knee extensor muscles especially at higher levels of contractile force had the effect of significantly improving endurance times and potentially increasing maximal knee extensor moment. Whether this neuromuscular adaptation to fatigue resulted from resistance training, endurance training or a combination of both, remains to be elucidated. In agreement with previous studies, RF appears more susceptible to fatigue, especially at higher levels of activity (80% MVC), highlighted by greater rates of decrease in MF compared to the *Vastii*. EMG variables were for the most part unable to detect potential intramuscular adaptations indicative of a shift in muscle fibre proportions. Overall, the trained group provided more reliable and reproducible EMG measures of fatigue and was more successful at maintaining their pre-set target during the 80% MVC contraction. Further research, focusing on alternative groups of trained individuals may help establish if adaptations observed in the current study were entirely as a result of resistance training, or if endurance training also played a role in enhancing the progressive knee extensor co-activation. In addition, examining a trained group focused on explosive anaerobic training may provide a more appropriate comparison of potential EMG spectral changes associated with shifts in muscle fibre proportions.

Chapter 5

A biomechanical assessment of ergometer task specificity in flat-water kayaking.

5.1: INTRODUCTION

The development of sports specific ergometers over the last 25 years has revolutionised the training and testing of elite athletes worldwide. Ergometers are primarily designed to simulate biomechanical movements and physiological stresses associated with a specific sport, allowing exercise to be performed in an indoor environment (Dal Monte *et al.,* 1988). In order to validate ergometer usage in laboratory testing of athletes, a quantitative assessment of task specificity must be established. Literature validating task specificity of various ergometer designs, using cardio-respiratory (Kenny *et al.,* 1995; Van Someran *et al.,* 2000; de Campos Mello *et al.,* 2009) or biomechanical variables such as kinematic and force data (Lamb, 1989; Elliott *et al.,* 2002) has been published. Over the last decade, the development of reliable, commercially available air-braked kayak ergometers has led to their usage in training and testing of elite flat-water kayakers. Investigations into the validity of on-ergometer versus on-water testing for metabolic and cardio-respiratory variables ($\dot{V}O_2$, heart rate and blood lactate) have concluded that while kayak ergometers accurately simulated physiological demands of short-term high-intensity kayaking, a biomechanical assessment is required to determine how accurately kayak ergometers simulated the on-water scenario (Van Someran *et al.,* 2000).

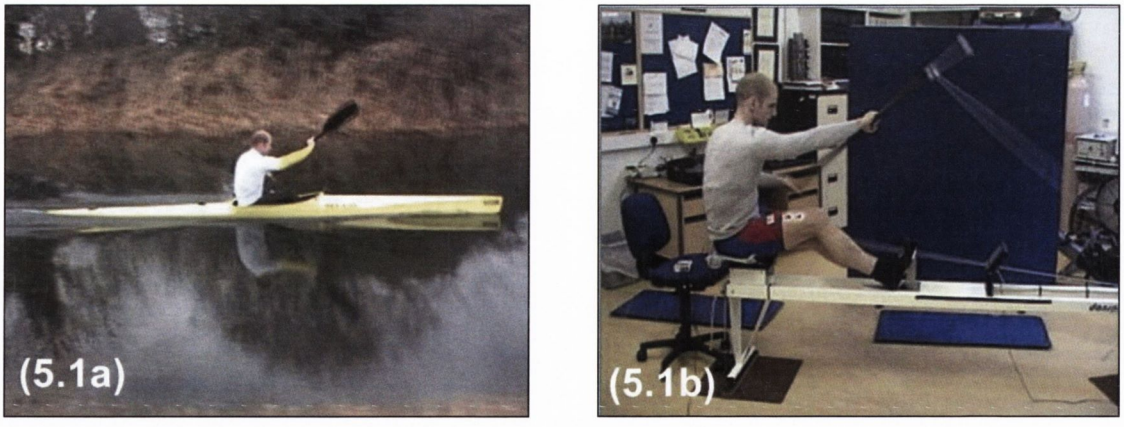

Plate 5.1: A kayaker completing the opposite draw phase of the kayak stroke cycle both on-water (5.1a) and on-ergometer (5.1b). Note the similarity in joint positions.

Surface electromyography (EMG) has been used for over 30 years as an effective technique for assessing muscle recruitment patterns during complex movements (De Luca, 1997) and more recently Nowicky *et al.* (2005) used EMG data in an assessment of rowing ergometer design. Nowicky *et al.* (2005) concluded that a direct biomechanical comparison to on-water rowing would further clarify the accuracy with which land-based ergometers simulated on-water rowing. Several laboratory based kinesiological EMG studies investigating kayaking (Yoshio *et al.*, 1974; Capousek and Bruggemann, 1990; Trevithick *et al.*, 2007) have been documented. Trevithick *et al.* (2007) investigated recruitment patterns of eight shoulder muscles in recreational kayakers and concluded that further research examining muscle recruitment patterns on-water kayaking was warranted, in order to establish if patterns observed during on-ergometer kayaking truly reflect the on-water scenario. Capousek and Bruggemann (1990) used EMG analysis during kayak-specific strength exercises and movement patterns to determine the most active muscles during the kayak stroke; reporting that *Anterior Deltoid* was the most active of the muscle groups investigated. To date, no literature validating the biomechanical task specificity of a kayak ergometer has been published. In addition, no quantitative analysis of EMG data during on-water kayaking has been reported.

5.2: AIMS AND HYPOTHESIS

The primary aim of this study was to validate the biomechanical task specificity of a commercially available kayak ergometer by analysing and comparing EMG, stroke force and 2D kinematic data during on-ergometer and on-water kayaking. A secondary aim was to assess the effect of increasing exercise intensity on recorded muscle activity patterns and stroke force. The study hypothesis was that on-water and on-ergometer kayaking would not differ significantly in duration, timing and magnitude of muscle activation, stroke force or kinematic data. Additionally muscle activity patterns and stroke force would progressively increase in line with exercise intensity.

5.3: MATERIALS AND METHODS

5.3.1: Participants

Ten (n=10) male international flat-water kayakers volunteered to perform this study (mean ± SD; age 20 ± 3yr, height 180 ± 6cm, body mass 73.5 ± 6.2kg). Personal best times for 500m were <110s for senior and <120s for junior kayakers. Prior to participation, enlisted kayakers completed a detailed medical questionnaire (Appendix 3) and underwent a medical examination by a qualified practitioner which included anthropometric, pulmonary and haematological assessments, in order to rule out any subclinical or medical contraindications to maximal exercise testing. All participants were fully informed of the procedures involved in the current study and provided informed consent to participate, see Appendix 3.

5.3.2: Experimental design

The study protocol consisted of three separate assessments and was approved by the Health Sciences Research Ethics Committee in Trinity College Dublin. Initially, a graded incremental test to volitional exhaustion was performed on a kayak ergometer to assess $\dot{V}O_2$, lactate and heart rate response profiles. Incremental test data were subsequently used to set individual exercise intensities (75, 85 and 95% $\dot{V}O_2$peak) for the task specificity trials. The first trial was on-ergometer; the second was on-water, time duration between task specificity trials was between 1 and 7 days and all trials were performed between 09:00 and 11:00 to reduce the potential for circadian variability. During task specificity trials, exercise intensity was matched using heart and stroke rate data attained during incremental testing and all individuals acted as their own control.

Kayakers performed their graded incremental test and on-ergometer task specificity trial on an air-braked, drag adjustable Dansprint kayak ergometer (Dansprint, Hvidovre, Denmark). The ergometer consisted of a fixed flywheel connected to a carbon shaft via a retractable cord attached at either end. Distance from seat to foot-bar was adjusted to match each individual's seat position in the kayak; hand position on the carbon shaft was also adjusted to match on-water paddling position. Ergometer drag setting was adjusted for body mass via a flywheel damper to equate to on-water drag forces associated with body mass

displacement. Power output per stroke (W), mean power output (W) and stroke rate (strokes.min^{-1}) were displayed on the ergometer's display monitor, allowing exercise intensity to be accurately controlled during incremental testing. Kayakers performed the on-water task specificity trial in a standard Nelo Olympic flat-water kayak (Nelo, Porto, Portugal). Kayak dimensions adhered to strict International Canoe Federation guidelines for flat-water racing; mass and length were 12kg and 5.2m, respectively. The seat used during the study was a fixed US model, identical to the seat on the kayak ergometer. Spray decks over the cockpit were not used as contact with EMG recording electrodes on *Vastus Lateralis* risked causing movement artefacts during paddling.

5.3.3: Maximal incremental test

Participants performed pre-trial maximal incremental tests on a Dansprint kayak ergometer, in order to attain specific exercise intensities necessary for the subsequent task specificity trials (see Chapter 2.8). Respiratory exchange variables, along with heart rate and blood lactate data were recorded during each increment of the test (see Chapters 2.9, 2.10 and 2.11, respectively). Data were subsequently used to attain target heart and stroke rates equivalent to 75, 85 and 95% of each participant's $\dot{V}O_2$peak.

5.3.4: Task specificity trials

A 10-min warm-up at heart rate equivalent to 50% of individual kayaker's $\dot{V}O_2$peak was performed prior to commencing task specific trials. Subsequent trials both on-ergometer and on-water consisted of 3 by 3 min bout of exercise at heart and stroke rates equivalent to 75, 85 and 95% of individual kayaker's $\dot{V}O_2$peak. Heart rate data were recorded and monitored using a Garmin Forerunner telemetric heart rate monitor (Garmin, Kansas, USA) and stroke rates were controlled via a digital metronome which kayakers listened to using a standard MP3 player and headphones. Kayakers were instructed to maintain the pre-determined stroke rate throughout and to gradually increase their heart rate over the initial 2 min until their target heart rate had been attained. They then maintained heart rate and stroke rate as close as possible to their individual targets for the final minute of the task specific exercise bout. See Plate 5.2 for a description of the task specificity trial setup.

5.3.5: EMG data

EMG data were recorded on the right side of the body from four muscles involved in the kayak stroke cycle: *Triceps Brachii (long head)* (TB), *Anterior Deltoid* (AD), *Vastus Lateralis* (VL) and *Latissimus Dorsi* (LD) (see Chapter 2.2 and Figure 5.1). Data were synchronised to 2D kinematic data recorded simultaneously, see Chapter 2.3. EMG data from 10 consecutive stroke cycles in the final minute of each task specificity trial, were amplitude processed via root mean squaring and normalised relative to isometric MVC, see Chapters 2.3 and 2.4, respectively. Subsequent temporal normalisation and averaging via cubic spline fitting (Chapter 2.5) produced an average rmsEMG ensemble for each muscle during task specificity trials.

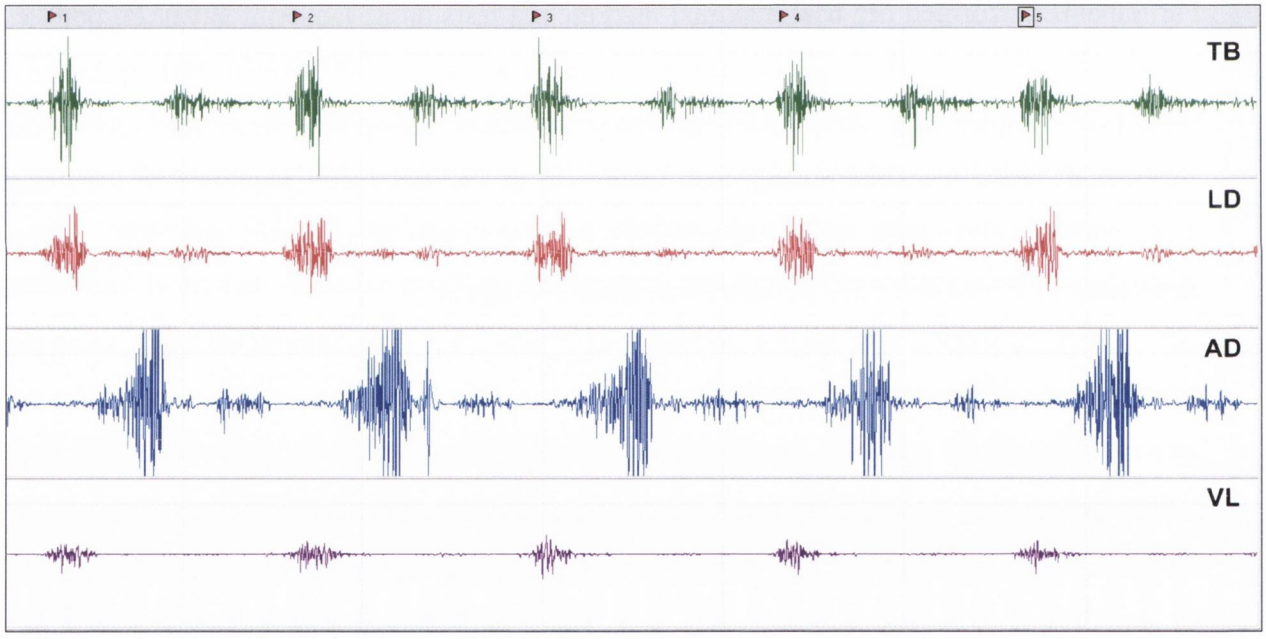

Figure 5.1: Raw EMG trace (bipolar scale: ±3000 μV per channel) recorded for 5 consecutive stroke cycles during on-water kayaking at 85% $\dot{V}O_2$peak. Flag markers at top of the trace indicate the onset of each stroke cycle (see Chapter 2.2 for methodolical description). Channels 1 to 4 (top to bottom) dispay raw EMG data recorded from TB, LD, AD and VL, respectively.

5.3.6: 2D Kinematic and stroke force data

2D video kinematic data were recorded during task specificity trials using a 50 Hz digital video camera (JVC, Yokohama, Japan) positioned orthogonally to the sagittal plane of the kayaker at a distance of 15 to 20m, see Chapter 2.2. In order to quantify the time duration of the draw phase and the draw/transition ratio, both the start and end of the draw phase were identified. Onset of stroke cycle was identified as the first video frame on paddle entry into the water (on-water trials) or the first video frame in which the paddle reference point crossed below the virtual water line (on-ergometer trials). The end of the draw phase was identified as the first video frame when the paddle fully emerged from the water (on-water trials) or the first video frame when the paddle reference point crossed above the virtual water line (on-ergometer trials). Stroke force data was recorded during both on-ergometer and on-water kayaking using strain gauge arrays integrated into two identical commercially available carbon paddle shafts, see Chapter 2.7 and Plate 5.2.

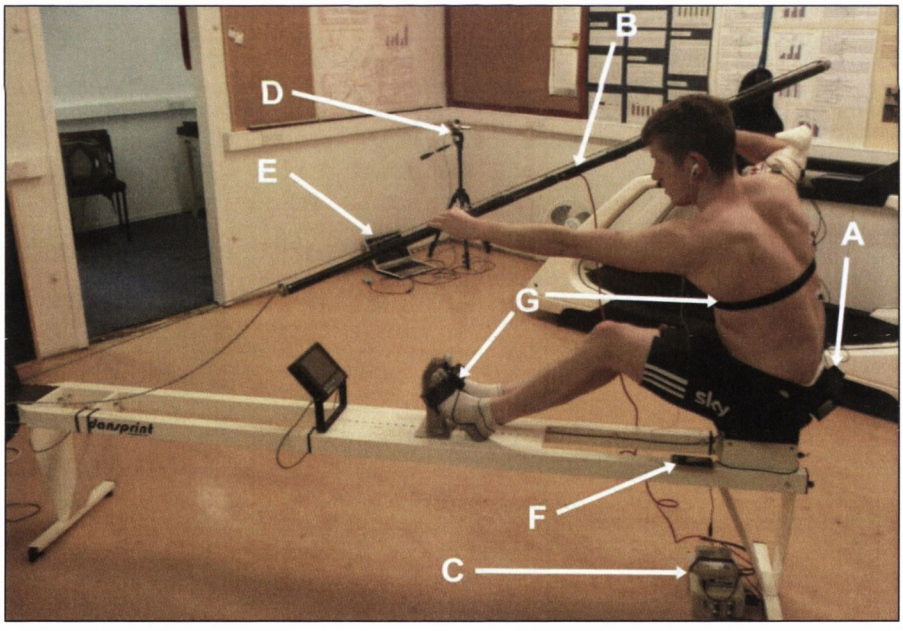

Plate 5.2: The task specificity trial setup. Shown is the ME6000 EMG recorder (A), the strain gauge integrated paddle shaft (B) connected to an amplifier and data logging system (C). Both EMG (A) and 2D kinematic data (D) were transmitted in real time to a laptop (E). A heart rate monitor and transmitter (G) and digital metronome (F) controlled exercise intensity.

5.3.7: Data reduction and statistical analysis

All EMG, force and kinematic data were transferred to Matlab (Mathworks, Massachusetts, USA) for data reduction. For statistical analysis, mean rmsEMG data were averaged for each 10% segment of the stroke cycle. Stroke force data were also averaged over the same 10 consecutive stroke cycles and temporally normalised to attain a group mean stroke force ensemble at each 2% of stroke cycle duration. Data were subsequently analysed to attain measures of peak force (N), absolute time to peak force (s), normalised time to peak force (%), rate of peak force development (RFD_{peak} in $N.s^{-1}$) and rate of 50% peak force development (RFD_{50} in $N.s^{-1}$) as outlined by Benson *et al.* (2011). Integration of the stroke force profile in the first 30% of the stroke cycle quantified the draw impulse (N.s). Paddle shaft angle at stroke cycle onset, time to vertical position, draw phase time and draw/transition ratio were computed from kinematic data attained during trials both on-water and on-ergometer.

Unless otherwise stated, all data are presented as group mean ± SEM and normality assessed using Kolmogorov-Smirnoff tests. Statistical analyses of EMG and stroke force data were performed using 2-way repeated measures ANOVA (condition x intensity), *post-hoc* Tukey tests quantified detected differences. Comparison of kinematic data across conditions (on-water vs. on-ergometer), were performed using paired Student's T-tests. Statistical analyses were performed using Sigma Stat (Systat Software, Chicago, USA) and $P < 0.05$ inferred statistical significance.

5.4: RESULTS

5.4.1: Group physiological characteristics

The group had a mean ± SEM $\dot{V}O_2$peak of 56.4 ± 1.7 mL.kg^{-1}.min^{-1}, BMI of 22.5 ± 0.4 kg.m^{-2} and percentage body fat of 11.6 ± 0.4 %. During incremental testing mean maximal power output at volitional failure was 203 ± 13 W. For each incremental test; heart rate, blood lactate, $\dot{V}O_2$ and stroke rate data were plotted against power output (W). Subsequently, lactate threshold (T_{Lac}) defined as the point of inflection on the lactate curve was determined graphically (Beaver *et al.,* 1986). The mean (± SEM) power, HR and BLa at T_{Lac} were 140 ± 11 W, 171 ± 4 beats.min^{-1} and 3.0 ± 0.2 mmol.L^{-1}, respectively. Mean heart rates equivalent to 75, 85 and 95% of the group $\dot{V}O_2$peak were 168 ± 2, 177 ± 2 and 184 ± 2 beats.min^{-1} and, respectively. Mean stroke rates equivalent to 75, 85 and 95% of the group $\dot{V}O_2$peak were 74 ± 2 , 81 ± 2, and 89 ± 2 stroke.min^{-1}, respectively. During the task specificity trials, no significant differences were observed in heart or stroke rate data recorded during the final minute of exercise across any of the exercise intensities.

5.4.2: 2D Kinematics

Kinematic analysis of the paddle shaft angle at entry, time to vertical position, time of draw phase and transition phase calculated during the 75, 85 and 95% trials are presented in Table 5.1. Time to vertical paddle position occurred significantly earlier comparing on-ergometer with on-water at all exercise intensities ($P < 0.05$). No significant differences were observed between exercise conditions for angle of paddle at entry, draw time or draw/transition ratio. Draw/transition ratio did progressively increase with exercise intensity and stroke rate, see Table 5.1.

In order to better interpret the results of the current study, a brief description of the kinematics of the kayak stroke cycle is necessary. The kayak stroke cycle is a contralateral movement of the upper body with four distinct phases (a draw and transition phase for both right and left sides). The cycle begins when the paddle blade enters the water initiating the draw phase, where the paddle is pulled through the water. The draw phase ends when the paddle blade is removed from the water. Once the paddle exits the water, a transition phase

occurs where the kayaker moves from the end of one draw phase to the start of the draw phase on the opposite side. Once the opposite draw phase is completed, a second transition phase brings the kayaker back to the original side for the onset of the next stroke cycle.

Variable	Intensity	On-ergometer	On-water
Stroke rate (strokes.min^{1})	75%	74 (2)	74 (3)
	85%	81 (2)	81 (2)
	95%	89 (2)	89 (3)
Angle of entry (°)	75%	133 (2)	133 (3)
	85%	134 (2)	133 (2)
	95%	132 (2)	131 (2)
Time to vertical (s)	75%	0.16 (0.02)*	0.19 (0.02)*
	85%	0.16 (0.02)*	0.19 (0.02)*
	95%	0.16 (0.01)	0.18 (0.02)*
Draw time (s)	75%	0.44 (0.02)	0.44 (0.01)
	85%	0.43 (0.01)	0.43 (0.01)
	95%	0.42 (0.01)	0.42 (0.01)
Draw/transition ratio (%)	75%	54.1 (1.7)	54.3 (1.5)
	85%	57.8 (1.4)	58.0 (1.3)
	95%	62.6 (1.3)	63.1 (1.4)

Table 5.1: Group mean (SEM) kinematic variables at 75, 85% and 95% $\dot{V}O_2$peak. Asterisk infer a significant difference between conditions (* $P <$ 0.05).

5.4.3: Muscle activity

2D kinematics synchronised to EMG data allowed us to observe the distinct phases of the stroke cycle during which each investigated muscle was active. As expected, both TB and LD were highly active during the draw phase of the stroke cycle (Figure 5.2a and 5.2b, respectively), when the abducted shoulder undergoes extension and internal rotation, coupled with eccentric elbow flexion which draws the paddle through the water. In addition, VL was active during the draw phase facilitating leg drive, a necessary element of flat-water kayak technique, aiding in the transfer of propulsive forces from the upper body to the kayak via the trunk, hips and legs, see Figure 5.2d. Activity in AD initiated as the paddle exited the water and increased throughout the transition phase. During this phase, the shoulder is externally rotated and begins abduction which facilitates the smooth exit of the paddle and subsequent transition to opposite draw phase. An additional phase of TB activity was observed during the opposite draw phase as the opposite paddle was drawn through the water, however, the level of activity observed during this phase varied greatly between kayakers and between conditions. Activity in AD was also observed towards the end of the opposite draw phase and during opposite transition phase of the stroke cycle, however, this phase of activity was significantly greater during on-ergometer kayaking, see Figure 5.2c. While the magnitude of activity was altered with increasing intensity, the overall patterns of muscle activity remained relatively consistent across exercise intensity (see Appendix 5).

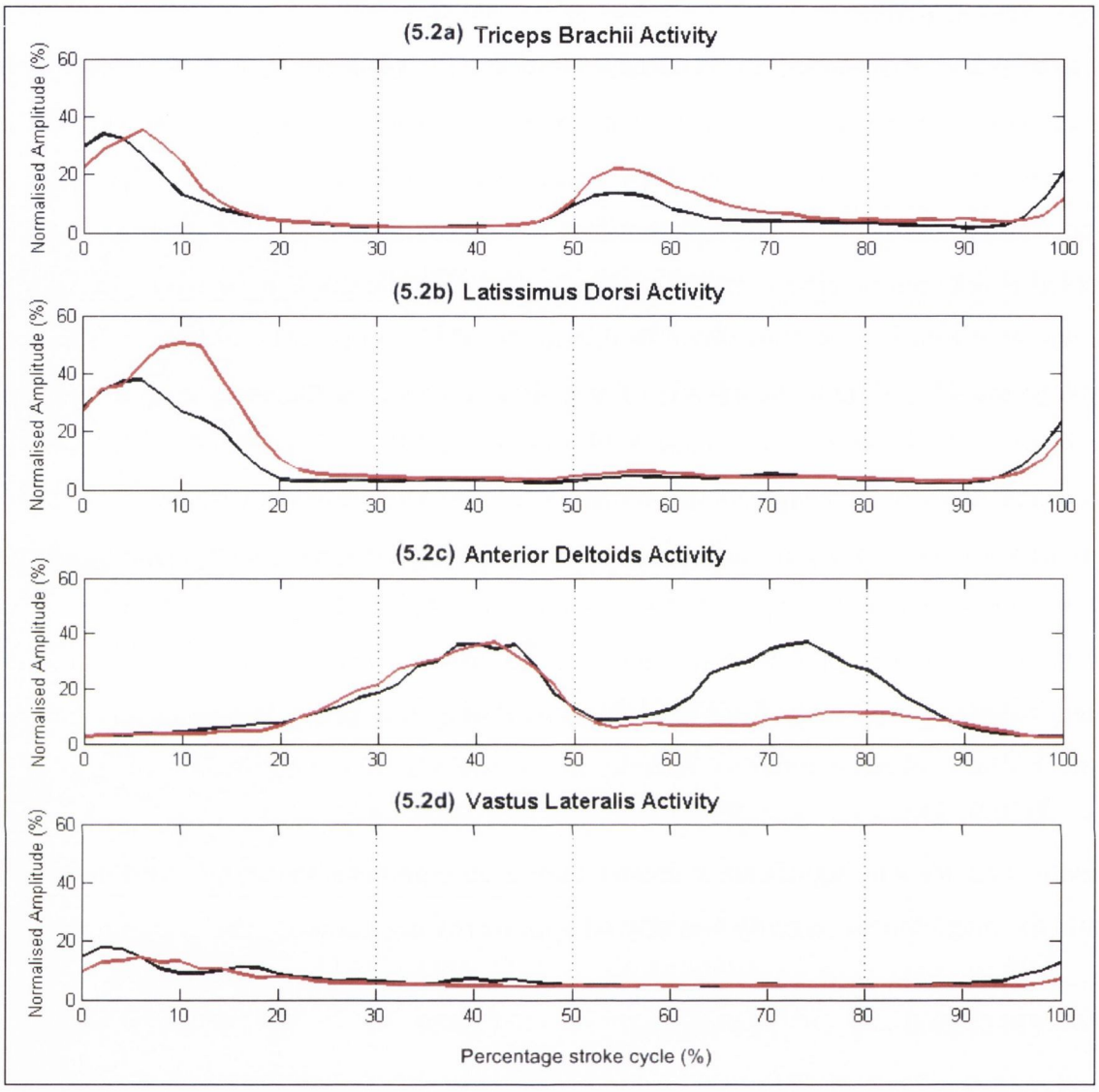

Figure 5.2: Group mean ensemble EMG traces (5.2a to 5.2d) recorded during on-water (red) and on-ergometer (black) kayaking at 85% $\dot{V}O_2$peak. The dashed vertical lines separate the approximate phases of the stroke cycle; draw phase (0-30%), transition phase (30-50%), opposite draw phase (50-80%) and opposite transition phase (80-100%).

Due to variations in the number of peaks and phases of muscle activity observed between kayakers and across conditions, overall muscle activity per stroke cycle was initially quantified using integrated EMG (iEMG) or area of rms amplitude per stroke cycle (Table 5.2). Comparison of mean iEMG data across conditions revealed significantly greater muscle activity during on-water kayaking for both TB ($P < 0.01$ at 75% and $P < 0.001$ at 85

and 95%) and LD ($P < 0.05$ at 85% and $P < 0.01$ at 95%). Unexpectedly, mean AD iEMG activity was significantly greater during on-ergometer kayaking ($P < 0.05$ at all intensities). No significant differences were observed for VL.

Variable	Intensity	On-ergometer	On-water
TB iEMG (μV.s)	75%	171 (14)**	222 (17)
	85%	179 (10)***	239 (15)
	95%	200 (14)***	275 (18)
LD iEMG (μV.s)	75%	152 (14)	172 (13)
	85%	137 (14)*	158 (12)
	95%	142 (15)**	173 (14)
AD iEMG (μV.s)	75%	514 (59)*	372 (46)
	85%	494 (66)*	340 (35)
	95%	487 (57)*	337 (31)
VL iEMG (μV.s)	75%	85 (10)	85 (8)
	85%	82 (9)	83 (6)
	95%	89 (11)	88 (7)

Table 5.2: Group mean (SEM) data for overall iEMG activity across condition and exercise intensity. Asterisk infer a significant difference between conditions (* $P < 0.05$, ** $P < 0.01$, *** $P < 0.001$).

In order to quantify where within the stroke cycle these differences occurred, EMG data was normalised to MVC and averaged for 10% intervals of the stroke cycle to produce group ensembles (Figures 5.3, 5.4 and 5.5). A 2-factor repeated measures ANOVA (intensity x condition) performed on these data revealed significant differences at discrete intervals within the stroke cycle. Mean TB activity was significantly greater during on-water kayaking at the 60% interval across all exercise intensities ($P < 0.01$ at 75 and 85%, $P < 0.05$ at 95%). As exercise intensity increased, differences in mean TB activity also appeared at the 70% and 80% intervals (Figures 5.4a and 5.5a). Mean LD activity was significantly greater during on-water kayaking at the 20% interval, across all exercise intensities ($P <$

0.001, see Figures 5.3b, 5.4b and 5.5b). During the 95% trial, mean LD activity was significantly greater comparing on-ergometer to on-water data at the 100% interval ($P < 0.01$). Pronounced differences were observed in AD activity across all intensities. Mean AD activity during on-ergometer kayaking were significantly greater than on-water at the 70, 80 and 90% intervals across all exercise intensities (Figures 5.3c, 5.4c and 5.5c). No significant differences in VL activity were observed across any of the exercise intensities.

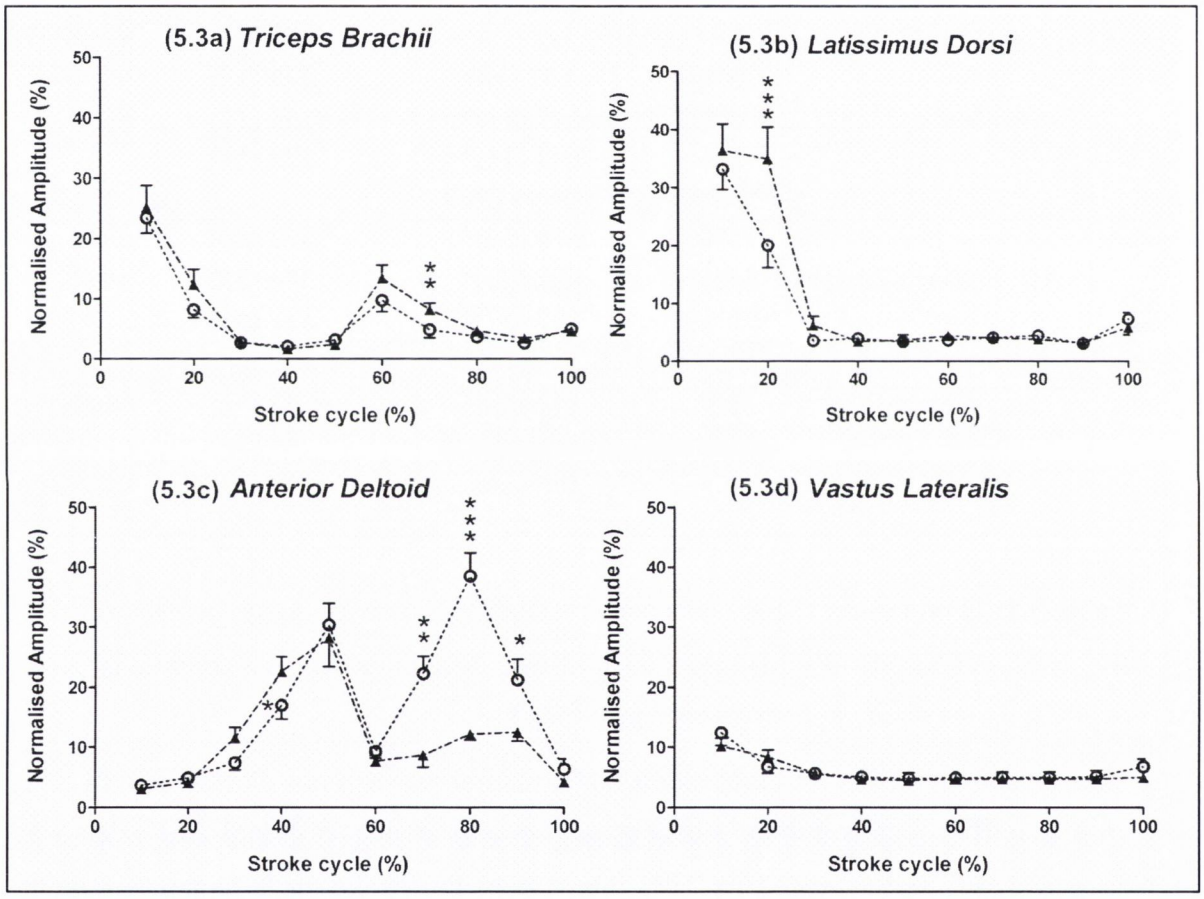

Figure 5.3: Group mean ± SEM (n=10) EMG profiles for on-ergometer (open circles) and on-water kayaking (closed triangles) stroke cycles at 75% $\dot{V}O_2$peak. Each point represents the mean rms amplitude for 10% of the stroke cycle normalised to maximal rms amplitude recorded during isometric MVCs. Asterisk infer difference between conditions at specific 10% intervals (*$P < 0.05$, ** $P < 0.01$, *** $P < 0.001$).

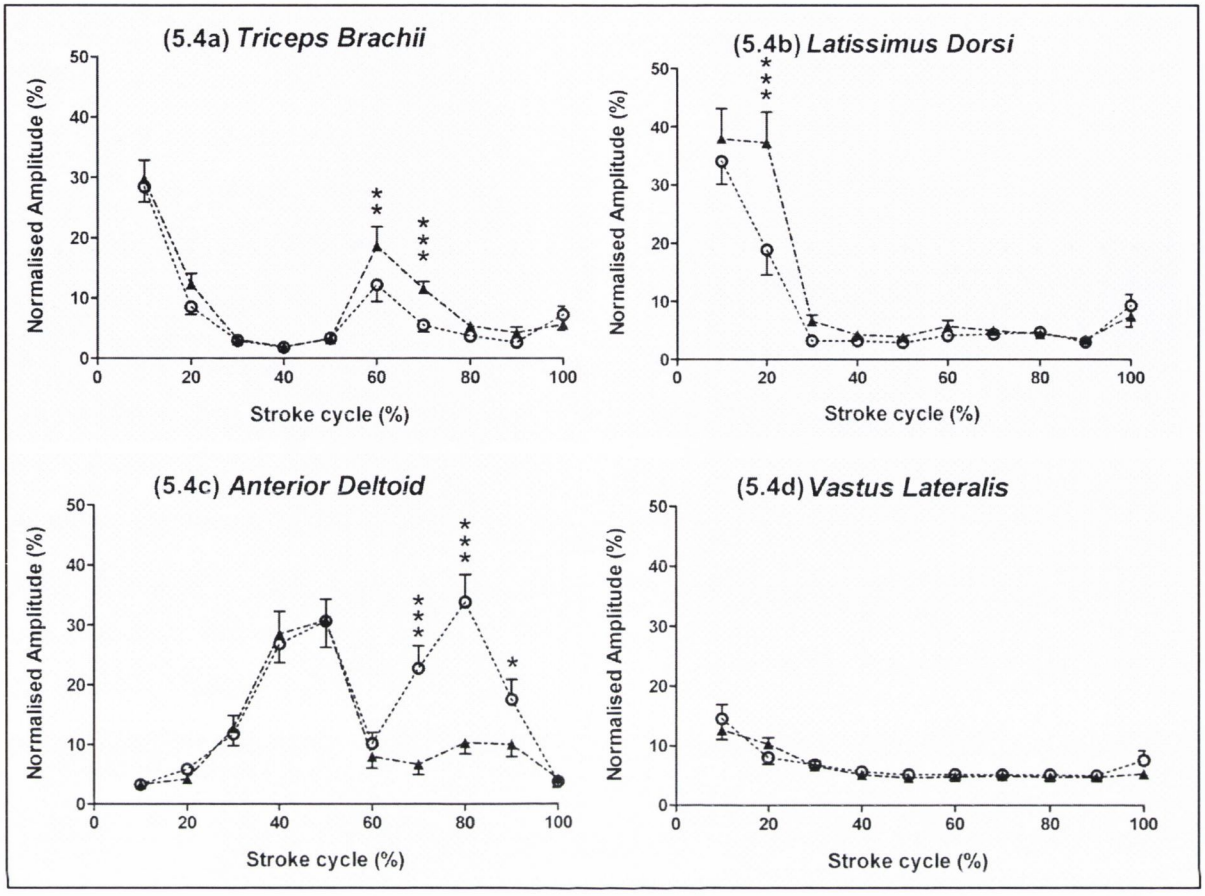

Figure 5.4: Group mean ± SEM (n=10) EMG profiles for on-ergometer (open circles) and on-water kayaking (closed triangles) stroke cycles at 85% $\dot{V}O_2$peak. Each point represents the mean rms amplitude for 10% of the stroke cycle normalised to maximal rms amplitude recorded during isometric MVCs. Asterisk infer difference between conditions at specific 10% intervals (*P < 0.05, ** P < 0.01, *** P < 0.001).

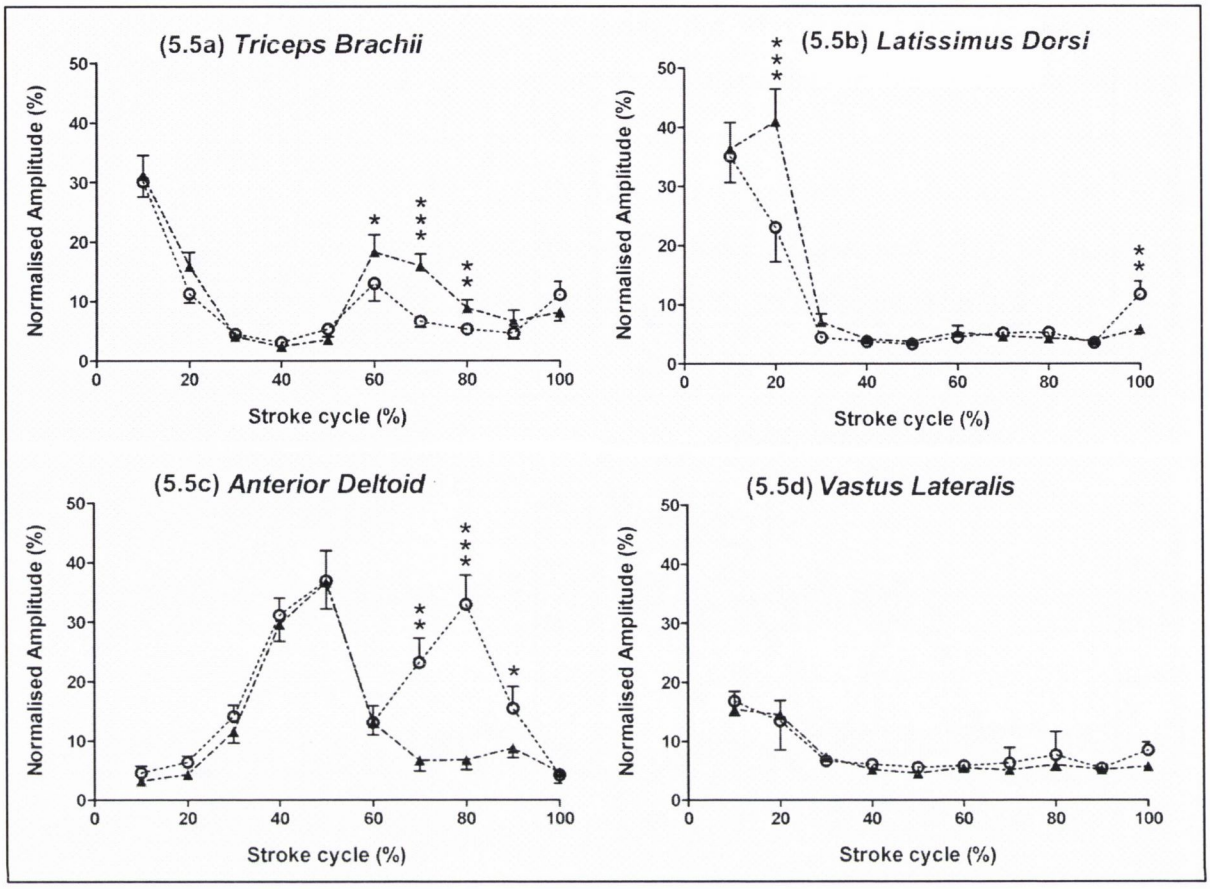

Figure 5.5: Group mean ± SEM (n=10) EMG profiles for on-ergometer (open circles) and on-water kayaking (closed triangles) stroke cycles at 95% $\dot{V}O_2$peak. Each point represents the mean rms amplitude for 10% of the stroke cycle normalised to maximal rms amplitude recorded during isometric MVCs. Asterisk infer difference between conditions at specific 10% intervals (* $P <$ 0.05, ** $P < 0.01$, *** $P < 0.001$).

5.4.4: Stroke force analysis

Due to minor technical problems during on-water trials (water interference with strain gauge array), only 7 full sets of stroke force data were attained. Therefore all statistical analysis was performed on a sub-group (n=7). Quantitative results for stroke force data are presented in Table 5.3. Analysis of rates of force development revealed that mean RFD_{50} was significantly greater on-water compared to on-ergometer at 75 ($P <0.05$), 85 ($P < 0.05$) and 95% $\dot{V}O_2$peak ($P < 0.001$). This can clearly be seen from Figure 5.6 as slower development

of force in the early portion of the on-ergometer compared to on-water draw phase. In contrast to RFD_{50}, mean RFD_{peak} was greater during the on-ergometer stroke cycle. The draw impulse (N.s) which quantified the overall forces applied during the draw phase revealed that greater forces were applied on-water, however this difference was not statistically significant at any exercise intensity (Table 5.3). Although not quantified, a noticeable difference in forces occurred during both the transition and opposite draw phases of the stroke cycle. During the transition phase, no detectable force was recorded on-water, the paddle is not in the water during this phase and minimal external forces are being exerted through the shaft. However, a noticeable force was recorded during the equivalent phase on-ergometer; see Figure 6 from 30 to 50% stroke cycle. This difference also manifest itself during the opposite draw phase, where a larger displacement of the shaft (by the opposite draw impulse) was observed on-ergometer. These differences are most likely due the external loading mechanism of the ergometer which exerts an elastic recoil force on the paddle shaft via the connecting ropes and elastic chord.

Variable	Intensity	On-ergometer	On-water
Peak force (N)	75%	208 (9)	195 (7)
	85%	224 (7)	238 (10)
	95%	232 (10)	245 (10)
Time to peak (s)	75%	0.16 (0.01)	0.19 (0.01)
	85%	0.16 (0.01)	0.19 (0.01)
	95%	0.17 (0.01)	0.20 (0)
Time to peak (%)	75%	10 (0.2)	12.3 (1.7)
	85%	11.7 (1.7)	13.4 (0.1)
	95%	13.2 (0.4)	13.9 (0.3)
RFD_{peak} ($N.s^{-1}$)	75%	1183 (64)	961 (48)
	85%	1215 (48)	1098 (37)
	95%	1285 (47)	1264 (56)
RFD_{50} ($N.s^{-1}$)	75%	1097 (47)*	1654 (70)
	85%	1165 (170)*	1834 (53)
	95%	1171 (25)***	2347 (133)
Impulse (N.s)	75%	68 (5)	77 (2)
	85%	67 (2)	79 (4)
	95%	78 (4)	89 (9)

Table 5.3: Presented are group mean (SEM) stroke force data across all exercise intensities. Asterisk infer a significant difference between conditions (* inferring $P < 0.05$, ** inferring $P < 0.01$).

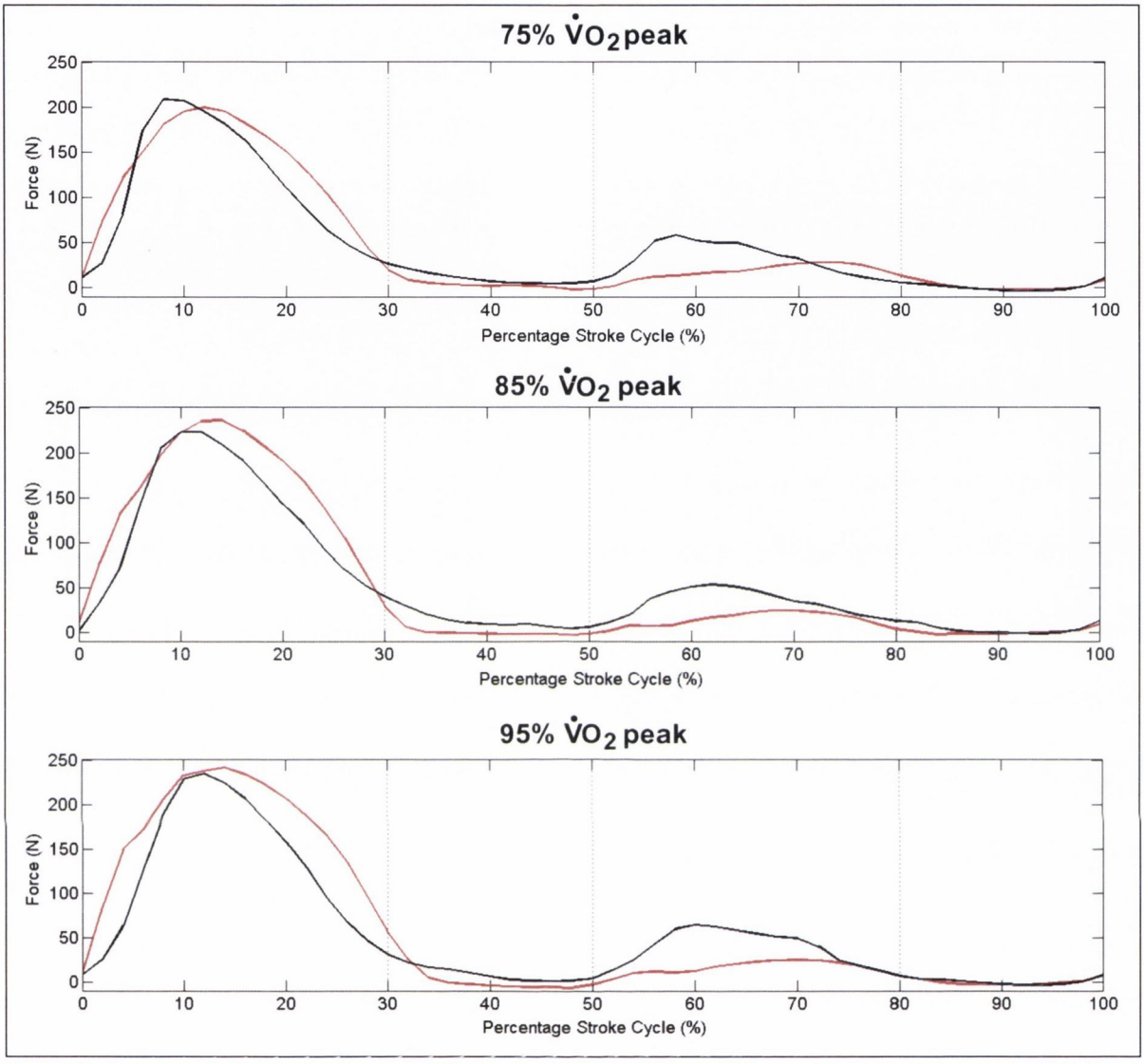

Figure 5.6: Group mean ensemble force-time profiles recorded during on-water (red) and on-ergometer (black) kayaking at 75, 85 and 95% $\dot{V}O_2$peak. The dashed vertical lines separate the approximate phases of the stroke cycle; draw phase (0-30%), transition phase (30-50%), opposite draw phase (50-80%) and opposite transition phase (80-100%).

5.4.5: Effect of exercise intensity

Exercise intensity had a varied effect on muscle activity patterns, depending on the investigated musculature. Significant increases in overall TB activity were observed as intensity increased, however these increases were more pronounced during the on-water condition ($P < 0.01$ for on-water, $P < 0.05$ for on-ergometer). No significant changes in overall LD or VL activity were observed with increasing exercise intensity. Unexpectedly, a trend towards decreasing overall AD activity was observed as exercise intensity increased (Table 5.2), however this trend did not attain statistical significance.

As expected, peak force increased significantly as exercise intensity increased, however this trend was more significant during on-water kayaking ($P < 0.01$ for on-water, $P < 0.05$ for on-ergometer). RFD_{peak} and RFD_{50} both increased significantly in line with exercise intensity ($P < 0.05$ and $P < 0.01$, respectively). While a trend towards increasing forces was observed in stroke impulse (Table 5.2), this trend did not achieve statistical significance. No changes in absolute or normalised time to peak force were observed with increasing exercise intensity.

5.5: DISCUSSION

The primary aim of this study was to compare EMG, 2-D kinematics and stroke force profiles both on-water and on-ergometer in order to assess the accuracy with which the ergometer simulates the biomechanical demands of on-water kayaking. Significant differences in muscle activity patterns, stroke force and kinematic data suggested that the two biomechanical tasks are not perfectly matched. Some differences in muscle activity may be explained by subtle changes in kinematics during the draw phase. This is most likely the case with LD activity, where significantly earlier time to vertical position ($P < 0.05$, see Table 2) appears to have altered LD recruitment pattern during on-ergometer kayaking. Other more striking differences in muscle activity, such as those observed in AD during the latter stages of the ergometer stroke are most likely explained by the additional external forces associated with the ergometer loading mechanism being applied to the paddle shaft.

Increased AD activity manifest itself as a significant second phase of recruitment occurring between 60 and 90% of the stroke cycle, a pattern not evident during on-water kayaking at any exercise intensity, see Figures 5.3c, 5.4c and 5.5c. The most probable explanation for this difference was the ergometer loading mechanism exerting additional forces on the paddle shaft (Figure 5.7). In order to maintain constant tension on the pulleys connecting the paddle shaft and ergometer flywheel, an elastic chord exerts a recoil force. Analysis of strain gauge data from a stationary position has quantified this force at 20 ± 4N under normal recoil (see Chapter 6), however during dynamic movement both the direction and magnitude of this force constantly changed. Trevithick *et al.* (2007) previously suggested that this recoil force aided in the transition phase of the stroke cycle, resulting in less shoulder muscle activity than would be expected during on-water kayaking. With regards to AD activity, the results of the current study clearly contradict this hypothesis. During the latter stages of the stroke cycle (60 to 90%), the shoulder moves from abduction into forward flexion. As the opposite draw phase concludes, the shoulder is in its most flexed and forward position. Both kinematic and strain gauge data would suggest that the ergometer is exerting a downward recoil force on the paddle shaft at this point (Figure 5.7a). No such downward force is exerted during the equivalent phase of the on-water stroke (Figure 5.7b). In order to maintain optimal shoulder and arm position during these latter stages of the on-water stroke

cycle, the kayaker must resist this downward force via significant increases in AD recruitment, evident at the 70 ($P < 0.001$), 80 ($P < 0.001$) and 90% ($P < 0.05$) intervals.

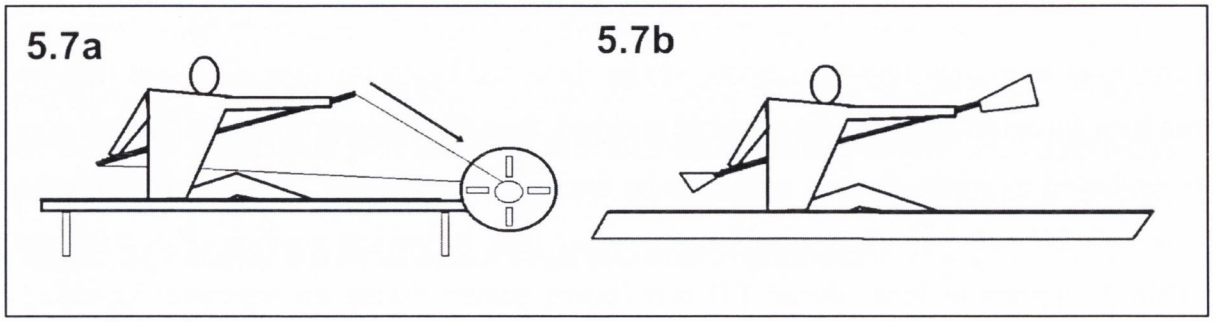

Figure 5.7: Diagrammatic representation of a time-point at the start of the opposite transition phase of the on-ergometer (5.7a) and on-water (5.7b) stroke cycle. The arrow in Figure 4a represents the elastic recoil force being applied to the paddle shaft which AD must work against. No such external force occurred on-water during this phase of the stroke cycle.

Stroke force profiles recorded during both conditions highlighted that propulsive forces are generated during the draw phase of the kayak stroke cycle, see Figure 5.6. During this phase, the shoulder is extended and internally rotated, facilitating the pulling motion of the paddle through the water (Logan and Holt, 1985). Since LD is responsible for both shoulder extension and internal rotation, it is considered a major propulsive muscle involved in the kayak stroke. Previous studies have reported that LD plays a primary role in generating propulsive forces during both kayak (Yoshio *et al.,* 1974; Trevithick *et al.,* 2007) and freestyle swimming stroke cycles (Pink *et al.,* 1991) and the current results are in agreement with this literature. The phase of LD activity in the current study was concurrent with the propulsive forces generated during the draw phase. In addition, time to peak LD activity closely matched time to peak stroke force for both conditions. Peak forces occurred later during the on-water stroke cycle, see Table 5.4, and peak LD activity also occurred later during on-water kayaking (Figure 5.2b). Moreover, significantly higher mean LD activity recorded in the 20% interval during on-water kayaking ($P < 0.001$ at all exercise intensities)

may explain the greater propulsive forces being generated in the latter stages of the on-water draw phase (15 to 30% of stroke cycle, Figure 5.6).

It is widely accepted that the maximum absolute acceleration occurs at and around the vertical paddle position (Mann & Kearney, 1980). The kinematic and stroke force data recorded are in agreement with this literature, since a close relationship between time to peak force and time to vertical paddle position existed during both on-ergometer and on-water trials (Tables 5.2 and 5.3, respectively). Significantly earlier time to vertical position observed on-ergometer may be a result of the recoil forces pulling the shaft forward on the opposite side earlier than during the on-water scenario. It is possible that this subtle change in stroke kinematics may have led to both the earlier peak forces and the significantly earlier peak LD activity observed during the on-ergometer draw phase; see Figures 5.2b and 5.6, respectively.

TB was also highly active during the draw phase of the stroke cycle. Prior to and directly at the onset of the draw phase, concentric contraction of TB ensure that maximal forward arm reach is attained (Logan & Holt, 1985). As the draw phase progresses however, the elbow joint is flexed (Tokuhara *et al.,* 1987; Baker *et al.,* 1999). Since TB is an elbow extensor, it may seem counter-intuitive to observe TB activity here, but progressive elbow flexion during the draw phase is actively resisted through an eccentric action of TB. Previously Tokuhara *et al.* (1987) reported that skilled kayakers did not recruit their elbow flexors during simulated arm pulling movements, even though elbow flexion occurs during the movement. In a multi-articular movement, the resultant propulsive force is limited by the weakest joint force within a multi-joint system (Kumamoto & Takagi, 1980). Since forces generated via shoulder extension exceed forces capable of being generated via elbow flexion, the optimal strategy for force development during the draw phase is one where forces are generated via shoulder extension and transmitted to the paddle via the elbow joint. Thus inhibition of elbow flexor recruitment and increased elbow extensor recruitment produce greater propulsive forces during the draw phase of the kayak stroke (Tokuhara *et al.,* 1987).

In addition to the initial draw phase, TB was also active during the opposite draw phase, although significant differences in the level of activity were observed between exercise conditions, see Figures 5.3a, 5.4a 5.5a. In order to effectively perform the opposite draw phase, the recovery arm acts as a support and aids in the forceful entry and pull of the opposite paddle through the water. Trevithick *et al.* (2007) reported that both *Upper Trapezius* and *Supraspinatus* were also active during the opposite draw phase of the kayak stroke cycle. The current results suggest that TB activity is also necessary in order to support the opposite draw phase, however, the reason why this phase of TB activity was significantly greater during on-water kayaking remains to be fully elucidated. It is possible that once again, recoil forces acting on the shaft are forcing kayakers to alter their muscle recruitment patterns. Differences in force profiles suggest that the ergometer is applying additional loads to the kayak shaft during this phase (50 to 70% of the stroke cycle). In order to maintain optimal joint position, it is possible that increased elbow flexion (via reduced TB activity) provides resistance to the recoil forces pulling the shaft forward earlier than required. Regardless of the exact mechanism, it is worth noting that the two best kayakers (based on personal best times) both showed markedly greater TB activity during the opposite draw phase when compared with other members of the group, both on-water and on-ergometer. This suggests that enhanced recruitment of TB during this phase of the stroke cycle may improve stroke biomechanics and thereby increase kayak velocity.

Logan and Holt (1985) reported that prior to the onset of the stroke cycle, the thorasic vertebrae are rotated anteriorly and the knee and hip joints are at their maximal degree of flexion. These joint articulations are made in an effort to maximally rotate the trunk and shoulders in the anterior direction, optimising the forward reach necessary for paddle entry. At the onset of the draw phase, the knee extensors are recruited in order to forcefully extend the knee joint from the maximal flexed position (Logan & Holt, 1985). This action aids in pelvic rotation and horizontal hip adduction, both of which enhance the rotational component that is desired in the trunk (Logan & Holt, 1985). Activity in VL was observed during the draw phase of the stroke cycle both on-ergometer and on-water (Figures 5.2d and 5.3d), in agreement with previous investigations evauating the role of VL in aiding body segment rotation (Mann & Kearney, 1980; Logan & Holt, 1985). While mean iEMG activity

in VL in the current study was lower than activity observed in upper body musculature (Table 5.2), the role of contralateral knee extension and flexion in enhancing pelvic and trunk rotation should not be underestimated. This point is highlighted by the fact that almost all elite kayakers have a strap on their footrest to enhance contralateral leg movements (Logan & Holt, 1985; Sanders & Baker, 1998).

Differences in the rate of force development in the initial stages of the draw phase were observed between the two exercise conditions. RFD_{50} was significantly greater during the on-water draw phase at all exercise intensities ($P < 0.05$, see Table 5.3). This difference is highlighted by a change in the slope of the ergometer stroke force profile at approximately 5% into the stroke cycle (Figure 5.6). A similar finding was reported for initial stroke force development comparing dynamic and stationary rowing ergometry (Kleshnev & Kleshneva, 1995; Benson *et al.*, 2011) and it was proposed that a disparity between handle and foot-stretcher forces may explain the altered stroke force development on stationary ergometers (Kleshnev and Kleshneva, 1995). In a similar fashion, it is possible that a disparity between initial force development at the shaft and opposing resistive forces at the flywheel may exist. A minor delay in transmission of forces from the shaft to the flywheel via the connecting ropes may impede optimal force development in the first 5% of the stroke cycle. During the on-water scenario, it appears no such delay in force generation occurs. Once the paddle enters the water, propulsive force can be generated effectively though the paddle shaft without any transmission delay.

The results of the current study suggest that the role of each muscle within the stroke cycle may determine what effect increased exercise intensity will have on its specific activity. Mean TB activity increased significantly, in line with exercise intensity. Since TB activity occurs during both the draw and opposite draw phases of the stroke cycle and hence plays a role in the development of propulsive force, these increases in activity were to be expected. However, LD activity did not show a significant trend towards increased activity despite being highly active during the propulsive draw phase of the stroke cycle. It is possible that LD activity while necessary for the development of the draw phase, works at a consistent level, independent of increaseses in stroke force. The unexpected decreases in AD activity

observed as exercise intensity increased are most likely due to increased stroke rates, which reduce the duration of the transition phase, thus potentially reducing the role of AD in this phase of the stroke cycle. As expected, many of the measurements of stroke force increased in line with exercise intensity. Peak force, RFD_{peak} and RFD_{50} were all significantly greater as intensity was increased. Further research examining the effect of stroke rate and intensity on both muscle activity and stroke kinematics is necessary in order to establish if changes in stroke rate alter the movement patterns and associated EMG of other muscles.

Study limitations must be considered before drawing definitive conclusions from the current results. Firstly, the biomechanical data presented represents controlled sub-maximal and near maximal exercise intensities. Kayakers exercised at a power outputs equivalent to 75, 85 and 95% of their $\dot{V}O_2peak$. A previous assessment of kayak ergometer task specificity concluded that simulated kayaking did not closely reflect open-water kayaking in the assessment of sub-maximal cardio-respiratory responses to exercise (Mitchell & Swaine, 1998). However, Van Someran *et al.* (2000) assessed cardio-respiratory variables at maximal exercise intensity and detected no significant differences between on-water and on-ergometer kayaking. The results of the current study are in agreement with Mitchell and Swaine (1998), however it remains to be seen if biomechanical differences are also evident during maximal exercise. Previous literature has reported stroke rates of 118 ± 4 (Mann & Kearney, 1980) and 96 ± 5 strokes.min^{-1} (Sanders & Kendal, 1992) during high intensity kayaking. The target stroke rates used in the current study (74 ± 2, 81 ± 2, and 89 ± 2 strokes.min^{-1}) were markedly lower. It is possible that at maximal stroke rates, differences between on-ergometer and on-water kayaking are not as significant as those observed in the current study. Further analysis of EMG, stroke force and kinermatic data, at maximal exercise intensity and stroke rate is warranted in order to fully assess biomechanical task specificity of the kayak ergometer. In addition, the number of available EMG channels limited our investigation to just four involved muscles. Kayaking is a complex multi-joint movement incorporating recruitment of many different muscles and joints, consequently analysis of recruitment patterns from other shoulder, arm and trunk muscles is warranted in order to provide a more complete assessment of kayak ergometer task specificity.

One of the main outcomes of the current study is that the recoil force associated with the ergometer loading mechanism appears to affect activity patterns in TB, LD and most notably in AD. In the case of LD activity, the subtle changes to stroke kinematics (earlier time to vertical position) brought about by this recoil foce, are most likely responsible for the altered activity patterns observed on-ergometer. In the case of TB and especially AD activity, it seems more likely that the altered recruitment patterns are as a result of the kayakers working to maintain optimal stroke kinematics. The subsequent chapter will outline a study which assessed the effect of varying kayak ergometer recoil forces on 3D kinematics and muscle activity patterns in order to clarify what effect this force has on AD, LD and TB activity.

5.6: CONCLUSION

The results of this study confirm that while the kayak ergometer may replicate the metabolic and cardiorespiratory demands of on-water kayaking (Van Someran *et al.,* 2000), it does not perfectly replicate the biomechanical demands of the sport. While the 2D kinematics appear closely matched (with the exception of time to vertical), measures of muscle activity and force production highlight that significant differences clearly exist between the two tasks. The most striking of these differences was the significantly greater AD activity recorded during on-ergometer kayaking. It is unclear as to whether this increased recruitment of AD during discrete phases of the stroke cycle has any implication for long term training. It should be noted that regardless of the findings of the current study, the kayak ergometer will remain a highly useful tool in the training and testing of elite kayakers. Therefore further research comparing EMG data from other active muscles and at maxiamal exercise intensities is warranted, in order to provide a more complete assessment of the biomechanical task specificity and potential training implications for ergometer usage. Finally, while increasing exercise intensity produced expected increases in stroke force data, the varying role of each muscle within the stroke cycle led to inconsistent changes in activity relative to intensity.

Chapter 6

An electromyographic and 3D kinematic analysis of ergometer kayaking under increasing levels of external recoil force.

6.1: INTRODUCTION

The results of the previous study (see Chapter 5) highlighted that significant differences in muscle activity patterns existed when comparing on-ergometer and on-water kayaking. It was hypothesised that these differences were potentially due to additional forces acting upon the ergometer paddle shaft during on-ergometer kayaking. This force applied via an adjustable elastic chord, maintained appropriate pulley tension between the paddle shaft and the ergometer flywheel. However, this elastic tension potentially has the additional effect of exerting an external force on the shaft which the kayaker must overcome at specific phases of the stroke cycle. In order to maintain optimal stroke biomechanics, the kayaker may resist this external force via altered recruitment of shoulder and arm musculature. Conversely, the external forces being applied on-ergometer may directly alter normal upper body joint kinematics, thus affecting associated muscle recruitment patterns. It remains to be seen whether differences in EMG observed during on-ergometer kayaking (vs. on-water) are the result of the kayaker's effort (conscious or otherwise) to maintain optimal upper body movement patterns or if the external forces are acting upon joints to create both altered movement patterns and EMG responses.

3-dimensional (3D) motion analysis has previously been used to analyse scapular, glenohumoral, elbow and wrist kinematics in a variety of complex biomechanical tasks including baseball pitching (Barrentine *et al.*, 1998; Murata, 2001), golf swing (Mitchell *et al.*, 2003; Nesbit, 2005) and tennis serve (Tanabe & Ito, 2007). Several studies have undertaken 3D motion analysis of the kayak stroke both on-water (Baker *et al.*, 1999) and on-ergometer (Begon *et al.*, 2008), however, these studies were limited to analysis of sport specific biomechanical variables (stroke length, stroke velocity, shaft angle and draw times) without assessing specific joint kinematics at the shoulder, elbow or wrist. The combination of EMG and joint kinematic analysis has previously been used to identify fatigue induced increases in lumbar motion and *Erector Spinae* activity during simulated 2000m ergometer rowing trials (Caldwell *et al.*, 2003).

6.2: AIMS AND HYPOTHESIS

The primary aim of this study was to assess the effect of recoil forces on both muscle activity and 3D upper body joint kinematics during the on-ergometer kayak stroke cycle. By increasing the elastic tension applied to the paddle shaft and comparing joint kinematics and associated EMG activity, the effect of this external force could be fully assessed and elucidated. We hypothesised that increasing the ergometer's elastic tension would result in increased EMG activity, without significant changes in the 3D joint kinematics.

6.3: MATERIALS AND METHODS

6.3.1: Participants

Ten (n=10) male international flat-water kayakers volunteered to perform this study (mean ± SD; age 21 ± 3yr, height 1.80 ± 0.06m, body mass 74.6 ± 5.8kg). All participants had previously performed both maximal graded incremental tests and task specificity trials both on-ergometer and on-water as part of the previous study (see Chapter 5). All participants were fully informed of the procedures involved in the current study and provided informed consent to participate, see Appendix 3. Ethical approval for this study was granted from the Trinity College Health Sciences ethics committee.

6.3.2: Experimental design

This study was approved by the university Health Sciences Ethics Committee in Trinity College Dublin and consisted of a two visits to separate locations. Initially, a graded incremental test to volitional exhaustion was performed on a Dansprint kayak ergometer (Dansprint, Hvidovre, Denmark) to assess $\dot{V}O_2$, lactate and heart rate response profiles. These tests were performed in the Human Performance Laboratory, Anatomy Department, Trinity College Dublin. Data acquired during incremental testing were used to set each individual's exercise intensity (85% $\dot{V}O_2$peak) for the subsequent 3D kinematic exercise trial. The kinematic trials were performed in the Exercise Laboratory, Trinity School of Physiotherapy, St. James's Hospital Dublin. During this trial, the elastic recoil forces

applied by the ergometer's loading mechanism were adjusted in order to assess their affect on muscle activity and joint kinematics of the shoulder, arm and back.

6.3.3: Maximal incremental test protocol

Maximal incremental tests were performed on a Dansprint kayak ergometer, in order to attain a specific exercise intensity of 85% $\dot{V}O_2$peak, necessary for the subsequent kinematic trials (see Chapter 2.8). Gas exchange variables, along with heart rate and blood lactate data were recorded during each increment of the test (see Chapters 2.9, 2.10 and 2.11, respectively).

6.3.4: Kinematic trial

A 10-min warm-up at heart rate equivalent to 50% of each individual kayaker's $\dot{V}O_2$peak was performed prior to commencing 3D kinematic trials. The exercise trial itself consisted of a series of 4 by 1 min intervals, with each interval followed by a 3 min rest period in order to eliminate any risk of fatigue affecting subsequent exercise bouts. Elastic tension applied to the ergometer paddle shaft via the connecting pulleys was varied in a fixed order between each exercise bout. Tension was increased in a stepwise fashion via a shortening of the ergometer's elastic chord. The elastic chord was shortened by fixed lengths of 10% relative to the overall chord length for each respective exercise bout. Thus kayakers exercised for 1 min bouts at gradually increasing elastic tensions from tension 1 through to tension 4 (T1 to T4). Throughout the entire trial, kayakers maintained a fixed power output (W) and stroke rate (strokes.min^{-1}) equivalent to 85% of their $\dot{V}O_2$peak. This was achieved via the ergometer's LCD screen which continually provided feedback of both power output and stroke rate. Since the exercise duration was significantly shorter than the previous study (1 vs. 3 min), power output instead of heart rate was considered a more appropriate means of quantifying exercise intensity.

6.3.5: EMG data

EMG data were recorded from three muscles on the right side of the body involved in the kayak stroke cycle: *Triceps Brachii (long head)* (TB), *Anterior Deltoid* (AD) and *Latissimus Dorsi* (LD), see Chapter 2.1. Synchronisation of EMG and video data using an audio-sync

trigger (Mega, Koupio, Finland) facilitated identification of onset of each stroke cycle on the EMG recording (see Chapter 2.3). EMG data from 10 consecutive stroke cycles in the latter stages of each task specificity trial, were amplitude processed via root mean squaring and normalised relative to isometric MVC, see Chapters 2.3 and 2.4, respectively. Subsequent temporal normalisation and averaging via cubic spline fitting (Chapter 2.5) produced an average rmsEMG ensemble for each muscle during task specificity trials.

6.3.6: Three-dimensional kinematic analysis

Three-dimensional (3D) movement patterns of discrete anatomical reference points were recorded using a CODA dual CX1 motion analysis system (Charnwood Dynamics, Rothley, UK, see Plate 6.1). The CODA motion analysis system uses active infra-red LED markers to measure positions within a 2 by 2 by 3 m^3 volume. The translational precision of the instrument has been shown to be within 0.5 mm in each direction, while rotational accuracy is within 1°, determined using factory calibration experiments (Mottram *et al.*, 2009). Two separate CX1 measurement units were placed equidistant (approximately 5m) and orthogonally to the left and right sides of the sagittal plane. Prior to motion capture, the CODA system was pre-calibrated by placing fixed reference points on the ground within the measurement volume. Marker positions were captured at 100 Hz and data transferred to PC for subsequent analysis using CODA software (CODAmotion V2.0, Charnwood Dynamics, Rothley, UK). All 3D kinematic data were presented in the X (length), Y (width), and Z (height) axes, as mm displacement from the pre-calibrated reference points. Since the ergometer was positioned behind the calibrated reference points, all marker positions were recorded as negative displacements in the X-axis, positive displacements in the Z-axis and both positive and negative displacements in the Y-axis, depending on relative position during the kayak stroke.

Previous studies have shown that skin mounted motion sensors are suitable to measure scapula rotation and translation (Karduna *et al.*, 2001; Lin *et al.*, 2005). While the accuracy of all skin-mounted marker-tracking systems is inherently limited (Mottram *et al.*, 2009), accuracy was deemed satisfactory for the purposes of the current study. Markers were attached to the head of the *Ulna* (wrist marker) and head of the *Radius* and *Lateral*

Epicondyle (elbow markers) in order to assess movement patterns of the arm. Additional markers were attached to the lateral tip of the *Acromion* (shoulder marker), and *Inferior Scapula* and medial border of the *Spinal Scapula* (scapular markers). Marker locations were identified via anatomical reference to bony prominences and all markers were secured to the skin with double-sided sticky tape (Sellotape, Henkel, Cheshire, UK).

Plate 6.1: The CODA CX1 motion capture system. (image location: www.codamotion.com)

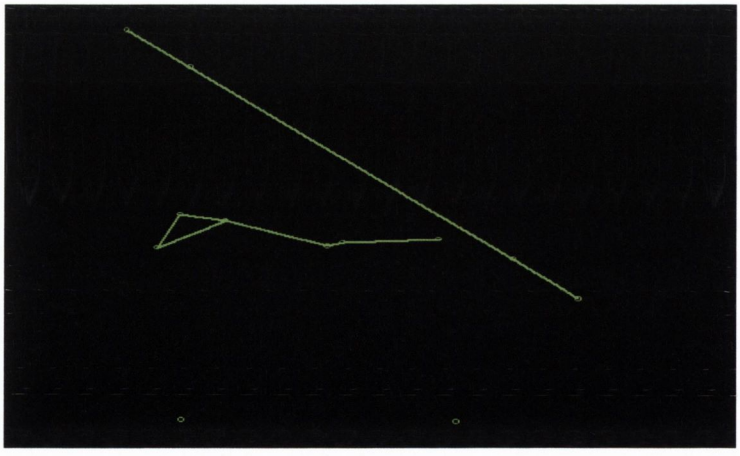

Plate 6.2: A screenshot of the CODAmotion software display of 3D marker positions during a kayak stroke cycle.

6.3.7: Stroke force data

In a similar fashion to Chapter 5, stroke force data was recorded during all kinematic trials using strain gauge arrays integrated into a carbon paddle shaft, see Chapter 2.7.

6.3.8: Data reduction and statistical analysis

All EMG, force and 3D motion data were transferred to Matlab (Mathworks, Massachusetts, USA) for data reduction. For statistical analysis, mean rms EMG data were averaged for each 10% interval of the stroke cycle. Stroke force data were also averaged over the same 10 consecutive stroke cycles and temporally normalised to attain a group mean stroke force ensemble at each 2% of stroke cycle duration. Data were subsequently analysed to attain measures of peak force (N), absolute time to peak force (s), normalised time to peak force (%), rate of peak force development (RFD_{peak} in $N.s^{-1}$) and rate of 50% peak force development (RFD_{50} in $N.s^{-1}$) as outlined by Benson *et al.* (2011). Integration of the stroke force profile in the first 30% of the stroke cycle quantified the draw impulse (N.s). 3D kinematic movement patterns for each anatomical marker were temporally normalised and averaged over 10 consecutive stroke cycles. 3D kinematic data were then averaged for each 10% interval of the stroke cycle in order to facilitate statistical analyses at comparative phases relative to the EMG data. Data are presented as group mean ± SEM unless otherwise stated. Normality of all data sets was assessed using Kolmogorov-Smirnoff tests. Statistical analyses were performed using 1-way repeated measures ANOVA; *post-hoc* Tukey tests quantified detected differences. Statistical analyses were performed using Sigma Stat (Systat Software, Chicago, USA) with $P < 0.05$ inferring statistical significance.

6.4: RESULTS

6.4.1 EMG data

Group mean (SEM) data for iEMG are presented in Table 6.1 and group mean (SEM) data for rmsEMG at each 10% interval of the stroke cycle are presented in Table 6.2. No significant differences were observed for iEMG data in any of the muscles investigated. However, when data were normalised to MVC and averaged for 10% intervals, significant differences were observed in *AD* activity at discrete phases of the stroke cycle. *AD* activity was significantly lower at T4 vs. T1 during the 40% interval ($P < 0.05$, see Figure 6.1 and Table 6.2), indicating that an increase recoil force reduced activity during this phase of the stroke cycle. The opposite effect was observed during later phases, as *AD* activity was significantly greater as tension increased during the 70, 80 and 90% intervals of the stroke cycle. During the 70% interval, *AD* activity was significantly greater (T4 vs.T1; $P < 0.05$: T4 vs.T2; $P < 0.05$) and during the 80 and 90% intervals (T4 vs. T1; $P < 0.001$: T4 vs. T2; $P < 0.05$), see Table 6.2 and Figure 6.2. In addition, activity at T3 was significantly greater than at T1 ($P < 0.01$) during both the 80 and 90% intervals. No significant differences in muscle activity for TB and LD were observed during any 10% intervals of the stroke cycle, see Table 6.2. Group mean (SD) ensemble EMG traces for each muscle across all tension levels are presented in Appendix 7.

6.4.2 Stroke force data

Group mean (SEM) stroke force data are presented in Table 6.1. The group mean stroke force profiles at each of the tension levels are presented in Figure 6.2. No significant differences were observed for peak force, time to peak force, normalised time to peak force, RFD_{peak}, RFD_{50}, or stroke impulse. Significant differences in the stationary forces applied to the paddle shaft were observed across all tension levels, see Table 6.1. Forces were significantly higher at T4 compared to T1, T2 and T3 ($P < 0.001$) and at T3 compared to T1 and T2 ($P < 0.001$). This outcome was expected, since increasing elastic tension, via the progressive shortening of the elastic chord, should increase the forces applied to the paddle shaft via the ergometer pulleys.

	Tension 1	Tension 2	Tension 3	Tension 4
EMG activity (n=10)				
iEMG of *TB* (μV.s)	161 (18)	157 (15)	164 (13)	170 (14)
iEMG of *LD* (μV.s)	163 (15)	163 (15)	163 (15)	164 (15)
iEMG of *AD* (μV.s)	402 (44)	437 (43)	458 (44)	466 (59)
Stroke force (n=9)				
Peak Force (N)	270 (12)	282 (16)	279 (13)	286 (15)
Time to peak (s)	0.15 (0.01)	0.15 (0.01)	0.15 (0.01)	0.15 (0.01)
Time to peak (%)	9.71 (0.40)	9.64 (0.60)	9.67 (0.50)	9.59 (0.50)
RFD_{peak} ($N.s^{-1}$)	1868 (125)	2025 (186)	2000 (166)	2065 (190)
RFD_{50} ($N.s^{-1}$)	1611 (135)	1765 (133)	1716 (120)	1759 (139)
Impulse (N.s)	66 (3)	68 (2)	72 (2)	70 (2)
Stationary recoil force (N)	20 (1)$^{***\$\$\$}$	29 (2)$^{***\$\$\$}$	37 (2)***	45 (2)$^{\$\$\$}$

Table 6.1: Presented are the group mean (SEM) iEMG and stroke force data. Asterisk infer a significant difference compared to T4 (*** inferring $P < 0.001$). Dollar symbols infer a significant difference compared to T3 ($^{\$\$\$}$ inferring $P < 0.001$).

Interval (% cycle)	Muscle	Tension 1	Tension 2	Tension 3	Tension 4
10	*TB*	26.2 (4.9)	25.1 (4.6)	25.3 (4.1)	25.6 (4.3)
	LD	35.9 (4.8)	32.7 (3.1)	33.5 (3.5)	32.8 (2.9)
	AD	2.9 (0.3)	2.9 (0.3)	2.9 (0.3)	2.9 (0.3)
20	*TB*	13.2 (3.7)	13.1 (3.5)	12.8 (2.7)	12.3 (3.0)
	LD	27.3 (2.8)	30.6 (3.4)	29.4 (2.8)	29.2 (3.0)
	AD	4.6 (0.7)	4.4 (0.8)	4.6 (0.7)	5 (0.9)
30	*TB*	2.5 (0.4)	2.5 (0.4)	2.8 (0.4)	3.5 (0.6)
	LD	8.0 (1.2)	8.0 (1.0)	7.9 (1.0)	9.8 (1.5)
	AD	7.7 (1.5)	7.3 (1.3)	6.6 (1.2)	7 (1.7)
40	*TB*	1.5 (0.2)	1.6 (0.2)	1.8 (0.3)	2.3 (0.4)
	LD	6.8 (0.8)	6.7 (0.7)	6.9 (0.8)	7.1 (0.8)
	AD	16.7 (2.1)*	15.3 (1.6)	14.1 (1.9)	11.9 (1.4)
50	*TB*	2.0 (0.3)	2.3 (0.3)	2.6 (0.4)	3 (0.4)
	LD	7.0 (0.9)	7.1 (0.9)	7.2 (0.9)	7.4 (1)
	AD	28.0 (2.4)	29 (3.3)	29.7 (3.2)	26.2 (3.2)
60	*TB*	7.6 (1.4)	7.3 (1.2)	8.7 (1.9)	9.1 (2.1)
	LD	7.2 (0.8)	7.0 (0.8)	7.2 (0.8)	7.3 (0.9)
	AD	8.6 (1.0)	10.7 (2.2)	11.3 (2.1)	11.7 (2.3)
70	*TB*	6 (1.4)	5.8 (1.3)	6.8 (1.9)	6.4 (1.6)
	LD	7.7 (0.8)	7.6 (0.7)	8.3 (1.)	8.3 (1.0)
	AD	10.6 (1.7)*	11.7 (1.9)*	14.9 (2.7)	18.1 (3.8)
80	*TB*	3.7 (0.4)	3.8 (0.4)	3.9 (0.4)	3.7 (0.4)
	LD	7.8 (1.0)	7.7 (0.8)	8.4 (1.3)	8.6 (1.3)
	AD	22.7 (3.5)*** ##	29.9 (4.2)*	32.3 (3.7)	37.6 (5.1)
90	*TB*	3.5 (1.1)	2.9 (0.5)	3.0 (0.5)	2.7 (0.3)
	LD	7.5 (1.1)	7.5 (1.4)	8.2 (1.4)	8.3 (1.3)
	AD	15.6 (2.8)*** ##	19.8 (3.3)*	24.1 (3.3)	26.3 (3.2)
100	*TB*	3.3 (0.8)	3 (0.6)	3 (0.6)	3 (0.6)
	LD	7.1 (0.8)	7 (0.8)	7.1 (0.8)	7.1 (0.9)
	AD	5.2 (0.6)	6 (0.8)	5.9 (0.8)	6.3 (0.7)

Table 6.2: Group mean (SEM) rms EMG data for each 10% interval of the stroke cycle across tension levels. Asterisk infer a significant difference from T4 (* $P<0.05$, *** $P<0.001$). Hash symbols infer a significant difference from T3 ($^{\#\#}$ $P<0.01$).

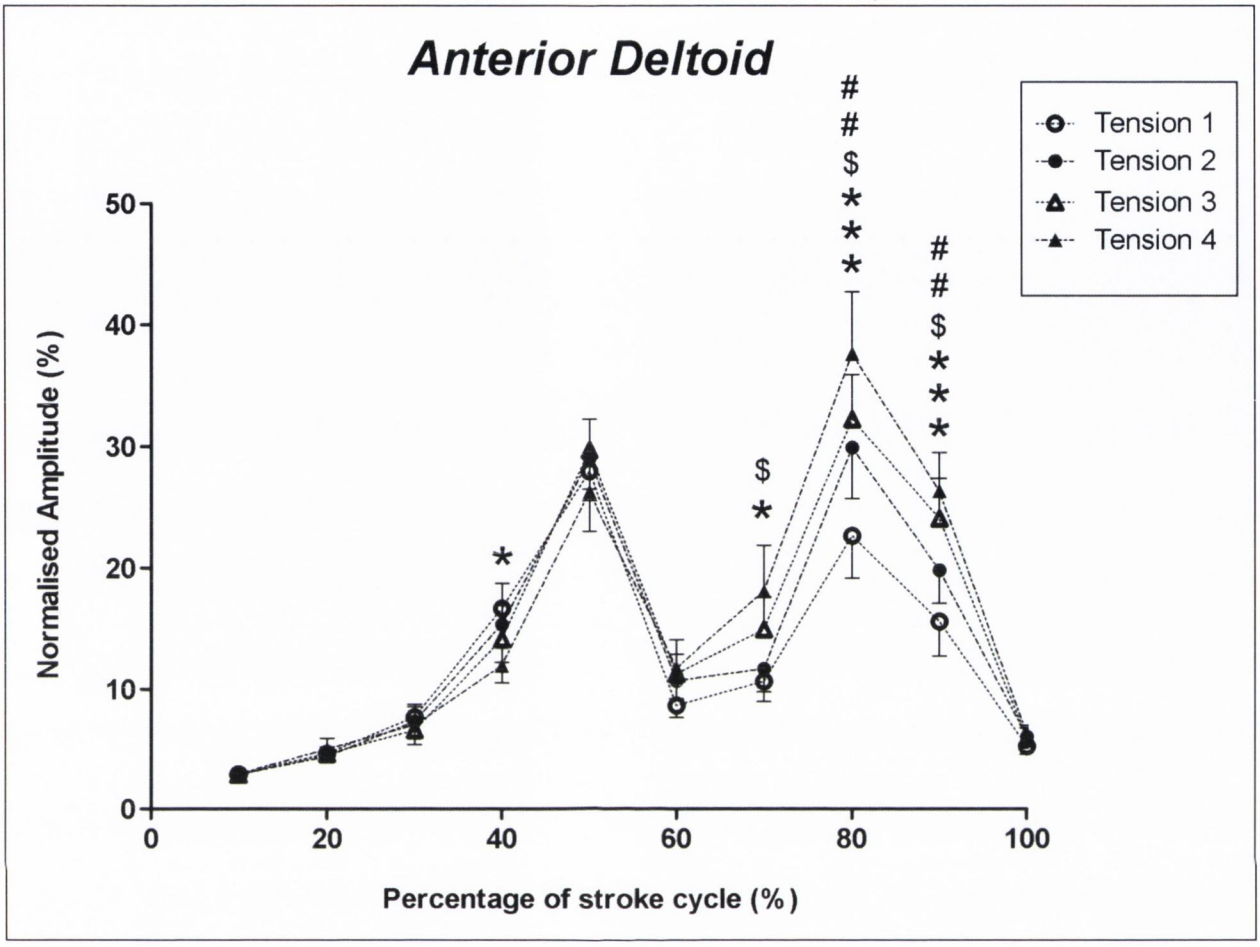

Figure 6.1: Group mean ± SEM (n=10) normalised EMG amplitude for *AD* at each 10% interval of the kayak stroke cycle across all tension levels. Each point represents the mean rmsEMG amplitude for 10% of the stroke cycle normalised to maximal rmsEMG amplitude recorded during isometric MVC. Asterisk infer a significant difference between T1 and T4 (* inferring $P < 0.05$, *** inferring $P < 0.001$). Dollar symbols infer a significant difference between T2 and T4 ($ inferring $P < 0.05$). Hash symbols infer a significant difference between T1 and T3 (## inferring $P < 0.01$).

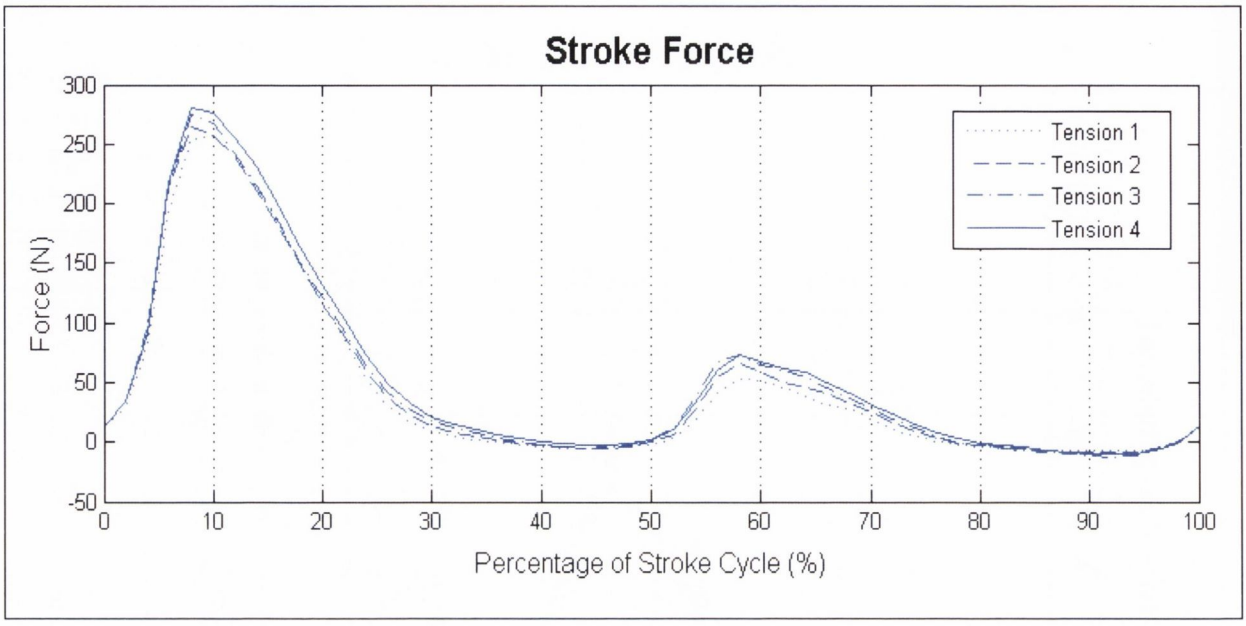

Figure 6.2: Group mean force-time profiles recorded across all tension levels. Each line represents the group mean stroke force data averaged for 2% intervals of the stroke cycle at a specific tension level.

6.4.3 3D kinematic data

Group mean (SD) kinematic data for each marker averaged over 10% intervals of the stroke cycle are presented in Appendix 6. In addition, range of movement (ROM) plots for each marker are presented in Figures 6.3 to 6.8. Statistical analysis of the 3D kinematic data averaged over 10% intervals revealed significant differences across tension levels, at discrete phases of the stroke cycle and within specific axes of orientation. Significant differences in marker position relative to the X-axis (horizontal) were observed for each of the markers at varying intervals of the stroke cycle, (see Appendix 6 for *P* values and specific intervals). In all cases, marker position at T4 was significantly greater than during T1 or T2, inferring a more forward position relative to the kayak ergometer. No significant differences in marker postion relative to the Y-axis were observed for any of the markers. Significant differences in marker position relative to the Z-axis (vertical) were observed in the elbow (head of the *Radius* and *Lateral Epicondyle of Humerus*), shoulder (*Acromion*) and scapular (*Inferior Scapula* and medial border of the *Spinal Scapula*) markers, at specific

phases of the stroke cycle, however, no significant differences were observed for the wrist (head of the *Ulna*) marker relative to the Z-axis. In all cases, Z-axis marker position at T4 was significantly greater than at T1 or T2, inferring that the joint position was significantly higher as elastic tension increased.

With respect to the X-axis, the wrist marker position was significantly more forward during the 10 to 30% and 60 to 100% phases of the cycle as tension increased (see Appendix 6.1 and Figure 6.3). Elbow marker position in the X-axis was significantly more forward during the 10 to 30% and 70 to 100% phases of the cycle as tension increased (see Appendix 6.2 and Figure 6.4). Shoulder and scapular marker positions in the X-axis were all significantly more forward during the 10 to 30%, 50 to 70% and 90 to 100% phases of the cycle as tension increased (see Appendices 6.4 to 6.6 and Figures 6.6 to 6.8, respectively).

With respect to the Z-axis, no significant differences in kinematics were observed for the wrist marker. Elbow marker positions in the Z-axis were significantly higher during the 60, 70 and 100% phases of the cycle as tension increased (see Appendix 6.2 and Figure 6.4 for *Radius* and Appendix 6.3 and Figure 6.5 for *Lateral Epicondyle*). Shoulder marker position in the Z-axis was significantly higher during the 40 to 100% phase of the cycle as tension increased. Scapular marker positions in the Z-axis were significantly higher at all phases of the cycle as tension increased. No significant differences in kinematic data were observed in the Y-axis for any of the markers investigated.

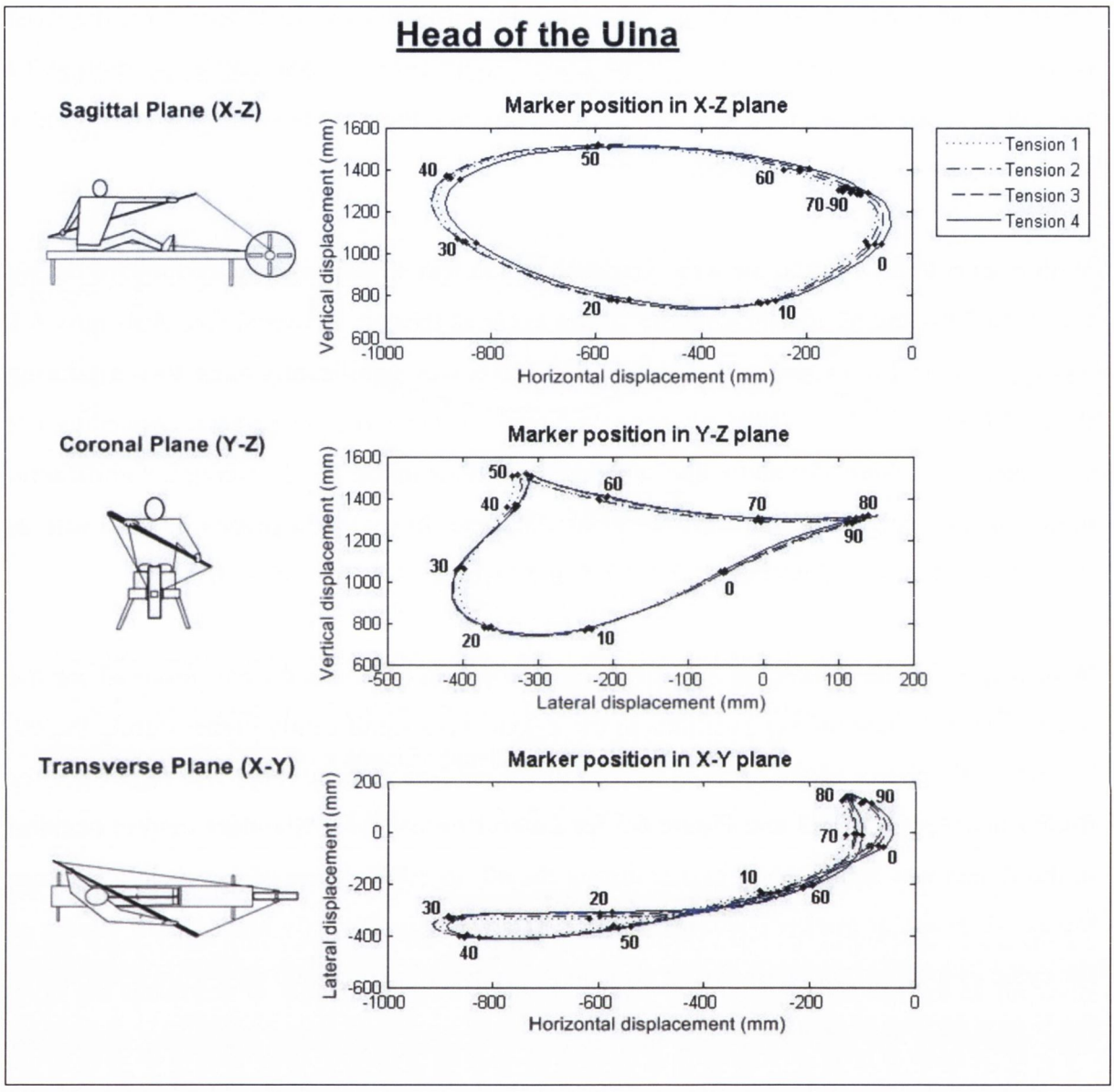

Figure 6.3: ROM plots for the head of the *Ulna* (wrist marker), recorded in the sagittal (X-Z), coronal (Y-Z) and transverse (X-Y) planes during the kayak stroke cycle. Data are presented as a group mean marker displacement (mm) at each 2% interval of the stroke cycle and separate lines represent specific kinematic data for each tension level. The 10% timepoints of the stroke cycle are marked (black dot) and numbered on each trace.

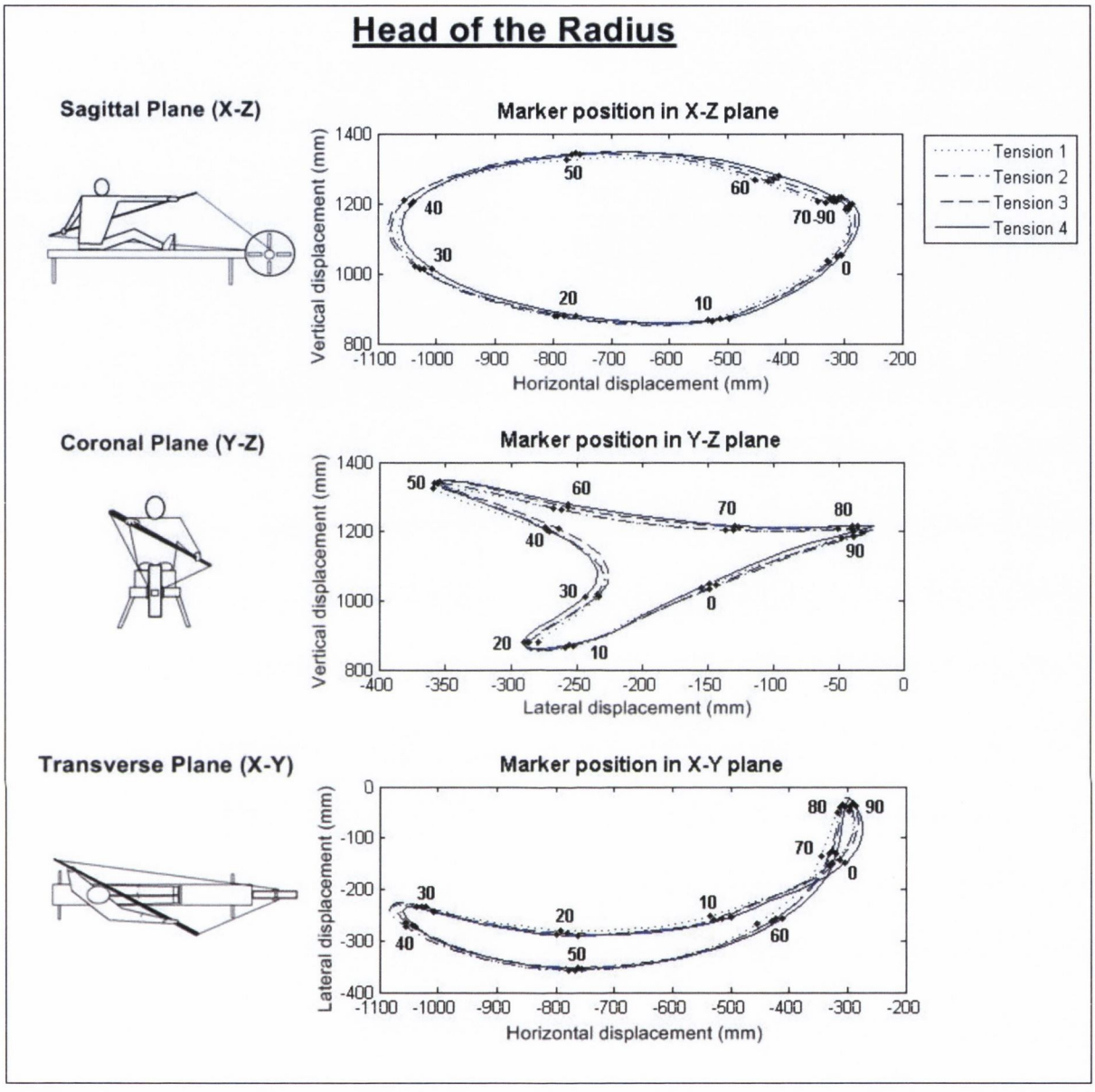

Figure 6.4: 3D kinematic data for the head of the *Radius* (elbow marker), recorded in the sagittal (X-Z), coronal (Y-Z) and transverse (X-Y) planes during the kayak stroke cycle. Data are presented as a group mean marker displacement (mm) at each 2% interval of the stroke cycle and separate lines represent specific kinematic data for each tension level. The 10% timepoints in the stroke cycle are marked (black dot) and numbered on each trace.

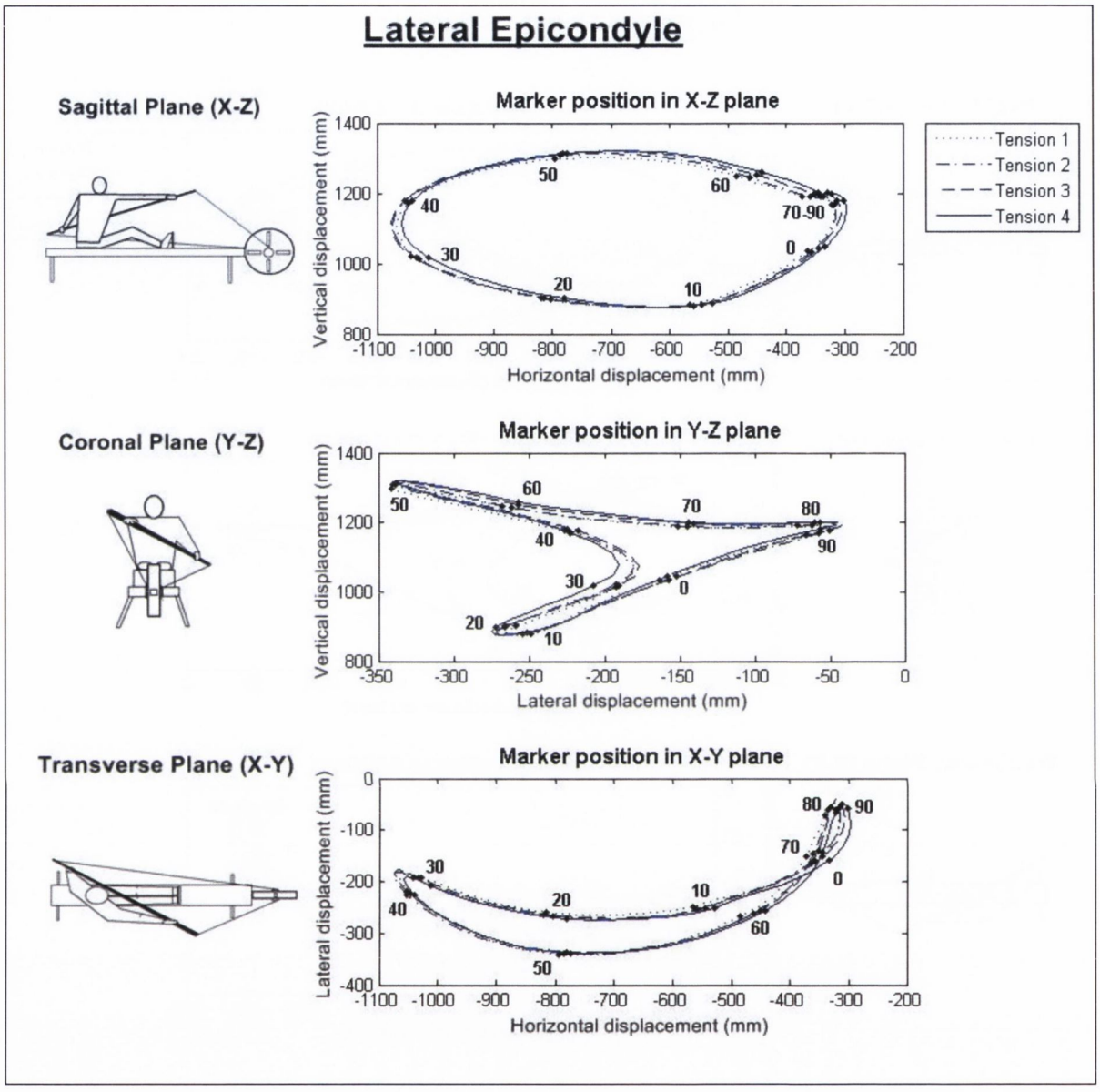

Figure 6.5: 3D kinematic data for the *Lateral Epicondyle* (elbow marker), recorded in the sagittal (X-Z), coronal (Y-Z) and transverse (X-Y) planes during the kayak stroke cycle. Data are presented as a group mean marker displacement (mm) at each 2% interval of the stroke cycle and separate lines represent specific kinematic data for each tension level. The 10% timepoints in the stroke cycle are marked (black dot) and numbered on each trace.

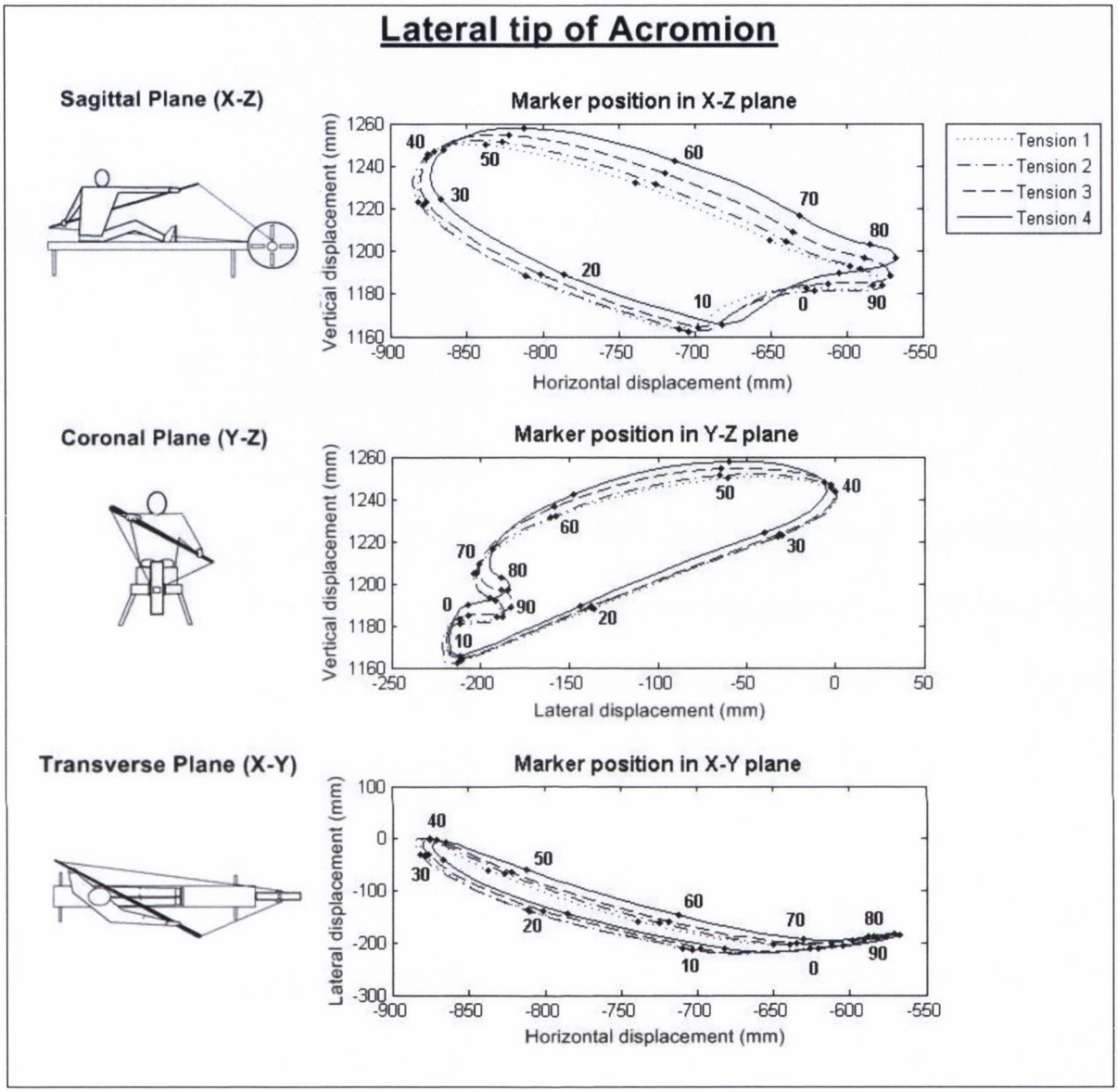

Figure 6.6: 3D kinematic data for the lateral tip of the *Acromion* (shoulder marker), recorded in the sagittal (X-Z), coronal (Y-Z) and transverse (X-Y) planes during the kayak stroke cycle. Data are presented as a group mean marker displacement (mm) at each 2% interval of the stroke cycle and separate lines represent specific kinematic data for each tension level. The 10% timepoints in the stroke cycle are marked (black dot) and numbered on each trace.

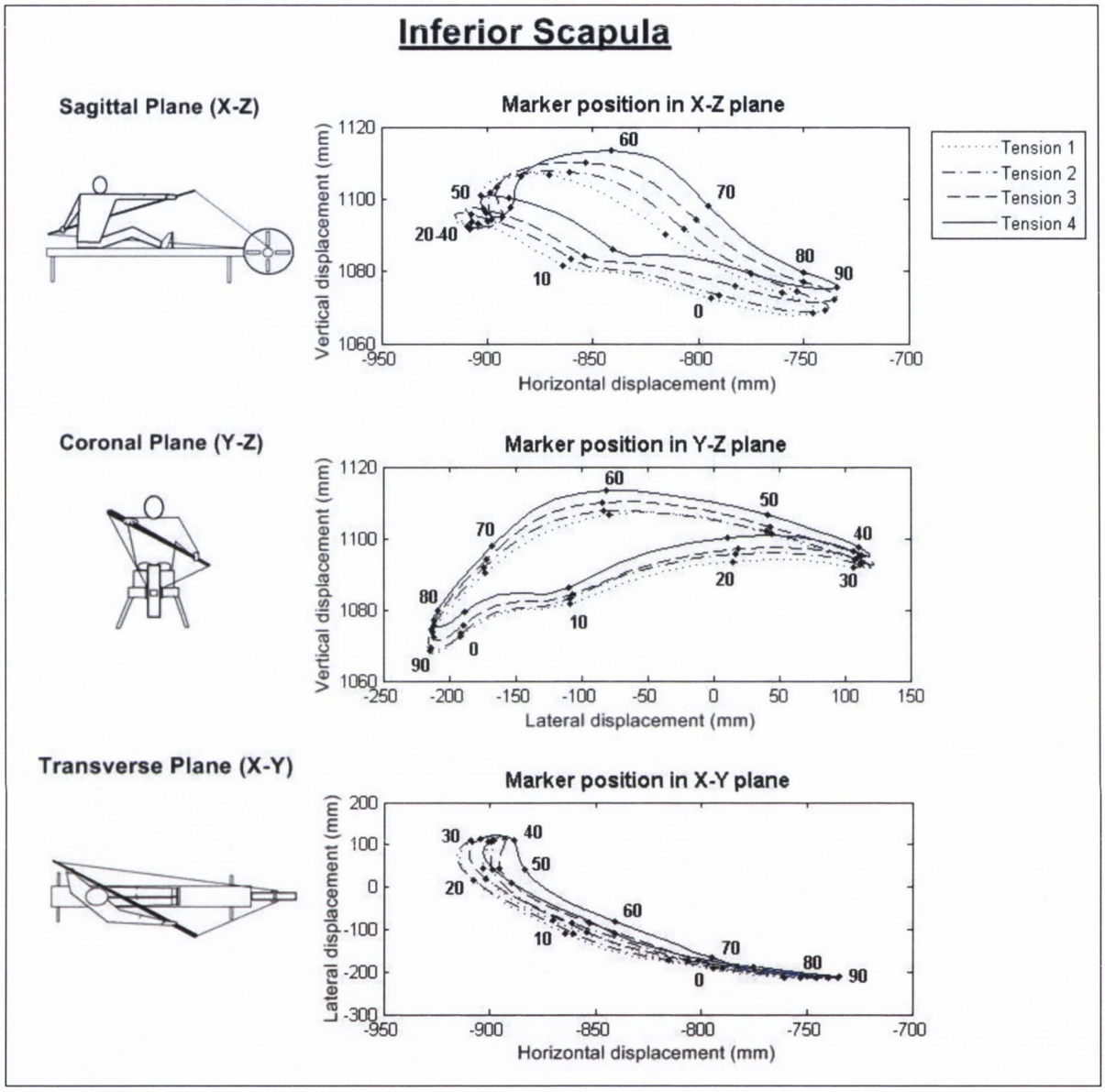

Figure 6.7: 3D kinematic data for the *Inferior Scapula* (scapular marker) recorded in the sagittal (X-Z), coronal (Y-Z) and transverse (X-Y) planes during the kayak stroke cycle. Data are presented as a group mean marker displacement (mm) at each 2% interval of the stroke cycle and separate lines represent specific kinematic data for each tension level. The 10% timepoints in the stroke cycle are marked (black dot) and numbered on each trace.

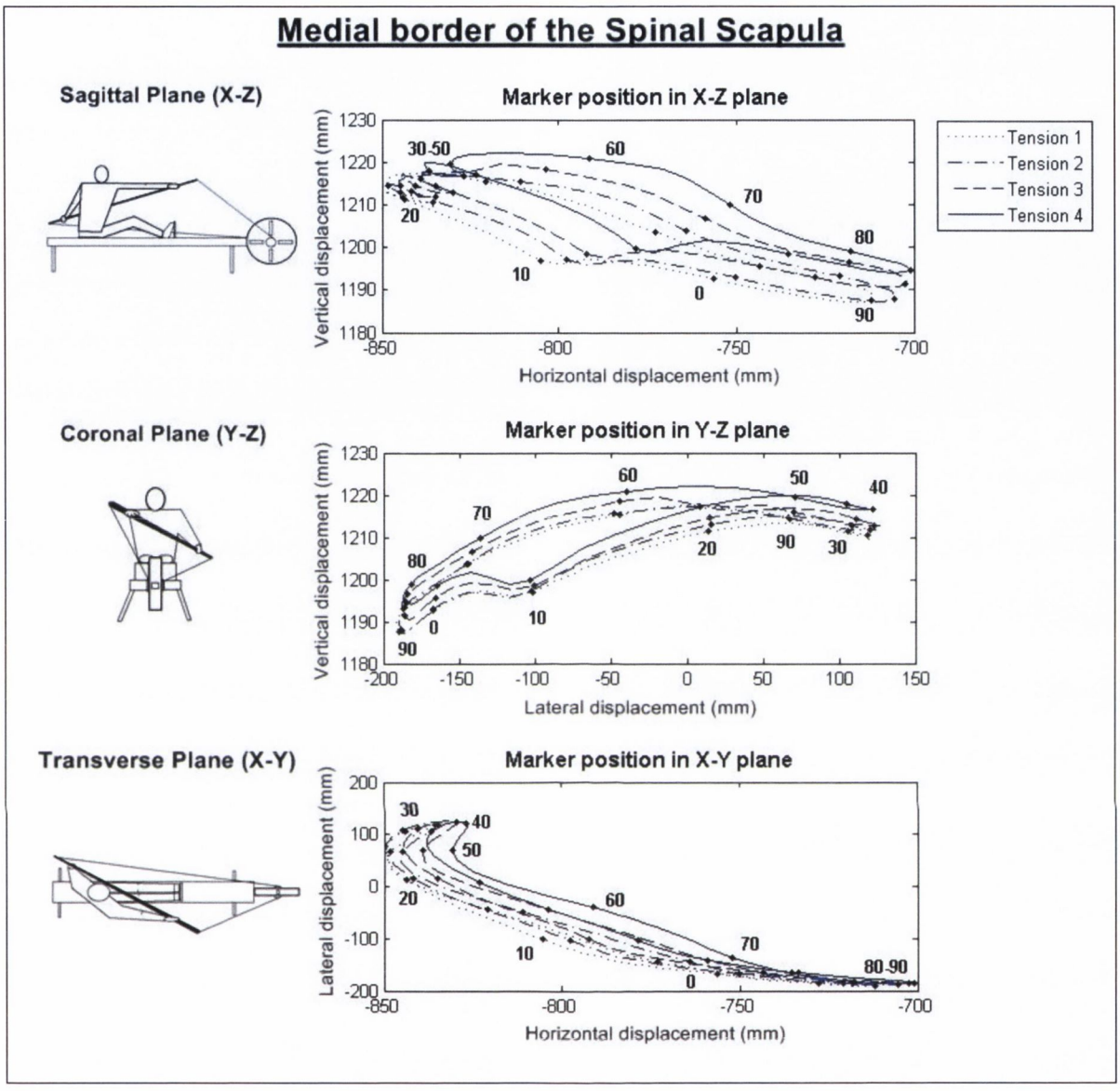

Figure 6.8: 3D kinematic data for the medial border of the *Spinal Scapula* (scapular marker), recorded in the sagittal (X-Z), coronal (Y-Z) and transverse (X-Y) planes during the kayak stroke cycle. Data are presented as a group mean displacement (mm) at each 2% interval of the stroke cycle and separate lines represent specific kinematic data for each tension level. The 10% timepoints in the stroke cycle are marked (black dot) and numbered on each trace.

6.5 DISCUSSION

The results of the previous study (see Chapter 5) suggested that differences in EMG activity between kayaking conditions were due to an additional external force experienced during on-ergometer kayaking which was not present during the on-water scenario. As such, the primary aim of the current study was to assess the extent to which this external force affected EMG and 3D kinematics, via increasing elastic tension. An additional aim was to establish if the changes in EMG activity were a manifestation of altered kinematic patterns, or the result of an effort to maintain optimal joint kinematics despite increased external forces acting upon the joints.

The most striking observation from the previous study was a significant second phase of *AD* activity during on-ergometer kayaking which was not clearly evident during the on-water scenario. This activity occurred between the 60 and 90% phase of the stroke cycle, when the shoulder was in a period of forward flexion. During this phase, the external recoil forces were acting in a downward trajectory from the paddle shaft towards the ergometer flywheel. Hence it was hypothesised that the increasing *AD* activity observed here, was a result of efforts to resist the downward forces acting upon the arm and shoulder. The current results confirm that the recoil forces associated with elastic tension were responsible for this significant second phase of *AD* activity observed during on-ergometer kayaking. *AD* activity was significantly higher at the 70, 80 and 90% intervals of the stroke cycle, as the elastic tension was increased (Figure 6.1). But were these increases in *AD* activity the result of the kayaker's effort to maintain optimal joint kinematics? Since the shoulder is in its most forward flexed position and the recoil forces are acting in a downward direction during this phase of the stroke cycle, the most likely changes to joint kinematics would be reduced forward flexion and a lowering of the arm from its normal height. Kinematic data confirmed that as elastic tension was increased, no signficant changes occurred in *Ulnar* marker height (Z-axis) during this phase of the stroke cycle (see Appendix 6.1 and Figure 6.3). Furthermore, an increase in both *Radial* and *Lateral Epicondyle* height were observed during the 60 and 70% phases of the stroke cycle. *Acromion* height during the latter phases of the stroke cycle was also significantly higher as tension increased. Collectively these kinematic data suggest that kayakers were actively resisting the downward force via

increased *AD* (and possibly other shoulder muscles) activity in order to maintain optimal wrist position during the latter stages of the stroke cycle. At higher levels of external recoil force (such as those experienced at T3 and T4), the increases in AD activity actually raised the height of shoulder and elbow markers while the corresponding height of the wrist marker remained unchanged (see Appendicess 6.1 to 6.4 and Figures 6.3 to 6.6, respectively).

Unexpectedly, elastic tension had the opposite effect on AD activity during the 40% interval of the stroke cycle, which is concurrent with the transition phase of the stroke cycle (see Chapter 5). During this phase, the shoulder is undergoing abduction as the kayaker transitions over to a draw phase on the opposite side. Mean AD activity at 40% of the stroke cycle was significantly lower at T4 when compared to T1 (Figure 6.1). At this phase of the stroke cycle, external recoil forces are acting to pull the paddle shaft forward as the kayaker raises it through the transition. Kinematic data from all markers show significant forward shifts in postion throughout the stroke. As such, it seems likely that any resistance to this forward pull during the transition phase would be achieved via increased shoulder transverse abduction and extension. This would most likely be achieved by an increase in *Posterior Deltoid, Infraspinatus* and *Teres Minor* activity (Hintermeister *et al.*, 1998) during the transition phase, which may explain the reduced reliance on AD activity as elastic tension increased.

No significant changes were detected in either TB or LD activity as elastic tension was increased. This would suggest that the forces applied by ergometer loading mechanism do not contribute to the altered EMG response observed when compared to on-water kayaking. An alternative explaination for these differences previously documented in Chapter 5, may be due to force transmission which on-water is almost instantateous (paddle contact with water) and on-ergometer requires the momentary transfer of force from the shaft through the pulleys before propulsive force can be exerted on the flywheel. Since differences in LD activity were isolated to the draw phase of the stroke cycle (see Chapter 5), this explaination is more likely to be a contributing factor with respect to this muscle. Other explainations include the lack of lateral movememt on the kayak ergometer or the inherrent instability of a flat-water kayak which invariably may alter EMG activity. It is worth noting however, that

even at T1, a significant level of external force (20 ± 4 N) was still being applied to the paddle shaft. It was not possible to lower this force any further due to the ergometer design. As such, the simple presence of an additional external force cannot be ruled out as a possible explaination for the differences in TB and LD activity when compared to the on-water condition.

The external forces applied by the ergometer's elastic tension are in general pulling the paddle shaft forward, towards the flywheel. However as was stated in the Chapter 5, during the dynamic kayaking movement the magnitude and exact direction at which the force acts is constantly changing. This was highlighted in the current study during the 60 to 90% phase of the cycle, where a more downward application of this external force resulted in significant increases in AD activity. Nonetheless, the overall effect of the elastic tension is a forward recoil force. This undoubtedly explains the significant changes in kinematic data relative to the X (horizontal) axis, which were observed in all markers in the current study (Figures 6.3 to 6.8 and Appendices 6.1 to 6.6). As tension increased, all joint positions were pulled into a more forward position. The exact mechanism as to how this was achieved remains to be elucidated. It is possible that the changes observed were due to increased shoulder protraction throughout the stroke cycle. Certainly, both the *Inferior Scapula* and medial border of the *Spinal Scapula* appear in a more forward position throughout the cycle, inferring a possible protraction of the scapula and connecting shoulder and arm. However, it is also possible that a progressive change in seating position via increased hip and lumbar flexion, could have resulted in a similar kinematic outcome. Since no markers were placed on anatomical positions in the lumbar or pelvic region, it remains to be evaluated if the consistent increases in marker position relative to the horizontal axis, were a result of increased shoulder protraction or hip and/or lumbar flexion. Additional 3D kinematic analysis is warranted in order clarify this issue.

Certain limitations must be considered before drawing definitive conclusions from the current results. Firstly, the biomechanical data presented only represents one sub-maximal exercise intensity. Kayakers exercised at a sub-maximal power output equivalent to 85% of their $\dot{V}O_2$peak; an exercise intensity in close proximity to their aerobic-anaerobic threshold

as assessed by T_{Lac}. Previous literature has reported stroke rates of 118 ± 4 (Mann & Kearney, 1980) and 96 ± 5 strokes.min^{-1} (Sanders & Kendal, 1992) during maximal intensity kayaking. The target stroke rates used in the current study (81 ± 2 strokes.min^{-1}) were markedly lower. It is possible that at higher stroke rates, the effect of elastic tension on AD activity and associated kinematic data is not as significant as those observed in the current study. The results of Chapter 5 however, highlighted that AD activity was consistently higher during ergometer kayaking, across a range of exercise intensities (75 to 95% $\dot{V}O_2$peak) and stroke rates (74 to 89 strokes.min^{-1}). This would suggest that even at higher stroke rates, kayakers continue to resist the external forces, in an effort to maintain optimal arm height during this phase of the stroke cyle. It is also worth noting that it was not possible to completely prevent the elastic tension from exerting forces on the paddle shaft. The presence or absence of this elastic tension may therefore still be responsible for the differences between kayaking conditions observed in TB and LD activity in the previous study.

6.6: CONCLUSION

From the results of the current study, the ergometer's built-in loading mechanism appears to be responsible for the significant second phase of AD activity observed during the latter stages of the on-ergometer stroke cycle. When the elastic tension was increased, AD activity during this phase progressively increased (Figure 6.1). In addition, it seems likely that these increases in AD activity are as a result of the kayaker's efforts to maintain optimal joint kinematics during this phase of the stroke cycle. The fact that *Ulnar* marker height remained unchanged despite increasing downward forces suggests that the kayaker strives to maintain optimal hand position at this key forward point within the cycle and will alter shoulder muscle activity in response to an external force, in order to achieve this goal. The lack of significant change in TB and LD activity as tension was increased suggests that the recoil forces associated with the ergometer loading mechanism, do not play as significant a role in altering recruitment patterns in these muscles during on-ergometer kayaking as was initially hypothesised. Finally, the overall changes in kinematics relative to the horizontal (X) axis, were most likely a result of the recoil forces. Further 3D kinematic analysis is warranted in order to elucidate if these alterations in kinematics were a result of increased shoulder protraction, hip flexion, or lumbar flexion.

Chapter 7

A biomechanical assessment of ergometer task specificity in rowing.

7.1: INTRODUCTION

For more than a century, rowers have used "dry-land" ergometer training to improve both fitness and rowing technique during poor weather (Halladay, 1990). During this time, a variety of ergometers have been designed to simulate the on-water rowing scenario (Steer *et al.*, 2006). The most popular modern rowing ergometers are air-braked stationary ergometers, such as the Concept II. On a stationary ergometer the flywheel and foot-stretcher are fixed while the seat slides back and forth on a rail, see Plate 7.1a. As such, when the rower's feet apply force to the stationary foot-stretcher, a reactive force moves the rower's seated body mass backwards along the ergometer rail. This fixed base for force transfer does not exist in the on-water scenario (Elliott *et al.*, 2001). Additionally, the rower's centre of gravity is continually shifted forward and backward on the ergometer rail and this has been cited as potentially increasing the risk of lower back injury in rowers (Bernstein *et al.*, 2002; Teitz *et al.*, 2002). More recently, air-braked dynamic ergometers such as the Rowperfect, have been designed in order to more accurately simulate the force transfer and biomechanics of on-water rowing. On a dynamic ergometer, the foot-stretcher, flywheel and seat are free to move along the ergometer rail, see Plate 7.1b. Therefore, the movement of body segments should be more closely matched to that of on-water rowing (Elliott *et al.*, 2001). In addition, the reduced horizontal displacement of the rower (Plate 7.2) may potentially reduce the risk of lower back injury (Bernstein *et al.*, 2002).

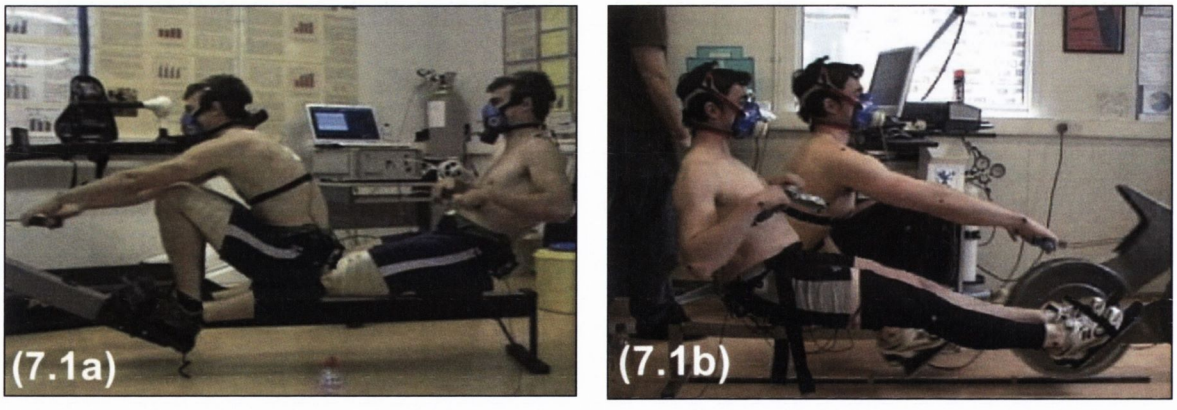

Plate 7.1: Overlapping images of a rower exercising on a stationary (7.1a) and dynamic ergometer (7.1b). Note the differences in horizontal displacement of the rower's body mass between the two ergometer designs.

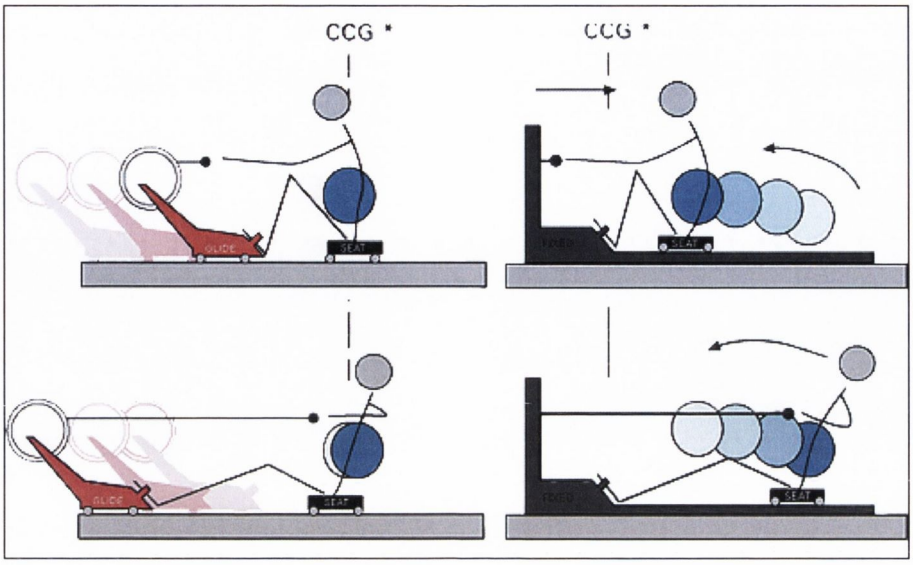

Plate 7.2: A comparison of horizontal displacement of the rower's centre of gravity on a stationary ergometer (right) and a dynamic ergometer (left). (Image location: http://www.rowperfect.ca/rowperfect.php)

Several studies have compared rowing ergometer designs, using biomechanical (Nowicky *et al.*, 2005; Steer *et al.*, 2006; Benson *et al.*, 2011) and physiological (Mahony *et al.*, 1999; Bernstein *et al.*, 2002; Benson *et al.*, 2011) variables. However, much of this published literature is contradictory in its findings. While Nowicky *et al.* (2005) reported no significant differences in hip and trunk activity or kinematics between two ergometer designs, Benson *et al.* (2011) observed significant differences in stroke biomechanics. In addition, Bernstein *et al.* (2002) reported no significant differences in physiological data, yet observed significant differences in stroke force profiles, stroke rate and stroke length, when comparing stationary and dynamic ergometers. With regards to task specificity, there is limited research assessing the accuracy with which either rowing ergometer simulates on-water rowing (Lamb, 1989; Elliott *et al.*, 2001; Kleshnev, 2005; de Campos Mello *et al.*, 2009) and the results of these published studies have also produced contradictory findings. While Elliott *et al.* (2002) reported that dynamic ergometry and sculling elicited similar biomechanics, Kleshnev (2005) observed shorter drive lengths and higher handle forces during rowing ergometry when compared to sculling. Lamb (1989) reported significant differences in arm kinematics, which were related to the removal of the oar from the water. Several authors have concluded that further research, comparing on-water rowing with

ergometry, is warranted in order to fully elucidate the accuracy with which rowing ergometers simulate the biomechanics of the on-water scenario (Caldwell *et al.*, 2003; Nowicky *et al.*, 2005).

The muscle activity patterns involved in the cyclic knee, hip and trunk movements of the rowing stroke cycle have been examined by several authors over the past 20 years (Wilson *et al.*, 1988; Clarys & Cabri, 1993; Caldwell *et al.*, 2003; Nowicky *et al.*, 2005). Early studies simply utilised EMG in order to identify the general patterns of muscle activity involved in the rowing stroke cycle (Wilson *et al.*, 1988; Clarys & Cabri, 1993). More recently, EMG has been used to compared activity patterns across ergometer design (Nowicky *et al.*, 2005) and to assess fatigue related changes in muscle activity during high intensity ergometer rowing (Caldwell *et al.*, 2003). A more recent paper (Turpin *et al.*, 2011), recorded 28 muscle recruitment patterns during dynamic ergometer rowing and identified 3 common muscle synergies which within the stroke cycle. To date however, no published literature examining muscle activity patterns during on-water rowing exists. A direct comparison of on-water and on-ergometer muscle activity patterns is therefore necessary in order to validate previous literature which examined EMG data during rowing ergometry.

7.2: AIMS AND HYPOTHESIS

The primary aim of the current study was to directly compare muscle activity patterns recorded during on-water and on-ergometer rowing across a range of exercise intensities. An additional aim was to compare EMG, biomechanical and kinematic data between stationary and dynamic ergometers and relate these findings to the on-water scenario; in order to assess which ergometer design best simulates activity patterns observed during on-water rowing. We hypothesised that muscle activity patterns would not differ significantly between the two investigated ergometer designs and the on-water scenario and that increasing exercise intensity would result in marked increase in muscle activity and stroke force independent of condition

7.3: MATERIALS AND METHODS

7.3.1: Participants

Ten (n=10) male intervarsity rowers volunteered to perform this study (mean ± SD; age 21 ± 2 yr, height 1.90 ± 0.05 m, body mass 83.3 ± 4.8 kg; BMI of 23.0 ± 1.8 $kg.m^{-2}$). All participants had a minimum of 3 years rowing experience and were proficient in both sweep and sculling technique. Prior to participation, enlisted rowers completed a detailed medical questionnaire and underwent a medical examination by a qualified medical practitioner which included anthropometric, pulmonary and haematological assessments, in order to rule out any subclinical or medical contraindications to maximal exercise testing.

7.3.2: Experimental design

This study was approved by the university Health Sciences Ethics Committee in Trinity College Dublin and consisted of a three visits to two separate locations. Initially, a graded incremental rowing test to volitional exhaustion was performed to assess $\dot{V}O_2$, lactate and heart rate response profiles. These tests were performed in the Human Performance Laboratory, Anatomy Department, Trinity College Dublin. Data acquired during incremental testing were subsequently used to set each individual's exercise intensities (75, 85, and 95% $\dot{V}O_2$peak) for the task specificity trials. The ergometer trials were also performed in the Human Performance Laboratory while the on-water trials were performed on the River Liffey at Dublin University Boat Club (DUBC). Time duration between task specificity trials was between 1 and 7 days and all trials were performed between 08:00 and 11:00 to reduce the potential for circadian variability. During task specificity trials, exercise intensity was matched using heart and stroke rate data attained during incremental testing and all individuals acted as their own control.

Rowers performed their graded incremental test and ergometer task specificity trial on an air-braked, drag adjustable rowing ergometer (RP3, Rowperfect, Hertogenbosch, The Netherlands). In order to facilitate comparison between stationary and dynamic ergometer designs, this rowing ergometer was modified, allowing the flywheel and foot-stretcher to be clamped in a stationary position. This facilitated assessment of both stationary and dynamic

rowing ergometry on the same machine. The chain was placed on the larger of two cogwheels and flywheel dampening was set at its lowest setting for all trials, in order to replicate the drag associated with single sculling as much as possible. The on-water task specificity trials were performed in a single scull (Empacher K10, Erbach, Germany) provided by the DUBC senior men's team, dimensions adhered to the FISA guidelines regarding single sculls; mass and length were 14kg and 8.2m, respectively. All participants in the study were competent single scullers and were accustomed to both dynamic and stationary rowing ergometer training.

7.3.3: Maximal incremental test

Prior to task specificity trials, maximal incremental tests were performed on the Rowperfect rowing ergometer using the protocol outlined in Chapter 2.7. Respiratory exchange variables, heart rate and blood lactate data were recorded during each increment of the test (see Chapters 2.8, 2.9 and 2.10, respectively). Data were subsequently used to attain target heart and stroke rates equivalent to 75, 85 and 95% of each participant's $\dot{V}O_2$peak.

7.3.4: On-ergometer task specificity trials

A 10-min warm-up at heart rate equivalent to 50% of individual rower's $\dot{V}O_2$peak was performed on the ergometer prior to commencing task specific trials. An additional series of 3 by 10 s maximal power starts were performed in order to attain maximal reference EMG data from investigated musculature. The subsequent on-ergometer trials consisted of 6 by 3 min bouts of exercise at heart and stroke rates equivalent to 75, 85 and 95% of individual rower's $\dot{V}O_2$peak. The ergometer flywheel and foot-stretcher were clamped on alternating exercise bouts such that rowers exercised at all intensities both on the stationary and dynamic ergometer setup. The order of both exercise intensity (75, 85 and 95% $\dot{V}O_2$peak) and ergometer setup (dynamic and stationary) was randomised for the group and a 5 min recovery period followed each exercise bout. Heart rate data were recorded and monitored throughout all trials using a Garmin Forerunner telemetric heart rate monitor (Garmin, Kansas, USA). Stroke rates were recorded and monitored via a laptop and RP3 software (Version 1.6) connected to the ergometer via a USB connection providing constant feedback of stroke rate and power output data.

7.3.5: On-water task specificity trials

All on-water task specificity trials were performed in a single scull. An initial 10-min warm-up at heart rate equivalent to 50% of individual rower's $\dot{V}O_2$peak was performed prior to commencing on-water task specific trials. An additional series of 3 by 10 s maximal power starts were also performed in order to attain maximal reference EMG data from investigated musculature. The subsequent on-water trial consisted of 3 by 3 min bouts of exercise at heart and stroke rates equivalent to 75, 85 and 95% of individual rower's $\dot{V}O_2$peak. The order of exercise intensity was randomised for the group and a 5 min recovery period followed each exercise bout. Heart rate data were recorded and monitored throughout trials using a Garmin Forerunner telemetric heart rate monitor (Garmin, Kansas, USA). Stroke rates were controlled throughout the on-water trial via a digital metronome which rowers listened to using a standard MP3 player and headphones. Rowers were instructed to maintain the pre-determined stroke rate throughout and to gradually increase their heart rate over the initial 2 min until their target heart rate had been attained. They then maintained their heart and stroke rates as close as possible to their individual targets for the final minute of the task specific exercise bout.

7.3.6: EMG data

EMG data were recorded on the right side of the body from four muscles involved in the rowing stroke cycle: *Rectus Femoris* (RF), *Vastus Medialis* (VM), *Biceps Femoris* (BF) *and Erector Spinae* (ES); see Chapter 2.1. Synchronisation of EMG and video data using an audio-sync trigger (Mega, Koupio, Finland) facilitated identification of onset of each stroke cycle on the EMG recording, see Chapter 2.3. EMG data from 10 consecutive stroke cycles in the final minute of each task specificity trial were amplitude processed via root mean squaring and normalised relative to isometric MVC, see Chapters 2.3 and 2.4, respectively. Subsequent temporal normalisation and averaging via cubic spline fitting (Chapter 2.5) produced an average rmsEMG ensemble for each muscle during task specificity trials both on-water and on-ergometer.

Attempts to normalise EMG data using standard isometric MVC procedures for each muscle were not successful in the current study. While this normalisation procedure was successful in previous studies (Chapters 5 and 6), peak EMG data recorded during rowing stroke cycle was often higher than the signal recorded during an isometric MVC manoeuvre, notably in RF and BF. The issue of EMG normalisation has previously been discussed by several authors (Burden & Bartlett, 1999; Rouffet & Hautier, 2008). In addition, Nowicky *et al.* (2005) encountered a similar problem when normalising their EMG data recorded during the rowing stroke cycle to an isometric MVC. Therefore EMG signals in the current study were normalised to the maximal EMG recorded during one of the pre-trial 10 s maximal power starts. This procedure has previously been suggested as a novel approach to the normalisation of dynamic EMG data (Rouffet & Hautier, 2008).

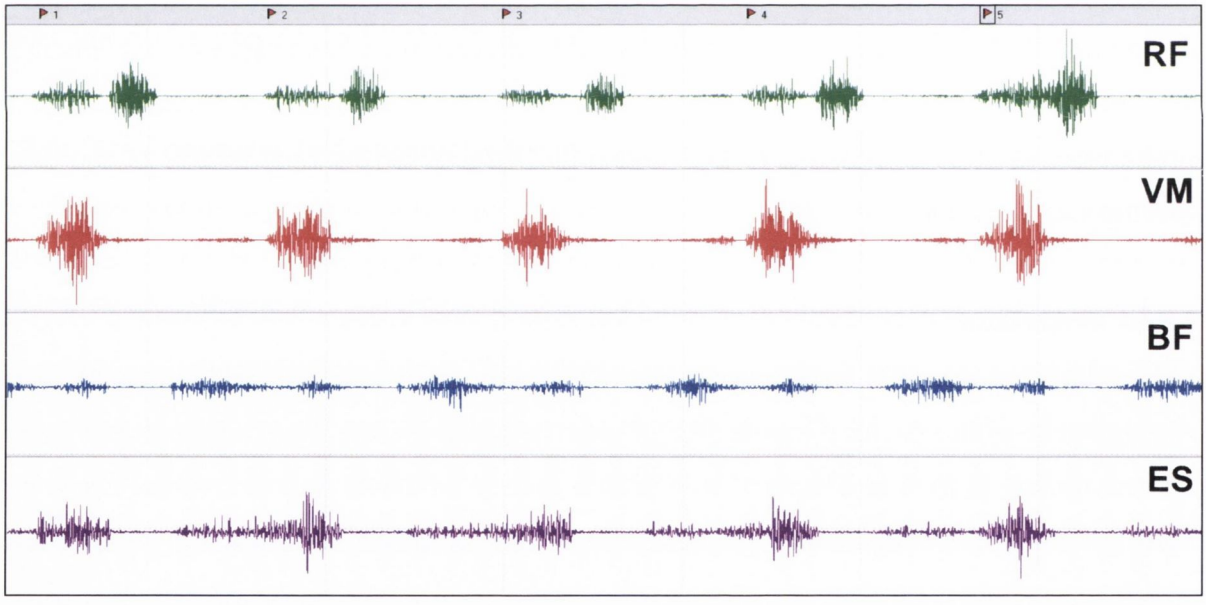

Figure 7.1: Raw EMG trace (bipolar scale: ±3000 μV per channel) recorded for 5 consecutive stroke cycles during on-water rowing at 85% $\dot{V}O_2$peak. Flag markers at top of the trace indicate the onset of each stroke cycle. Channels 1 to 4 (top to bottom) dispay raw EMG data recorded from RF, VM, BF and ES, respectively.

7.3.7: Stroke force data

Throughout all ergometer trials, stroke force data were measured using a load cell attached to the ergometer handle, see Chapter 2.7 and Plate 2.8.

7.3.8: Kinematic data

2D video kinematic data were recorded during task specificity trials using a 50 Hz digital video camera (JVC, Yokohama, Japan) positioned orthogonally to the sagittal plane of the rower at a distance of 5 to 10m. Video data were transferred in real-time to computer via firewire connection for subsequent processing and analysis. Onset of stroke cycle was identified as the first video frame where ergometer or oar handle was moved away from maximal forward position. End of drive phase was identified as the video frame where ergometer or oar handle was at its furthest displacement from maximal forward position. Stroke rate, drive time and drive-recovery ratio were calculated and averaged for 10 consecutive stroke cycles in each exercise condition across all exercise intensities.

7.3.9: Data reduction and statistical analysis

All EMG and force data were transferred to Matlab (Mathworks, Massachusetts, USA) for data reduction. For statistical analysis, mean rmsEMG data were averaged for each 10% segment of the stroke cycle. Stroke force data during on-ergometer task specificity trials were also averaged over the same 10 consecutive stroke cycles and temporally normalised to attain a group mean stroke force ensemble at each 2% of stroke cycle duration. Data were subsequently analysed to attain measures of peak force (N), absolute time to peak force (s), normalised time to peak force (%), rate of peak force development (RFD_{peak} in $N.s^{-1}$) and rate of 50% peak force development (RFD_{50} in $N.s^{-1}$) as outlined by Benson *et al.* (2011). Integration of the stroke force profile in the first 30% of the stroke cycle quantified the drive impulse (N.s).

All data are presented as group mean ± SEM. Normality was assessed using Kolmogorov-Smirnoff tests and log transformations of EMG data were performed in order to satisfy normality. Statistical analyses of iEMG data were performed using 2-way repeated measures ANOVA (condition by intensity); *post-hoc* Tukey tests quantified detected differences.

Comparison of iEMG and stroke force data across conditions (stationary ergometer vs. dynamic ergometer vs. on-water) were also performed using 2-way repeated measures ANOVA (condition by intensity). Statistical analyses were performed using Sigmastat (Systat Software, Chicago, USA) and $P<0.05$ inferred statistical significance.

7.4: RESULTS

7.4.1: Group physiological characteristics

The group had a mean ± SEM $\dot{V}O_2$peak of 66.0 ± 2.6 mL.kg^{-1}.min^{-1} and during incremental testing mean maximal power output at volitional failure was 393 ± 9 W. For each incremental test; heart rate, blood lactate, $\dot{V}O_2$ and stroke rate data were plotted against power output (W). Subsequently, lactate threshold (T_{Lac}) defined as the point of inflection on the lactate curve was determined graphically (Beaver *et al.*, 1986). The mean power, HR and BLa at T_{Lac} were 280 ± 10 W, 179 ± 3 beats.min^{-1} and 2.4 ± 0.1 mmol.L^{-1}, respectively. Mean heart rates equivalent to 75, 85 and 95% of the group $\dot{V}O_2$peak were 162 ± 5, 174 ± 4 and 186 ± 2 beats.min^{-1}. During the task specificity trials, no significant differences between conditions were observed in heart rate data recorded at any of the exercise intensities, suggesting that exercise intensity was closely matched between the three task specificity trials.

7.4.2: Stroke force and kinematics

The group mean (SEM) data for stroke kinematics and force are presented in Tables 7.1 and 7.2, respectively. In addition, stroke force profiles during both stationary and dynamic ergometry are presented in Figure 7.2. No stroke force data were collected during the on-water trials; data were only recorded via an integrated load cell during on-ergometer task specificity trials. Significant differences in kinematic data were observed between the on-ergometer and on-water trials across all exercise intensities. Most notably, on-water rowing differed significantly from dynamic ergometry across several kinematic variables. Draw times were significantly greater comparing on-water rowing to dynamic ergometry ($P<0.001$ at all exercise intensities). In addition, drive/recovery ratios were significantly greater comparing on-water rowing to dynamic ergometry ($P<0.01$ at all exercise intensities). Increased exercise intensity and stroke rate had a significant effect on both drive times and drive/recovery ratios across all conditions. Differences in the two ergometer designs were also observed when comparing drive time and drive-recovery ratios. Draw time was significantly longer during stationary ergometry ($P<0.05$ at all intensities). In addition, the drive-recovery ratio was significantly greater during stationary ergometry at the 85 and 95%

intensities ($P<0.05$). These results suggest that as a whole, rowers were completing the drive phase of the stroke cycle significantly faster during dynamic ergometry compared to both stationary ergometry and on-water rowing. As exercise intensity and stroke rate increased drive times progressively decreased ($P<0.001$), this observation was expected, however, drive/recovery ratios progressively increased ($P<0.001$). This effect was consistent across all conditions (Table 7.1) and suggests that while drive times are reduced with increasing stroke rate, the corresponding reduction in recovery times was of a greater magnitude.

Variable	Intensity	On-Ergometer		On-Water
		Stationary	Dynamic	
Stroke rate (strokes.min^{-1})	75%	20 (1)	20 (1)	20 (1)
	85%	23 (1)	23 (1)	23 (1)
	95%	27 (1)	27 (1)	27 (1)
Drive time (s)	75%	1.06 (0.02)*#	1.00 (0.03)***	1.13 (0.05)
	85%	1.00 (0.02) #	0.94 (0.02)***	1.05 (0.03)
	95%	0.94 (0.01) #	0.88 (0.01)***	0.99 (0.02)
Drive-recovery ratio (%)	75%	35 (1)	33 (1)**	36 (1)
	85%	39 (1) #	37 (1)**	40 (1)
	95%	42 (1) #	40 (1)**	44 (1)

Table 7.1: Group mean (SEM) stroke kinematic data. Asterisk infer a significant difference compared to on-water (* $P<0.05$, ** $P<0.01$, *** $P<0.001$). Hash symbol infers a significant difference compared to dynamic ergometer at $P<0.05$.

Comparing stroke force data between stationary and dynamic ergometry trials revealed no significant differences in peak force, RFD_{peak}, RFD_{50} or impulse (Table 7.2). While no differences were observed in absolute time to peak force, a significant difference in normalised time to peak force was observed at 95% $\dot{V}O_2$peak. At this high exercise intensity, peak force occurred significantly earlier during stationary ergometry ($P<0.05$). Increasing exercise intensity had a significant effect on peak force ($P<0.01$), RFD_{peak} ($P< 0.001$) and RFD_{50} ($P<0.001$), with all variables increasing as exercise intensity increased. These effects were consistent across ergometer design (Table 7.2). While absolute time to peak force was reduced as exercise intensity increased ($P<0.001$), when time to peak force was expressed as a percentage of overall stroke cycle duration no significant differences were observed across intensity. Although not quantified, a noticeable difference in the initial development of force was observed between the two ergometer designs. This can clearly be seen from Figure 7.2 as greater force production in the first 10% of the drive phase during dynamic ergometry. No significant change in stroke impulse was observed with increasing exercise intensity.

Variable		Stationary	Dynamic
Peak force (N)	75%	843 (58)	844 (53)
	85%	915 (54)	912 (51)
	95%	1007 (34)	981 (33)
Time to peak (s)	75%	0.43 (0.02)	0.43 (0.02)
	85%	0.38 (0.02)	0.38 (0.02)
	95%	0.35 (0.01)	0.36 (0.01)
Time to peak (%)	75%	14.63 (0.67)	14.88 (0.73)
	85%	14.91 (0.89)	15.63 (1.02)
	95%	15.01 (0.83) *	15.92 (0.69)
RFD_{peak} ($N.s^{-1}$)	75%	2058 (266)	2095 (259)
	85%	2529 (277)	2501 (234)
	95%	2974 (177)	2737 (150)
RFD_{50} ($N.s^{-1}$)	75%	2649 (281)	3017 (622)
	85%	3229 (383)	3312 (426)
	95%	3694 (305)	3736 (451)
Impulse (N.s)	75%	398 (16)	398 (12)
	85%	412 (11)	403 (11)
	95%	418 (9)	406 (7)

Table 7.2: Group mean (SEM) stroke force data during on-ergometer task specificity rowing trials. Asterisk infers a significant difference compared to the dynamic ergometer condition at $P<0.05$.

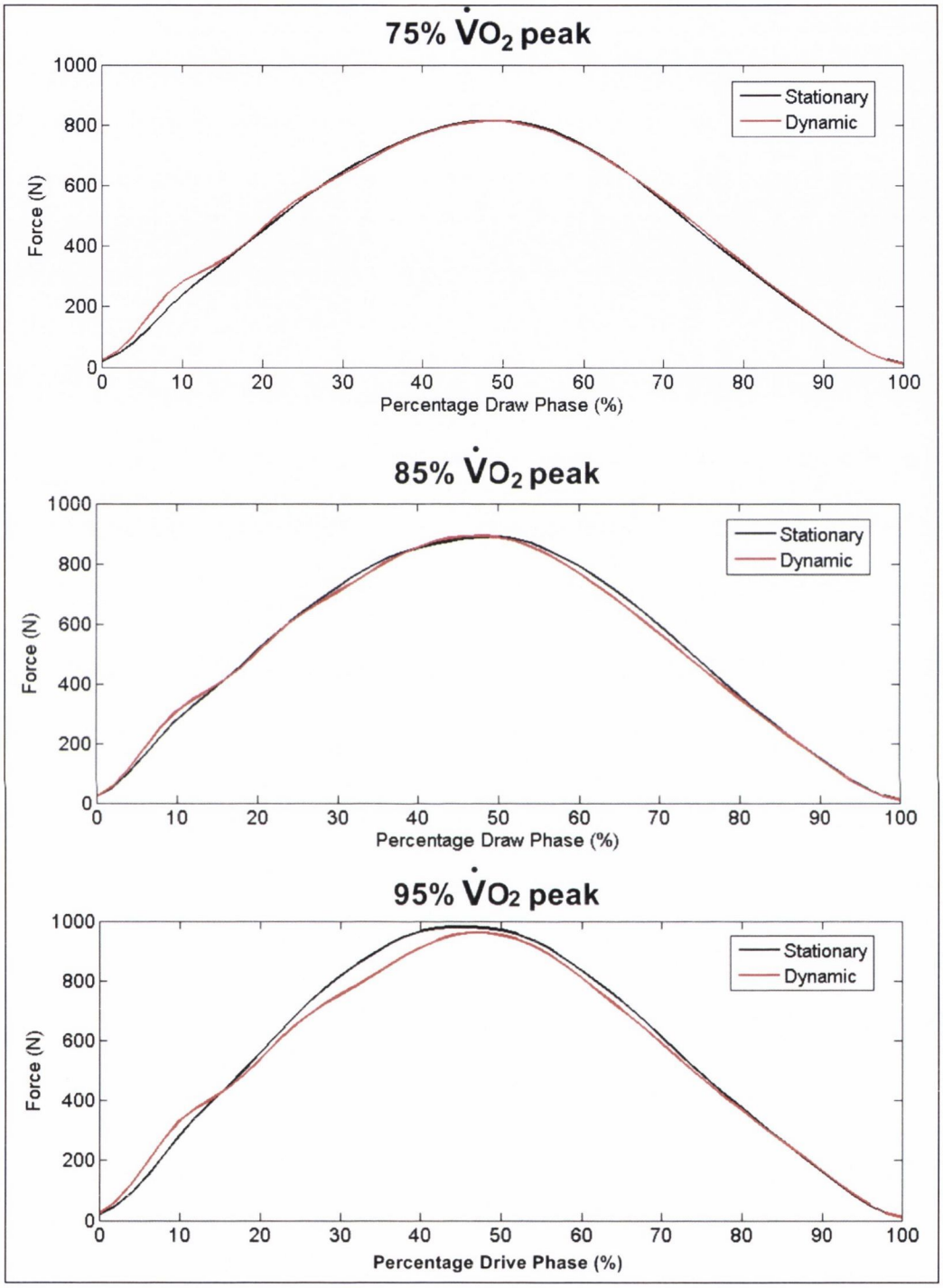

Figure 7.2: Group mean ensemble force-time profiles normalised to the drive phase duration of stationary (red) and dynamic (black) ergometer rowing stroke cycles.

7.4.3: EMG data

Synchronisation of 2D kinematic and EMG data facilitated quantification of the distinct phases of the rowing stroke cycle during which each investigated muscle was active. As expected, the knee extensor muscles (RF and VM) were highly active during the majority of the drive phase (0-30% of stroke cycle, see Figures 7.3 and 7.4). The drive phase involves synchronous knee and hip extension, which drives the body backwards and facilitates the powerful pulling of the oar through the water. It is worth noting that magnitude of RF activity during the drive phase of the stroke cycle varied greatly across both condition and intensity (Figure 7.3). Both BF and ES activity were also observed during drive phase. This is due to their role in hip and trunk extension, respectively, which is especially necessary in the latter stages of the drive phase, in order to maximise stroke length (Figures 7.5 and 7.6). A second distinct phase of RF activity was observed during the 30-50% phase of the stroke cycle which corresponded to the end of the drive and onset of the recovery phases. The recovery phase initially involves progressive hip and trunk flexion followed by knee flexion, which facilitates the forward movement of the rower's body in preparation for the subsequent stroke. Since RF is a bi-articulate muscle and is involved in both knee extension and hip flexion, RF activity during 30-50% of the stroke cycle is indicative of the role of RF in the controlled flexion of the hip joint during the recovery phase. Finally, low level BF activity in the latter stages of the stroke cycle (60-100%) was observed and is most likely due to the progressive knee flexion during the recovery phase of the stroke (Figure 7.5).

Overall muscle activity per stroke cycle was initially quantified using integrated EMG (iEMG) or area of rms amplitude per stroke cycle (Table 7.3). While no significant differences were observed across exercise condition, intensity had a significant effect on RF and VM activity ($P<0.01$). Both knee extensor muscles showed significant increases in overall EMG activity as exercise intensity increased. Unexpectedly, there was a progressive decrease in BF activity as exercise intensity increased; see Table 7.3, especially during on-water rowing, however, this effect did not reach a significant level. Overall, iEMG activity in ES remained relatively unchanged throughout.

Variable	Intensity	On-Ergometer		On-Water
		Stationary	Dynamic	
RF iEMG (μV.s)	75%	105 (10)	109 (19)	141 (22)
	85%	122 (9)	113 (22)	146 (20)
	95%	149 (12)	130 (23)	161 (24)
VM iEMG (μV.s)	75%	207 (26)	195 (23)	217 (36)
	85%	230 (31)	231 (29)	243 (36)
	95%	266 (32)	249 (24)	283 (32)
BF iEMG (μV.s)	75%	174 (15)	182 (13)	196 (14)
	85%	155 (13)	170 (11)	179 (12)
	95%	155 (14)	177 (14)	158 (11)
ES iEMG (μV.s)	75%	227 (28)	243 (28)	263 (33)
	85%	256 (26)	229 (22)	260 (28)
	95%	255 (28)	236 (19)	258 (27)

Table 7.3: Mean (SEM) data for iEMG activity across exercise condition and intensity, n=10.

While no significant differences were observed for overall muscle activity, analysis of discrete 10% time intervals within the stroke cycle highlighted several specific differences in muscle activity between conditions. The most striking differences were observed in RF, see Figures 7.7a, 7.8a and 7.9a. Mean RF activity during on-water rowing was significantly greater than either on-ergometer condition at the 50, 60 and 70% intervals of the stroke cycle see Figures 7.7a, 7.8a and 7.9a. In addition, mean on-water RF activity was significantly greater than dynamic ergometry during the initial 10 and 20% intervals of the stroke cycle. Both these differences appeared consistent across all exercise intensities. No significant differences in RF activity were observed comparing stationary and dynamic ergometry at the 75% exercise intensity, however, as intensity increased significantly greater activity was observed during stationary ergometry at the 10 and 20% intervals (Figures 7.8a

and 7.9a). Mean VM activity during on-water rowing was significantly greater than ergometry at the 10% interval during all exercise intensities (Figures 7.7b, 7.8b and 7.9b). As intensity increased greater on-water mean VM activity also occurred at the 20 and 30% intervals on-water. Significantly greater mean ES peak activity during on-water rowing was observed at the 75% exercise intensity ($P<0.05$, see Figure 7.7d), however, this difference did not manifest itself at higher intensities. No significant differences in mean BF activity were observed at any of the exercise intensities.

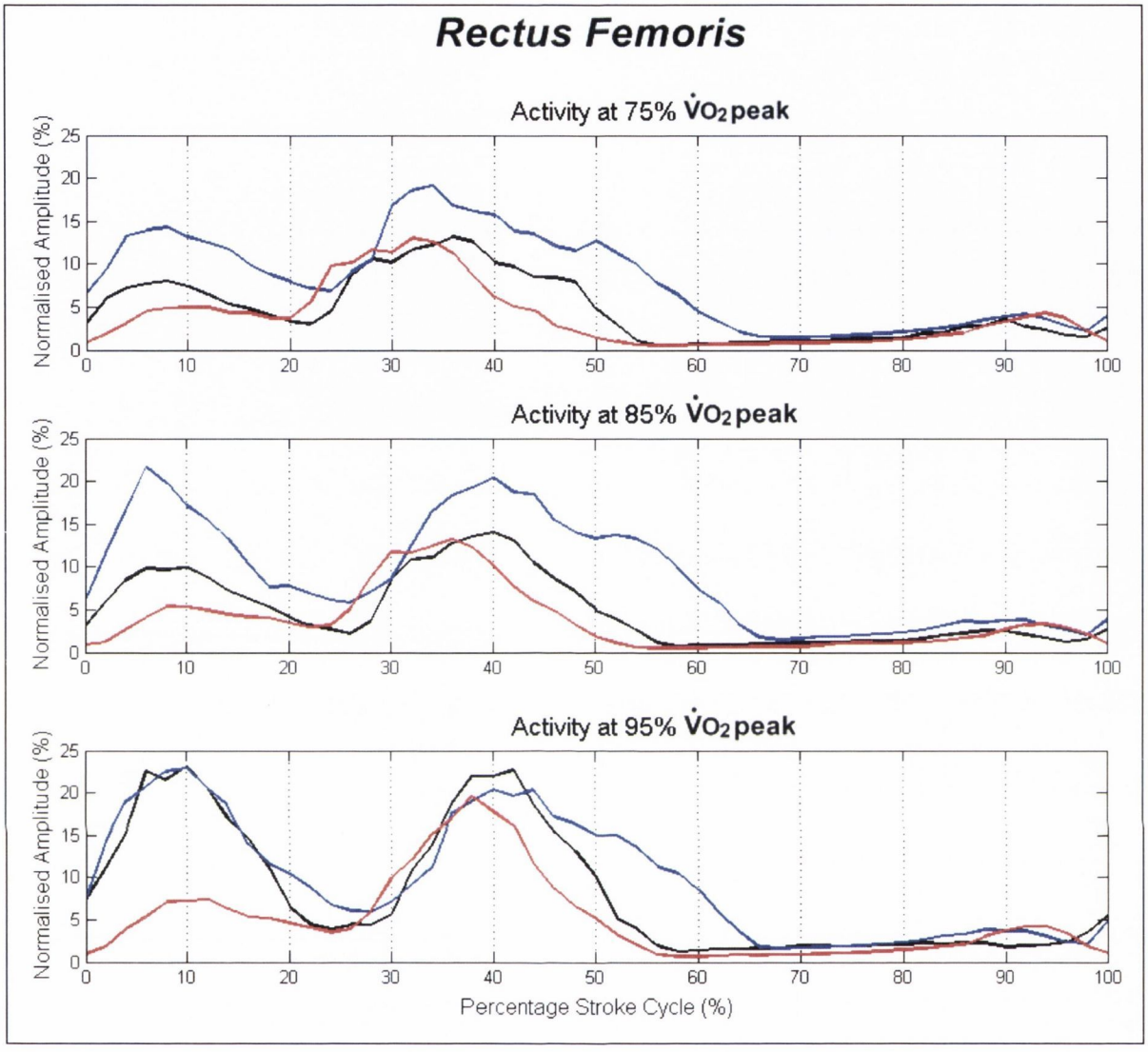

Figure 7.3: Group mean ensemble EMG traces for RF recorded during on-water (blue), stationary ergometer (black) and dynamic ergometer (red) rowing at 75, 85 and 95% $\dot{V}O_2$peak.

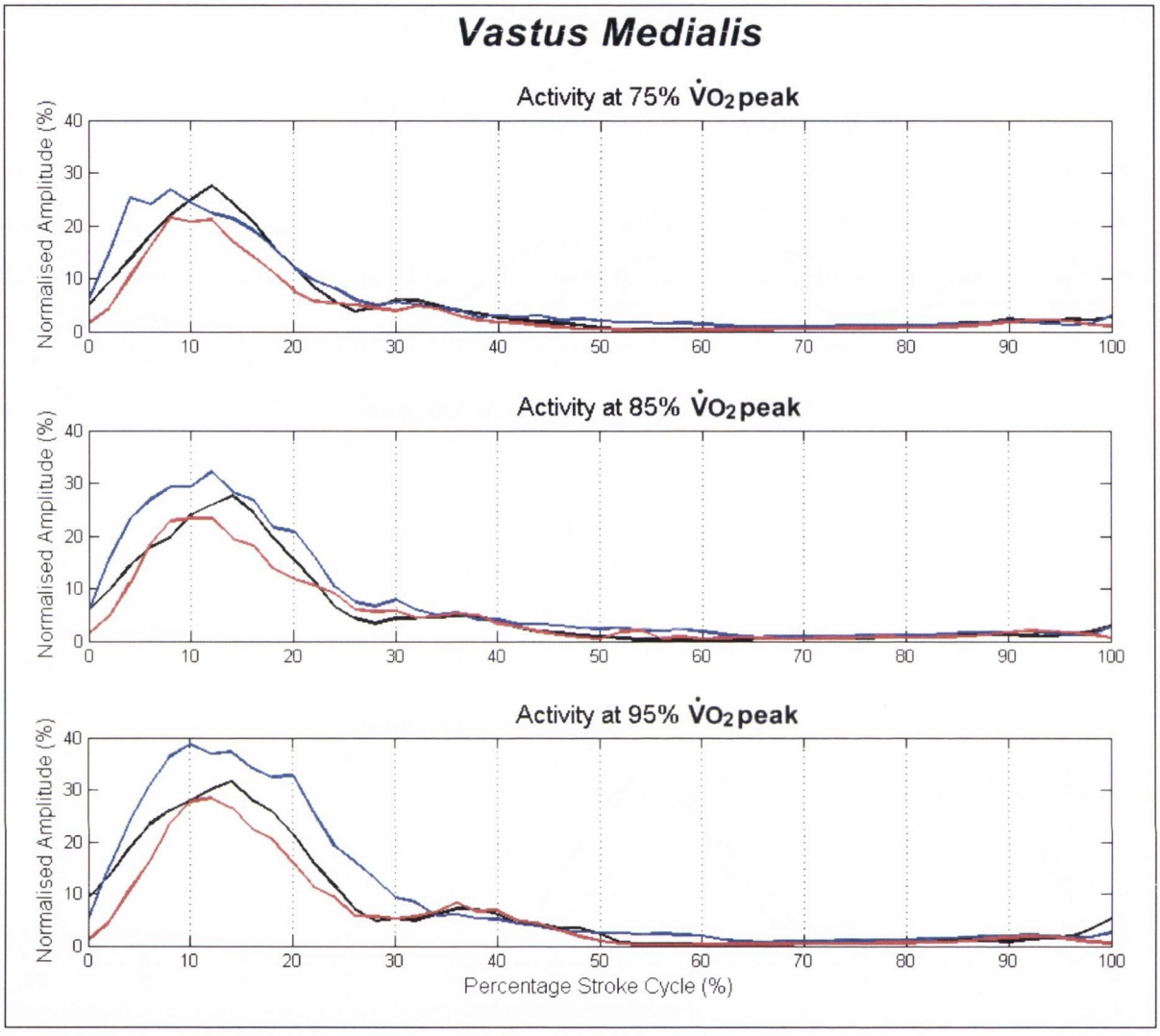

Figure 7.4: Group mean ensemble EMG traces for VM recorded during on-water (blue), stationary ergometer (black) and dynamic ergometer (red) rowing at 75, 85 and 95% $\dot{V}O_2$peak.

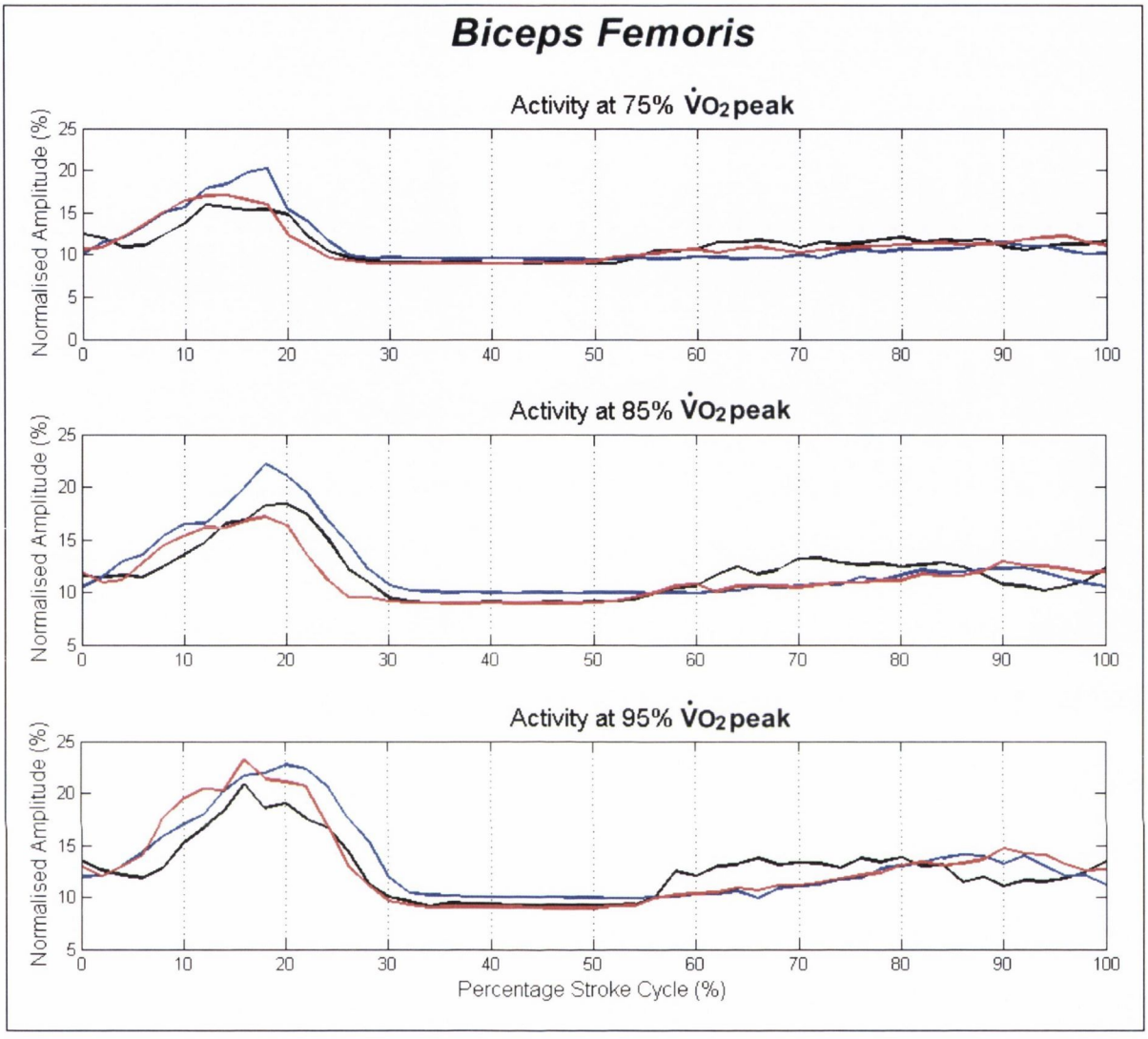

Figure 7.5: Group mean ensemble EMG traces for BF recorded during on-water (blue), stationary ergometer (black) and dynamic ergometer (red) rowing at 75, 85 and 95% $\dot{V}O_2$peak.

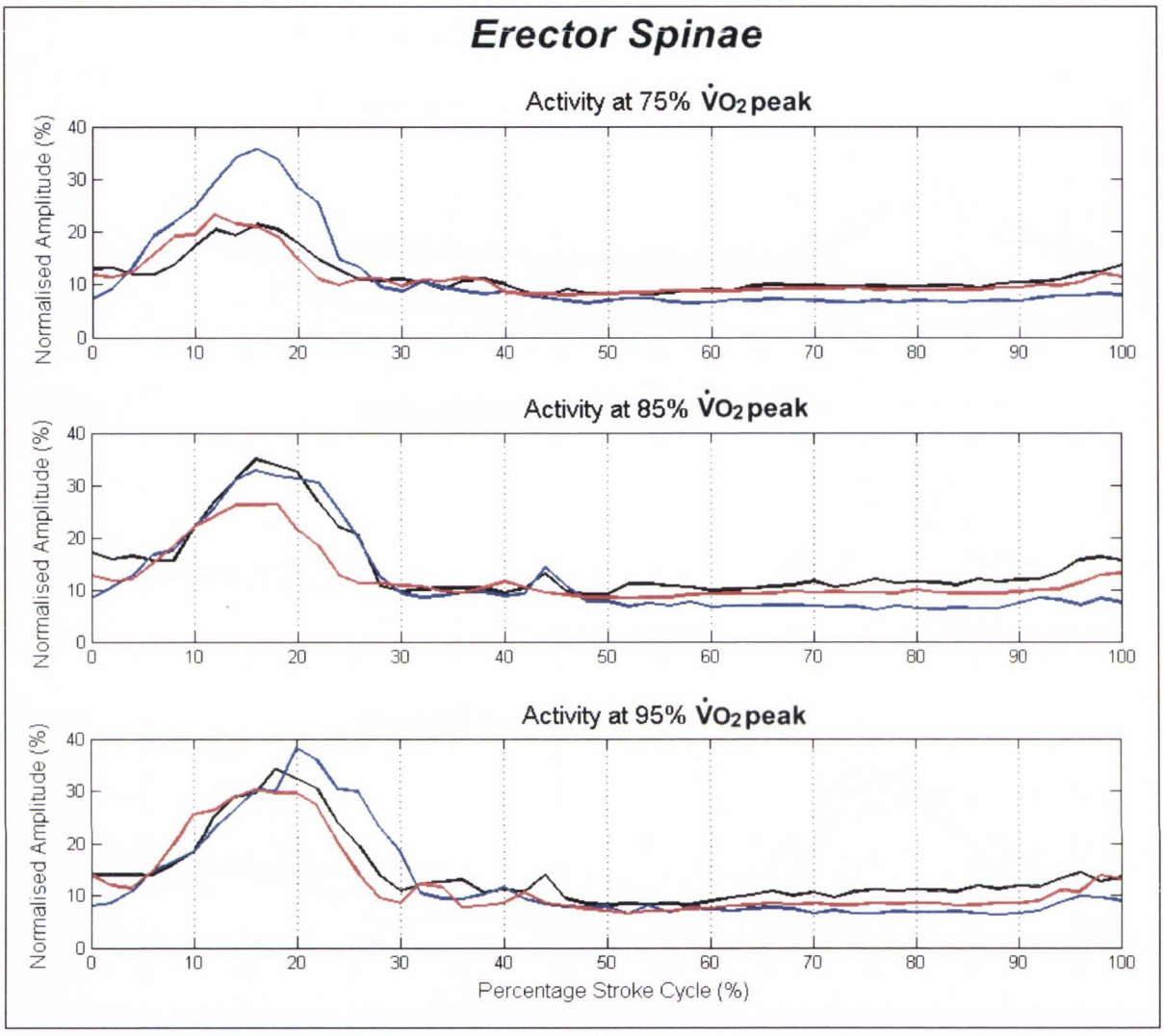

Figure 7.6: Group mean ensemble EMG traces for ES recorded during on-water (blue), stationary ergometer (black) and dynamic ergometer (red) rowing at 75, 85 and 95% $\dot{V}O_2$peak.

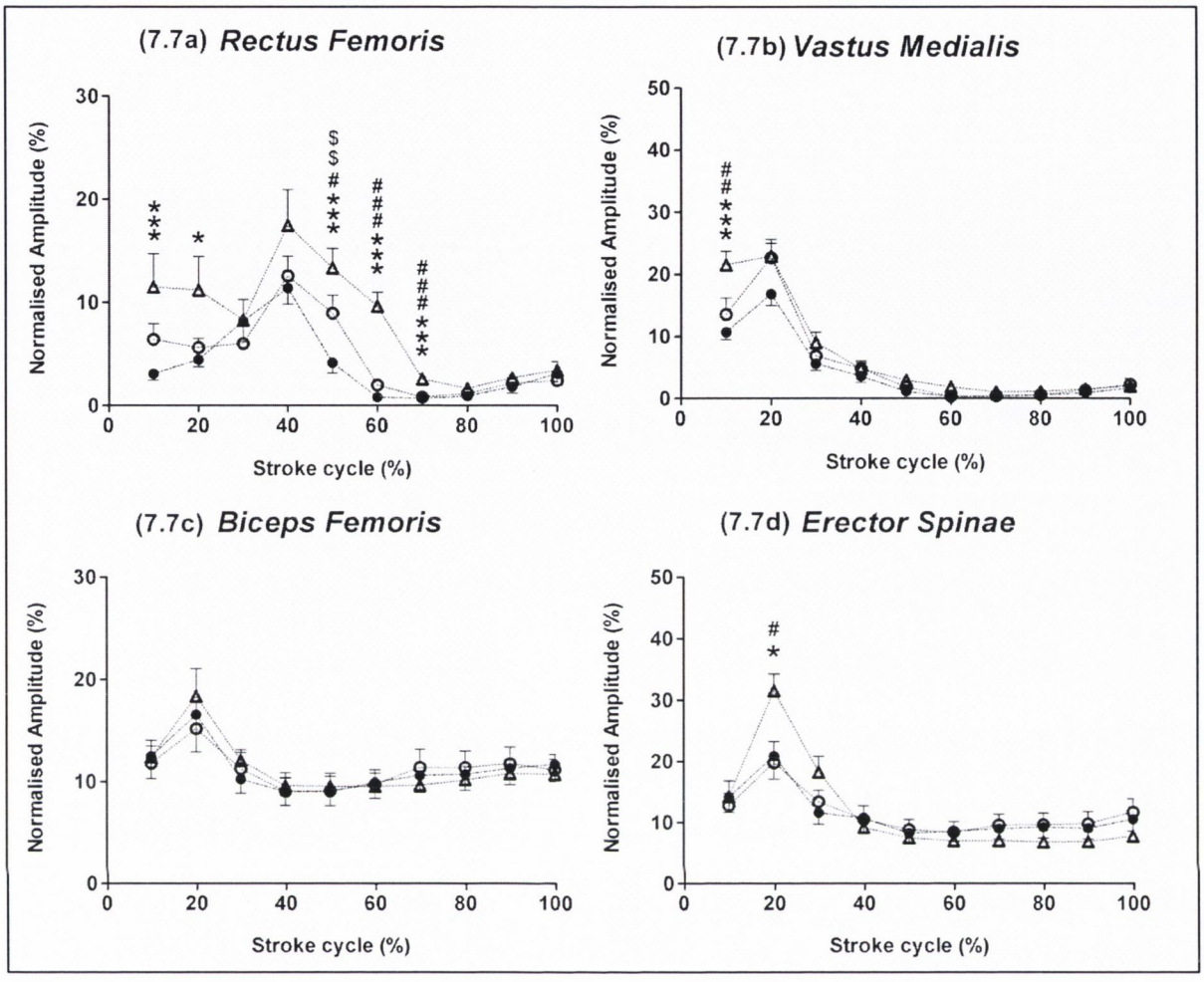

Figure 7.7: Group mean ± SEM (n=9) EMG profiles for stationary (open circles), dynamic (closed circles) and on-water (closed triangles) rowing stroke cycles at 75% $\dot{V}O_2$peak. Each point represents mean rms amplitude for 10% of the stroke cycle normalised to maximal rms amplitude recorded during pre-trial sprints. Asterisk infer a significant difference between on-water and dynamic at specific 10% intervals (* $P<0.05$, ** $P<0.01$, *** $P<0.001$). Hash symbols infer significant differences between on-water and stationary (# $P<0.05$, ### $P<0.001$). Dollar symbol infer significant differences between dynamic and stationary ($$ $P<0.01$).

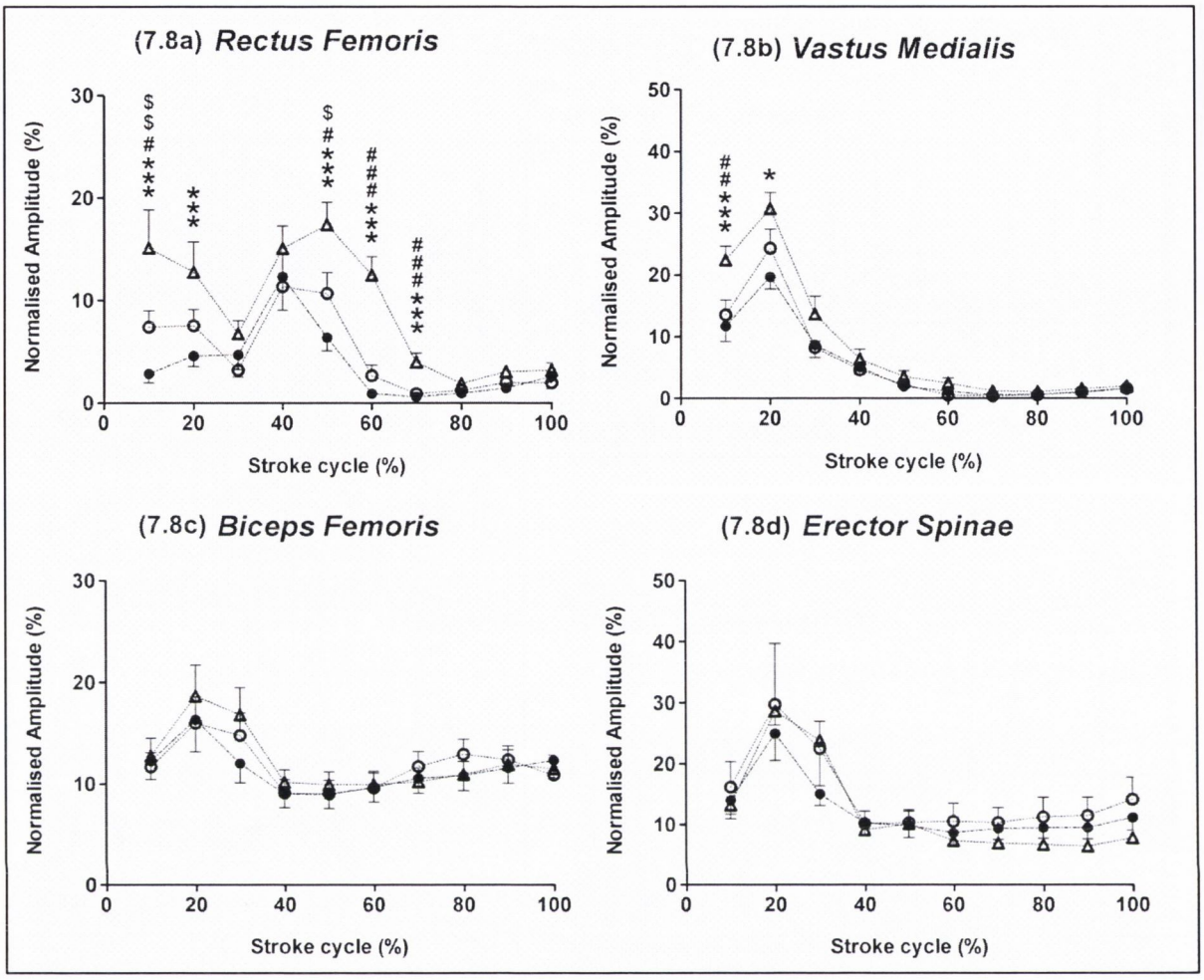

Figure 7.8: Group mean ± SEM (n=9) EMG profiles for stationary (open circles), dynamic (closed circles) and on-water (closed triangles) rowing stroke cycles at 85% $\dot{V}O_2$peak. Each point represents mean rms amplitude for 10% of the stroke cycle normalised to maximal rms amplitude recorded during pre trial sprints. Asterisk infer significant differences between on-water and dynamic at specific 10% intervals (* $P<0.05$, ** $P<0.01$, *** $P<0.001$). Hash symbol infer significant differences between on-water and stationary (# $P<0.05$, ### $P<0.001$). Dollar symbol infer significant differences between dynamic and stationary ($ $P<0.05$, $$ $P<0.01$).

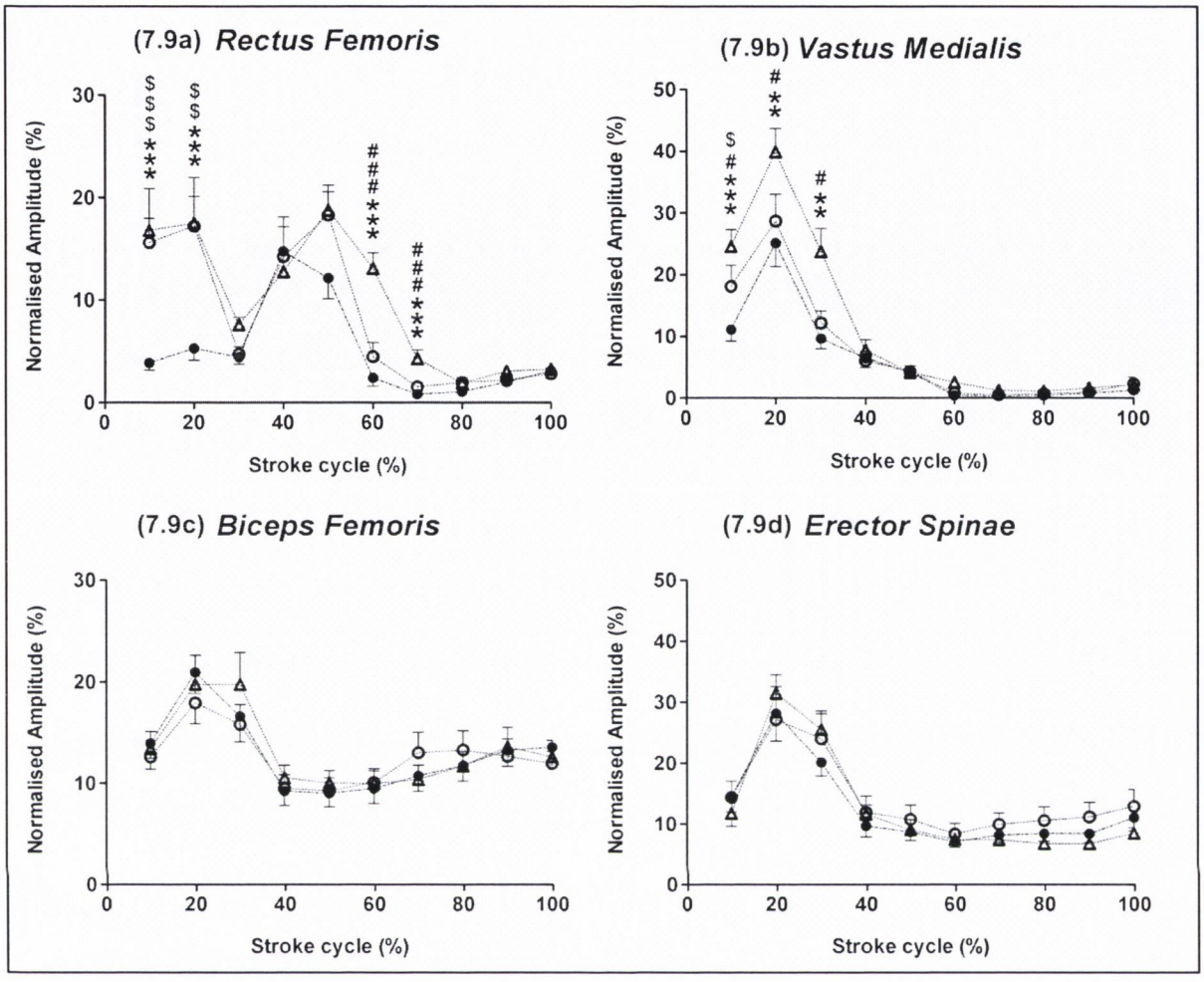

Figure 7.9: Group mean ± SEM (n=9) EMG profiles for stationary (open circles), dynamic (closed circles) and on-water (closed triangles) rowing stroke cycles at 95% $\dot{V}O_2$peak. Each point represents mean rms amplitude for 10% of the stroke cycle normalised to maximal rms amplitude recorded during pre-trial sprints. Asterisk infer difference between on-water and dynamic at specific 10% intervals (* $P<0.05$, ** $P<0.01$, *** $P<0.001$). Hash symbol infer significant differences between on-water and stationary (# $P<0.05$, ### $P<0.001$). Dollar symbol infer significant differences between dynamic and stationary ($ $P<0.05$, $$ $P<0.01$, $$$ $P<0.001$).

7.5: DISCUSSION

The primary aim of the current study was to compare muscle activity patterns and associated kinematic data recorded during on-water rowing with data recorded during rowing ergometry, in order to assess the biomechanical task specificity of two contrasting ergometer designs. To the best of this author's knowledge, this is the first study which utilises telemetric EMG to identify the muscle activity patterns of the on-water rowing stroke cycle. The results of this study highlighted several differences in muscle activity patterns between on-water and ergometer rowing, most notably in RF activity. In addition, stroke kinematic data (normalised and absolute drive times) suggest that differences exist in the velocity at which rowers execute the drive phase of the stroke. It is possible that these kinematic differences played a role in altering muscle recruitment patterns between the ergometer designs and on-water scenario.

The differences in RF activity between exercise conditions were extensive and appeared across all exercise intensities (Figures 7.7a, 7.8a and 7.9a). In order to better interpret these results, it is appropriate to group the differences in RF activity into two specific categories; those which occurred during the early drive phase (10 and 20% intervals) and those which occurred during the early recovery phase (40, 50 and 60% intervals). Due to the bi-articulate nature of RF, these two phases of activity are resultant from varying joint articulations, however, the underlying biomechanical mechanism which elicited the differences may be common to both. Activity during the early drive phase (10 and 20% intervals) was due to the muscle's role as a knee extensor while activity during the early recovery phase (40 to 60% intervals) was due to its role as a hip flexor. In general, the overall pattern of RF activity observed in current study is in agreement with previous EMG data reported by Nowicky *et al.* (2005). With regards to the early drive phase, RF activity progressively increased both on-water and on the stationary ergometer as stroke rate and intensity increased; however, no such increase in activity was observed during dynamic ergometer rowing. The differences in RF activity were therefore most pronounced at 95% $\dot{V}O_2$peak, see Figure 7.9a. It is most likely that these differences were due to the increased acceleration and deceleration of the moving masses during the stroke cycle. Bernstein *et al.* (2002) highlighted that during the rowing stroke cycle, the kinetic energy of the moving masses must be reduced to zero at the

end of both the drive and recovery phases. This kinetic energy can be as much as 6 time higher on a stationary ergometer and it is likely that this extra energy is absorbed by the muscles working eccentrically in order to decelerate the moving masses (Bernstein *et al.*, 2002). Conversely, these muscles must also work concentrically, in order to generate the kinetic energy necessary to overcome the inertial forces and accelerate the moving masses at the onset of the each phase of the stroke cycle. As stroke rate increases, the velocity and hence momentum of the moving masses must increase in order to complete both the drive and recovery phases more rapidly. It appears that increased concentric RF activity in the early drive phase is responsible for producing the kinetic energy necessary to accelerate greater moving masses both on the stationary ergometer and on-water. Since the moving mass on the dynamic ergometer is approximately 19kg (the mass of the flywheel and foot-stretcher), increasing its acceleration at higher stroke rates does not appear to require additional concentric RF activity. The kinematic data would appear to corroborate this hypothesis, since drive times were significantly shorter during dynamic ergometry (Table 7.1). This suggests that rowers were able to accelerate the moving masses on the dynamic ergometer more successfully than on either the stationary ergometer or on-water during the drive phase especially at higher stroke rates.

Increased RF activity during the on-water recovery phase was observed across all exercise intensities (40, 50 and 60% intervals, see Figures 7.7a, 7.8a and 7.9a) due to the increased role of RF in hip flexion. While the increased hip flexion during the on-water recovery phase may be due to a greater hip angle being generated at the end of the drive phase, previous data would suggest that this is most likely not the case (Elliott *et al.*, 2001; Nowicky *et al.*, 2005). Authors have reported maximal hip angles of approximately 120° which remained unchanged on both dynamic and stationary rowing ergometers (Nowicky *et al.*, 2005) and during on-water rowing (Elliott *et al.*, 2001). It is more likely that the differences in RF activity during the recovery phase are once again due to differences in the inertial forces and kinetic energy required to accelerate the moving masses from the end of the drive phase (Bernstein *et al.*, 2002). It may also be possible that the instability associated with on-water rowing requires additional activation of the hip and trunk flexors, in order to maintain core stability balance during the recovery phase. Whatever the mechanism, both

the duration and magnitude of RF activity during the on-water recovery phase was significantly greater than that recorded from both ergometer designs, highlighting its increased role as a hip flexor during the on-water recovery phase.

On-water rowing appears to utilise VM activity to a greater extent than either stationary or dynamic ergometry during force production in the drive phase of the stroke cycle (Figures 7.7b, 7.8b and 7.9b). Previous authors have highlighted the role that knee extension plays in generating the propulsive forces in rowing (Wilson *et al.*, 1988; Hagerman, 2000; Parkin *et al.*, 2001) and as such VM activity is crucial for the development of that force. It is worth noting that VM activity during the drive phase (10, 20 and 30% intervals) progressively increased with exercise intensity during on-water rowing. The increases observed during on-ergometer rowing were much less pronounced as exercise intensity increased (Figure 7.4). It is possible that VM is preferentially recruited during on-water rowing, while VL is recruited to a greater extent during on-ergometer rowing. Further research assessing activity in both the *Vastii* and RF is required in order to fully elucidate the reason for greater VM activity observed during on-water rowing.

Unexpectedly, RF and VM activity on-water were markedly higher than during dynamic ergometry, both in the early drive (RF and VM) and recovery phase (RF). These differences appeared more pronounced as the stroke rate and exercise intensity increased. Several authors have hypothesised that the dynamic rowing ergometer would better simulate the movement patterns associated with on-water rowing by reducing the kinetic energy of the moving body mass and more closely matching the inertial forces associated with on-water rowing (Elliott *et al.*, 2001; Bernstein *et al.*, 2002). The pattern of RF activity observed in the current study would suggest that the Rowperfect ergometer underestimates the kinetic energy required to accelerate moving masses during on-water rowing. The energy necessary to accelerate the mass of the ergometer flywheel and foot-stretcher (17kg) does not appear to match the energy necessary to accelerate the mass of the single scull plus body mass in the water. However, Benson *et al.* (2011) recently compared the sliding Concept 2 ergometer (mass of 35kg) and suggested that it may more closely simulate the on-water condition. It is

possible that by simply increasing the mass of the Rowperfect foot-stretcher, a more accurate simulation of the on-water stroke cycle could potentially be accomplished.

Previous literature reporting peak handle forces during dynamic and stationary ergometer rowing are contradictory in their findings (Buck *et al.*, 2000; Elliott *et al.*, 2001; Benson *et al.*, 2011). Buck *et al.* (2000) reported peak handle forces ranging between 575 and 970 N recorded during stationary and dynamic ergometry, while Benson *et al.* (2011) reported mean (SD) peak forces of 793 (115) and 900 (110) N for male collegiate rowers on dynamic and stationary ergometers, respectively. In contrast, Elliott *et al.* (2001) reported substantially lower peak handle forces during dynamic ergometry (range 318 to 541 N). In addition, while Benson *et al.* (2011) reported significantly greater peak handle forces on the stationary ergometer, Buck *et al.* (2000) reported no significant differences between conditions. The current study reports mean peak handle forces ranging from 843 to 1007 N during stationary ergometer rowing and 844 to 981 N during dynamic ergometer rowing, with no significant differences detected across condition. While the current data is higher than previously published literature, it is for the most part in agreement with Buck *et al.* (2000) regarding ergometer design comparison. Benson *et al.* (2011) reported significantly earlier time to peak force during stationary ergometry (13.8 vs. 15.8 %). The current study also reports significantly earlier time to peak force during stationary ergometry at 95% $\dot{V}O_2$peak ($P<0.05$). Mean RFD_{peak} data recorded in the current study (Table 7.2) did not differ greatly from those reported by Benson *et al.* (2011). It is worth noting that greater handle forces were generated in the first 10% of the drive phase during dynamic ergometry. This anomaly was consistent across all exercise intensities, see Figure 7.2, and has also been previously reported by several authors (Elliott *et al.*, 2001; Bernstein *et al.*, 2002; Kleshnev, 2005; Benson *et al.*, 2011). Kleshnev (2005) suggested that this difference may be due to a disparity between foot-stretcher and handle forces; however, it is also possible that the difference could be due the smaller moving mass being accelerated more rapidly in the initial stages of the drive phase.

In order to draw meaningful conclusions from the biomechanical data attained in the current study, one must be confident that trials were performed at matched physiological intensities.

Other studies assessing ergometer task specificity or rowing ergometer design have performed race simulations at maximal intensity (de Campos Mello *et al.*, 2009; Benson *et al.*, 2011), fatiguing exercise trials of a longer duration (Bernstein *et al.*, 2002) or set sub-maximal power outputs based on absolute stroke rate and power (Nowicky *et al.*, 2005). While performing trials at maximal intensity ensures that a group are theoretically exercising at matched physiological intensity across conditions, these studies fail to take into consideration variations in stroke rate which may occur due to conditional differences. This may limit the scope for identifying changes in muscle recruitment and kinematics, since rowers may adapt to an ergometer's design by altering their normal stroke rate and mechanics. Of the previous studies published in this field, only Nowicky *et al.* (2005) controlled stroke rate during their exercise trial, however, a nominal stroke rate of 23 strokes.min^{-1} and target power of 300W were chosen. By choosing an absolute stroke rate and power output, the authors failed to account for potential variations in the relative fitness level and anthropometrics of each rower. Depending on aerobic fitness level, a target power output of 300W may represent an exercise intensity of 75% $\dot{V}O_2$peak for one rower and 95% $\dot{V}O_2$peak for another. In addition, a tall rower may perform the task at a stroke rate of 21 strokes.min^{-1}; while a smaller rower may perform the same power output at 25 strokes.min^{-1}, due to variations in lower limb length.

Finally, to date none of the published literature has assessed the potential biomechanical changes which may occur with increasing exercise intensity and stroke rate. By using data acquired during pre-trial incremental testing, the current protocol set sub-maximal and near-maximal exercise intensities (75, 85, and 95% $\dot{V}O_2$peak) at each individual's own heart and stroke rates. Since no significant differences in heart or stroke rate data were observed across exercise conditions, one can be confident that physiological exercise intensity was matched across all trials.

7.6: CONCLUSION

The results of the current study would suggest that with regards to muscle activity patterns, the dynamic ergometer design may underestimate the contribution of the knee extensor muscles (RF and VM) to the normal on-water rowing stroke cycle. On-water rowing appears to require greater activity in both RF and VM in order to accelerate the moving masses and generate effective stroke force. This appears to be especially true at higher stroke rates and exercise intensity where RF and VM activity during the on-water drive phase were at their most pronounced. It is worth noting that the Concept II ergometer appears to better simulate RF activity patterns associated with on-water rowing especially at higher stroke rates. Further research comparing EMG from other active muscles and at maximal exercise intensities and stroke rates is warranted, in order to provide a more complete assessment of the biomechanical ergometer task specificity. In addition, research examining the effect of increasing the dynamic ergometer moving mass (flywheel and foot-stretcher) on muscle activity patterns during the rowing stroke cycle is warranted. It may be possible that the differences observed in the current study are simply a product of the light moving masses encountered on the dynamic ergometer and by increasing these masses a more accurate simulation of the on-water scenario can be produced.

Chapter 8

General discussion

8.1: EMG and the assessment of ergometer task specificity.

One of the main aims in this series of studies was to use EMG as a means of assessing ergometer biomechanical task specificity. By comparing muscle activity patterns, along with other more common measurements (kinematics and force), it was envisaged that a clear assessment of the accuracy with which ergometers simulate their on-water condition, could be established. This approach was based on the novel work of Nowicky *et al.* (2005) who used EMG and joint kinematic patterns as a means of comparing two rowing ergometer designs. While the authors did not report any difference in muscle activity patterns, they nonetheless concluded that a direct comparison of EMG was warranted, in order to quantify the accuracy with which ergometers simulate the on-water condition (Nowicky *et al.*, 2005). The main finding from the current research is that while many of the measurements were consistent across conditions, several striking differences in muscle activity patterns were observed, comparing both kayak and rowing ergometry to their on-water counterpart (see Chapter 5 and 7, respectively).

In the case of kayak ergometry, it was established that the ergometer's loading mechanism, which applies an elastic recoil force to maintain tension between the paddle shaft and flywheel, was responsible for the markedly higher AD recruitment observed during ergometer kayaking, see Figures 5.2c and 6.1. In addition, analysis of 3D joint kinematics suggests that the increased AD activity was most likely due to an altered motor recruitment strategy; aimed at preserving optimal kinematics, despite additional external forces working against the shoulder joint, see Section 6.5. This observation contradicts a previously published hypothesis eluded to by Trevithick *et al.* (2007) suggesting that the ergometer's loading mechanism would aid shoulder movement patterns and hence reduce activity in the associated musculature. More subtle differences identified as lower activity in both TB and LD activity during on-ergometer kayaking were most likely due to altered paddle shaft kinematics, namely the shorter time to vertical position (Section 5.6).

It remains unclear as to whether the altered recruitment patterns observed during ergometer kayaking could have negative implications for training and performance. The possibility that long term ergometer training may increase the risk of shoulder injury or lead to a

deterioration in kayak stroke technique cannot be ruled out. It is this author's opinion however, that in the case of elite kayakers, the kayak ergometer remains an effective substitute for on-water training. Thousands of hours of on-water practice have allowed these athletes to perfect the complex movement patterns associated with the kayak stroke cycle, so much so that they are sensitive to the application of any external force and can thus alter their recruitment strategy in order to maintain optimal stroke technique during ergometer kayaking. Anecdotal evidence suggests that elite kayakers are equally capable of altering their motor recruitment strategies when they encounter external forces on the water. Elite kayakers are well trained to adapt to headwind, crosswind or tailwind conditions in order to maintain their optimal technique (Cox, 1992b). Adapting to the forces encountered on the ergometer is simply another extension of the sensitivity and proprioception induced through years of kayak training. In contrast, untrained kayaker may struggle to replicate their on-water technique when performing on the ergometer. External recoil forces applied by the ergometer's pulleys may push and pull their joints (shoulder and elbow in particular) from their optimal position. Since the untrained kayaker's proprioception and motor recruitment strategies are not as well trained as their elite counterpart, they may not be as sensitive to deviations from the optimal movement patterns. It is therefore the view of this author, that the kayak ergometer is a poor substitute for on-water kayaking when it comes to the teaching and development of kayak technique to beginners and those developing in the sport. It nonetheless remains an extremely useful aid in the training and testing of elite kayakers.

In the case of rowing, the most striking difference in recruitment patterns was observed in RF activity. This difference manifested itself as a lower level of RF recruitment comparing the dynamic ergometer to the stationary ergometer and also comparing on-ergometer and on-water rowing scenarios. The findings reported in Chapter 7 suggest that RF activity is extensively utilised during on-water rowing, both as a knee extensor during the early drive phase and as a hip flexor during the late drive and early recovery phase of the stroke cycle. The level of RF recruitment was significantly lower during on-ergometer rowing. This was especially true of the dynamic ergometer design where consistently lower RF activity was observed at all stroke rates and intensities, see Figure 7.3. These data suggests that in the

case of the dynamic rowing ergometer, the forces required to accelerate the body segments through the drive phase are markedly lower than those encountered during on-water rowing. Rekers (1993) designed the dynamic ergometer in order to more closely simulate the body segment movements of on-water rowing (Rekers, 1993; Elliott *et al.*, 2001). However, while the current research suggests that while body segment movements may closely replicate on-water rowing, the forces necessary to accelerate and decelerate the moving masses are underestimated. The moving masses on the dynamic ergometer equate to the mass of the flywheel and foot-stretcher (17kg). While this is a similar mass to that of a single scull, the on-water stroke cycle involves acceleration of both the boat and the rower's body mass. The results of this study, identifying reduced recruitment of both RF and VM in the early drive phase, suggest that the acceleration of the moving masses in dynamic rowing ergometry (and to a lesser extent in stationary ergometry) can be achieved with less effort than is necessary during on-water rowing, see Section 7.5. Unexpectedly, on the basis of EMG data, the stationary ergometer appears to simulate the on-water stroke cycle more effectively than the dynamic ergometer, especially during high intensity rowing (Figure 7.9). This contradicts the conclusions of several published papers which compared rowing ergometer designs or on-ergometer and on-water rowing (Elliott *et al.*, 2001; Bernstein *et al.*, 2002; de Campos Mello *et al.*, 2009). However, it should be noted that to the best of this author's knowledge, the current research is the first to directly compare on-ergometer and on-water rowing using EMG data and as such offers a more comprehensive comparison of ergometer task specificity.

The results of this research suggest that in the case of certain discrete muscle recruitment patterns, ergometer task specificity is not as highly accurate as one would desire. However, based on the findings presented in this thesis it may be possible to improve ergometer biomechanical task specificity through minor alterations in ergometer design. In the case of the kayak ergometer, the elastic loading mechanism is unfortunately a necessary component in the mechanical workings of the machine. While it may not be possible to completely eliminate the effect of elastic recoil, it is highly recommended that kayakers use as low an elastic tension as possible during ergometer training. This will minimise the effects of elastic tension on muscle recruitment patterns and provide as close a simulation to on-water

kayaking as possible. The current results suggest that the dynamic rowing ergometer underestimates the forces necessary for the acceleration of the moving masses encountered during on-water rowing. By increasing the mass at both the flywheel and possibly the seat, it may be possible to more accurately simulate the on-water scenario, especially in the recruitment of knee extensor muscles in the early part of the drive phase. Finally these results highlight that while external comparisons of task specificity, by way of kinematics, force or even metabolic variables may suggest accurate task specificity, EMG can identify subtle biomechanical differences which are not otherwise detectable to the naked eye. EMG provides a window into the internal recruitment strategies being utilised by the athlete to perform a given task and is therefore an extremely useful tool in the assessment of ergometer task specificity. Further assessment of other recruitment patterns from other discrete muscles is warranted in order to provide a better assessment of task specificity across a large range of active musculature.

8.2: EMG and the quantification of neuromuscular fatigue

Another key aim in this series of studies was to assess the identification of neuromuscular fatigue via EMG across a range of tasks and actions. The results reported in Chapter 3 suggest that T_{EMG} is identifiable across a variety of tasks and from a number of discrete active muscles. Overall, 75% of the raw EMG traces recorded from discrete muscles exercising during incremental testing (cycling, kayaking and rowing) exhibited non-linear increases in rmsEMG amplitude. These non-linear increases in rmsEMG amplitude facilitated the consistent identification of T_{EMG} during rowing and kayaking ergometry and the relative exercise intensity (Figure 3.1 and Appendix 5) at which these thresholds occurred did not significantly differ between conditions. The observation that T_{EMG} occurred at significantly higher relative intensities comparing cycling and rowing, led the author to postulate that T_{EMG} was sensitive to differences in testing protocol, in a similar fashion to ventilatory thresholds. However, an additional validation study which compared T_{EMG} attained during both continual and intermittent incremental cycling tests did not corroborate this postulation (see Appendix 4). There is tentative evidence to suggest that T_{EMG} and ventilator thresholds are more sensitive to subtle changes in exercise protocols than lactate measurements. While global T_{EMG} and ventilatory thresholds identified differences between

the cycling and rowing sub-groups which were also identified in the ventilatory thresholds, see Figures 3.6 and 3.7, differences across conditions were not observed in either T_{Lac} or OBLA.

There is still much debate in the literature as to the mechanisms underlying the neuromuscular fatigue threshold which occurs around the aerobic-anaerobic transition. While peripheral mechanisms of fatigue such as the increase in lactate and associated exercise metabolites remain the most likely cause, central mechanisms have also been suggested to contribute along with the peripheral changes within the active motor units (Moritani & De Vries, 1980; Bigland-Ritchie *et al.*, 1986). The EMG response to incremental testing in several discrete muscles assessed, suggest that central alterations in recruitment strategy do play a significant role in the occurrence of the neuromuscular fatigue threshold. The most striking change in recruitment was observed in RF during incremental rowing. Initial monophasic recruitment in the early stages of the test gave way to biphasic recruitment as exercise intensity increased (Figure 3.2a). Alterations in the recruitment of BB during incremental kayaking were also observed (Figure 3.3b). While these alterations in muscle recruitment strategy suggest a central component to the neuromuscular fatigue threshold, it is also possible that they are primarily a response to significant changes in the velocity of execution of the movement. Each exercise element of both incremental kayaking and rowing tests were performed at freely chosen stroke rates. As such, participants gradually increased their stroke rate in response to increases in the target power output. In contrast, cycling tests were performed within a fixed range of cadence (80 to 90 $rev.min^{-1}$) and no such alterations in recruitment strategy were observed during cycling ergometry. Further research examining the mechanisms surrounding alterations in muscle recruitment strategy is warranted in order to establish if these changes are a result of increased velocity of movement execution or in response to fatigue and increases in power output.

Comparing T_{EMG} across a range of tasks and muscles required the use of a novel analysis method. Thresholds attained from the EMG of discrete muscles were averaged together to provide a "global" T_{EMG} in each sub-group. While this method has yet to be validated, statistically comparing thresholds attained from individual muscles across sub-groups was

considered an inappropriate means of comparison from a physiological perspective. Finally, no evidence of intramuscular alterations in fibre typing between trained and untrained groups was observed (see Chapter 4). It was initially postulated that the frequency content of the EMG signal may be altered due to long term training induced shifts in muscle fibre typing. No such alterations in either MF or MPF were observed. Only an alteration in the amplitude of RF activity was observed during fatiguing isometric knee extensions, see Figure 4.13. This altered recruitment of RF was most likely a result of centrally mediated training adaptations such as enhanced agonist co-activation.

8.3: The unique role of RF activity in rowers

Of the four discrete knee muscles which make up the *Quadriceps Femoris*, RF is unique in that it is biarticular. The actions of RF are therefore twofold; RF can act as both a knee extensor and a hip flexor. These joint actions also play a crucial role in the propulsive force development of the rowing stroke cycle. It is not surprising therefore, that the results of several of the studies undertaken highlighted that rowers possess a unique and altered strategy when it comes RF recruitment. This was observed not only in the attainment of neuromuscular fatigue thresholds (Chapter 3) but also in the study of isometric fatigue (Chapter 4) and rowing ergometer task specificity (Chapter 7). The EMG data from the rowing trials reported in this thesis suggest that rowers can alter their recruitment of RF depending on the level of force and acceleration required for the completion of the stroke cycle. At low stroke rates, rowers adopt a strategy of utilising RF activity primarily as a hip flexor. We therefore observed monophasic RF recruitment at low stroke rates and power outputs (Figures 3.2a and 7.3). However, as both stroke rate and power output increased rowers appeared to alter their recruitment strategy and began utilising RF as both a knee extensor and hip flexor. Biphasic RF recruitment was thus observed at higher stroke rates and power outputs (Figures 3.2a and 7.3). Further evidence of the unique adaptations in RF recruitment was observed during isometric knee extensions to fatigue. Untrained participants demonstrated progressive de-recruitment of RF during 80% MVC contractions. This observation was in agreement with previous results reported by Mathur *et al.* (2005). In contrast, rowers were capable of progressively increasing their recruitment of RF over the course of the fatiguing contraction, which most likely aided in their ability to maintain the

required level of force for longer, see Chapter 4. It would appear from the presented results that untrained individuals are less capable of recruiting RF as a knee extensor and are more reliant on the actions of the *Vastii* to accomplish this knee articulation. Rowers in contrast, through years of training have adapted to more effectively utilise RF as a knee extensor. They can thus alter their neural strategies during highly intense, fatiguing work and recruit RF as a knee extensor to provide additional force whether during rowing at high power output and stroke rate, or during fatiguing isometric contractions.

8.4: Limitations and further research

The primary limitation in all studies undertaken in this dissertation was undoubtedly the limited number of muscles from which EMG data were recorded. All EMG data collection was performed using a 4-channel telemetric recorder, see Section 2.1. This limited the scope of assessing recruitment patterns to just four muscles during any given task. In early work for this dissertation, the author made preliminary attempts at repeating exercise trials on two separate occasions in order to double the number of recorded muscles. However, it quickly became clear that validating the consistency of exercise intensity, movement patterns and force production across repeat trials would be too difficult. In addition, the level of confidence one could have in recorded EMG data during repeated trials to failure would be low, even during more controlled efforts such as isometric contraction. Complex movement patterns such as those which form the basis of the kayaking and rowing stroke cycles require the coordination of many muscles in distinct patterns of recruitment. As such, further research investigating other muscles involved in these movements, both during on-ergometer and on-water exercise, is highly recommended.

A second limitation encountered was the lack of consistency in methods used to normalise EMG amplitude. It was initially envisaged that all EMG data recorded during task specificity trials would be normalised to data recorded during pre-trial isometric MVC contractions. However, problems were encountered during the rowing task specificity trials, as EMG amplitude data recorded during these trials were in many cases greater than maximal data recorded during the isometric MVC contractions. Previous authors have also reported this problem in isometric MVC normalisation (Jobe *et al.*, 1984; Nowicky *et al.*,

2005). In order to overcome this problem, it was decided to use a novel EMG normalisation protocol initially proposed by Rouffet and Hautier (2008). This protocol involved normalising data to the maximal EMG amplitude recorded during maximal power dynamic sprints which the participant performed prior to task specificity trials. This method has previously been used to normalise cycling data (Rouffet & Hautier, 2008), however, to the best of this author's knowledge, this is the first time it has been applied to on-water EMG data in rowing. A more detailed discussion of EMG normalisation methods is presented in Section 1.3.2.

A final limitation in this dissertation relates to the lack of stroke force data from on-water rowing. It was initially envisaged that stroke force data would be recorded and compared during both on-ergometer and on-water kayaking and rowing. The development and integration of laser trimmed strain gauge arrays on to two identical kayak paddle shafts facilitated the quantification and comparison of stroke force in both kayaking conditions. While handle forces during ergometer rowing were measured via the application of a load cell to the handle-chain coupling, the author was unable to measure stroke force data during on-water rowing. A conference discussion with biomechanists specialising in the measurement of rowing stroke force highlighted several technical issues with the development of force measurement equipment for on-water rowing. These technical issues mostly focus around the effect of longditudonal forces on the rowing oar, which may lead to overestimations of stroke force unless measured and accounted for. In addition, Elliott *et al.* (2001) previously reported significant differences in stroke force related to variations in the measurement of force from either the ergometer handle or on-water oar. Since it was deemed impractical to directly compare forces measured from a load cell to forces measured from the bending moment of a carbon rowing shaft, the development of an on-water measurement device for rowing stroke force was not completed.

As a follow on from this dissertation it would be beneficial to assess additional muscles involved in the execution of kayaking and rowing stroke cycles, in order to better assess ergometer biomechanical task specificity in these sports. Additional data describing the recruitment patterns involved in the performance of these sports on-water would

undoubtedly be of benefit, since there is limited published research in this field. In addition, 3D kinematic analysis of ergometer rowing may provide useful insight into the acceleration of body segments which is occurring during the stroke cycle. Repeating the methodology described in Chapter 7 with a group of rowers exercising on stationary and dynamic ergometers would facilitate this. With regards to the assessment of neuromuscular fatigue, it may be beneficial to assess other athletic populations possessing altered adaptations to training than those exhibited by the rowing group. Comparing this endurance trained group with an untrained population in Chapter 4, highlighted adaptations in the recruitment of RF during a high intensity (80%MVC) fatigue exercise. A comparison to an explosively trained group such as weightlifters or rugby players may provide further insight into whether this adaptation is sport specific or a neuromuscular response, common to various resistance trained groups.

References

Allen DG, Lamb GD & Westerblad H. (2008). Skeletal muscle fatigue: Cellular mechanisms. *Physiol Rev* **88,** 287-332.

Allison GT, Marshall RN & Singer KP. (1993). EMG signal amplitude normalisation technique in stretch-shortening cycle movements. *J Electromyog Kinesiol* **3,** 236-244.

Amiridis IG, Martin A, Morlon B, Martin L, Cometti G, Pousson M & van Hoecke J. (1996). Co-activation and tension-regulating phenomena during isokinetic knee extension in sedentary and highly skilled humans. *Eur J Appl Physiol Occup Physiol* **73,** 149-156.

Anderson G & Rhodes E. (1989). A review of blood lactate and ventilatory methods of detecting transition thresholds. *Sports Med* **8,** 43-55.

Asmussen E. (1934). Untersuchungen über die mechanische Reaktion der Skelettmuskelfease. *Scand Arch Physiol* **70,** 233-272.

Asmussen E. (1979). Muscle fatigue. *Med Sci Sports Exerc* **11,** 313-321.

Baker J, Rath D, Sanders RH & Kelly B. (1999). A three-dimensional analysis of male and female elite sprint kayak paddlers. In *Proceedings of the XVIIth International Symposium on Biomechanics in Sports*, ed. Sanders RH & Gibson BJ, pp. 53-56. Perth, Australia.

Baldwin K, Campell P & Cooke D. (1977). Glycogen, lactate, and alanine changes in muscle fibre types during graded exercise. *J Appl Physiol* **43,** 288-291.

Barrentine SW, Matsuo T, Escamilla RF, Fleisig GS & Andrews JR. (1998). Kinematic analysis of the wrist and forearm during baseball pitching. *J Appl Biomech* **14,** 24-39.

Basmajian JV & De Luca CJ. (1985). *Muscles alive: Their functions revealed by electromyography*. Williams and Wilkins, Baltimore, Md.

Beaver L, Wasserman K & Whipp J. (1986). A new method for detecting anaerobic threshold by gas exchange. *J Appl Physiol* **60,** 2020-2027.

Beck TW, Housh TJ, Johnson GO, Weir JP, Cramer JT, Coburn JW & Malek MH. (2005). The effects of interelectrode distance on electromyographic amplitude and mean power frequency during isokinetic and isometric muscle actions of the biceps brachii. *J Electromyog Kinesiol* **15,** 482-495.

Beck TW, Housh TJ, Mielke M, Cramer JT, Weir JP & Malek MH. (2007). The influence of electrode placement over innervation zone on electromyographic amplitude and mean power frequency versus isokinetic torque relationships. *J Neurosci Methods* **15,** 72-83.

Begon M, Lacouture P & Colloud F. (2008). 3D kinematic comparison between on-water and on-ergometer kayaking. In *Proceedings of the XXVIth International Symposium on Biomechanics in Sports,*, ed. Kwon YH, Shim J, Shim J & Shin IK, pp. 502-505. Seoul, South Korea.

Benson A, Abendroth J, King D & Swensen T. (2011). Comparison of rowing on a Concept 2 stationary and dynamic ergometer. *J Sports Sci Med* **10,** 267-273.

Bernstein IA, Webber O & Woledge RC. (2002). An ergonomic comparison of rowing machine designs: Possible implications for safety. *Br J Sports Med* **36,** 108-112.

Bigland-Ritchie B, Dawson N, Johansson R & Lippold O. (1986). Reflex origin for the slowing of motoneurone firing rates in the fatigue of human voluntary contractions. *J Physiol* **379,** 451-459.

Bigland-Ritchie B, Donovan E & Roussos C. (1981). Conduction velocity and EMG power spectrum changes in fatigue of sustained maximal efforts. *J Appl Physiol* **51,** 1300-1305.

Bigland-Ritchie B & Woods JJ. (1984). Changes in muscle contractile properties and neural control during human muscular fatigue. *Muscle Nerve* **7,** 691-699.

Bilodeau M, Cincera M, Bertrand Arenault A & Gravel D. (1997). Normality and stationarity of EMG signals of elbow flexor muscles during ramp and step isometric contractions. *J Electromyog Kinesiol* **7,** 87-96.

Binder-Macleod S & Guerin T. (1990). Preservation of force output through progressive reduction of stimulation frequency in human quadriceps femoris muscle. *Phys Ther* **70,** 619-625.

Boonstra T, Daffertshofer A, van Ditshuizen J, van den Heuvel M, Hofman C, Willigenburg N & Beek P. (2008). Fatigue-related changes in motor-unit synchronization of quadriceps muscles within and across legs. *J Electromyog Kinesiol* **18,** 717-731.

Brody L, Pollock M, Roy S, De Luca C & Celli B. (1991). pH-induced effects on median frequency and conduction velocity of the myoelectric signal. *J Appl Physiol* **71,** 1878-1885.

Broman H, Bilotto G & De Luca CJ. (1985). Myoelectric signal conduction velocity and spectral parameters: Influence of force and time. *J Appl Physiol* **58,** 1428-1437.

Brooks GA. (1985). Anaerobic threshold: Review of the concept and directions for future research. *Med Sci Sports Exerc* **17,** 22-34.

Brooks GA. (1986). The lactate shuttle during exercise and recovery. *Med Sci Sports Exerc* **18,** 360-368.

Buck DP, Smith RM & SInclair PJ. (2000). Peak ergometer handle and foot stretcher force on Concept II and Rowperfect rowing ergometers. In *Proceedings of the XVIII International Symposium on Biomechanics in Sport*, ed. Hong Y & Johns D, pp. 622-625. The Chinese University of Hong Kong, Hong Kong, China.

Burden A. (2010). How should we normalise electromyograms obtained from healthy participants? What we have learned from over 25 years of research. *J Electromyog Kinesiol* **20,** 1023-1035.

Burden A & Bartlett R. (1999). Normalisation of EMG amplitude: An evaluation and comparison of old and new methods. *Med Eng Phys* **21,** 247-257.

Burden A, Trew M & Baltzopoulos V. (2003). Normalisation of gait EMGs: A re-examination. *J Electromyog Kinesiol* **13,** 519-532.

Caiozzo VJ, Davis JA, Ellis JF, Azus JL, Vandagriff CA & McMaster WC. (1982). A comparison of gas exchange indices used to detect anaerobic threshold. *J Appl Physiol* **53,** 1184-1189.

Caldwell JS, McNair PJ & Williams M. (2003). The effects of repetitive motion on lumbar flexion and erector spinae muscle activity in rowers. *Clin Biomech* **18,** 704-711.

Campanini I, Merlo A, Degola P, Merletti R, Vessosi G & Farina D. (2007). Effect of electrode location on EMG signal envelope in leg muscles during gait. *J Electromyog Kinesiol* **17,** 515-526.

Capousek JB & Bruggemann P. (1990). An ergonomic electromyographic investigation of specific strength exercises and specific movements in kayak. In *Proceedings of the International Seminar on Kayak-Canoe Coaching and Sciences*, ed. Vrijens J, Verstuyft J & De Clercq D, pp. 69-82. Budapest.

Carolan B & Cafarelli E. (1992). Adaptations in co-activation after isometric resistance training *J Appl Physiol* **73,** 911-917.

Cescon C, Rebecchi P & Merletti R. (2008). Effect of electrode array position and subcutaneous tissue thickness on conduction velocity estimation in upper trapezius muscle. *J Electromyog Kinesiol* **18,** 628-636.

Chicharro JL, Hoyos J & Lucia A. (2000). Effects of endurance training on the isocapnic buffering and hypocapnic hyperventilation phases in professional cyclists. *Br J Sports Med* **34,** 450-455.

Chwalbinska-Moneta J, Kaciuba-Uscilko H, Krysztofiak H, Ziemba A, Krzemiski K, Kruk B & Nazar K. (1998). Relationship between EMG, blood lactate and plasma catecholamine thresholds during graded exercise in men. *J Physiol Phamacol* **49,** 433-441.

Clarys JP & Cabri J. (1993). Electromyography and the study of sports movements: A review. *J Sport Sci* **11,** 379-448.

Clarys JP, Scafoglieri A, Tresignie J, Reilly T & Van Roy P. (2010). Critical appraisal and hazards of surface electromyography data acquisition in sport and exercise. *Asian J Sports Med* **1**, 69-80.

Cox R. (1992a). Anatomical and physiological factors. In *The Science of Canoeing: A guide for competitors and coaches to understanding and improving performance in sprint and marathon kayaking* ed. William R, pp. 57-113. Coxburn Press, Cheshire.

Cox R. (1992b). Biomechanical factors. In *The Science of Canoeing: A guide for competitors and coaches to understanding and improving performance in sprint and marathon kayaking*
ed. William R, pp. 36-56. Coxburn Press, Cheshire.

Coyle EF, Sidossis LS, Horowitz JF & Beltz JD. (1992). Cycling efficiency is related to the percentage of Type 1 muscle fibers. *Med Sci Sports Exerc* **24,** 782-788.

Dal Monte A, Faina M & Menchinelli C. (1988). Sport-spectific ergometric equipment. In *Endurance in sports*, ed. Shepard R & Astrand P, pp. 201-207. Blackwell Scientific, London.

Dal Monte A & Lupo S. (1989). Specific ergometry in the functional assessment of top class sportsmen. *J Sport Med Phys Fit* **29,** 4-8.

Davis JA, Vodak P, Wilmore J, Vodak J & Kurtz P. (1976). Anaerobic threshold and maximal aerobic power for three modes of exercise. *J Appl Physiol* **41,** 544-550.

de Campos Mello F, de Moraes Bertuzzi R, Grangeiro P & Franchini E. (2009). Energy systems contributions in 2000m race simulation: A comparison among rowing ergometers and water. *Eur J Appl Physiol* **107,** 615-619.

De Luca CJ. (1997). The use of surface electromyography in biomechanics. *J Appl Biomech* **13,** 135-163.

De Luca CJ & Erim Z. (2002). Common drive of motor units of a synergistic muscle pair. *J Neurophysiol* **87,** 2200-2204.

De Nooij R, Kallenberg LAC & Hermens H. (2009). Evaluating the effect of electrode location on surface EMG amplitude of the m. erector spinae p. longissimus dorsi. *J Electromyog Kinesiol* **19,** e257-e266.

De Souza A, Oliveira C & Goncalves M. (2009). EMG amplitude and frequency parameters of muscular activity: Effect of resistance training based on electromyographic fatigue threshold. *J Electromyog Kinesiol* **19,** 295-303.

De Vries HA. (1968). Method of evaluation of muscle fatigue and endurance from electromyographic fatigue curves. *Am J Phys Med* **47,** 125-135.

Diederichsen LP, Nerregaard J, Dyhre-Poulsen P, Winther A, Tufekovic G, Bandholm T, R. RL & Krogsgaard M. (2007). The effect of handedness on electromyographic activity of human shoulder muscles during movement. *J Electromyog Kinesiol* **17,** 410-419.

DiPrompero PE, Cortelli G, Celantano F & Cerretelli P. (1971). Physiological aspects of rowing. *J Appl Physiol* **31,** 853-857.

Donovan CV & Brooks GA. (1983). Endurance training affects lactate clearance not lactate production. *Am J Physiol* **244,** E83-E92.

Duchateau J & Baudry S. (2010). Training Adaptation of the Neuromuscular System. In *Neuromuscular Aspects of Sport Performance, Volume XVII of the Encyclopedia of Sports Medicine* ed. Komi PV, pp. 216-253. Wiley-Blackwell, Oxford.

Dubo HI, Peat M, Winter D, Quanbury AO, Hobson DA, Steinke T & Reimer G. (1976). Electromyographic temporal analysis of gait: Normal human locomotion. *Arch Phys Med Rehabil* **57,** 415-420.

Durnin JV & Womersley J. (1974). Body fat assessed from total body density and its estimation from skinfold thickness: measurements on 481 men and women aged from 16 to 72 years. *Br J Nutr* **32,** 77-97.

Eason RG. (1960). Electromyographic study of local and generalised muscular impairment. *J Appl Physiol* **15,** 479-482.

Ebenbichler G, Kollmitzer J, Quittan M, Uhl F, Kirtley C & Fialka V. (1998). EMG fatigue patterns accompanying isometric fatiguing knee-extensions are differences in mono- and bi-articular muscles. *Electroencephalogr Clin Neurophysiol* **109,** 256-262.

Eberhart HD & Inman T. (1951). An evaluation of experimental procedures used in a fundametal study of human locomotion. *Ann N Y Acad Sci* **51** 1213-1228.

Edmans KAP & Lou F. (1990). Changes in force and stiffness induced by fatigue and intracellular acidification in frog muscle fibres. *J Physiol* **424,** 133-149.

Edwards RG & Lippold OCJ. (1956). The relation between force and integrated electrical activity in fatigued muscle. *J Physiol* **132,** 677-681.

Elfving B, Liljequist D, Mattssonn E & Nemeth G. (2002). Influence of interelectrode distance and force level on the spectral parameters of surface electromyographic recordings from the lumbar muscles. *J Electromyog Kinesiol* **12,** 295-304.

Elfving B, Nemeth G, Arvidsson I & Lamontagne M. (1999). Reliability of EMG spectral parameters in repeated measurements of back muscle fatigue. *J Electromyog Kinesiol* **9,** 235-243.

Elliott B, Lyttle A & Birkett O. (2001). The rowperfect ergometer: A training aid for on-water single scull rowing. *Sports Biomech* **1,** 123-134.

Enoka RM & Duchateau J. (2008). Muscle fatigue: What, why and how it influences muscle function. *J Physiol* **568,** 11-23.

Enoka RM & Stuart DG. (1992). Neurobiology of muscle fatigue. *J Appl Physiol* **72,** 1631-1648.

Eston R & Reilly T. (2001). *Kinanthropometry And Exercise Physiology Laboratory Manual: Volume 2: Exercise Physiology Tests, Procedures and Data*, vol. 2. Routledge.

Exton JH & Park CR. (1967). Control of gluconeogenesis in liver. General features of gluconeogenesis in the perfused livers of rats. *J Biol Chem* **242,** 2622-2636.

Farina D, Cescon C & Merletti R. (2002). Influence of anatomical, physical, and detection-system parameters on surface EMG. *Biol Cybern* **86,** 445-456.

Farina D, Ferguson RA, Macaluso A & De Vito G. (2007). Correlation of average muscle fibre conduction velocity measured during cycling exercise with myosin heavy chain composition, lactate threshold and $V_{O_2}max$. *J Electromyog Kinesiol* **17,** 393-400.

Farina D, Merletti R & Enoka R. (2004). The extraction of neural strategies from the surface EMG. *J Appl Physiol* **96,** 1486-1495.

Favero TG, Zable AC & Coletr D. (1997). Lactate inhibits Ca^{2+} activated Ca^{2+} channel activity from skeletal muscle sarcoplasmic reticulum. *J Appl Physiol* **82,** 447-452.

Favier RJ, Constable SH, Chen M & Holloszy JO. (1986). Endurance exercise training reduces lactate production. *J Appl Physiol* **61,** 885-889.

Fink WJ, Costill DL & Pollock M. (1977). Sub-maximal and maximal working capacity of elite distance runners. Part II: Muscle fibre composition and enzyme activities. *Ann N Y Acad Sci* **301,** 323-327.

Fitts RH & Metzger JM. (1988). Mechanisms of muscular fatigue. In *Principals of Exercise Biochemistry*, ed. Poortmans JR, pp. 212-229. Karger, Basel.

Fleming N, Donne B & Mahony N. (2007). Electromyographic and kinesiological analysis of the kayak stroke: Comparison of on-water and on-ergometer data across exercise intensity. In *Proceedings of the 12th annual congress of the European College of Sports Science*, ed. Kallio J, Komi PV, Komulainen J & Avela J, pp. 177.

Fry RW & Morton AR. (1991). Physiological and kinanthropometric attributes of elite flatwater kayakers. *Med Sci Sports Exerc* **23,** 1297-1301.

Fuglevand AJ, Winter D, Patla AE & Stashuk D. (1992). Detection of motor unit action portentials with surfact electrodes: Influence of electrode size and spacing. *Biol Cybern* **67,** 143-153.

Gandevia SC. (2001). Spinal and supraspinal factors in human muscle fatigue. *Physiol Rev* **81,** 1725-1789.

Ganter N, Witte K, Edelmann-Nusser J, Heller M, Schwab K & Herbert W. (2007). Spectral parameters of surface electromyography and performance in swim bench exercises during the training of elite and junior swimmers. *Eur J Sport Sci* **7,** 143-155.

Gerdle B, Karlsson S, Crenshaw AG, Elert J & Friden J. (2000). The influences of muscle fibre proportions and areas upon EMG during maximal dynamic knee extensions. *Eur J Appl Physiol* **81,** 2-10.

Gollnick PD. (1986). Metabolic regulation in skeletal muscle: Influence of endurance training as exerted by mitochondrial protein concentratioin. *Acta Physiol Scand* **128,** 53-66.

Gollnick PD, Armstrong RB, Saubert EW, Piehl K & Saltin B. (1972). Enzyme activity and fibre composition in skeletal muscle of untrained and trained men. *J Appl Physiol* **33,** 312-319.

Gollnick PD, Piehl K & Saltin B. (1974). Selective glycogen depletion pattern in human muscle fibres after exercise of varying intensity and at varying pedalling rates. *J Physiol* **241,** 45-57.

Green HJ & Patla AE. (1992). Maximal aerobic power: Neuromuscular and metabolic considerations. *Med Sci Sports Exerc* **24,** 38-46.

Hagberg M. (1981). Muscular endurance and surface electromyogram in isometric and dynamic exercise. *J Appl Physiol* **51,** 1-7.

Hagerman FC. (1984). Applied physiology of rowing. *Sports Med* **1,** 303-326.

Hagerman FC. (2000). Physiology of competitive rowing. In *Exercise and Sport Science*, ed. Garrett WE & Kirkendall DT, pp. 862-868. Lipincott, Williams & Wilkins.

Hagerman FC, Hagerman GR & Mickelson TC. (1979). Physiological profiles of elite rowers. *Phys Sports Med* **7,** 74-81.

Hagerman FC & Staron RS. (1983). Seasonal variations among physiological variables in elite oarsmen. *Can J Appl Sports Sci* **8,** 143-148.

Hakkinen K & Komi PV. (1983). Electromyographic changes during strength training and detraining. *Med Sci Sports Exerc* **15,** 455-460.

Halladay E. (1990). Rowing in England: A Social History., pp. 5-15. Manchester University Press, Manchester, UK.

Henneman E. (1957). Relation between size of neurons and their susceptibility to discharge. *Science* **126,** 1345-1346.

Hermens H, Freriks B, Disselhorst-Klug C & Rau G. (2000). Development of recommendations for SEMG sensors and sensor placement procedures. *J Electromyog Kinesiol* **10,** 361-374.

Hermens H & Vollenbroek-Hutten MM. (2004). Effect of electrode dislocation on electromyographic activity and relative rest time: Effectiveness of compensation by a normalisation procedure. *Med Biol Eng Comput* **42,** 502-508.

Hill AV & Lupton H. (1923). Muscular exercise, lactic acid and supply and utilization of oxygen. *Q J Med* **16,** 135-171.

Hintermeister RA, Lange GW, Schultheis JM, Bey MJ & Hawkins RJ. (1998). Electromyographic activity and applied load during shoulder rehabilitation exercises using elastic resistance. *Am J Sports Med* **26,** 210-220.

Hodgson JA, Finni T, Lai AM, Edgerton VR & Sinha S. (2006). Influence of structure on the tissue dynamics of the human soleus muscle observed in MRI studies during isometric contraction. *J Morphol* **267,** 585-601.

Hoffmann P. (1910). Beitrag zur Kenntnis der menschlichen Reflexe mit besonderer Berucksichtigung der elektrischen Erscheinungen. *Arch Anat Physiol* **1,** 223–246.

Holloszy JO. (1976). Adaptations of muscular tissue in training. *Prog Cardiovasc Dis* **18,** 445-458.

Housh TJ, De Vries HA, Johnson D & Housh SA. (1995). Electromyographic fatigue thresholds of the superficial muscles of the quadriceps femoris. *Eur J Appl Physiol* **71,** 131-136.

Hug F, Decherchi P, Maqueste T & Jammes Y. (2004). EMG versus oxygen uptake during cycling exercise in trained and untrained subjects. *J Electromyog Kinesiol* **14,** 187-195.

Hug F & Dorel S. (2009). Electromyographic analysis of pedaling: A review *J Electromyog Kinesiol* **19,** 182-189.

Hug F, Faucher M, Kipson N & Jammes Y. (2003). EMG signs of neuromuscular fatigue related to the ventilatory threshold during cycling exercise. *Clin Physiol Funct Imaging* **23,** 208-214.

Hunter AM, St. Claire Gibson A, Lambert M & Noakes TD. (2002). Electromyographic (EMG) normalisation method for cycle fatigue protocols. *Med Sci Sports Exerc* **24,** 83-89.

Ivy JL, Withers RT, Van Handel PJ, Elger DH & Costill DL. (1980). Muscle respiratory capacity and fibre type as determinants of the lactate threshold. *J Appl Physiol* **48,** 523-527.

Jacobson WC, Gabel RH & Brand RA. (1995). Surface vs. fine-wire electrode ensemble-averaged signals during gait. *J Electromyog Kinesiol* **5,** 37-44.

Jensen C, Vasseljen O & Westgaard RW. (1993). The influence of electrode position on bipolar surface electromyogram recordings of upper trapezius muscle. *Eur J Appl Physiol* **67,** 266-273.

Jensen C & Westgaard RW. (1997). Functional subdivision of the upper trapezius muscle during low-level activation. *Eur J Appl Physiol Occup Physiol* **76,** 335-339.

Jobe FW, Radovich D, Tibone JE & Perry J. (1984). An EMG analysis of the shoulder in pitching: a second report. *Am J Sports Med* **12,** 218-220.

Jurimae J, Duvillard SPV, Maestu J, Cicchella A, Purge P, Ruosi S, Jurimae T & Hamra J. (2007). Aerobic-anaerobic transition intensity measured via EMG signals in athletes with different physical activity patterns. *Eur J Appl Physiol* **101,** 341-346.

Karduna AR, McClure PW & Michener LA. (2001). Dynamic measurements of three-dimensional scapular kinematics: A validation study. *J Biomech Eng* **123,** 184-190.

Karlsson S & Gerdle B. (2001). Mean frequency and signal amplitude of the surface EMG of the quadriceps muscles increase with increasing torque - a study using the continuous wavelet transform. *J Electromyog Kinesiol* **11,** 131-140.

Keenan KG, Farina D, Maluf KS, Merletti R & Enoka RM. (2005). Influence of amplitude cancellation on the simulated surface electromyogram. *J Appl Physiol* **98,** 120-131.

Kellis E & Baltzopoulos V. (1996). The effects of normalisation method on antagonistic activity patters during eccentric and concentric isokinetic knee extension and flexion. *J Electromyog Kinesiol* **6,** 235-245.

Kellis E & Katis A. (2009). Reliability of EMG power-spectrum and amplitude of the semitendinosus and biceps femoris muscles during ramp isometric contractions. *J Electromyog Kinesiol* **18,** 351-358.

Kendal SJ & Sanders RH. (1992). The technique of elite flatwater kayak paddlers using the wing paddle. *Int J Sport Biomech* **8,** 233-250.

Kenny G, Reardon F, Marion A & Thoden J. (1995). A comparative analysis of physiological responses at sub-maximal workloads during different laboratory simulations of field cycling. *Eur J Appl Physiol Occup Physiol* **71,** 409-415.

Kindermann W, Simon G & Keul J. (1979). The Significance of the Aerobic-anaerobic Transition for the Determination of Work Load Intensities During Endurance Training. *Eur J Appl Physiol* **42**.

Kleine BU, Schumann NP, Stegeman DF & Scholle HC. (2000). Surface EMG mapping of the human trapezius muscle: The topography of monopolar and bipolar surface EMG amplitude and spectrum parameters at varied forces and in fatigue. *Clin Neurophysiol* **111,** 686-693.

Kleshnev V. (2005). Comparison of on-water rowing with its simulation on Concept 2 and RowPerfect machines. In *Proceedings of XXIII International Symposium on Biomechanics in Sports*, ed. Wang Q, pp. 130-133. China Institute of Sport Science.

Kleshnev V & Kleshneva E. (1995). Biomechanical features of rowing on devices with mobile or stationary workplace. In *Proceedings of XVth Congress of the International Society of Biomechanics*, pp. 482-483. Jyvaskyla, Finland.

Knutson LM, Soderberg GL, Ballantyre BT & Clarke WR. (1994). A study of normalization procedures for within day electromyographic data. *J Electromyog Kinesiol* **4,** 47-59.

Kumamoto M & Takagi K. (1980). Dynamic and neuro-physiological features of serial multijoint movements. In *Regulation of Physical Activity*, ed. Kumamoto M & Takagi K, pp. 207-229. Kyorin Shoin, Tokyo.

Kumar DK, Pah ND & Bradley A. (2003). Wavelet analysis of surface electromyography to determine muscle fatigue. *IEEE Transactions on Neural Systems and Rehabilitation Engineering* **11,** 400-406.

Kupa EJ, Roy SH, Kandarian SC & De Luca CJ. (1995). Effects of muscle fibre type and size on EMG median frequency and conduction velocity. *J Appl Physiol* **79,** 23-32.

Lamb D. (1989). A kinematic comparison of ergometer and on-water rowing. *Am J Sports Med* **17,** 367-373.

Larsson B, Kadi F, Lindvall B & Gerdle B. (2006). Surface electromyography and peak torque of repetitive maximum isokinetic plantar flexions in relation to aspects of muscle morphology. *J Electromyog Kinesiol* **16,** 281-290.

Li L & Caldwell GE. (1998). Muscle coordination in cycling: Effect of surface incline and posture. *J Appl Physiol* **85**, 927-934.

Lin J, Hanten WP, Olson SL, Roddey TS, Soto-quijano DA, Lim HK & Sherwood AM. (2005). Functional activity characteristics of individuals with shoulder dysfunctions. *J Electromyog Kinesiol* **15,** 576-586.

Lindstrom L, Magusson R & Peterson I. (1970). Muscular fatigue and action potential conduction velocity changes studied with frequency analysis of EMG signals. *Electromyography* **4,** 341-356.

Lippold O. (1952). The relation between integrated action potentials in a human muscle and its isometric tension. *J Physiol* **117,** 492-499.

Lippold O. (1960). The electromyography of fatigue. *Ergonomics* **3** 121-131.

Logan K & Holt L. (1985). The flatwater kayak stroke. *NSCA J* **7,** 4-11.

Lucia A, Sanchez O, Carvajal A & Chicharro JL. (1999). Analysis of the aerobic-anaerobic transition in elite cyclists during incremental exercise with the use of electromyography. *Br J Sports Med* **33,** 178-185.

Macintyre DL, Slawnych MP, Reid WD & McKenzie DC. (1998). Fatigue of knee extensor muscles following eccentric exercise. *Electromyogr Clin Neurophysiol* **38,** 3-9.

Maestu J, Cicchella A & Purge P. (2006). Electromyographic and neuromuscular fatigue thresholds as concepts of fatigue. *J Strength Cond Res* **20,** 824-828.

Mahony N, Donne B & O'Brien M. (1999). A comparison of physiological responses to rowing on friction-loaded and air-braked ergometers. *J Sport Sci* **17,** 143-149.

Mann RV & Kearney JT. (1980). A biomechanical analysis of the Olympic-style flatwater kayak stroke. *Med Sci Sports Exerc* **12,** 183-188.

Marsden CD, Meadows JC & Merton PA. (1971). Isolated single motor units in human muscle and their rate of discharge during maximal voluntary effort. *J Physiol (Lond)* **217,** 12P-13P.

Marey, EJ. (1868). Du mouvement dans les fonctions de la vie. Leçons faites au Collège de France. Paris: Baillière

Marsh AP & Martin PE. (1995). The relationship between cadence and lower extremity EMG in cyclists and noncyclists. *Med Sci Sports Exerc* **27,** 217-225.

Martin TP & Bernfield YS. (1998). Effect of stroke rate on velocity of a rowing shell. *Med Sci Sports Exerc* **12,** 250-256.

Martindale WO & Robertson DG. (1984). Mechanical energy in sculling and in rowing an ergometer. *Can J Appl Sports Sci* **9,** 153-163.

Masuda K, Masuda T, Sadoyama T, Inaki M & Katsuta S. (1999). Changes in surface EMG parameters during static and dynamic fatiguing contractions. *J Electromyog Kinesiol* **9,** 39-46.

Mateika JH & Duffin J. (1994a). Coincidental changes in ventilation and electromyographic activity during consecutive incremental exercise tests. *Eur J Appl Physiol* **68,** 54-61.

Mateika JH & Duffin J. (1994b). The ventilation, lactate and electromyographic thresholds during incremental exercise tests in normoxia, hypoxia and hyperoxia. *Eur J Appl Physiol* **69,** 110-118.

Mateika JH & Duffin J. (1995). A review of the control of breathing during exercise. *Eur J Appl Physiol* **71,** 1-27.

Mathiassen SE, Winkel J & Hagg GM. (1995). Normalization of surface EMG amplitude from the upper trapezius muscle in ergonomic studies - A review. *J Electromyog Kinesiol* **5,** 197-226.

Mathur S, Eng JJ & Macintyre DL. (2005). Reliability of surface EMG during sustained contractions of the quadriceps. *J Electromyog Kinesiol* **15,** 102-110.

Maughan RJ & Nimmo MA. (1984). The influence of variations in muscle fibre composition on muscle strength and cross-sectional area in untrained males. *J Physiol* **351,** 299-311.

McArdle W, Katch F & Katch V. (2005). Optimising body composition. In *Essentials of Exercise Physiology*, pp. 580-581. Williams & Wilkins, Baltimore.

Merton PA. (1954). Voluntary strength and fatigue. *J Physiol (Lond)* **123,** 553–564,.

Merton PA, Hill DK, Morton HB (1981). Indirect and direct stimulation of fatigued human muscle, in *Human Muscle Fatigue: Physiological Mechanisms.* Porter R, Whelan J (eds) London, Pitman Medical Ltd., pp 120-129.

Mesin L, Merletti R & Rainoldi A. (2009). Surface EMG: The issue of electrode location. *J Electromyog Kinesiol* **19,** 719-726.

Mickelson TC & Hagerman FC. (1982). Anaerobic threshold measurements of elite oarsmen. *Med Sci Sports Exerc* **14,** 440-444.

Millar NC & Homsher E. (1990). The effect of phosphate and calcium on force generation in glycerinated rabbit skeletal muscle fibres: A steady-state and transient kinetic study. *J Biol Chem* **265,** 20234-20240.

Mirka GA. (1991). The quantification of EMG normalisation error. *Ergonomics* **34,** 343-352.

Mitchell A & Swaine IL. (1998). Comparison of cardiorespiratory responses to open-water and simulated kayaking. *Biol Sport* **15,** 229-236.

Mitchell K, Banks S, Morgan D & Sugaya H. (2003). Shoulder motions during the golf swing in male amateur golfers. *J Orthop Sports Phys Ther* **33,** 196-203.

Moritani T & De Vries HA. (1980). Anaerobic threshold determination by surface electromyography. *Med Sci Sports Exerc* **12,** 86.

Moritani T, Takaishi T & Matsumoto T. (1993). Determination of maximal power output at neuromuscular fatigue threshold. *J Appl Physiol* **74,** 1729-1734.

Mosso A. (1892), *Die Ermüdung.* Hirzel, Leipzig. P 333

Mottram SL, Woledge RC & Morrissey D. (2009). Motion analysis study of a scapular orientation exercise and subjects' ability to learn the exercise. *Man Ther* **14,** 13-18.

Murata A. (2001). Shoulder joint movement of the non-throwing arm during baseball pitch-comparison between skilled and unskilled pitchers. *J Biomech* **34,** 1643-1647.

Nagata A, Muro M, Moritani T & Yoshida T. (1981). Anaerobic threshold determination by blood lactate and myoelectric signals. *Jpn J Physiol* **31,** 585-597.

Narici MV, Roi GS, Ladoni L, Minetti AE & Cerretelli P. (1989). Changes in force, cross-sectional area and neural activation during strength training and detraining of the human quadriceps. *Eur J Appl Physiol Occup Physiol* **59,** 310-319.

Naylor JM, Kronfeld DS & Freeman DE. (1984). Hepatic and extrahepatic lactate metabolism in sheep: The effects of lactate loading and pH. *Am J Physiol* **247,** E747-E755.

Nesbit SM. (2005). A three dimensional kinematic and kinetic study of the golf swing. *J Sports Sci Med* **4,** 499-519.

Nowicky AV, Burdett R & Horne S. (2005). The impact of ergometer design on hip and trunk muscle activity patterns in elite rowers: An electromyography assessment. *J Sports Sci Med* **4,** 18-28.

Ounpuu S & Winter D. (1989). Bilateral electromyographical analysis of the lower limbs during walking in normal adults. *Electroencephalogr Clin Neurophysiol* **72,** 429-438.

Owles WH. (1930). Alterations in the lactic acid content of the blood as a result of light exercise, and associated changes in CO_2 combining power of the blood and into alveolar CO_2 pressure. *J Physiol* **69,** 214-237.

Paiss O, Inbar GF. (1987). Autoregressive modeling of surface EMG and its spectrum with application to fatigue. *IEEE Trans Biomed Engng* **34,** 761-770

Palmieri RM, Ingersoll CD & Hoffman MA. (2004). The Hoffmann reflex: Methodological considerations and applications for use in sports medicine and athletic training research. *J Ath Train* **39,** 268-277.

Parkin S, Nowicky AV, Rutherford OM & McGregor AH. (2001). Do oarsmen have asymmetries in the strength of their back and leg muscles? *J Sport Sci* **19,** 521-526.

Pate E & Cooke R. (1989). Addition of phosphate to active muscle fibres probes actomyosin states within the powerstroke. *Pflugers Arch* **414,** 73-81.

Person RS. (1960). Electrophysiological study of the activity of the motor apparatus of man in fatigue. *Fiziol Zh SSSR* **46,** 945-954.

Person RS & Kudina LP. (1972). Discharge frequency and discharge pattern of human motor units during voluntary contraction of muscle. *Electroencephalogr Clin Neurophysiol* **32,** 471-483.

Pflagenhoef S. (1980). Biomechanical analysis of Olympic flatwater kayaking and canoeing. *Res Q* **50,** 443-459.

Piitulainen H, Rantalainen T, Linnamo V, Komi PV & Avela J. (2009). Innervation zone shift at different levels of isometric contraction in the biceps brachii muscle. *J Electromyog Kinesiol* **19,** 667-675.

Place N, Matkowski B & Martin A. (2006). Synergists activation pattern of the quadriceps muscle differs when performing sustained isometric contractions with different EMG biofeedback. *Exp Brain Res* **174,** 595-603.

Polger J, Johnson D, Weightman D & Appleton D. (1973). Data on fibre type in thirty-six human muscles: An autopsy study. *J Neurol Sci* **19,** 307-318.

Popivanov D, Todorov A. (1986). Statistical procedures for interference EMG power spectra estimation. *Med Biol Engng Comp* **24,** 344-350.

Potvin JR & Bent LR. (1997). A validation of techniques using surface EMG signals from dynamic contractions to quantify muscle fatigue during repetitive tasks. *J Electromyog Kinesiol* **7,** 131-139.

Prince RP, Hikida RS & Hagerman FC. (1976). Human muscle fibre types in power lifters, distance runners and untrained subjects. *Pflugers Arch* **363,** 19-26.

Pucci A, Griffin L & Caferelli. (2006). Maximal motor unit firing rates during isometric resistance training in men. *Exp Physiol* **91,** 171-178.

Rainoldi A, Bullock-Saxton JE, Cavarretta F & Hogan N. (2001). Repeatability of maximal voluntary force of surface EMG variables during voluntary isometric contractions of quadriceps muscles in healthy subjects. *J Electromyog Kinesiol* **11,** 425-438.

Rainoldi A, Galardi G, Maderna L, Comi G, Conte LL & Merletti R. (1999). Repeatability of surface EMG variables during voluntary isometric contractions of the biceps brachii muscle *J Electromyog Kinesiol* **9,** 105-119.

Rainoldi A, Nazzaro M, Merletti R, Farina D, Caruso I & Gaudenti S. (2000). Geometrical factors in surface EMG of the vastus medialis and lateralis muscles. *J Electromyog Kinesiol* **10,** 327-336.

Rasmussen P, Secher NH & Peterson NT. (2007). Understanding central fatigue: where to go? *Exp Physiol* **92,** 369-370.

Redgrave S. (1995). In *Complete Book of Rowing*, pp. 298. Partridge Press, London.

Reilly T & Lees A. (1984). Exercise and sports equipment: Some ergonomics aspects. *Appl Ergo* **15,** 259-279.

Rekers C. (1993). Verification of the Rowperfect ergometer. In *ARA Senior Rowing Conference*. London.

Roeleveld K, Stegeman DF, Vingerhoets HM & Van Oostrom A. (1997). Motor unit potential contribution to surface electromyography. *Acta Physiol Scand* **160,** 175-183.

Rouffet DM & Hautier CA. (2008). EMG normalisation to study muscle activation in cycling. *J Electromyog Kinesiol* **18,** 866-878.

Sale DG. (1988). Neural adaptations to resistance training. *Med Sci Sports Exerc* **20,** S135-145.

Saltin B, Henriksson J, Nygaard E & Andersen P. (1977). Fibre types and metabolic potentials of skeletal muscles in sedentary man and endurance runners. *Ann N Y Acad Sci* **301,** 3-29.

Sanders RH & Baker J. (1998). Evolution of technique in flatwater canoeing. In *Science and Practice of Canoe/Kayak High-Performance Training*, ed. Issurin V, pp. 67-81. Wingate Institute for Physical Education and Sport, Tel Aviv, Israel.

Sanders RH & Kendal SJ. (1992). A description of olympic flatwater kayak stroke technique. *Aust J Sci Med Sport* **24,** 25-30.

Shiavi R, Green N, McFadyen B, Frazer M & Chen J. (1987). Normative childhood EMG gait patterns. *J Orthop Res* **5,** 283-295.

Soderberg GL & Knutson LM. (2000). A guide for use and interpretation of kinesiological electromyographic data. *Phys Ther* **80,** 485-498.

Solomonow M, Baten C, Smith J, Baretta R, Hermens H, D'Ambrosia R & Shoji H. (1990). Electromyogram power spectral frequencies associated with motor unit recruitment strategies. *J Appl Physiol* **68,** 1177-1185.

Soper C & Hume PA. (2004). Towards an ideal rowing technique for performance: The contributions from biomechanics. *Sports Med* **34,** 825-848.

Staudenmann D, Roeleveld K, Stegeman DF & Van Dieen JH. (2010). Methodological aspects of SEMG recordings for force estimation - A tutorial and review. *J Electromyog Kinesiol* **20,** 375-387.

Steer RR, McGregor AH & Bull AMJ. (2006). A comparison of kinematics and performance measures of two rowing ergometers. *J Sports Sci Med* **5,** 52-59.

Swaine IL & Reilly T. (1983). The freely chosen swimming stroke rate in a maximal swim and on a biokinetic swim bench. *Med Sci Sports Exerc* **15,** 370-375.

Tanabe S & Ito A. (2007). A three-dimensional analysis of the contributions of upper limb joint movements to horizontal racket head velocity at ball impact during tennis serving. *Sports Biomech* **6,** 418-433.

Tanaka K & Matsuuram Y. (1984). Marathon performance, anaerobic threshold, and onset of blood lactate accumulation. *J Appl Physiol* **57,** 640-643.

Taylor AD & Bronks R. (1994). Electromyographic correlates of the transition from aerobic to anaerobic metabolism in treadmill running. *Eur J Appl Physiol Occup Physiol* **69,** 508-515.

Teitz CC, O'Kane J, Lind BK & Hannafin JA. (2002). Back pain in intercollegiate rowers. *Am J Sports Med* **30,** 674-679.

Tesch P. (1983). Physiological characteristics of elite kayak paddlers. *Can J Appl Sports Sci* **8,** 87-91.

Tesch P. (1984). Blood lactate accumulation during arm exercise in world class kayak paddlers and strength trained athletes. *Eur J Appl Physiol* **52,** 441-445.

Tesch P, Piehl K, Wilson G & Karlsson J. (1976). Physiological investigations of Swedish elite canoe competitors. *Med Sci Sports Exerc* **8,** 214-218.

Trevithick BA, Ginn KA, Halaki M & Bainave R. (2007). Shoulder muscle recruitment patterns during a kayak stroke performed on a paddling ergometer. *J Electromyog Kinesiol* **17,** 74-79.

Turpin NA, Guevel A, Durand S & Hug F. (2011). No evidence of expertise-related changes in muscle synergies during rowing. *J Electromyog Kinesiol* **21,** 1030-1040.

Urhausen A, Coen B & Kindermann W. (2000). Individual assessment of the aerobic-anaerobic transition by measurements. In *Exercise and Sport Science*, ed. Garrett WE & Kirkendall DT, pp. 267-275. Lippincott Williams & Wilkins.

Van Someran KA, Phillips GR & Palmer GS. (2000). Comparison of physiological responses to open water kayaking and kayak ergometry. *Int J Sports Med* **21,** 200-204.

Viitasalo J, Luhtanen P, Rahkila P & Rusko H. (1985). Electromyographic activity related to aerobic and anaerobic threshold in ergometer bicycling *Acta Physiol Scand* **124,** 287-293.

Vollestad NK. (1997). Measurement of human muscle fatigue. *J Neurosci Methods* **74,** 219-227.

Walsh ML & Banister EW. (1988). Possible mechanisms of the anaerobic threshold: A review. *Sports Med* **5,** 269-302.

Wasserman K, Beaver WL & Whipp BJ. (1986). Mechanisms and patterns of blood lactate increase during exercise in man. *Med Sci Sports Exerc* **18,** 344-352.

Wasserman K & McIlroy M. (1964). Detecting the threshold of anaerobic metabolism in cardiac patients during exercise. *Am J Cardiol* **14,** 844-852.

Wasserman K, Whipp BJ, Koyal SN & Beaver WL. (1973). Anaerobic threshold and respiratory gas exchange during exercise. *J Appl Physiol* **35,** 236-243.

Wilmore JH, Costill DL & Kennedy WL. (2008). Adaptations to Resistance Training. In *Physiology of Sport and Exercise*, ed. Costill DL & Kenney WL, pp. 202-219. Human Kinetics, Champaign, Il.

Wilson JM, Gordon D, Robertson E & Stothart JP. (1988). Analysis of lower limb muscle function in ergometer rowing. *Int J Sport Biomech* **4,** 315-325.

Winter D & Yack HJ. (1987). EMG profiles during normal human walking: stride-to-stride and inter-subject variability. *Electroencephalogr Clin Neurophysiol* **67,** 402-411.

Wong Y & Ng G. (2010). Resistance training alters the sensorimotor control of vastii muscles. *J Electromyog Kinesiol* **20,** 180-184.

Yang J & Winter D. (1983). Reliability of non-normalised and normalised integrated EMG during maximal isometric contractions in females *Arch Phys Med Rehabil* **64,** 417-420.

Yang J & Winter D. (1984). Electromyographic amplitude normalisation methods: Improving their sensitivity as diagnostic tools in gait analysis. *Arch Phys Med Rehabil* **65,** 517-521.

Zhukov EK. (1959). Synchronized action potentials during muscular activity in man. *Fiziol Zh SSSR* **45,** 17-23.

Zijdewind I, Zwarts MJ & Kernell D. (2000). Potentiating and fatiguing cortical reactions in a voluntary fatigue test of a human hand muscle. *Exp Brain Res* **130,** 529-532.

Zipp P. (1978). Effect of electrode parameters on the bandwidth of the surface EMG power-density spectrum. *Med Biol Eng Comput* **16,** 537-541.

Appendix 1

Abstracts

2009 Physiological Society Conference, University College Dublin, Ireland.

IDENTIFICATION OF THE AEROBIC-ANAEROBIC TRANSITION IN MALE ROWERS USING SURFACE ELECTROMYOGRAPHY DURING GRADED INCREMENTAL EXERCISE.

Neil Fleming[1], Bernard Donne[1], Nick Mahony[2]

[1]Department of Physiology, [2]Department of Anatomy, Trinity College Dublin.

The aim of this study was to assess the use of surface electromyography (EMG) as a non-invasive determinant of the metabolic response to incremental exercise in male rowers. The relationship between EMG threshold (T_{EMG}) and more commonly used variables for detection of the aerobic-anaerobic threshold (blood lactate threshold (T_{Lac}), onset of blood lactate accumulation, OBLA) was assessed.

Thirteen male rowers (age 21±4yr, height 1.88±0.04m, mass 84±7kg, $\dot{V}O_2max$ 61.0±6.0mL.kg^{-1}.min^{-1}) performed graded tests to volitional exhaustion on a Concept II ergometer. This ethically approved study involved intermittent exercise bouts at power outputs (start power 120W, duration 3 min, rest 1 min, increment 40W) during which root-mean-squared-EMG data (rmsEMG) were recorded from *Rectus Femoris* (RF), *Vastus Lateralis* (VL), *Biceps Femoris* (BF) and upper portion of *Trapezius* (UT). The rest period between increments facilitated earlobe blood sampling for lactate determination. Computed rms-EMG data for each muscle were averaged over 10 consecutive stroke cycles during the final minute of each exercise increment. Individual power at EMG threshold were identified using the V-slope method and compared against power at T_{Lac} and OBLA using a repeated measures ANOVA.

Correlation analysis showed strong association between blood lactate and rmsEMG activity in *RF* (r=0.82), *VL* (r=0.63) and *BF* (r=0.71), and lower association in *UT* (r=0.42). Analysis revealed no significant differences between T_{Lac} (257±7W) and T_{EMG} in *RF* (266±6W) and *VL* (267±7W), however T_{EMG} occurred at significantly higher power outputs (P<0.01) for

BF (270±7W) and *UT* (274±10W). No significant differences were observed comparing T_{EMG} and OBLA (280±9W) in any of the muscles investigated.

Our results suggest that T_{EMG} is strongly associated to both OBLA and T_{Lac} (r=0.75 to 0.94) and that there are differing recruitment strategies relative to increasing exercise intensity between the muscles analysed in the current study. Further analysis is required to assess overall changes in recruitment associated with the aerobic-anaerobic transition.

	Power @ T_{EMG}	Correlation to BLa
Rectus Femoris	266±6W	r=0.82
Vastus Lateralis	267±7W	r=0.63
Biceps Femoris ($P<0.01$)	270±7W	r=0.71
Upper Trapezius ($P<0.01$)	274±10W	r=0.42

ECSS 2010, Antalya, Turkey

A BIOMECHANICAL ASSESSMENT OF KAYAK ERGOMETER TASK SPECIFICITY

Fleming, N., Donne, B., Fletcher D

Physiology Department, Trinity College Dublin, Ireland.

Introduction

Ergometer and on-water kayaking were not significantly different comparing metabolic and cardiovascular variables; however biomechanical differences may exist between modalities. Electromyographic (EMG) analysis of ergometer kayaking has investigated shoulder muscle recruitment patterns during task performance (Trevithick *et al.* 2007). The current study assessed task specificity by direct biomechanical comparison of ergometer and on-water kayaking via EMG, force application and stroke kinematics.

Methods

Male flat-water kayakers (n=10) performed matched exercise protocols on a kayak ergometer (Dansprint) and on-water. Protocols consisted of 3 min bouts at heart and stroke rates equivalent to 75, 85 and 95% of $\dot{V}O_2max$ (assessed via incremental tests). EMG data were recorded from *Anterior Deltoids* (AD), *Triceps Brachii* (TB), *Latissimus Dorsi* (LD) and *Vastus Lateralis* (VL) via wireless telemetry (ME6000, Mega Ltd). Simultaneous video data recorded at 50 Hz with audio triggers pre- and post-exercise facilitated synchronisation of EMG and kinematic data. Force was recorded via strain gauge arrays on paddle and ergometer shafts. EMG data were root mean squared (20ms window), temporally and amplitude normalised, and averaged over 10 consecutive cycles for each kayaker. Mean rmsEMG data for each decile (10%) of the stroke cycle were compared using 2 way repeated measures ANOVA, Tukey *post-hoc* tests quantified significant differences ($P<0.05$).

Results

During the draw phase (deciles 1 and 2), stroke force and EMG activity (TB, LD and VL) increased significantly ($P<0.05$) with exercise intensity, however no intensity effect in AD was observed in either modality. Analysis of kinematic and force data revealed AD activity was concurrent with phases of non-force production (transition phases, deciles 3 to 5 and 7 to 9). Comparison across modalities revealed significantly ($P<0.01$) greater AD activity on-ergometer during the 7^{th} to 9^{th} deciles (27.3±9.7 vs. 11.1±2.1, 24.6±8.3 vs. 8.9±2.0 and 23.8±8.7 vs. 7.4±1.2 at 75, 85 and 95%, respectively), in addition LD activity was significantly greater ($P<0.01$) during the 10^{th} decile. Subsequent analysis revealed an external force of 21±2 N associated with the ergometer loading mechanism being applied to the shaft.

Discussion

Significantly greater on-ergometer AD and LD activity can be attributed to the ergometer loading mechanism applying additional forces during non-force production phases of the stroke cycle (transition phases). These external forces are not observed on-water when the muscles can therefore remain in a more inactive state. These results contradict a previous hypothesis (Trevithick *et al.* 2007) on shoulder muscle recruitment during on-water kayaking.

References

Trevithick B, Ginn K, Halaki M, Bainave R. (2007). J Electromyog Kinesiol 17, 74-79.

ECSS 2010, Antalya, Turkey

TRAINING INDUCED ALTERATIONS IN NEUROMUSCULAR FATIGUE INDICES RECORDED DURING ISOMETRIC KNEE EXTENSION.

Fleming, N., Donne, B

Physiology Department, Trinity College Dublin. Dublin 2, Ireland

Introduction

Short term resistance training reportedly alters frequency and amplitude of muscle fatigue indices during subsequent sustained isometric contractions. We investigated if potential changes associated with resistance training and/or muscle fibre type shifts could be identified via spectral analysis of EMG fatigue indices recorded from knee extensor musculature.

Methods

Collegiate level, resistance trained male rowers (n=10) and sedentary controls (n=10) performed isometric knee extensions to failure at 70° of knee flexion on a Cybex II dynamometer. Both groups performed trials at 80 and 20% of their maximal isometric force. Visual feedback of force production was provided and failure was defined when the applied force dropped 10% below target despite verbal encouragement. Trials were repeated on a separate day to establish reliability. EMG data were recorded from *Rectus Femoris* (RF), *Vastus Lateralis* (VL) and *Vastus Medialis* (VM) throughout all trials. Data collected over a 5s window following onset and preceding the end point were averaged using discrete FFT methods (Hamming window processing, 256 samples, overlap 75%) in order to obtain a single measure for initial and final median frequency (MF), mean power frequency (MPF) and average EMG (AEMG), and rates of change of spectral variables across trials were calculated.

Results

The trained group produced significantly greater maximal isometric force in both legs ($P<0.05$), and mean time to failure data were significantly greater during both 80% (102 ±

39 vs. 59 ± 13 s, $P<0.01$) and 20% trials (603 ± 124 vs. 411 ± 87 s, $P<0.001$). The trained group also exhibited better reliability (ICC: trained 0.74 to 0.97, untrained 0.13 to 0.91) compared to untrained. Analysis revealed no significant differences within VL or VM for any measured variables. However, RF revealed significant differences in rate of change for AEMG during the 80% trial (45.3 ± 48.9 vs. -51.9 ± 60.4 $\mu V.min^{-1}$, $P<0.001$). The decline in AEMG exhibited by RF in the untrained group was unexpected as AEMG should progressively increase with neuromuscular fatigue during sustained contractions.

Discussion

The current study failed to observe any significant differences in investigated EMG variables during the 20% trial which might have been linked to contrasting fibre typing within the musculature. Differences observed for AEMG in RF during the 80% trial, were most likely resultant from enhanced recruitment strategies brought about by resistance training. Further research should focus on enhanced spectral processing of the EMG signal and comparison between contrasting trained groups. Muscle fibre type differences between sprint and endurance trained groups would be more pronounced and perhaps more clearly identifiable via spectral EMG analysis.

Full paper published in the Journal of Sport Science and Medicine (2012) 11, 16-25.

TITLE: A biomechanical assessment of ergometer task specificity in elite flat-water kayakers.

AUTHORS: Fleming, N.[1], Donne, B.[1], Fletcher D[1], Mahony, N.[2]

[1]Physiology Department, Trinity College Dublin, Ireland.

[2]Anatomy Department, Trinity College Dublin, Ireland

ABSTRACT

The current study compared EMG, stroke force and 2D kinematics during on-ergometer and on-water kayaking. Male elite flat-water kayakers (n=10) performed matched exercise protocols consisting of 3 min bouts at heart and stroke rates equivalent to 85% of $\dot{V}O_2$peak (assessed by prior graded incremental test). EMG data were recorded from *Anterior Deltoid* (AD), *Triceps Brachii* (TB), *Latissimus Dorsi* (LD) and *Vastus Lateralis* (VL) via wireless telemetry. Video data recorded at 50 Hz with audio triggers pre- and post-exercise facilitated synchronisation of EMG and kinematic variables. Force data were recorded via strain gauge arrays on paddle and ergometer shafts. EMG data were root mean squared (20ms window), temporally and amplitude normalised, and averaged over 10 consecutive cycles. In addition, overall muscle activity was quantified via iEMG and discrete stroke force and kinematic variables computed. Significantly greater TB and LD mean iEMG activity were recorded on-water (239 ± 15 vs. 179 ± 10 μV.s, $P<0.01$ and 158 ± 12 vs. 137 ± 14 μV.s, $p < 0.05$, respectively), while significantly greater AD activity was recorded on-ergometer (494 ± 66 vs. 340 ± 35 μV.s, $P<0.01$). Time to vertical shaft position occurred significantly earlier on-ergometer ($P<0.05$). Analysis of stroke force data and EMG revealed that increased AD activity was concurrent with increased external forces applied to the paddle shaft at discrete phases of the on-ergometer stroke cycle. These external forces were associated with the ergometer loading mechanism and were not observed on-water. The current results contradict a previous published hypothesis on shoulder muscle recruitment during on-water kayaking.

Full paper accepted for publication in the Journal of Sport Science and Medicine.

TITLE: Effect of kayak ergometer elastic tension on upper limb EMG activity and 3D kinematics.

AUTHORS: Fleming, N.[1], Donne, B.[2], Fletcher, D.[2]

[1]Department of Kinesiology, Recreation and Sport, Indiana State University, Indiana, USA.

[2]Physiology Department, Trinity College Dublin, Dublin 2, Ireland.

Despite the prevalence of shoulder injury in kayakers, limited published research examining associated upper limb kinematics and recruitment patterns exists. Altered muscle recruitment patterns on-ergometer vs. on-water kayaking were recently reported, however, mechanisms underlying changes remain to be elucidated. The current study assessed the effect of ergometer recoil tension on upper limb recruitment and kinematics during the kayak stroke. Male kayakers (n=10) performed 4 by 1 min on-ergometer exercise bouts at 85% VO_2max at varying elastic recoil tension; EMG, stroke force and three-dimensional 3D kinematic data were recorded. While stationary recoil forces significantly increased across investigated tensions (125% increase, $p < 0.001$), no significant differences were detected in assessed force variables during the stroke cycle. In contrast, increasing tension induced significantly higher *Anterior Deltoid* (AD) activity in the latter stages (70 to 90%) of the cycle ($p < 0.05$). No significant differences were observed across tension levels for *Triceps Brachii* or *Latissimus Dorsi*. Kinematic analysis revealed that overhead arm movements accounted for 39 ± 16% of the cycle. Elbow angle at stroke cycle onset was 144 ± 10°; maximal elbow angle (151 ± 7°) occurred at 78 ± 10% into the cycle. All kinematic markers moved to a more anterior position as tension increased. No significant change in wrist marker elevation was observed, while elbow and shoulder marker elevations significantly increased across tension levels ($p < 0.05$). In conclusion, data suggested that kayakers maintained normal upper limb kinematics via additional AD recruitment despite ergometer induced recoil forces.

Appendix 2

EMG sensor locations

Appendix 2.1: Anterior Deltoid

Muscle	*Anterior Deltoid*
Abbreviation:	AD
Origin	Anterior border, superior surface, lateral third of the clavicle.
Insertion	Deltoid tuberosity of the humerus.
Action	Anterior flexion and medial rotation of the shoulder
Electrode Location	One finger width distal and anterior to the acromion.
Orientation	In the direction of the line between the acromion and the thumb.
Reference Electrode	Clavicle,spinal scapula or spinous process of C7.

Sensor Location:

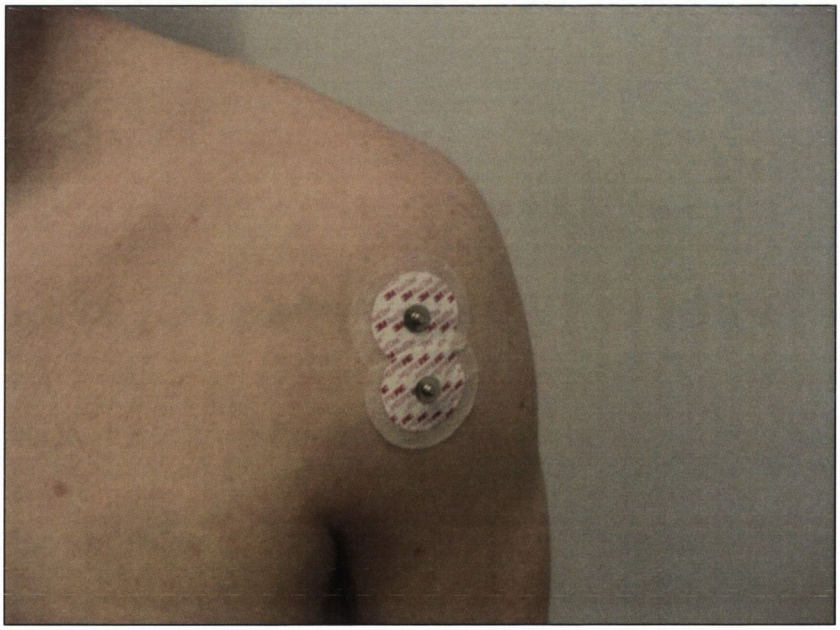

Appendix 2.2: Triceps Brachii

Muscle	*Triceps Brachii* (long head)
Abbreviation:	TB
Origin	Infraglenoid tubercle of scapula.
Insertion	Posterior surface of olecranon process of ulna and antebrachial fascia.
Action	Extension of the elbow joint. The long head also adducts and may assist in extension of the shoulder joint.
Electrode Location	At 50 % on the line between the posterior crista of the acromion and the olecranon at 2 finger widths medial to the line (SENIAM).
Orientation	In the direction of the line between the posterior crista of the acromion and the olecranon (SENIAM).
Reference Electrode	Lateral tip of acromion or lateral epicondyle.

Sensor Location:

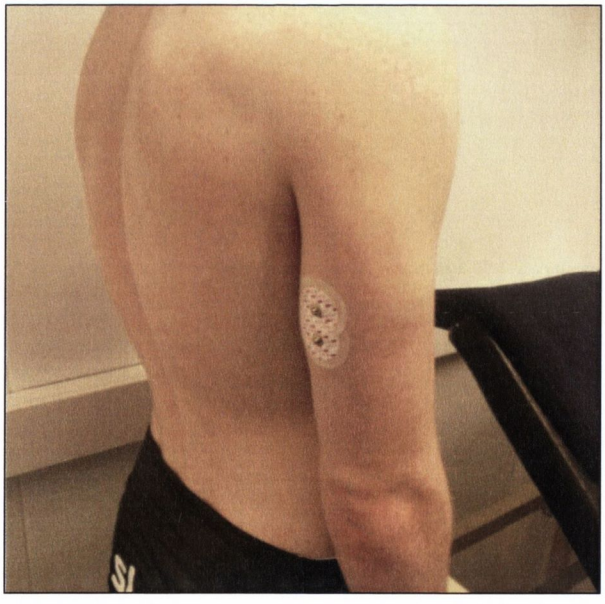

Appendix 2.3: Biceps Brachii

Muscle	*Biceps Brachii* (long head)
Abbreviation:	BB
Origin	Supraglenoid tubercle of scapula.
Insertion	Radial tuberosity and bicipital aponeurosis into deep fascia on medial part of forearm.
Action	Elbow flexion
Electrode Location	On the line between the medial acromion and the cubital fossa at a third distance from the cubital fossa (SENIAM).
Orientation	In the direction of the line between the acromion and the fossa cubit (SENIAM).
Reference Electrode	Lateral tip of acromion or lateral epicondyle.

Sensor Location:

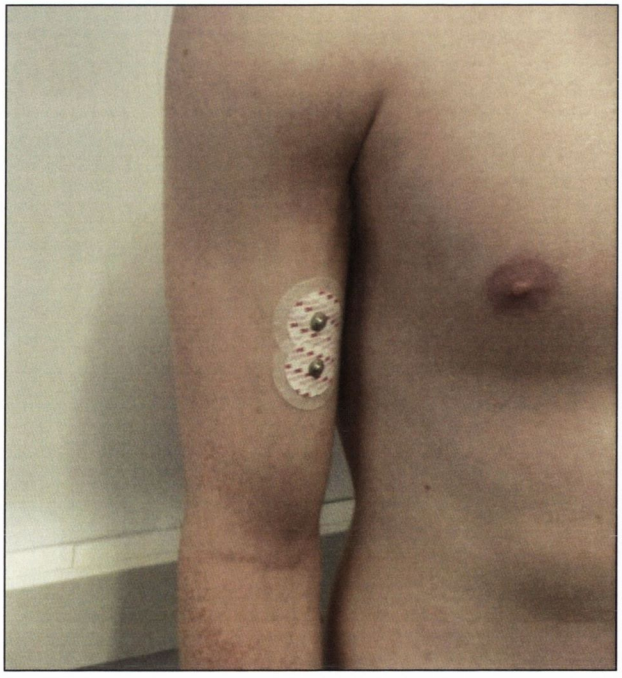

Appendix 2.4: Latissimus Dorsi

Muscle	*Latissimus Dorsi*
Abbreviation:	LD
Origin	Spinous processes of thoracic T7-L5, thoracolumbar fascia, iliac crest and inferior 3 or 4 ribs, inferior angle of scapula.
Insertion	Floor of intertubercular groove of the humerus.
Action	Adduction, extension and internal rotation of the shoulder
Electrode Location	Three fingerlengths inferior and laterally from the inferior angle of the scapula
Orientation	45° relative to vertical in the direction of the acromion.
Reference Electrode	Spinous processes from L1 to T6.

Sensor Location:

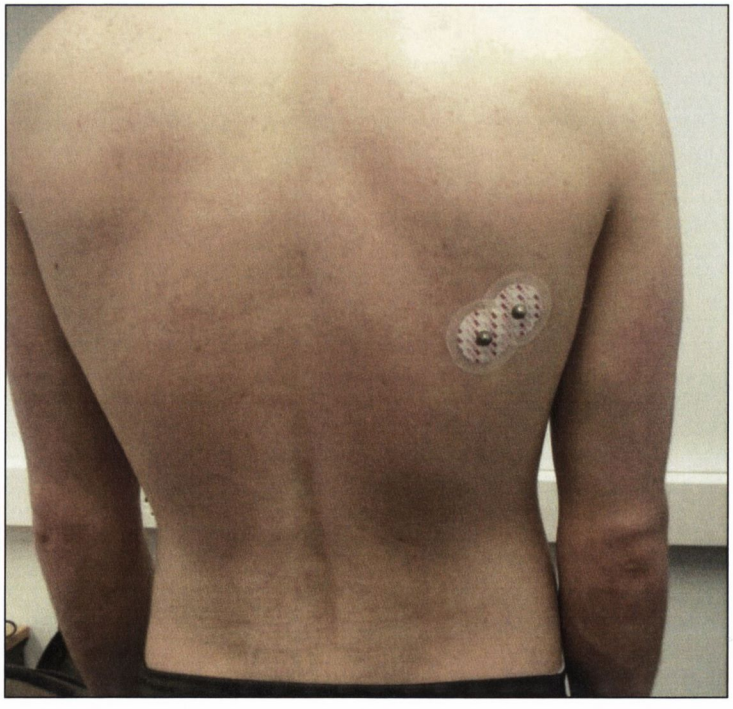

Appendix 2.5: Upper Trapezius

Muscle	*Upper Trapezius*
Abbreviation:	UT
Origin	External occipital protuberance, medial third of superior nuchal line, ligamentum nuchae, and spinous process of vertebra C7.
Insertion	Lateral third of clavicle and acromion process of scapula.
Action	Shoulder elevation and scapular stabilisation.
Electrode Location	50% on the line from the acromion to the spine on vertebra C7 (SENIAM).
Orientation	In the direction of the line between the acromion and the spine on vertebra C7 (SENIAM).
Reference Electrode	Spinous process of vertebra C7.

Sensor Location:

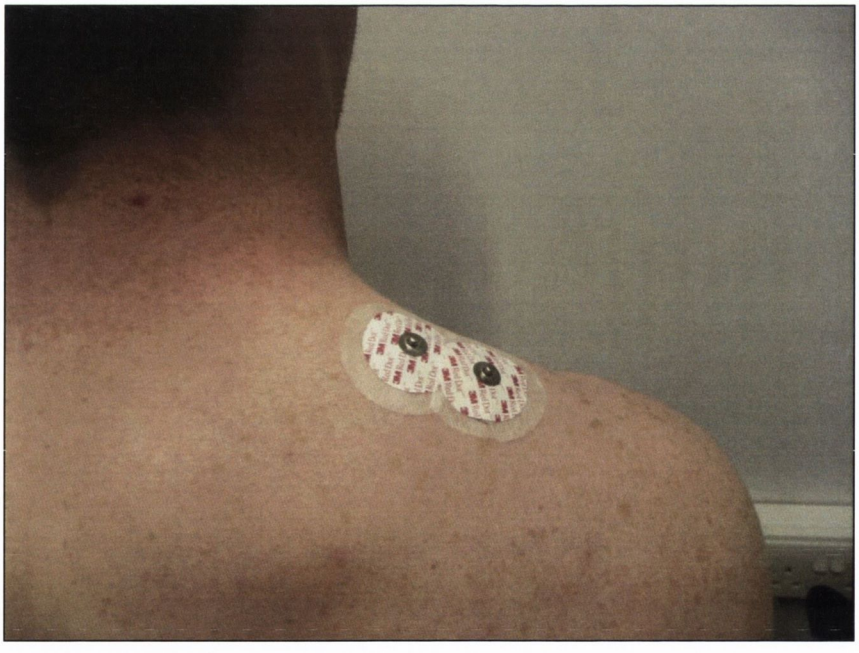

Appendix 2.6: Erector Spinae

Muscle	*Erector Spinae (longissimus)*
Abbreviation:	ES
Origin	Spinous processes of T9 to T12 thoracic vertebræ.
Insertion	Spinous processes of T1 and T2 thoracic vertebrae and the cervical vertebrae.
Action	Extension of the vertebral column.
Electrode Location	2 finger widths laterally from the spinous process of L1 (SENIAM).
Orientation	Vertical (SENIAM).
Reference Electrode	Spinous process of C7 or iliac crest.

Sensor Location:

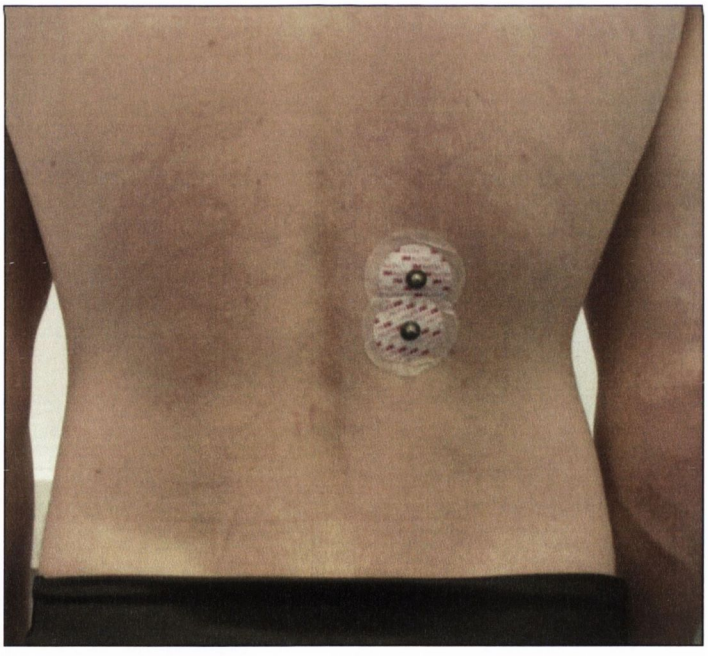

Appendix 2.7: Rectus Femoris

Muscle	*Rectus Femoris*
Abbreviation	RF
Origin	Anterior inferior iliac spine and the exterior surface of the bony ridge which forms the iliac portion of the acetabulum.
Insertion	Proximal border of the patella and through patellar ligament.
Action	Knee extension and hip flexion.
Electrode Location	50% on the line from the anterior spina iliaca superior to the superior part of the patella (SENIAM).
Orientation	In the direction of the line from the anterior superior iliac spine superior to the superior part of the patella (SENIAM).
Reference Electrode	Iliac crest or superior patella

Sensor Location:

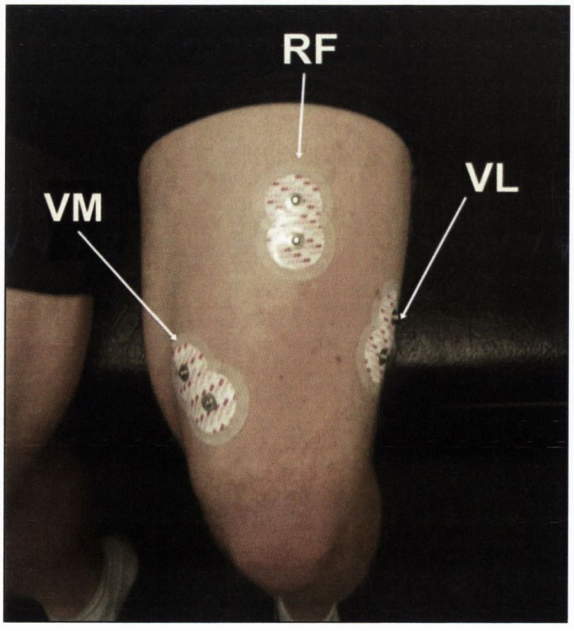

Appendix 2.8: Vastus Medialis

Muscle	*Vastus Medialis*
Abbreviation	VM
Origin	Distal half of the intertrochanteric line, medial lip of line aspera, proximal part of medial supracondylar line, tendons of adductor longus and adductor magnus and medial intermuscular septum.
Insertion	Proximal border of the patella and through patellar ligament.
Action	Knee extension.
Electrode Location	80% on the line between the anterior spina iliaca superior and the joint space in front of the anterior border of the medial ligament (SENIAM).
Orientation	Almost perpendicular to the line between the anterior spina iliaca superior and the joint space in front of the anterior border of the medial ligament (SENIAM).
Reference Electrode	Iliac crest or medial side of patella.

Sensor Location:

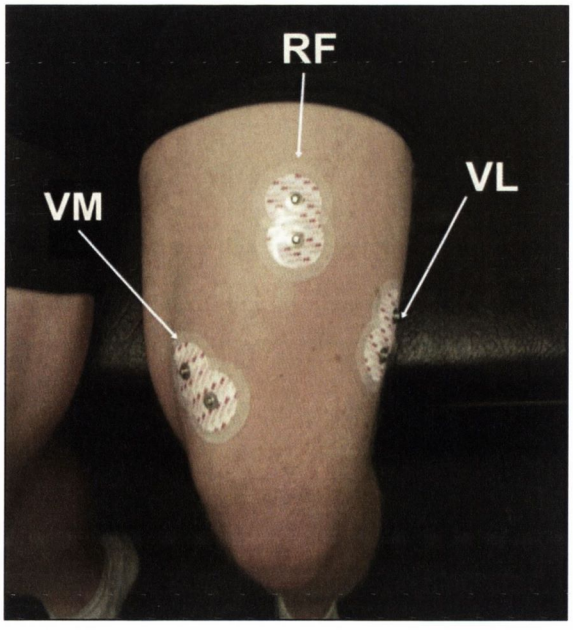

Appendix 2.9: Vastus Lateralis

Muscle	*Vastus Lateralis*
Abbreviation	VL
Origin	Proximal parts of intertrochanteric line, anterior and inferior borders of greater trochanter, lateral lip of gluteal tuberosity, proximal half of lateral lip of linea aspera, and lateral intermuscular septum.
Insertion	Proximal border of the patella and through patellar ligament.
Action	Knee extension.
Electrode Location	Approximately 60% on the line from the anterior spina iliaca superior to the lateral side of the patella (SENIAM).
Orientation	In the direction of the muscle fibres (SENIAM).
Reference Electrode	Iliac crest or lateral side of patella.

Sensor Location:

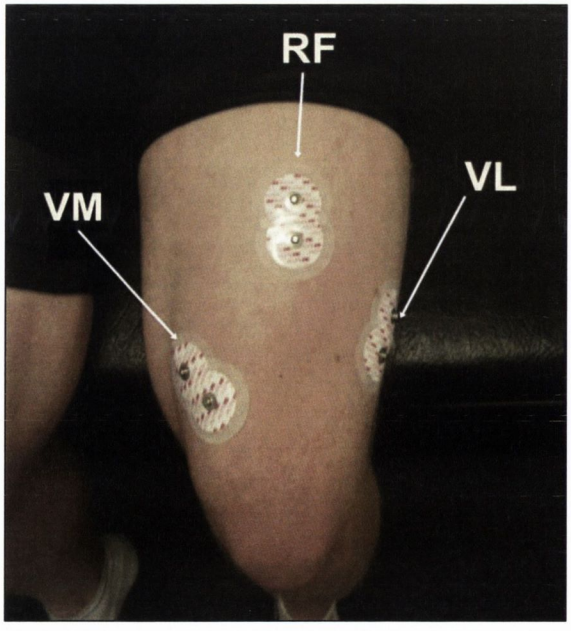

Appendix 2.10: Biceps Femoris

Muscle	*Biceps Femoris* (long head)
Abbreviation	BF
Origin	Distal part of sacrotuberous ligament and posterior part of tuberosity
Insertion	Lateral side of head of fibula, lateral condyle of tibia, deep fascial on lateral side of leg.
Action	Knee flexion and lateral rotation. Hip extension.
Electrode Location	50% on the line between the ischial tuberosity and the lateral epicondyle of the tibia (SENIAM).
Orientation	In the direction of the line between the ischial tuberosity and the lateral epicondyle of the tibia (SENIAM).
Reference Electrode	Greater trochanter of the femur.

Sensor Location:

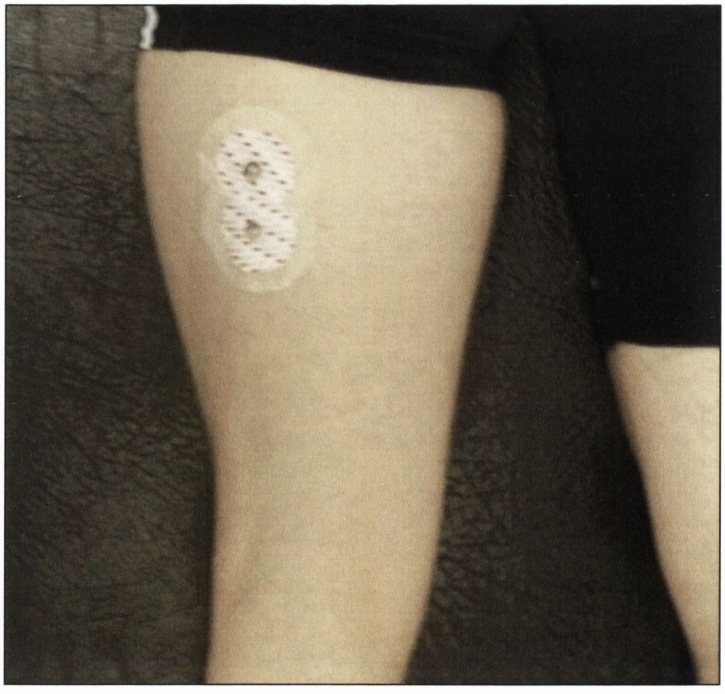

Appendix 2.11: Gastrocnemius

Muscle	*Gastrocnemius (Medialis)*
Abbreviation	GA
Origin	Proximal and posterior part of medial condyle and adjacent part of the femur, capsule of the knee joint.
Insertion	Middle part of posterior surface of calcaneus.
Action	Heel flexion and assisting knee flexion.
Electrode Location	Electrodes need to be placed on the most prominent bulge of the muscle (SENIAM).
Orientation	In the direction of the lower leg (SENIAM).
Reference Electrode	Medial side of patella, or ankle.

Sensor Location:

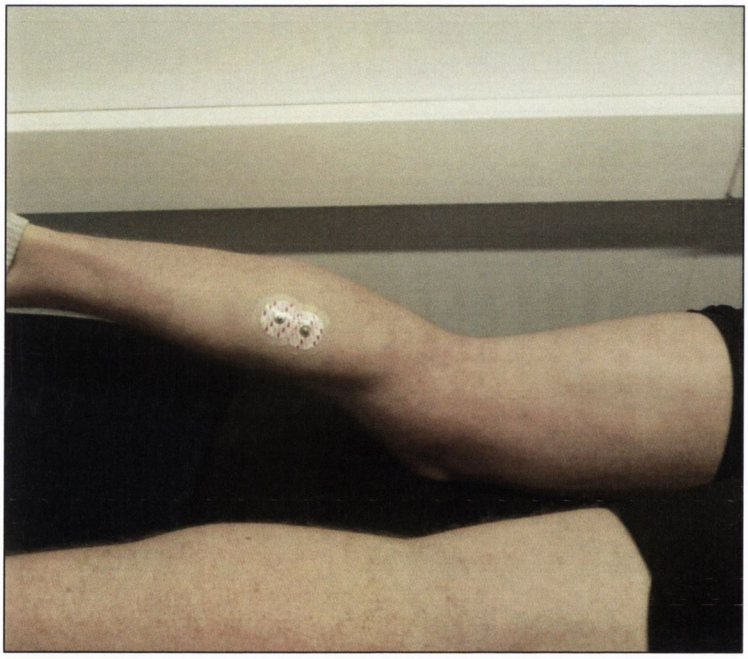

Appendix 2.12: Tibialis Anterior

Muscle	*Tibialis Anterior*
Abbreviation	TA
Origin	Lateral condyle and proximal half of lateral surface of tibia, interosseus membrane, deep fascia and lateral intermuscular septum.
Insertion	Medial and plantar surface of medial cuneiform bone, base of first metatarsal bone.
Action	Dorsiflexion of the ankle joint and assistance in foot inversion.
Electrode Location	A third of the distance on the line between the tip of the fibula and the tip of the medial malleolus.
Orientation	In the direction of the line between the tip of the fibula and the tip of the medial malleolus (SENIAM).
Reference Electrode	Lateral side of patella, or ankle.

Sensor Location:

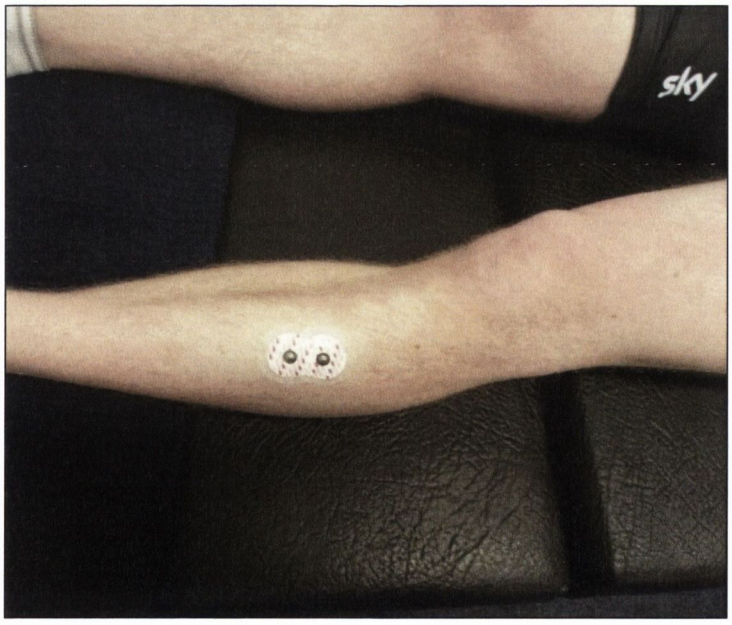

Appendix 3

Informed consent form and medical questionaire.

SUBJECT INFORMATION LEAFLET
Physiology Department, Trinity College Dublin.

Title of Study: Reliability and reproducibility of EMG parameters in the assessment of neuromuscular fatigue in the knee extensors of trained and untrained male volunteers

Principal Researcher: Neil Fleming

Introduction: In order to have confidence in the results of any test, we must know that good reliability and reproducibility exists for the data being analysed. Surface electromyography (EMG) has been used to test muscle fatigue for many years however there is a lack of published material assessing the reliability and reproducibility of these measurements. The main aim of this study is to assess the reliability and reproducibility of measuring muscle fatigue using EMG. A secondary aim is to compare reliability and reproducibility of EMG measurements between trained and untrained volunteer groups. Only healthy males over the age of 18 will participate in this study. All testing will be performed in the Human Performance Laboratory, Anatomy Department, Trinity College Dublin. Testing will involve performing a series of knee extensions at a fixed angle on a Cybex dynamometer which is specifically designed to measure your muscle strength. Using a portable EMG recorder, muscle activity in your knee extensor muscles will be recorded during these tests. The recorded data will then be used to assess the reliability and reproducibility of measurements.

Procedure: You will attend the laboratory on 3 occasions in total; each testing session will last approximately 45 minute. On the first occasion you will receive a full medical assessment by a qualified doctor. You will also have a chance to practice performing isometric knee extensions on the Cybex dynamometer during a familiarisation session. During the 2 subsequent testing sessions, you will perform a series of knee extensions at a fixed knee angle of 70°, while EMG is recorded from your knee extensor muscles. You will initially perform 3 maximal contractions of each knee. The results of these contractions will be used to calculate your target forces for the 2 subsequent fatigue tests. During these fatigue tests, you will attempt to maintain a constant target force equivalent to 80% and 20% of your maximum force for as long as possible.EMG will be recorded during all your knee contractions and these data will be used to calculate the reliability and reproducibility of using EMG to assess muscle fatigue. Both testing sessions will require approximately 45 minutes to complete and there will be a minimum of 24 hours rest between testing sessions.

Benefits: You will receive the result of the haematological assessment outlining your full blood count. You will also receive detailed information on your strength in both your legs with regard to knee extension.

Risks: There are no major risks involved in undertaking this study. All procedures in the study are non-invasive. EMG recording often involves shaving portions of the skin in order to stick on electrodes required for recording muscle activation. As part of the pre-trail medical assessment, a small blood sample will be taken by a qualified doctor. This is standard practice before any testing performed in the laboratory and no major risks are

envisaged, however there may be some small bruising and soreness associated with this procedure.

Exclusion from participation: Any person presenting with any health abnormalities, respiratory difficulties or symptoms of a cold on the trail day. Anyone with an injury affecting their legs and specifically their knees will be excluded.

Confidentiality: Your identity will remain confidential. Your name will not be published and will not be disclosed to anyone outside the study group. All data will be stored safe and secure within the department for a period of five years. Blood samples and associated data collected during the study will not be used for any purpose other than those related to the variables of interest in this study.

Compensation: The medical investigator involved in this study is covered by standard medical malpractice insurance. This study is covered by standard institutional indemnity insurance. Nothing in this document restricts or curtails your rights

Voluntary Participation: You have volunteered to participate in this study. You may quit at any time. If you decide not to participate, or if you quit, you will not be penalised and will not give up any benefits that you had before entering the study.

Stopping the study: You understand that the investigators may stop your participation in the study at any time without your consent.

Permission: This project has received approval from the Health Sciences Faculty Research Ethics Group.

Further Information: You can get more information or answers to your questions about the study, your participation in the study, and your rights, from Neil Fleming who can be telephoned at 086 8524341 or Bernard Donne (01 8962012). If the study team learns of important new information that might affect your desire to remain in the study, you will be informed at once.

SUBJECT CONSENT FORM

Physiology Department, Trinity College Dublin

PROJECT: Reliability and reproducibility of EMG parameters in the assessment of neuromuscular fatigue in the knee extensors of trained and untrained male volunteers

PRINCIPAL INVESTIGATOR: Neil Fleming

INTRODUCTION: In order to have confidence in the results of any test, we must know that good reliability and reproducibility exists for the data being analysed. Surface electromyography (EMG) is no exception to this rule, however currently there is a lack of published studies assessing the reliability and reproducibility of EMG measurements of muscle fatigue. Therefore the primary aim of this study is to establish if the use of EMG to test muscular fatigue is a reliable and reproducible measurement. A secondary aim will assess if trained volunteers who regularly exercise their knee extensor muscles in dynamic sporting activities provide a more reliable subject group than untrained volunteers.

PROCEDURES:

This study will undertake an EMG (electromyography) analysis of the muscles involved in knee extension during fatiguing muscle contractions. Trials will be carried out on a Cybex dynamometer which is especially designed to test muscle strength. Participants will perform 2 identical trials on separate days. The EMG data collected over these two trials will then be used to assess reliability and reproducibility. Between 24 and 30 healthy, male volunteers over the age of 18 will participate in this study. This group will be split into trained and untrained sub-groups in order to assess if differences in training status affects the reliability and reproducibility of measurements.

All testing will be performed in the Human Performance Laboratory in the Anatomy Department in Trinity College. Volunteers will visit the laboratory on three separate occasions. On the first occasion, a full medical assessment and familiarisation session on the Cybex machine will be performed. During the two subsequent visits, a full isometric muscle test will be carried out on the knee extensor muscles. This test involves initially performing 3 maximum contractions of the knee, at a fixed angle of 70°. The results of these contractions will be used to calculate 80 and 20% of maximum voluntary contraction (MVC) which will be used in 2 subsequent fatigue tests. During the 2 fatigue tests,

volunteers will maintain a constant force equivalent to 80% and 20% of their MVC for as long as possible. During all tests, EMG will be recorded and used to assess the reliability and reproducibility of measurements. There will be a minimum of 24 hours rest between subsequent testing sessions.

DECLARATION:

I have read, or had read to me, this consent form. I have had the opportunity to ask questions and all my questions have been answered to my satisfaction. I freely and voluntarily agree to be part of this research study, though without prejudice to my legal and ethical rights. I have received a copy of this agreement and I consent that any medical abnormalities identified during my medical examination can be passed on to my designated general practitioner.

I understand I may withdraw from the study at any time.

PARTICIPANT'S NAME: .....

CONTACT DETAILS: .....

PARTICIPANT'S SIGNATURE: .....

Date: .....

Statement of investigator's responsibility: I have explained the nature and purpose of this research study, the procedures to be undertaken and any risks that may be involved. I have offered to answer any questions and fully answered such questions. I believe that the participant understands my explanation and has freely given informed consent.

INVESTIGATOR'S SIGNATURE: ..... **Date:** .....

Pre-participation Medical Questionnaire & Examination Form. **Date / / 11**

Name:	Preferred Event: .....
Age:	Age of entry into sport: .....
Date of Birth:	Club: .....
Occupation:	Contact Tel No.: .....
Address:	Email: .....
.....	G.P's name: .....
.....	G.P's address: .....
	.....

Training *No of sessions per week*

AM Resting HR: .....beats.min^{-1}	Aerobic Interval
Sleep: .....hr.day^{-1}	Speed Resistance
Mood: 1 2 3 4 5 6 7 8 9 10	Last training Session *(time/details)*
Fatigue: 1 2 3 4 5 6 7 8 9 10	.....

Personal & Family History *Detail any other family illnesses*

Circle			*Circle*		
Smoking	Y	N	Heart Disease	Y	N
Alcohol	Y	N	Strokes	Y	N
Tea	Y	N	Diabetes	Y	N
Coffee	Y	N	Asthma	Y	N
Vegetarian	Y	N	Epilepsy	Y	N

Drug History			*State Details*
Medication	Y	N	
Over The Counter Meds	Y	N	
Allergies	Y	N	
Vitamins	Y	N	

Current medical Problems last 3 months

Recent Illnesses:	Recent Injuries:

Last 7 days	*Circle*		*At any time...*	*Circle*		*Details*
Flu Symptoms	Y	N	Hospital admissions	Y	N	
Sore Throat	Y	N	Operations	Y	N	
Cough	Y	N	Fractures	Y	N	
Wheeze	Y	N	Sports Injuries	Y	N	
Chest Pains	Y	N	Diabetes	Y	N	
Palpitations	Y	N	Asthma	Y	N	
Nausea	Y	N	Epilepsy	Y	N	
Vomiting	Y	N	Jaundice	Y	N	
Diarrhea	Y	N	Kidney problem	Y	N	
Headaches	Y	N	Heart Murmur	Y	N	
Fits or Faints	Y	N	Eye Problems	Y	N	
Others	Y	N	Other Illness			

General Examination Doctors Use Only

Obs: Pulse .....beats.min^{-1} Reg. / Irreg.		
BP ...../.....mmHg		
Head: Nose	Throat	FBC Result: .....
Neck: Nodes	Thyroid	.....
CVS: Apex beat	Heart Sounds	PFT Result: .....
RS: Exp^{n}	Perc. / Ausc.	.....

Medical Summary

Fit for Exercise Test to Exhaustion Y N Signature: .....

Appendix 4

Validation study examining the appearance of the neuromuscular fatigue threshold during continuous and intermittent incremental tests.

INTRODUCTION

The results of Chapter 3 suggested that both V_{T2} and T_{EMG} possessed a shared sensitivity for alterations in the exercise-recovery ratio of an incremental test protocol. Significant differences were observed in both variables comparing their occurrence in cycling and rowing incremental tests. It was postulated that these differences may have been due to the contrasting test protocols that were used. While the cycling sub-group performed a continuous incremental test, the rowing sub-group performed an intermittent test. During an intermittent incremental test, a 1 min rest period is afforded between increments. This is done in order to facilitate blood lactate measurement; however this rest period can impact on the physiological processes occurring during the test. As the participant reaches their aerobic-anaerobic transition, the rest period between increments of the test affords them the opportunity to buffer the accumulation of H^+ ions in the blood, via respiratory compensation through hyperventilation. This may have the effect of altering the appearance of thresholds, especially those measured via gas exchange variables. It is unclear however, if EMG measures of neuromuscular fatigue may also be impacted on by this mechanism.

AIMS AND HYPOTHESIS

As a consequence of the findings in Chapter 3, the current validation study was undertaken, in order to investigate if T_{EMG} was capable of detecting alterations in incremental protocol. It was hypothesised that changes in the incremental protocol would alter the appearance of T_{EMG} and ventilatory derived thresholds, due to the mechanisms previously outlined above.

MATERIALS AND METHODS

Eight (n=8) male cyclists participated in this study. Participants visited the laboratory twice, in order to perform two separate incremental cycling tests. One of the tests was performed using the continuous incremental protocol, while the other was performed using the intermittent protocol, see Figure 2.3. Trial order was randomised for the group and the time duration between tests was 2 to 7 days. Incremental testing was carried out in the methods previously described (Chapter 2.8) during which, respiratory exchange variables (Chapter 2.9), blood lactate (Chapter 2.10) and heart rate data (Chapter 2.11) were collected. In addition, raw EMG data were recorded from the *Rectus Femoris* (RF) and *Vastus Medialis*

(VM) muscles during the final minute of each increment, see Chapter 2.1. EMG data were processed and thresholds attained in a similar fashion to the methods described in Chapter 3.3. In addition to these methods, average EMG data were normalised to peak amplitude and temporally normalised (Chapter 2.5) in order to graphically compare across varying power outputs. Statistical analysis was performed using paired Student's T-tests with $P<0.05$ inferring significance.

RESULTS

Non-linear increases in EMG recorded from RF and VM were observed in all participants during all incremental protocols, see Figure 1. Comparison of thresholds attained from blood lactate, ventilatory and EMG data across exercise protocol revealed significant differences. With the exception of OBLA, all measures of the aerobic-anaerobic transition occurred at significantly greater power outputs during the intermittent incremental protocol, see Table 1. In addition, power at Pmax was significantly greater ($P<0.01$) during the intermittent protocol, highlighting that the participants were capable of reaching higher power outputs during this test. However, when threshold data were normalised to Pmax, no significant differences were observed for any of the measures, see Table 2.

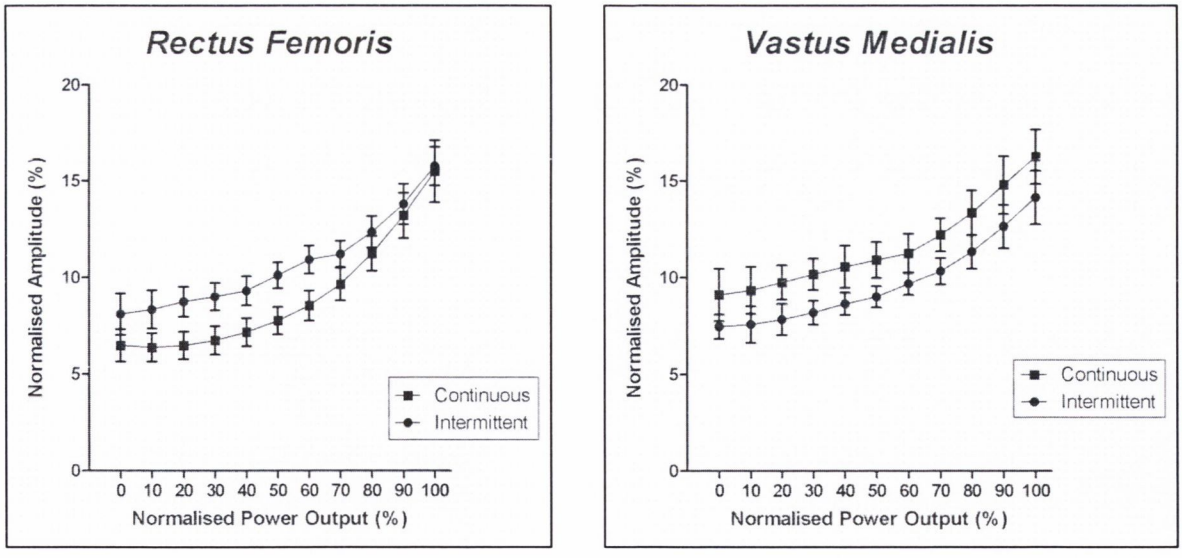

Figure 1: Group mean (SEM) rmsEMG data recorded during continuous and intermittent incremental cycling tests for RF and VM. EMG data were normalised to peak amplitude and temporally normalised to Pmax.

	Continuous	Intermittent
$\dot{V}O_2$peak ($mL.kg^{-1}.min^{-1}$)	61.3 (2.5)	60.6 (2.5)
Power at T_{Lac} (W)	249 (9)*	260 (10)
Power at OBLA (W)	288 (11)	295 (10)
Power at T_{EMG} RF (W)	261 (6)**	287 (7)
Power at T_{EMG} VM (W)	264 (6)**	287 (10)
Power at VT1 (W)	254 (5)***	273 (7)
Power at VT2 (W)	273 (3)**	294 (8)
Power at Pmax (W)	333 (9)**	349 (9)

Table 1: Group mean (SEM) data for $\dot{V}O_2$peak, Pmax, lactate, EMG and ventilatory thresholds recorded during continuous and intermittent incremental testing. Asterisk infer significant differences from intermittent test (* $P<0.05$, ** $P<0.01$ and *** $P<0.001$).

	Continuous	Intermittent
Power at T_{Lac} (%)	75 (1)	74 (1)
Power at OBLA (%)	86 (2)	84 (1)
Power at T_{EMG} RF (%)	78 (2)	82 (1)
Power at T_{EMG} VM (%)	79 (2)	82 (1)
Power at VT1 (%)	77 (1)	79 (1)
Power at VT2 (%)	82 (2)	84 (1)

Table 2: Group mean (SEM) data lactate, EMG and ventilatory thresholds normalised to Pmax, recorded during continuous and intermittent incremental testing.

DISCUSSION

The results of the current validation study were not in agreement with the hypothesis put forward following the results from Chapter 3. While all measures were capable of detecting greater absolute power at the aerobic-anaerobic transition, these thresholds were most likely a result of the significantly higher Pmax values attained during intermittent tests. When data were normalised to Pmax, none of the measures of the aerobic-anaerobic transition differed significantly across testing condition.

As described in the introduction, the 1 min rest which participants are afforded during an intermittent protocol facilitates respiratory compensation, which should impact on the subsequent appearance of ventilatory thresholds. V_{T1} and V_{T2} would therefore by expected to occur later relative to Pmax during an intermittent protocol. It is worth noting that both the ventilatory and EMG thresholds did increase relative to Pmax during the intermittent test (Table 2), while no increases were observed in blood lactate thresholds. While it may be tempting to suggest that these increases are a sign of a shared physiological mechanism which alters their response due to increased recovery, these results did not attain statistical significance. The hypothesis that T_{EMG} and ventilatory thresholds are in some way sensitive to alterations in testing protocol must therefore be rejected, based on the results of this validation study.

Appendix 5

Group ensemble EMG traces during on-water and on-ergometer kayaking.

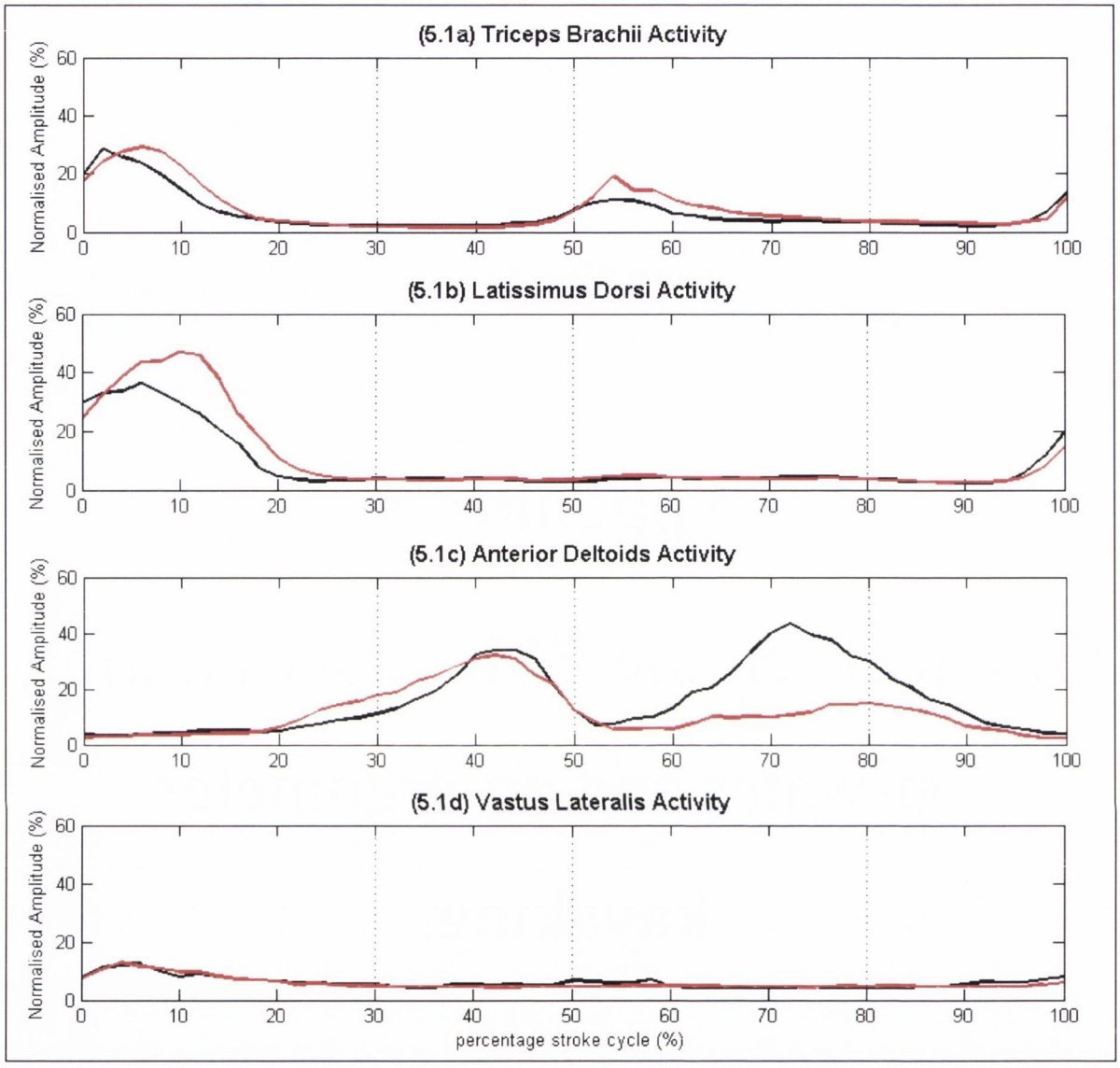

Appendix 5.1: Group mean ensemble EMG traces (5.1a to 5.1d) recorded during on-water (red) and on-ergometer (black) kayaking at 75% $\dot{V}O_2$peak. The dashed vertical lines separate the approximate phases of the stroke cycle; draw phase (0-30%), transition phase (30-50%), opposite draw phase (50-80%) and opposite transition phase (80-100%).

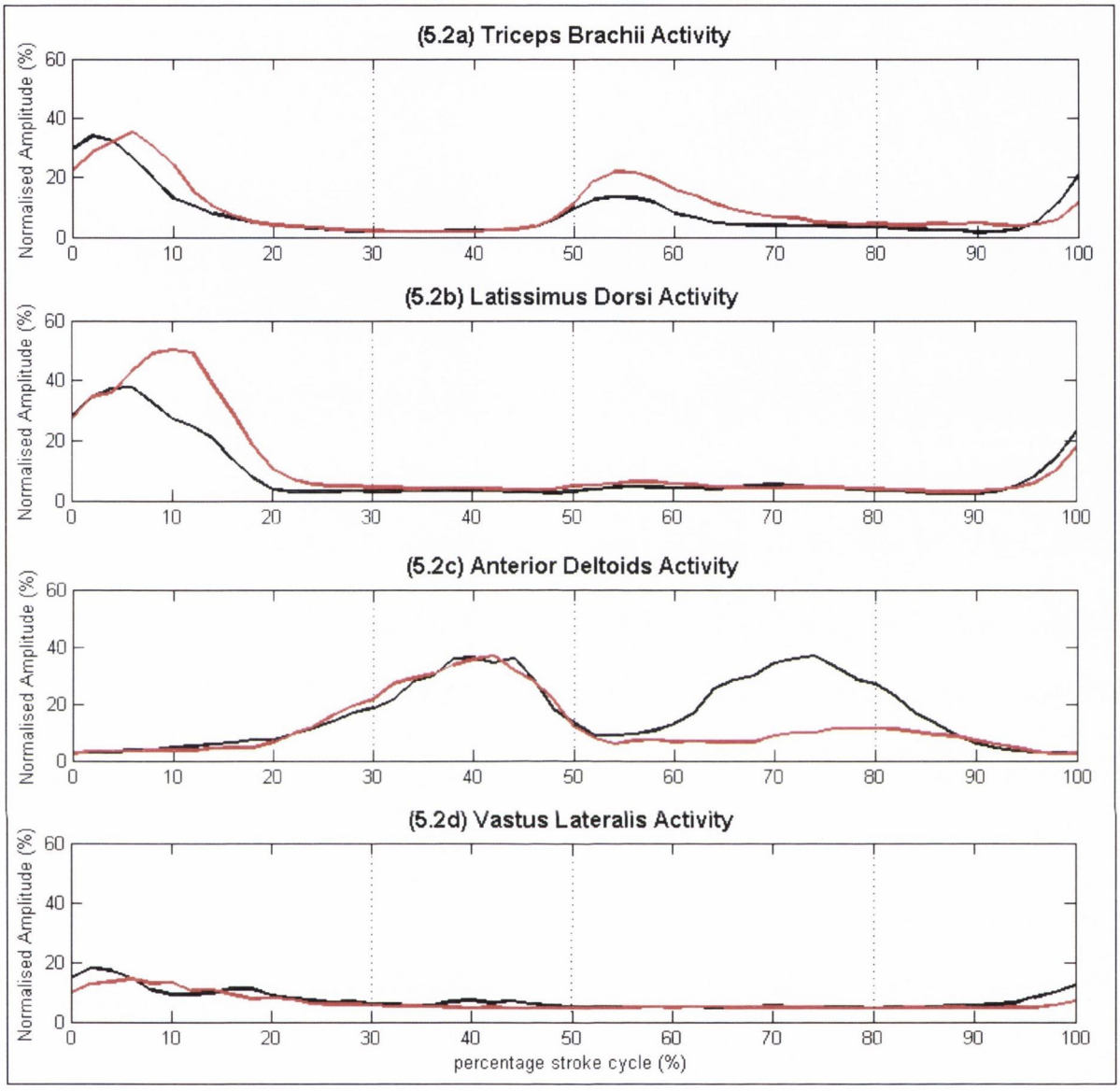

Appendix 5.2: Group mean ensemble EMG traces (5.2a to 5.2d) recorded during on-water (red) and on-ergometer (black) kayaking at 85% $\dot{V}O_2$peak. The dashed vertical lines separate the approximate phases of the stroke cycle; draw phase (0-30%), transition phase (30-50%), opposite draw phase (50-80%) and opposite transition phase (80-100%).

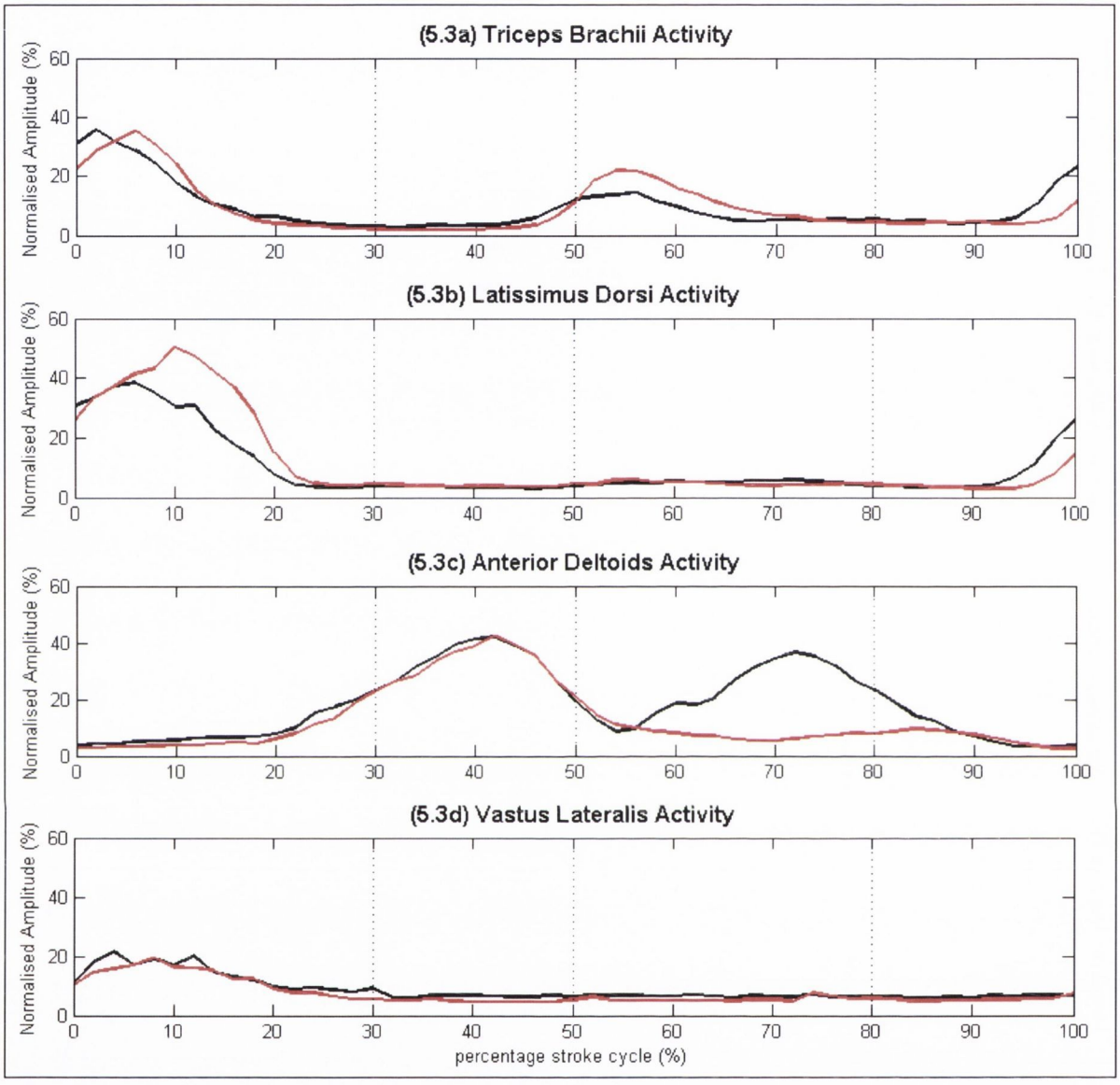

Appendix 5.3: Group mean ensemble EMG traces (5.3a to 5.3d) recorded during on-water (red) and on-ergometer (black) kayaking at 95% $\dot{V}O_2$peak. The dashed vertical lines separate the approximate phases of the stroke cycle; draw phase (0-30%), transition phase (30-50%), opposite draw phase (50-80%) and opposite transition phase (80-100%).

Appendix 6

3D marker data

Interval (% cycle)	Axis	Tension 1	Tension 2	Tension 3	Tension 4
10	X	-166 (35)***#	-163 (29)***	-151 (32)	-138 (36)
	Y	-129 (27)	-134 (30)	-130 (28)	-133 (19)
	Z	922 (38)	907 (27)	913 (28)	912 (23)
20	X	-397 (38)**	-395 (31)**	-380 (29)	-361 (39)
	Y	-282 (32)	-291 (32)	-290 (33)	-285 (38)
	Z	754 (53)	749 (47)	751 (51)	755 (51)
30	X	-691 (60)*	-701 (50)	-687 (44)	-662 (52)
	Y	-389 (38)	-398 (44)	-399 (43)	-397 (42)
	Z	879 (82)	883 (70)	874 (68)	872 (74)
40	X	-885 (57)*	-898 (57)	-893 (53)	-866 (55)
	Y	-374 (59)	-372 (53)	-373 (57)	-377 (57)
	Z	1186 (98)	1202 (69)	1191 (72)	1180 (81)
50	X	-795 (65)	-795 (60)	-794 (53)	-771 (55)
	Y	-334 (55)	-324 (49)	-317 (56)	-317 (57)
	Z	1434 (89)	1449 (67)	1444 (69)	1431 (76)
60	X	-452 (90)*	-423 (59)	-421 (58)	-402 (60)
	Y	-307 (65)	-302 (62)	-291 (56)	-286 (60)
	Z	1481 (66)	1481 (59)	1487 (66)	1481 (67)
70	X	-181 (76)*	-157 (44)	-154 (41)	-138 (37)
	Y	-137 (73)	-133 (64)	-127 (58)	-129 (54)
	Z	1346 (39)	1339 (44)	1353 (45)	1357 (41)
80	X	-133 (60)*	-121 (50)	-118 (46)	-108 (36)
	Y	56 (68)	64 (60)	68 (56)	60 (47)
	Z	1294 (41)	1291 (56)	1303 (44)	1303 (40)
90	X	-130 (58)*	-126 (57)	-124 (56)	-113 (44)
	Y	132 (50)	141 (50)	147 (48)	138 (39)
	Z	1302 (48)	1304 (57)	1316 (45)	1313 (41)
100	X	-81 (45)**	-76 (41)**	-69 (42)	-56 (37)
	Y	59 (39)	63 (39)	67 (41)	56 (31)
	Z	1216 (36)	1212 (40)	1223 (39)	1224 (36)

Appendix 6.1: Presented are group mean (SD) 3D kinematic data for the head of the *Ulna*. Data are mean displacement (mm) from reference point at each 10% interval of the stroke cycle across tension levels. Asterisk infers significantly different from T4 (* inferring $P < 0.05$, ** inferring $P < 0.01$, *** inferring $P < 0.001$). Hash symbols infers significantly different from T3 ($^{\#}$ inferring $P < 0.05$, $^{\#\#}$ inferring $P < 0.01$).

Interval (% cycle)	Axis	Tension 1	Tension 2	Tension 3	Tension 4
10	X	-414 (30)***#	-409 (24)***	-396 (25)	-385 (32)
	Y	-201 (24)	-200 (23)	-195 (18)	-198 (16)
	Z	954 (47)	949 (37)	958 (34)	959 (35)
20	X	-630 (42)**	-627 (29)**	-611 (32)	-594 (44)
	Y	-269 (22)	-277 (22)	-275 (21)	-275 (23)
	Z	861 (41)	859 (36)	862 (37)	864 (38)
30	X	-896 (61)*	-906 (40)	-891 (41)	-872 (47)
	Y	-263 (35)	-268 (38)	-268 (38)	-275 (38)
	Z	926 (39)	928 (38)	925 (40)	926 (45)
40	X	-1052 (46)	-1068 (31)	-1060 (33)	-1042 (34)
	Y	-236 (46)	-238 (52)	-232 (54)	-242 (52)
	Z	1088 (50)	1096 (44)	1091 (43)	1089 (49)
50	X	-962 (56)	-965 (40)	-963 (39)	-951 (44)
	Y	-314 (39)	-315 (47)	-308 (53)	-314 (49)
	Z	1260 (65)	1272 (60)	1272 (62)	1270 (64)
60	X	-631 (73)	-612 (47)	-604 (42)	-596 (48)
	Y	-335 (29)	-330 (30)	-326 (30)	-327 (24)
	Z	1317 (55)*	1322 (51)	1329 (54)	1331 (59)
70	X	-400 (65)*	-380 (34)	-372 (28)	-363 (28)
	Y	-216 (45)	-209 (43)	-204 (41)	-205 (38)
	Z	1236 (37)*	1233 (40)*	1242 (38)	1250 (37)
80	X	-333 (53)*	-322 (40)	-317 (37)	-312 (31)
	Y	-95 (47)	-87 (43)	-83 (42)	-87 (36)
	Z	1204 (40)	1203 (49)	1212 (40)	1214 (40)
90	X	-310 (43)	-306 (42)	-303 (41)	-299 (33)
	Y	-41 (39)	-31 (39)	-26 (37)	-30 (30)
	Z	1202 (44)	1202 (52)	1213 (45)	1214 (45)
100	X	-296 (33)**	-292 (31)**	-286 (29)	-279 (24)
	Y	-81 (32)	-73 (33)	-67 (30)	-74 (23)
	Z	1141 (43)**#	1142 (45)**#	1155 (44)	1160 (44)

Appendix 6.2: Presented are group mean (SD) 3D kinematic data for the head of the *Radius*. Data are mean displacement (mm) from reference point at each 10% interval of the stroke cycle across tension levels. Asterisk infers significantly different from T4 (* inferring $P < 0.05$, ** inferring $P < 0.01$, *** inferring $P < 0.001$). Hash symbols infers significantly different from T3 ($^{\#}$ inferring $P < 0.05$, $^{\#\#}$ inferring $P < 0.01$).

Interval (% cycle)	Axis	Tension 1	Tension 2	Tension 3	Tension 4
10	X	-446 (25)***#	-441 (22)**	-427 (24)	-416 (29)
	Y	-205 (23)	-204 (23)	-199 (18)	-202 (17)
	Z	960 (43)	956 (35)	963 (31)	965 (32)
20	X	-658 (43)***	-655 (31)**	-639 (35)	-620 (44)
	Y	-260 (20)	-267 (20)	-265 (19)	-266 (22)
	Z	879 (37)	878 (35)	880 (34)	881 (37)
30	X	-912 (62)	-921 (42)**	-907 (45)	-885 (44)
	Y	-233 (41)	-238 (41)	-239 (41)	-250 (43)
	Z	941 (32)	944 (35)	941 (36)	942 (41)
40	X	-1054 (43)	-1064 (33)	-1060 (38)	-1043 (33)
	Y	-190 (44)	-190 (55)	-186 (52)	-199 (53)
	Z	1077 (40)	1084 (36)	1080 (36)	1081 (45)
50	X	-969 (54)	-970 (40)	-970 (40)	-960 (42)
	Y	-277 (30)	-279 (46)	-273 (47)	-278 (44)
	Z	1228 (53)	1240 (46)	1240 (49)	1240 (53)
60	X	-655 (71)	-637 (43)	-629 (38)	-621 (44)
	Y	-324 (27)	-321 (29)	-317 (29)	-318 (23)
	Z	1291 (48)*#	1297 (46)	1304 (49)	1307 (52)
70	X	-431 (62)*	-411 (30)	-402 (23)	-393 (23)
	Y	-222 (40)	-215 (39)	-210 (37)	-211 (35)
	Z	1219 (33)*	1217 (37)*	1225 (35)	1234 (33)
80	X	-358 (50)*	-348 (39)	-342 (34)	-334 (26)
	Y	-114 (42)	-106 (38)	-101 (37)	-105 (32)
	Z	1189 (35)	1188 (45)	1196 (35)	1199 (35)
90	X	-333 (41)*	-329 (40)	-325 (37)	-315 (30)
	Y	-62 (36)	-52 (36)	-46 (33)	-51 (26)
	Z	1185 (38)	1186 (46)	1196 (39)	1196 (38)
100	X	-323 (31)**	-320 (30)**	-312 (26)	-301 (23)
	Y	-96 (31)	-88 (32)	-82 (28)	-90 (24)
	Z	1129 (37)*#	1130 (41)*	1142 (39)	1144 (36)

Appendix 6.3: Presented are group mean (SD) 3D kinematic data for the *Lateral Epicondyle*. Data are mean displacement (mm) from reference point at each 10% interval of the stroke cycle across tension levels. Asterisk infers significantly different from T4 (* inferring $P < 0.05$, ** inferring $P < 0.01$, *** inferring $P < 0.001$). Hash symbols infers significantly different from T3 ($^{\#}$ inferring $P < 0.05$, $^{\#\#}$ inferring $P < 0.01$).

Interval (% cycle)	Axis	Tension 1	Tension 2	Tension 3	Tension 4
10	X	-662 (22)**	-657 (22)*	-648 (18)	-637 (23)
	Y	-216 (19)	-218 (18)	-215 (16)	-214 (14)
	Z	1177 (22)	1174 (22)	1178 (24)	1181 (27)
20	X	-747 (27)***	-742 (28)***	-734 (28)*	-718 (28)
	Y	-186 (22)	-188 (22)	-187 (23)	-190 (28)
	Z	1171 (27)	1171 (27)	1172 (29)	1173 (31)
30	X	-845 (35)**	-847 (34)**	-839 (35)	-825 (27)
	Y	-94 (42)	-93 (41)	-93 (42)	-102 (44)
	Z	1202 (26)	1203 (27)	1204 (28)	1204 (29)
40	X	-880 (26)	-883 (29)	-878 (29)	-871 (24)
	Y	-11 (48)	-10 (48)	-11 (51)	-18 (50)
	Z	1232 (24)	1233 (24)	1233 (26)	1234 (28)
50	X	-865 (22)*	-860 (22)	-856 (22)	-848 (23)
	Y	-18 (32)	-21 (38)	-21 (44)	-22 (44)
	Z	1248 (24)**	1249 (23)**	1251 (26)	1253 (28)
60	X	-801 (23)**	-789 (18)	-783 (17)	-774 (25)
	Y	-101 (19)	-105 (21)	-103 (25)	-96 (32)
	Z	1245 (26)**	1245 (23)**	1249 (26)	1254 (29)
70	X	-701 (32)*	-688 (23)	-682 (14)	-676 (18)
	Y	-182 (16)	-184 (12)	-181 (18)	-170 (26)
	Z	1221 (30)**	1221 (26)**	1226 (28)	1232 (31)
80	X	-626 (39)	-617 (35)	-613 (28)	-610 (23)
	Y	-200 (14)	-200 (11)	-198 (10)	-193 (20)
	Z	1199 (30)*	1198 (29)*	1202 (31)	1209 (35)
90	X	-589 (37)*	-582 (37)	-578 (34)	-575 (28)
	Y	-191 (21)	-188 (19)	-184 (18)	-185 (15)
	Z	1190 (28)*	1189 (28)*	1194 (30)	1201 (35)
100	X	-592 (28)**	-586 (30)	-580 (27)	-576 (22)
	Y	-197 (25)	-195 (24)	-190 (24)	-192 (18)
	Z	1183 (24)*	1182 (24)*	1186 (27)	1194 (32)

Appendix 6.4: Presented are group mean (SD) 3D kinematic data for the lateral tip of the *Acromion*. Data are mean displacement (mm) from reference point at each 10% interval of the stroke cycle across tension levels. Asterisk infers significantly different from T4 (* inferring $P < 0.05$, ** inferring $P < 0.01$, *** inferring $P < 0.001$). Hash symbols infers significantly different from T3 ($^{\#}$ inferring $P < 0.05$, $^{\#\#}$ inferring $P < 0.01$).

Interval (% cycle)	Axis	Tension 1	Tension 2	Tension 3	Tension 4
10	X	-827 (13)***	-822 (19)***	-816 (12)	-805 (10)
	Y	-162 (28)	-162 (27)	-161 (23)	-161 (24)
	Z	1077 (16)***	1078 (16)**	1080 (17)	1083 (18)
20	X	-882 (20)***	-879 (25)***	-873 (21)*	-859 (17)
	Y	-64 (44)	-63 (42)	-62 (40)	-67 (38)
	Z	1087 (19)***	1089 (18)*	1090 (19)	1093 (20)
30	X	-912 (31)**	-913 (36)**	-907 (33)	-899 (26)
	Y	60 (46)	65 (38)	66 (40)	58 (37)
	Z	1093 (20)***	1095 (19)*	1097 (20)	1100 (23)
40	X	-903 (34)	-903 (38)	-899 (36)	-895 (29)
	Y	113 (27)	117 (24)	119 (27)	115 (25)
	Z	1092 (20)*	1092 (19)	1093 (21)	1096 (23)
50	X	-901 (30)**	-899 (33)*	-894 (30)	-887 (23)
	Y	89 (18)	89 (19)	92 (20)	89 (18)
	Z	1096 (19)**	1097 (19)*	1098 (20)	1101 (22)
60	X	-894 (27)***	-888 (29)**	-883 (22)	-870 (19)
	Y	-6 (21)	-10 (19)	-9 (18)	-10 (20)
	Z	1105 (19)**	1105 (19)**	1107 (20)	1110 (22)
70	X	-849 (29)**	-839 (29)*	-832 (17)	-821 (18)
	Y	-118 (18)	-122 (17)	-121 (13)	-118 (16)
	Z	1102 (22)***##	1103 (19)***#	1106 (21)**	1110 (23)
80	X	-792 (32)	-784 (35)	-779 (23)	-777 (22)
	Y	-194 (19)	-195 (14)	-193 (12)	-189 (13)
	Z	1082 (22)***#	1083 (20)***	1086 (21)*	1089 (22)
90	X	-751 (26)	-744 (32)	-740 (26)	-741 (24)
	Y	-215 (18)	-215 (15)	-213 (12)	-212 (12)
	Z	1071 (20)***#	1072 (19)***	1075 (20)	1078 (20)
100	X	-758 (19)	-753 (27)	-747 (22)	-744 (19)
	Y	-209 (21)	-208 (19)	-207 (14)	-206 (14)
	Z	1069 (17)***#	1069 (17)***	1072 (18)**	1076 (18)

Appendix 6.5: Presented are group mean (SD) 3D kinematic data for the *Inferior Scapula*. Data are mean displacement (mm) from reference point at each 10% interval of the stroke cycle across tension levels. Asterisk infers significantly different from T4 (* inferring $P < 0.05$, ** inferring $P < 0.01$, *** inferring $P < 0.001$). Hash symbols infers significantly different from T3 ($^{\#}$ inferring $P < 0.05$, $^{\#\#}$ inferring $P < 0.01$).

Interval (% cycle)	Axis	Tension 1	Tension 2	Tension 3	Tension 4
10	X	-780 (15)***	-774 (16)*	-767 (12)	-756 (19)
	Y	-143 (33)	-143 (32)	-142 (29)	-141 (29)
	Z	1196 (19)*	1196 (19)*	1198 (20)	1200 (22)
20	X	-820 (20)***	-814 (23)**	-807 (20)*	-794 (20)
	Y	-61 (49)	-62 (47)	-61 (46)	-65 (46)
	Z	1203 (22)*	1204 (23)	1205 (23)	1207 (25)
30	X	-847 (33)*	-847 (37)*	-842 (35)	-833 (28)
	Y	58 (49)	61 (44)	62 (44)	55 (44)
	Z	1213 (25)***#	1214 (25)**	1216 (26)	1219 (28)
40	X	-839 (38)	-840 (42)	-835 (40)	-832 (32)
	Y	115 (33)	119 (30)	121 (33)	118 (33)
	Z	1211 (27)***	1212 (26)**	1213 (27)*	1217 (29)
50	X	-840 (34)*	-838 (38)	-832 (34)	-828 (27)
	Y	104 (19)	104 (20)	108 (23)	107 (22)
	Z	1211 (25)***	1212 (26)***	1213 (27)**	1217 (28)
60	X	-843 (26)**	-838 (28)*	-831 (21)	-821 (18)
	Y	25 (16)	23 (16)	26 (16)	28 (18)
	Z	1216 (24)**	1216 (24)**	1218 (26)*	1221 (27)
70	X	-801 (21)***#	-790 (19)*	-783 (10)	-773 (14)
	Y	-87 (20)	-91 (17)	-88 (16)	-82 (18)
	Z	1212 (24)***	1212 (23)***	1214 (23)*	1218 (25)
80	X	-754 (23)	-746 (24)	-742 (16)	-738 (16)
	Y	-166 (23)	-167 (17)	-164 (13)	-160 (14)
	Z	1198 (23)***#	1199 (22)***	1202 (24)	1205 (25)
90	X	-718 (19)	-711 (22)	-709 (19)	-708 (19)
	Y	-190 (23)	-189 (20)	-187 (15)	-185 (15)
	Z	1191 (23)***#	1191 (22)***#	1194 (24)	1197 (24)
100	X	-723 (14)*	-717 (18)	-712 (16)	-709 (17)
	Y	-185 (26)	-183 (23)	-182 (18)	-181 (17)
	Z	1188 (20)***#	1188 (20)***#	1191 (21)*	1195 (22)

Appendix 6.6: Presented are group mean (SD) 3D kinematic data for the medial border of the *Spinal Scapula*. Data are mean displacement (mm) from reference point at each 10% interval of the stroke cycle across tension levels. Asterisk infers significantly different from T4 (* inferring $P < 0.05$, ** inferring $P < 0.01$, *** inferring $P < 0.001$). Hash symbols infers significantly different from T3 ($^{\#}$ inferring $P < 0.05$).

Appendix 7

Group ensemble EMG traces for on-ergometer kayaking at varying elastic tension levels.

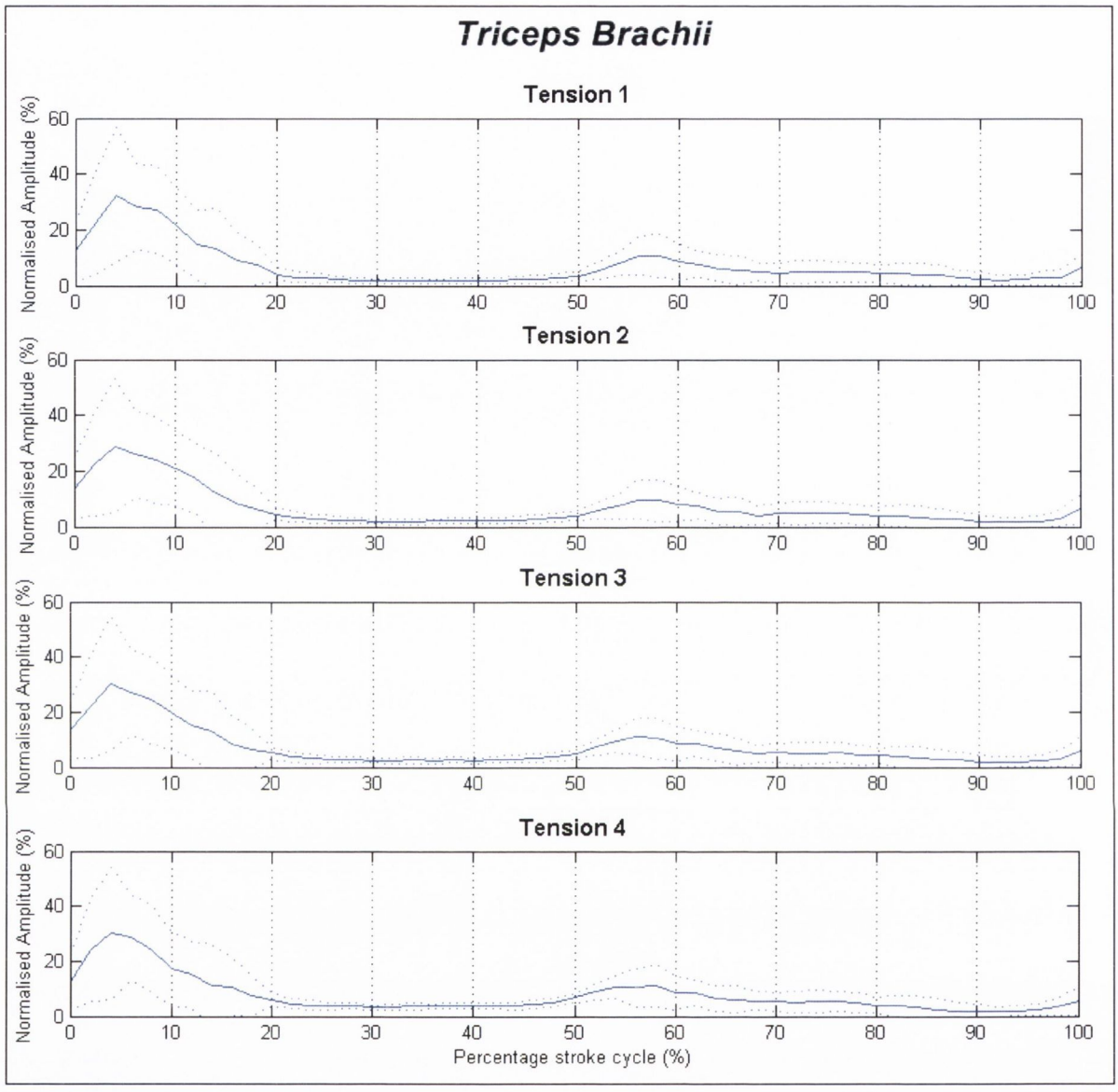

Appendix 7.1: Group mean (± SD) ensemble EMG traces for TB recorded at each tension level. Solid line represents group mean rmsEMG data at 2% intervals of the stroke cycle normalised to maximal rmsEMG amplitude recorded during isometric MVC. Dashed lines above and below represent group SD.

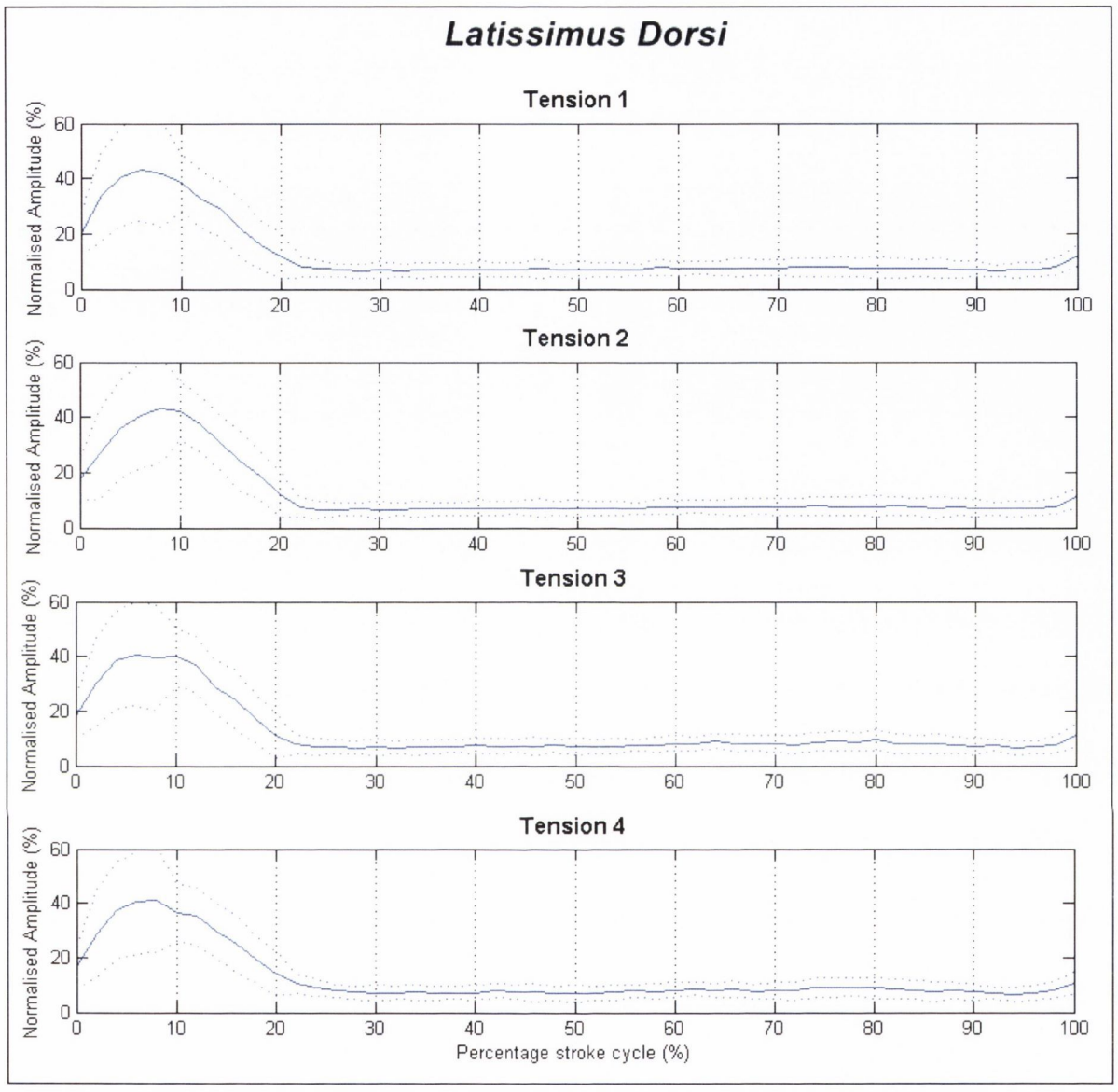

Appendix 7.2: Group mean (± SD) ensemble EMG traces for LD recorded at each tension level. Solid line represents group mean rmsEMG data at 2% intervals of the stroke cycle normalised to maximal rmsEMG amplitude recorded during isometric MVC. Dashed lines above and below represent group SD.

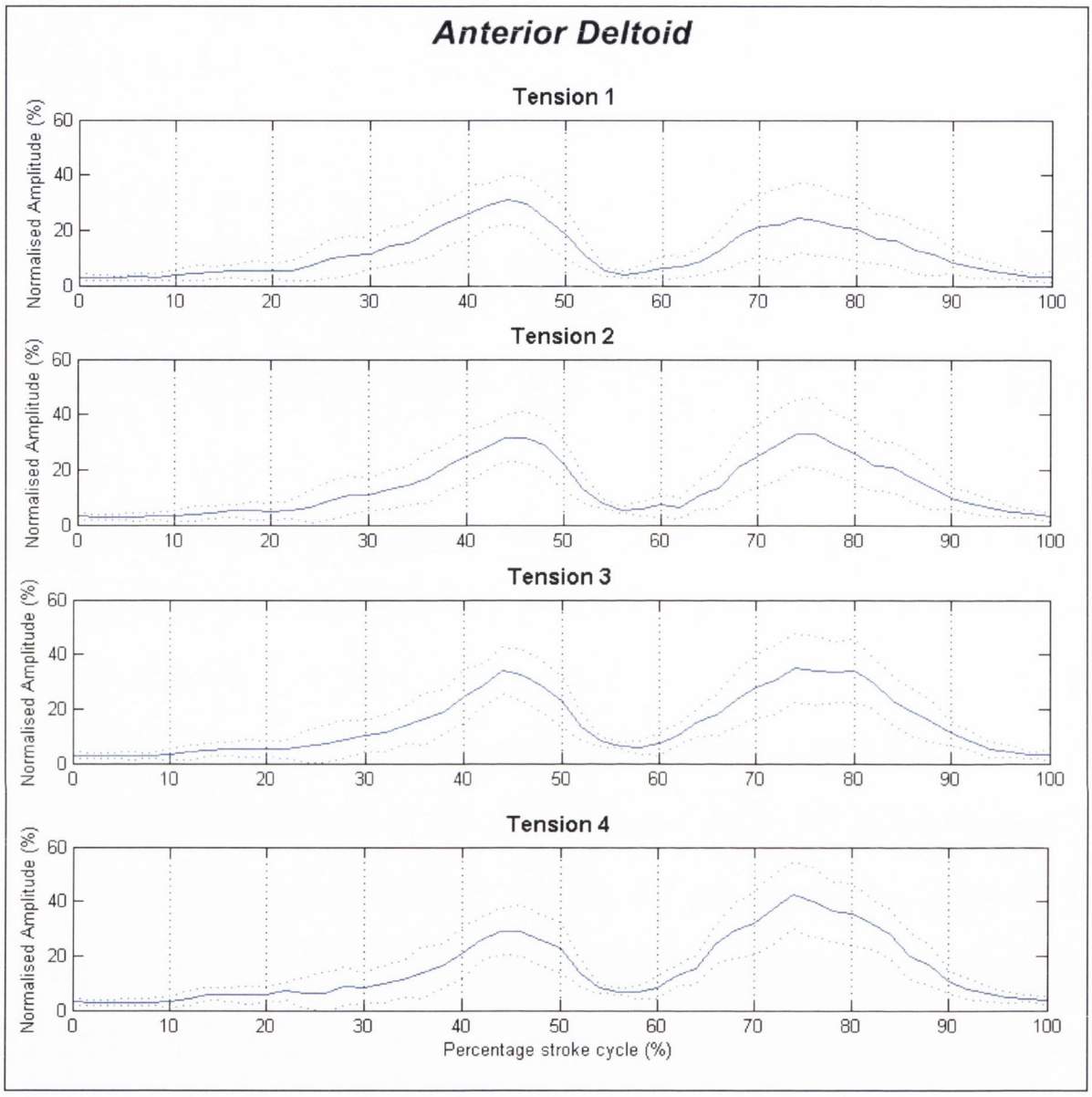

Appendix 7.3: Group mean (± SD) ensemble EMG traces for AD recorded at each tension level. Solid line represents group mean rmsEMG data at 2% intervals of the stroke cycle normalised to maximal rmsEMG amplitude recorded during isometric MVC. Dashed lines above and below represent group SD. Progressive increases in *AD* activity occurred between the 60 and 90% phase of the stroke cycle as elastic tension increased.